PALESTINE POLYTECHNIC UNIVERSITY

AL-QUDS UNIVERSITY

Master Program of Renewable Energy and Sustainability

Investigate the Influence of the Penetration level of PV Distributed Generation and Energy Storage Integration on the Medium Voltage Distribution Network

By

Haitham Zidan Alqadi

Supervisors

Dr. Maher Maghalseh **Dr. Nassim Iqteit**

December, 2019

Joint mAster of Mediterranean Initiatives on renewabLe and sustainAble energy

Palestine Polytechnic University

Deanship of Graduate Studies and Scientific Research

Master Program of Renewable Energy and Sustainability

Investigate the Influence of the Penetration Level of PV Distributed Generation and Energy Storage Integration on the Medium Voltage Distribution Network

---

By

Haitham Zidan Alqadi

Supervisor

Dr. Maher Maghalseh Dr. Nassim Iqteit

Thesis submitted in partial fulfillment of requirements of the degree

Master of Science in Renewable Energy & Sustainability

December, 2019

The undersigned hereby certify that they have read, examined and recommended to the Deanship of Graduate Studies and Scientific Research at Palestine Polytechnic University and Al-Quds University the approval of a thesis entitled:

Investigate the Influence of the Penetration level of PV Distributed Generation and Energy Storage Integration on the Medium Voltage Distribution Network

Submitted by

Haitham Zidan Alqadi

In partial fulfillment of the requirements for the degree of Master in Renewable Energy & Sustainability.

Graduate Advisory Committee:

Dr. Maher Maghalseh
(Supervisor), Palestine Polytechnic University.

Signature: _____ Date: _____

Dr. Nassim Iqteit
(Co-Supervisor), Palestine Polytechnic University.

Signature: _____ Date: _____

Prof. Abdel-karim Daud
(Internal committee member), Palestine Polytechnic University.

Signature: _____ Date: _____

Prof. Samer Alsadi
(External committee member), Palestine Technical University.

Signature: _____ Date: _____

Thesis Approved by:

Name: Dr. Murad Abu Sbeih

Dean of Graduate Studies & Scientific Research

Palestine Polytechnic University

Signature: …… Date: ……

Investigate the Influence of the Penetration level of PV Distributed Generation and Energy Storage Integration on the Medium Voltage Distribution Network

Submitted by

Haitham Zidan Alqadi

ABSTRACT

Electrical Power System is centralized energy frames, power flows from generation plant to distribution network through transmission lines of the grid, which means that the conventional system has a unidirectional power flow. The increasing of electrical energy consumption and the immediate need of electricity today leads to enhance and develop the electrical power system. Using of renewable energy systems, especially solar energy is one of the solutions to produce sustainable and environmentally friendly electrical energy systems. This study supports the photovoltaic (PV) system as a renewable source, but the intermittency of the solar energy and variation of weather conditions, besides of high impact of the high penetration of PV systems are stands as a main drawback of the grid connected PV system. However, in the field of operation and planning of electrical power systems point of view, using an Energy Storage System (ESS) integrated with grid connected PV systems are filling the gap of the grid-tied PV system by reduce the PV impact, maximizing the penetration level of DG and enhancing the grid stability through getting a backup source of the system.

The objective of this thesis is investigating the effects and performance of integrating grid-tied PV system with the conventional power system through the conduction of a real case study 230 kWp PV power plant on the Palestine Polytechnic University (PPU) distribution medium voltage feeder and determine the penetration level of the PV system on the PPU feeder. Moreover, battery energy storage system (BESS) proposed to be integrated with the grid-tied PV system due to maximize the allowable PV Penetration and eliminate the grid connected PV system impact issues to the grid.

However, a modelling of the case study PPU feeder and the PV station and the proposed BESS was conducted using Electrical Transient Analyzer Power (ETAP) software where the daily load profile built to be inserted to the system model in the form of four scenarios: i) electrical network alone, ii) electrical grid with PV system integration, iii) electrical grid with BESS and iv) electrical grid with PV and BESS integration, the aim of studying these cases is to improve the strengthen power networks and to verify the results with the IEEE standard. In the results of this thesis, it is shown that the PV hosting capacity of a distribution power grid can be increased using the investigated methods, in addition to that the technical impact of the PV power plant minimized especially of the PF, voltage drop and power issues.

دراسة تأثير مستوى إسهام الإنتاج الموزع الكهروضوئي وتكامله مع أنظمة تخزين الطاقة على شبكة توزيع الجهد المتوسط

ملخص:

نظام الطاقة الكهربائية بشكلٍ عام، عبارة عن نظام مركزي في إنتاج الطاقة الكهربائية؛ حيث أن الطاقة المنتَجة تتدفق من محطة التوليد إلى المستهلكين عن طريق نظامي النقل والتوزيع الخاصيّن بالشبكة، أي أنه نظام أحادي الإتجاه (من المنتج إلى المتسهلك)، ويسمى هذا النظام بالنظام التقليدي. مع زيادة الإستهلاك والحاجة إلى الطاقة في كافة مناحي الحياة في يومنا الحاضر، كان لا بدّ من تطوير وتعزيز نظام الطاقة الكهربائية التقليدي و المساهمة في خلق نظامٍ كهربائي قادرٌ على تلبية الحاجات الكهربائية المختلفة حيث تمثلت هذه المساهمة في استخدام أنظمة الطاقة المتجددة على اختلاف أنواعها، وأهمها الطاقة الشمسية الكهروضوئية لأنها وسابقاتها تعد من المصادر المستدامة والصديقة للبيئة حيث أنها تعمل على تخفيف الآثار البيئية الناجمة عن الطرق التقليدية في توليد الطاقة الكهربائية. تقوم هذه الدراسة على اعتماد نظام الطاقة الشمسية كمصدر الطاقة المتجدد الخاص بالشبكة المستخدمة، ولكن، نتيجة للتغيرات الجوية اللحظية المتكررة والتي تؤثر على إنتاجية الخلايا من الطاقة، إلى جانب نسبة الإسهام العالي من الطاقة الكهربائية الناتجة عن محطات الطاقة الكهروضوئية الموزعة، كلتاهما أوجدتا عيوبًا ذمّت النظام وكوّنتا فجوةً فيه، ومع ذلك فإن هناك حلًا متاحًا يتمثل في استخدام نظامٍ آخر مرافق لنظام الطاقة الشمسية يكون في ذات الوقت قادرًا على تغطية الفجوة الناجمة، هذا النظام هو (نظام بطاريات تخزين الطاقة- "Battery Energy Storage System" BESS)؛ تتكامل البطاريات مع الخلايا من أجل تقليل نسب الإسهام من محطات التوليد الكهروضوئية، وتعزز استقرار الشبكة في حالاتٍ تكون فيها الخلايا غير قادرة على تزويد الطاقة لأي سبب كان، كما وأنها تمثل مصدرًا إحتياطيًا للطاقة في النظام.

إن الهدف الأساسي من هذه الأطروحة يتمثلُ في دراسة تأثيرات وأداء النظام الكهروضوئي على صعدٍ عدة، كأن يتم ربطها مع شبكة الطاقة، كما في الحالة الحقيقية المستخدمة في الدراسة، حيث بلغت سعةُ نظام الطاقة الشمسية المرتبط بنظام الشبكة الجهد المتوسط خاصةً بجامعة بوليتكنك فلسطين 230 KWp ، يتم فيها تحديد مستوى الإسهام من النظام الكهروضوئي على الشبكة. بعد ذلك يتم دمج نظام تخزين الطاقة (البطاريات) مع نظام الخلايا المرتبط بالشبكة لمعرفة الحد الأقصى المسموح به للإسهام، ولإزالة التأثيرات السلبية الناجمة عن تركيب الخلايا وحيدةً كـ مولدات طاقة متجددة مستفردةً على الشبكة.

تقوم الدراسة على عمل نمذجة أو محاكاة لمغذيات جامعة بوليتكنك فلسطين ونظام الخلايا المرتبط بها، ونظام تخزين الطاقة المقترح أيضًا، ليتم دراسة حالتها، وذلك باستخدام برنامج ETAP (Electrical Transient Analyzer Power)، حيث تم خلال العمل تحديد الحمل اليومي وبناؤه بما يناسب البرنامج وادخاله على الشبكة المصممةٍ فيه؛ تقوم الدراسة على أربعِ سيناريوهات مختلفة: أ) دراسة خصائص الشبكة وحدها، ب) تكاملٌ ما بين الشبكة ونظام الخلايا الشمسية، ج) دراسة الشبكة مع نظام التخزين كنظام مركب، د) دراسة الشبكة مدمجة مع كلٍ من نظامي الطاقة الشمسية والتخزين؛ تكمن الأهداف الرئيسة لدراسة هذه الحالات في تحسين وتقوية خصائص الشبكة الكهربائية، ومقارنة النتائج مع المعايير العالمية المعتمدة من قِبل IEEE؛ من الجدير بالذكر أن النتائج التي تم الحصول عليها في هذه الأطروحة تشير إلى أنه يمكن زيادة سعة الإسهام الكهروضوئي على شبكات التوزيع من خلال الطريقة التي تم توضيحها، وعلى نفس النهج، تشير إلى أنه يمكن تقليل التأثيرات التقنية السلبية الناجمة على الشبكة نتيجة استخدام الخلايا الشمسية وحدها، أهم هذه التأثيرات تتمحور حول تغيراتٍ في قيم الجهد إلى قيم أقل مما يُسمح به، أو قضايا تتعلق بمعامل القدرة (PF).

DECLARATION

I declare that the Master Thesis entitled "**Investigate the influence of the Penetration level of PV Distributed Generation and Energy Storage Integration on the Medium Voltage Distribution Network**" is my own original work, and herby certify that unless stated, all work contained within this thesis is my own independent research and has not been submitted for the award of any other degree at any institution, except where due acknowledgement is made in the text.

Student Name: Haitham Zidan Alqadi

Signature: _____. Date: _____.

STATEMENT OF PERMISSION TO USE

In presenting this thesis in partial fulfillment of the requirements for the joint Master's degree in Renewable Energy & Sustainability at Palestine Polytechnic University and Al-Quds University, I agree that the library shall make it available to borrowers under rules of the library.

Brief quotations from this thesis are allowable without special permission, provided that accurate acknowledgement of the source is made.

Permission for extensive quotation from, reproduction, or publication of this thesis may be granted by my main supervisor, or in his absence, by the Dean of Graduate Studies and Scientific Research when, in the opinion of either, the proposed use of the material is for scholarly purposes.

Any coping or use of the material in this thesis for financial gain shall not be allowed without my written permission.

Student Name: Haitham Zidan Alqadi

Signature: _____. Date: _____.

DEDICATION

Say: Truly, my prayer and my service of sacrifice, my life and my death, are all for Allah, the Cherisher of the Worlds [162, Al-An'am]

This thesis is dedicated to:

The sake of Allah, my Creator and my Master,

My great teacher and messenger, Mohammed (PBUH), who taught us the purpose of life,

My great parents, who never stop giving of themselves in countless ways,

My beloved brothers and sisters; for their support,

My lecturers for help me until the end,

My friends; whom give me Positive sentiment and support,

Palestine Polytechnic University and Al-Quds University, my second magnificent home;

My supervisors Dr. Maher Maghalseh and Dr. Nassim Iqteit,

To all the people in my life who touch my heart,

To our great Palestine

I dedicate this research to all who made this work is possible

ACKNOWLEDGEMENT

I would like to express my gratitude towards all the people who have contributed their precious time and efforts to help me in completing this thesis, without whom it would not have been possible for me to understand and analyze the thesis.

I would like to thank my thesis Supervisors Dr. Nassim Iqteit, and Dr. Maher Maghalseh for their guidance, support, motivation and encouragement throughout the period of this work. Their readiness for consultation at all times, their educative comments, his concern, and assistance have been invaluable. Thanks, are extended to Eng. Mohammad Al-Tamimi and Eng. Samer Sultan for their time and effort to make this work possible, and many thanks for Prof. Sameer Khader Head of Department of JAMILA project and for Dr. Hussein Samamreh the coordinator for JAMILA master at al-Quds university, for providing the necessary facilities. I am also grateful for my friends Mr. Manfred Backer, Eng. Yehya Hassouneh and Eng. Yunis Badran for continues encouragement.

Finally, my ultimate thanks go to the great all instructors and engineers who helped me during the first stages of my master thesis

TABLE OF CONTENTS

LIST OF FIGURES

LIST OF TABLES

LIST OF ABBREVIATIONS

AC	Alternative Current.
BESS	Battery Energy Storage System.
DC	Direct Current.
DG	Distributed Generation.
ESS	Energy Storage System.
ETAP	Electrical Transient Analysis Program.
HEPDS	Hebron Electrical Power Distribution System.
IEC	Israel Electrical Company.
IEEE	Institute Electrical and Electronics Engineer.
IHD	Individual Harmonic Distortion.
KWh	Kilo Watt Hour.
LV	Low Voltage.
MPPT	Maximum Power Point Tracking.
MV	Medium Voltage.
NRM	Newton-Raphson Method.
OLTC	On Load Tap Changer.
PCC	Point of Common Coupling.
PCU	Power Conditioning Unit.
PEPS	Palestinian Electrical Power System.
PF	Power Factor.
PSH	Peak Sun Hour.
PV	Photovoltaic.
SCC	Short Circuit Capacity.
SLD	Single Line Diagram.
SVR	Step Voltage Regulator.
THD	Total Harmonic Distortion.

1

Chapter One

Introduction

1.1: Introduction.

1.2: Overview.

1.3: Problem formulation.

1.4: Thesis objectives.

1.5: Motivation.

1.6: Research Questions.

1.7: Thesis structure.

1.1: Introduction.

The main reason for climate changes is the greenhouse gases emitted from the burning of fossil fuels such as oil and its derivatives. In addition, around 80% of the released greenhouse gases came from generation and consumption of electrical energy. However, the turning to renewable energy resources revolution was appear all over the world, sustainability and low carbon energy technologies which play an important role in this energy revolution. Several types of renewable energy resources support this revolution especially solar and wind. Fig.1.1 illustrates the amount of global PV and wind installed between 2000 and 2018 [1].

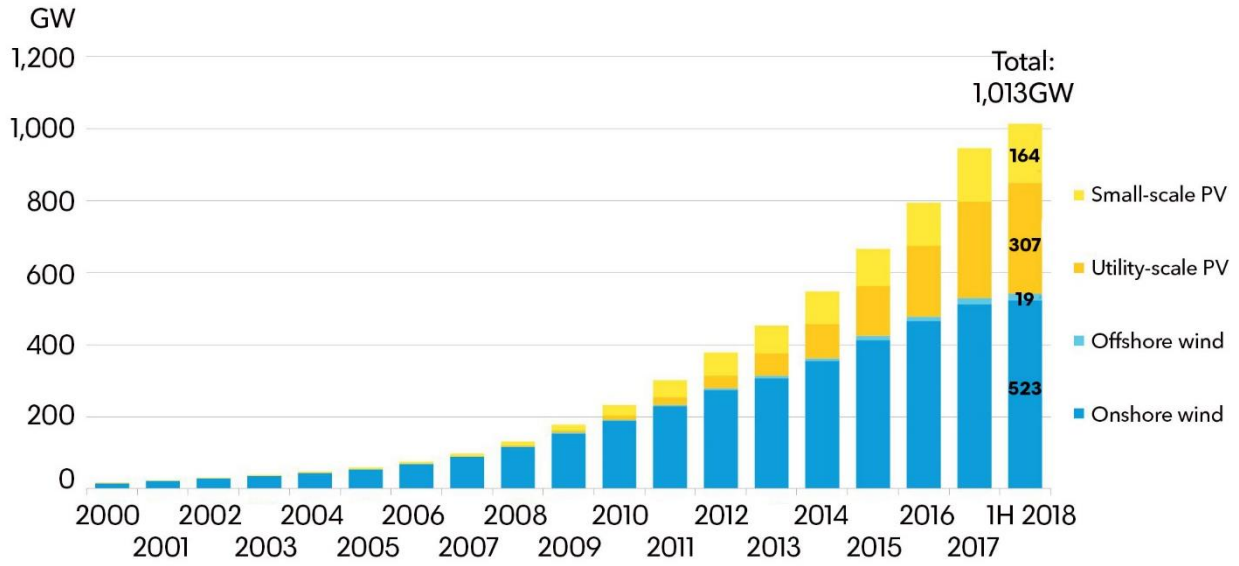

Figure 1.3: Evolution of global wind & solar cumulative installed capacity 2000-2018 (MW) [1].

In the past decade, traditional and unsustainable sources of energy pose a major threat to the environment. Nowadays the world offers all facilities and resources to find solutions to this problem and to increase reliance on renewable and clean energy. Photovoltaic (PV) technology is one of these solutions. PV technology is one of the most promising approach of renewable energy due to the continues increasing of its efficiency and performance. It's worth mentioning that the PV system contains a semiconductor panel converting sunlight into direct current and an inverter that converts direct current to alternative current which used in the grid [2].

The distribution generation systems are integrated with the electrical power system in order to decentralize the distribution feeders and to deliver it to distributed loads. With the increasing share of distributed generation, and particularly photovoltaics, power flow started to invert at certain points in time. This immediately rises some new challenges. Means that the hosting capacity of the DG is limited in the distribution grid and the researchers are aiming to maximize it. Maximizing approach that supported by this thesis is integrating the energy storage system with the PV-DGs. Moreover, the grid moves toward a smart grid for decentralizing the power source, energy efficiency and the intermittent production of DGs [3].

1.2: Overview.

The increasing of pollution caused by fuel combustion for electrical power production has become a serious concern for the ecosystem due to the increasing on the electricity demand. Consequently, the world is turning to use the renewable energy, which is considered sustainable and environmentally friendly especially in generating electricity, while traditional methods of power generation have become less used. Meanwhile the developed countries are depending widely on solar, wind and other environmentally friendly sources to produce the electrical power as a main power plant or even in distributed generation forms. However, distribution generator (DG) represents one of the most widespread power sources in the electrical power system. In Palestine, solar energy sources are widely used. Nevertheless, the usage of DG causes some critical issues in distribution networks and the capacity on the network is limited. In this thesis, the explanation of these DG affects the grid and how much is the hosting capacity of the DG in distribution network by focusing on a case study selected.

1.3: Problem formulation.

The penetration levels of distributed PV system in power distribution systems are increasing at a rapid rate to cover the rapid increasing in the load demand and overcome a significant change in the design, operation and control of the distribution feeders. But this increasing of the penetration is limited by network reliability and component. In addition, the high penetration of intermittency renewable sources like PV, generate some critical impacts to the distribution network such as voltage rising on the PV plant feeder, reverse power flow and islanding operation …etc. especially at the peak production period and to observe the hourly effect on the distribution grid parameters profile an hour by hour analysis should be concern.

1.4: Thesis Objectives.

The main objectives of this thesis are as follows:

1. Modeling and analysis a real case study of distribution feeder and specifying the power system quality parameters and conducting a single line diagram.
2. Generate a load profile for the main feeder and for each load in the feeder to obtain an hour by hour analysis for the feeder parameters from voltage, current, active and reactive power, apparent power, power factor, power losses, voltage drop and harmonics analysis.
3. Conducting the real case study system feeder and making the analysis using an Electrical Transient Analyzer Power ETAP software.
4. Study the hourly profiles of the feeder in four scenarios, Case 1: Electrical network only, Case 2: Electrical network with PV system only, Case 3: Electrical network with PV system and Energy storage system and Case 4: Electrical network with Energy storage system only.
5. Determining the current PV penetration on the real feeder and the simulation results at that point.
6. Study the PV penetration level. And reaching the maximum point in addition to maximize the hosting capacity of the distribution system.
7. Testing the maximizing approach which was selected (adding energy storage system) and its effect on the penetration level in addition to enhance the performance of the grid.
8. Study the effect of the PV system and the ESS especially on the reliability and the quality of the electrical feeder with and without PV system and ESS.

1.5: Motivations

Due to the increasing demand on the electrical energy and regarding to the good performance of the PV systems in Palestine due to its location, in addition to the advantages of the spreading of the PV and its connection with the grid which reduces the dependency on the conventional energy sources which cause many environmental problems. The PV generation is increasingly widespread in the distribution network but still there are some technical problems have been detected that may affect the operation and quality of the network, on the other hand the limitation of increasing the PV hosting capacity on the distribution system is set to be another technical problem which considered to be studied in this thesis.

1.6: Research Questions.

The main research question of this thesis is: “How much PV can be integrated into the distribution power system and how to maximize it?”. This question will be answered as two parts, firstly by the investigation of the case study modeling and analysis, the second part will be achieved using one of the main supportive technique for the distribution power system which is battery energy storage system. However, the main constraints are the voltage profile variation and rising and over loading of the distribution grid components such as cables and transformers. Moreover, the other research question of this thesis is how do the PV penetration levels change the distribution grid, and study the profiles of the grid parameters at the current state of the case study.

1.7: Thesis Structure.

This thesis is structured and divided into six chapters, the literature studies that deals with the integration of PV system and energy storage system with the grid and its effect on the medium voltage network, in addition to the modeling of the grid and the standard issues are concerned in chapter 2. The electrical network, load analysis and case study discretion are given in chapter 3. Chapter 4 illustrates the simulation results and discussion of the current state analysis of the real case study with many technical observation, chapter 5 includes the simulation results and discussion of the proposed scenarios of different penetration levels in the selected feeder. Finally, the conclusions of the work and some ideas for future work are listed in chapter 6 of the thesis.

2

Chapter Two

Impact assessment of Grid Connected Photovoltaic and Energy Storage System in the Electrical Network

2.1: Introduction

Traditional and unsustainable source of energy such as nonrenewable ones represents the main energy supplier of the worldwide economy, but this energy poses a major threat to the environment. Besides, the increasing of energy demands, and the limited resources of traditional energy led the world now devotes all its resources to find solutions to this problem and to increase reliance on renewable and clean energy as an alternative source for power generation [4].

Meanwhile, the increases in the demand for electricity is very large and there are some shortages of energy in peak load hours, so the demand for installation of renewable energy sources was increased significantly. However, renewable energy resources when implemented in a large scale without any specialized investigation of technical studies, which create an impact of the quality, reliability and stability of the power grid. The problem, nonetheless, cannot be solved easily as a new problem arises from the variable and intermittent nature of solar power as an example. Even if the most optimistic situation assumed in which the weather and the panels always have an uninterrupted view of the sun, the power generated from the PV power system changes drastically throughout a day. When the sunlight is shading by clouds or from surroundings, the power from the PV system can be dropped sharply [4, 5].

Solar energy source is one of the most important renewable sources, as the sun is the largest energy source of life while at the same time it is the ultimate source of most of renewable energy sources. Solar energy can be used to generate electricity in a direct way with the usage of photovoltaic phenomena, using solar thermal or concentrating solar power to produce heat for generating electricity by steam turbines [6], but in this thesis the PV system was only considered.

Due to the development of PV system components such a PV panels and power electronic converters besides the cost of the PV system decreases in recent years, the opportunity to obtain electrical energy from the sun to generate electrical energy has been realized. Therefore, in a distribution network PV generation has appeared as one of the major distributed generation sources particularly in the regions that have a high solar radiation, and the installations of PV grid-connected systems in many countries have been supported by utilities [7].

A distributed generation such Grid tied PV systems are installed to enhance the performance of the electrical networks also the PV production provides energy at the load side or to the distribution system. Despite of the many advantages of the photovoltaic systems associated with the distribution network, the PV integration with the grid can also impose several undesirable impacts, especially if their penetration level is high. The voltage level raises apparently under high PV penetration level due to reverse power of distribution generation to the electrical network [7, 8]. A traditional-technics used to mitigate this potential issue and regulating the voltage within the normal voltage range in the distribution system on load tap changer (OLTC) transformer and step voltage regulator (SVR). However, these voltage regulation technologies suffering from increasing work stress resulting in reduced system lifetime under high penetration PV applications.

The impact of PV integration is not only to the voltage profile of the distribution network but also due to the intermittency nature of this type of renewable energy source, current flow active, reactive and apparent power in addition to the current and voltage harmonics, grid islanding protection, and other power quality issues, the PV integration leads to some effects can be listed as follows, flicker and stress on distribution transformer [9, 10]. Moreover, Energy Storage System (ESS) integrated with a grid tied PV system also proposed to be mitigation criteria for the voltage raising issue in the distribution network. But instead of curtailment, the excess energy from PV can be redirected to the storage system for later use or injected back to the grid latter if necessary and this approach reduces the voltage rising and shaves the peak [8].

In addition, decentralized grid integration of the renewable energy systems improves the uncertainties associated with variability, location and coordination of available DG capacities. Implementation of PV embedded generation reduces the substation transformer losses in peak generation in general, but with low consumption the loss increases due to reverse power flow [11].

In this thesis, the performance and effects of using BESS with grid-tied PV system will be considered, for verification issue a real case study conducted and the outcome results will be compared with the IEEE standards. After collecting required data, the PV penetration level is going to be determined and enhanced by integrating BESS, four scenarios will conduct (i. electrical network alone ii. With PV only iii. with PV and BESS iv. with BESS only) using an Electrical Transient Analyzer Program (ETAP) modelling software.

2.2: Electrical Power system.

The electric grid contains an alternating current (AC), modern grid was sooner or later designed using Tesla's generators, transformers and other power system components. AC system proved to be more economically and practically efficient to transmit and use of electrical energy [12]. This design of the grid was established in 1888, which is still the same design and infrastructure up today. It has evolved since its initiation making use of better and more efficient and complex components. But the rapidly increasing on the energy demand leads the researchers to care about an advanced energy storage system, load management strategies and renewable resources. These are the main points of the future grid. This technology will help the electrical grid to shift towards a future smart grid.

Conventional electrical power systems are formed as main three stages, electrical power generation, transmission and distribution stage. Present production of electricity is clearly centralized and often a long distance away from its users approximately until now [13].

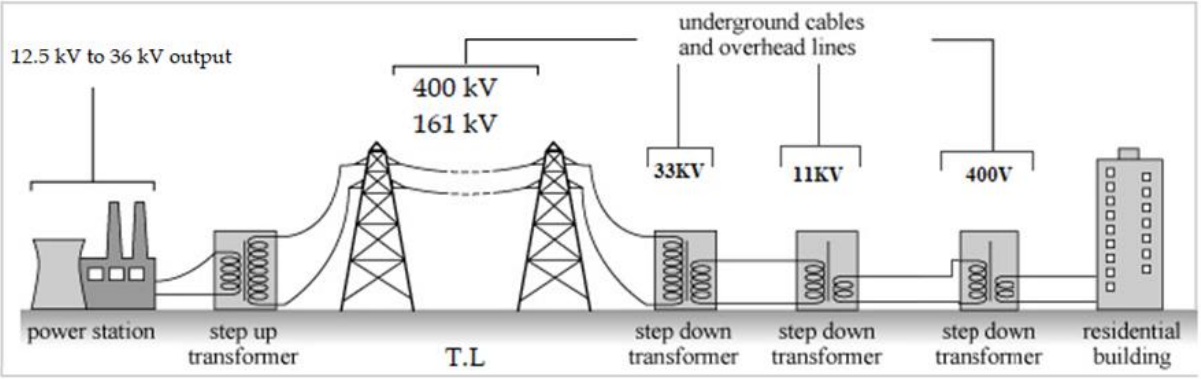

Figure 2.1: Conventional Electrical Power System

The conventional power systems can be characterised as:

- Central configuration of power generation.
- Ability to control the generation stage, but not loads.
- The generation pattern follows the load configuration.
- Limited grid access for new producers.
- One directionality power flow.
- Power system operation is primarily based on experience of operators and historical data.
- The detection of overloading in the power system is by the operators.
- Rerouting of power flow in the case of overload is performed by the operators.
- It's possible for an events of costly power blackout.

Traditionally power flow in the distribution power systems has always been a unidirectional from electrical power distribution grid to the loads of the user, the intelligent of the distributed energy sources is transforming the unidirectional distribution networks into bidirectional networks, where power can also flow in the reverse direction from the side of the load buses to the network. Bidirectional power flow has introduced new operational issues to the grid, one of them is voltage rise along the feeders when power flows toward the network [8].

2.3: Distributed Generation.

Distributed generation (DG) is an electric power source that tied directly with the distribution power system at the Medium voltage level or even the low voltage load side of the end users. Distributed energy resources can be any electrical production source either it is a renewable or non-renewable energy technologies [14].

Renewable distributed generators are the most commonly installed with the distribution system such a wind, solar, hydro or even geothermal. In addition, this type of DGs can advantage the environment if its usage reduces the amount of electrical energy that must be produced at centralized power plants, which result in reducing the environmental impacts of centralized generation. By using local energy sources, distributed generation reduces or eliminates the "line loss" that happens during transmission and distribution in the electricity delivery system [15, 16].

DG facilities offer potential advantages for improving the transmission of power. As they produce power locally for users, they assist the grid either by reducing demand during peak times, by minimizing crowding demand of power on the network, or by building large numbers of localized power generation which increase the flexibility of the distribution system. Moreover, DG technologies may improve the security of the grid. Decentralized power generation helps reducing the extreme demands condition that conventional power system facilitate. In addition, to reduce the transmission loss and improving the power quality of the power system [17].

DGs can contribute deferring transmission upgrades and growths at a time when investments in such facilities remain constrained. Which is may provide advantages in the form of more reliable power for industries that requires uninterrupted service [18]. For the environmentally wise DG is environmentally friendly particularly when it is renewable energy sources.

On the other hand, DG had some draw backs that appear after integration with the grid especially when it is renewable source, such as initial investment amount is often larger than for nonrenewable source and it's needs a specific requirement of the site for power generation. Furthermore, the unpredictability production of renewable systems also means a higher cost for balancing the electricity grid and maintaining reserve capacity [19].

Contrasting of the conventional distribution system, distributed energy systems deliver power from a number of sources to a great number of loads, consequently the uncontrollable number of generators tied to the distribution network some technical issues including power quality problems will arise [20]. But the question is how DG changing the Grid? And the answer depends on the rating of the DG and on the power system itself. the problems are complex and have many related aspects that have to be studied thoroughly.

2.4: PV system technology.

The main component of the photovoltaic system is the PV modules which are consisted of discrete cells integrated together in the purpose of convert the sun radiation into an electrical energy. It's worth mentioning that PV cells produce direct-current (DC), however the electricity supplied by the electric distribution system which used by industrial and residential end-users is AC electricity, means that this energy produced should be converted from DC to AC using Power Conditioning Unit (PCU) which known as inverter. Usually, an additional power conditioning circuits may be required if the solar panel is connected to the electric grid [21].

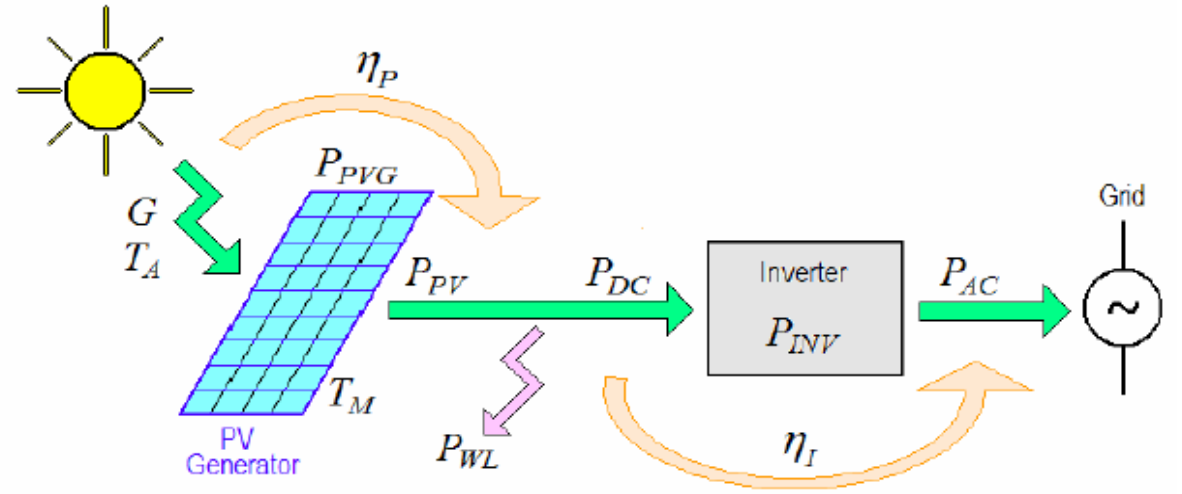

Figure 2.2: PV system power conversion chain.

The classifications of Photovoltaic systems regarding to their ratings was categorized into three different groups, small systems rated at 10kW and less, intermediate PV systems rated 10kW to 500kW, and large PV systems rated above 500kW. In a distribution system the first two categories are dominant to install but the last category is usually installed on the transmission system as a main power generation plant[22]. Moreover, the PV system configurations can be listed as follows:

2.4.1: PV system configuration

1- Stand-alone system:

The main feature of this type is the independence of the systems fig 2.3 illustrates the schematic diagram of the Stand-Alone System. Which has the following Specifications [23]:

- Operate autonomously, independent of utility grid operation.
- In all cases the energy storage system is needed, typically usage energy storage is batteries.
- backup source may be integrated to form a hybrid system use engine generator.
- The components number in the system is much higher and the system complexity too.

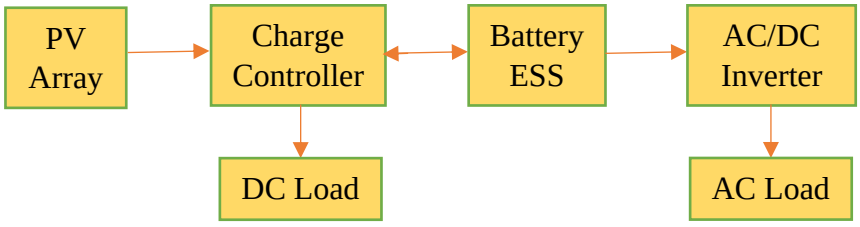

Figure 2.3: Stand Alone PV System block diagram.

2- Grid tie PV System

Grid connected PV system is a type of PV configurations which is dependent sharply on the operation of the grid itself, fig 2.4 illustrates the configuration of the system, which has the following Specifications [24]:

- PV system stands as an on-site energy usage, leading to make an electrical loads supplied by either the PV system or utility or a combination of both, depending on the PV production value and magnitude of the load.
- Grid connected PV system can be combined as PV array is directly connected to the inverter, and the inverter AC output connected to the utility grid and loads in parallel.
- PV system operates in parallel and it must be synchronized with the electrical grid.

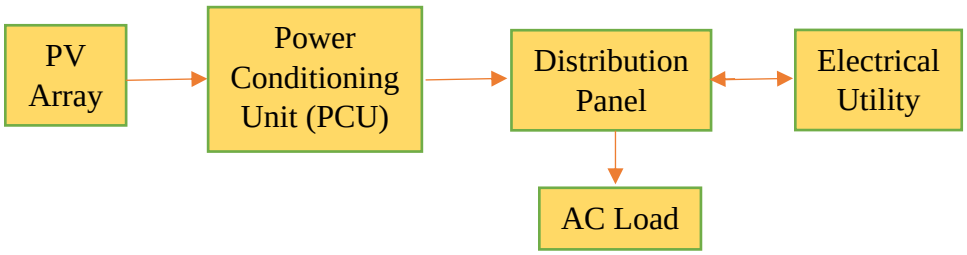

Figure 2.4: Grid-tie PV System block diagram.

3- *Utility Interactive PV System with Battery ESS.*

Grid connected PV system covering it's shortage of energy demand totally by the grid power and the stand-alone system using BESS as a back-up source, in this type of PV configuration, the two benefits of these connections are used and fig 2.5 illustrates the configuration of the system, which has the following Specifications [23]:

- PV, inverter, Charger/inverter and battery energy storage system interface between the customer's load and main service low voltage bus, and Can operate either in grid-tie or stand-alone mode but not simultaneously, it depends on the daily load profile.
- In grid interconnected mode, excess energy that produced by PV and not required for battery charging nor load, it sent back to utility.
- When the grid de-energizes, inverter and charger/inverter will be isolated from grid and loads, and this case will be the worst because of the lost energy from two sources PV and BESS. At the moment that islanding operation mode occurs through a day time the PV produce energy to charge the BESS, but if it occurs at night time "no PV production" the BESS can't cover the load alone so it must be islanded totally.
- In advanced control mode and in Islanding mode from the grid a load emergency distribution board can be founded and it should not exceed the BESS capacity to use the BESS for continuing feeding a critical demanding need.
- One of the main goals of interacting the BESS and grid tied-PV system is to make a demand side management at the load side, and shaving the peak concentrated load at midday time.

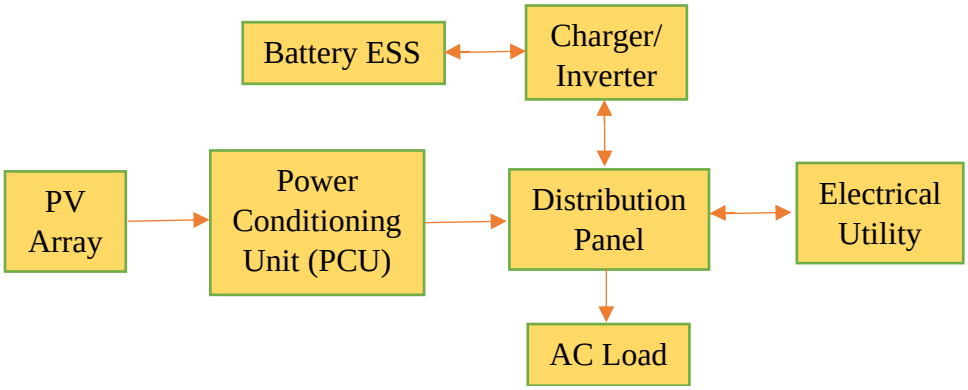

Figure 2.5: PV integrated Utility Interactive PV System with Battery ESS.

2.5: PV as distributed Generation.

Photovoltaic system is one of the possible forms of solar energy directly conversion into electricity which occurs in a semiconductor known as photovoltaic cells. Solar energy conversion occurring in these photovoltaic cells by absorption of the photons to generate an electron–hole pair. Then the electrons and holes are separated by the apparatus structure, electrons on the negative terminal and holes on the positive terminal, generating a voltage difference, hence, electricity [12]. When photovoltaic cells are assembled together in panels, they give origin to the photovoltaic module, utilized in solar generation systems.

Distributed photovoltaic systems tied to the grid by different installation approach, the produced power from the PV-DG either feeding energy to a specific consumer or directly connected with grid feeder. According to Hoff et al in [25], the benefits of solar distributed generation include increasing reliability of the power systems, increase in generation capacity, avoiding costs of transmission and distribution, reduction in losses in transformers substation and transmission lines, possibility to control reactive power and the fact that they are environmentally friendly generator. Furthermore, Olga et al in [14] illustrates the solar energy is sustainable and widely available, it has minimal environmental impacts and the environmental benefits can be measured in terms of greenhouse gas emissions.

According to the benefits of PV-DG consist of the peak load shaving, the closeness of PV systems to the load, and the peak solar radiation which means peak electricity generation from the PV, that almost at the same time, so large PV generation systems can take share of the peak load with the grid demanding and reducing transmission losses. If the peak load occurs during sunlight hours then the PV systems will have an effect in reducing this peak demand and thus assist the utility operation to be more efficient [23, 24].

Grid connected distributed photovoltaic systems increasing reliability of the systems but this configuration of the PV connection suffering from islanding mode of operation which is the protection technique of the grid connected inverters activated when grid missing even in the fault cases or for the maintenance issues [14]. Fig 2.6 illustrates the PV production in different conditions.

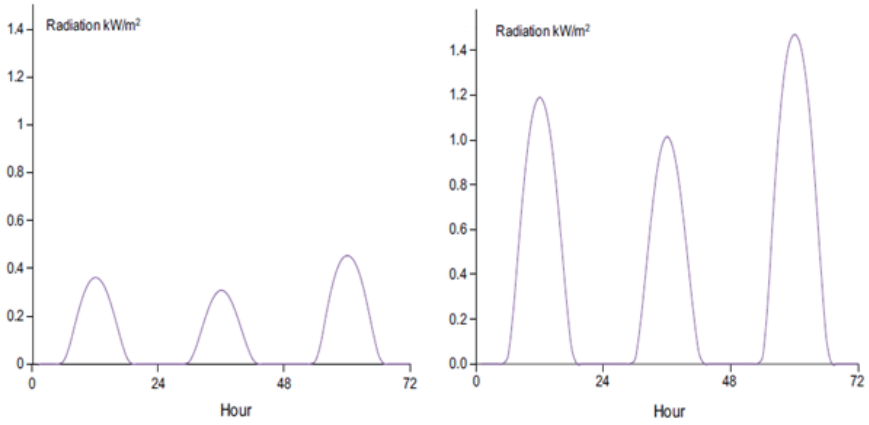

Figure 2.6: hourly PV system production with varying solar radiation [14].

Another important issue for a grid-tied PV is electrical power quality issue. Power quality involves voltage, frequency and waveforms in power system. The power systems are designed to operate at a sinusoidal voltage of a given voltage and frequency with a prescribed range. Any significant change in the voltage magnitude, frequency, and purity of the waveform is considered as power quality problem. Changing in solar radiation will produce a variation in operating point of solar cell, which mean variation in operating voltage and current. As the power supply system can only control the voltage but not the currents, therefore the important mission in this case is to maintain the voltage operation range within an acceptable limit to ensure the power quality is maintained, and not affected by the PV generators connected to distribution networks [26].

In case of multi PV system as distributed generation in high concentration, in the instant of the power production exceeds the immediate power consumption. As a result, the imbalance in power produces a net power flow returns through the MV network from LV transformers sides, so it is important to determine the limit of penetration level of PV that can be fed into a power network without causing problem to the power system. It is important to distinguish how to identify these limits, and what the possibilities of maximizing them [28].

Harmonics produced by distributed energy systems is another important issue that should be concerned. Solar PV systems generate DC, therefore the need of usage a power conditioning unit to match with the electrical grid. These inverters contain a power electronic component which produce harmonic currents. In recent years the inverter topologies has improved significantly and as a result of this improvement, the level of harmonics produced by inverters has decreased unusually [28].

2.6: Integration Issues of PV-DG system.

Due to the intermittency production of the PV-DG and regarding to the conditions around the PV with significant variation such a radiation, temperature, shadowing and limited time to provide electricity during a day, some technical issues appears in distribution system. However, the stability of the distribution network depends on the voltage and the frequency. If there is a significant rise or fall in the value of voltage or the frequency, the system will be unstable and that will influence the quality of supply to the end user leading to serious problems, there are many other issues and these issues will be discussed in this section.

2.6.1: Voltage Levels and Fluctuation Consideration.

High penetrations of PV can impact network voltage as a voltage rise or variations caused by fluctuations in solar PV generation. These effects are particularly pronounced when large amounts of solar PV are installed near the less loaded feeders [29]. Also, voltage quality can be affected by the intermittency of PV power output in distribution system [30]. In general, PV-DG generation type which affected by the climate changes, it can create irradiance fluctuations either for a short or long period of time. Therefore, this can affect the voltage output of PV in Point of Common Coupling (PCC).

The rising voltage phenomena can be observed as follows, when the PV system integrated with the distribution power system near the load with high PV penetration there is a reverse voltage flow, which leads to reduce the voltage drop due to the losses along the distribution feeders. As the output voltage of the grid connected PV system limited to the rated distributed grid voltage, so the output PV voltage is higher than the received voltage to the load. As a result, fig. 2.7 illustrates the reverse voltage phenomena [31].

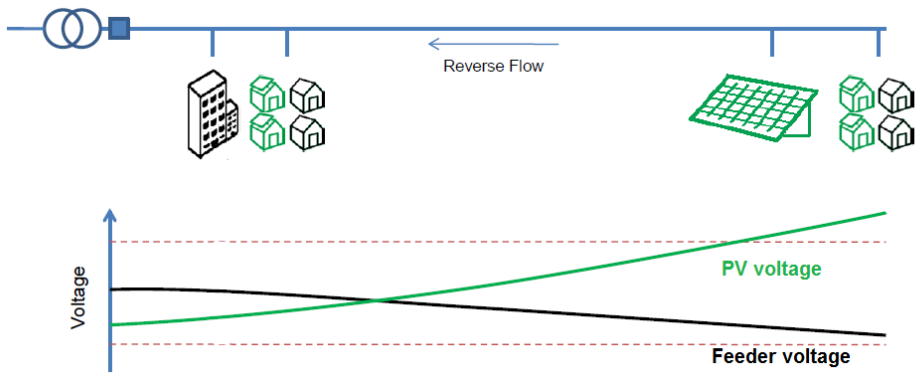

Figure 2.7: Reverse power flow, PV and feeder voltage profile [31].

The voltage problem of distribution system that has been come with PV can be characterized as voltage rise, voltage unbalance and flickers in the network. Fig. 2.8 shows the voltage profile on the medium voltage (MV) feeder during light load and the maximum nominal load conditions, with and without PV integration power [32]. Means that the installing PV systems have already increasing voltage levels which can cause over voltages in the load side particularly at light loads and enhancing the voltage drop at critical high loading [33].

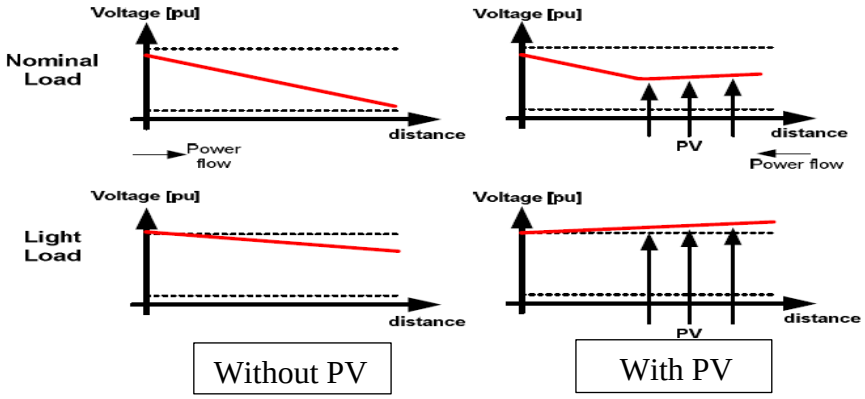

Figure 2.8: Typical voltage profile in a MV feeder with and without PV inverter [29]

2.6.2: Active and Reactive Power

Photovoltaic system inverters normally operate at unity power factor to prevent the inverters to operate in the voltage regulation mode, and the metering system of small domestic PV systems in the incentive programs are revenue only for kw.h yield, not for k-ampere hour production. So, it is better that the inverters operate at unity power factor to enhance the active power produced and accordingly their return. As a result, the active power requirements of existing loads are partially met by PV systems, reducing the active power supply from the electrical network [32].

The active power losses reduction attractions more attention form the electrical network operators, since it reduces the efficiency of the power that transmitted to customers. However, reactive power losses are not less important, due to the fact that reactive power flow in the system should be maintained at a specific amount for appropriate voltage level. Thus, reactive power makes it possible to transfer active power through transmission lines to customers [34]. However, the losses can be reduced by an optimal placement of DG along the electric feeder, it can be very useful if the decision maker is committed to reduce losses and to enhance network performance by maintaining the investments in DGs field to a sensible level [35].

2.6.3: Power Factor

The relationship between active and reactive power is represented by fig. 2.9, therefore the vector summation of active and reactive power is called apparent power, which magnitude is the length of the hypotenuse and its common unit of measure is the kilovolt- ampere (kVA). cosine of the angle φ represents power factor (PF) at the fundamental power line [36].

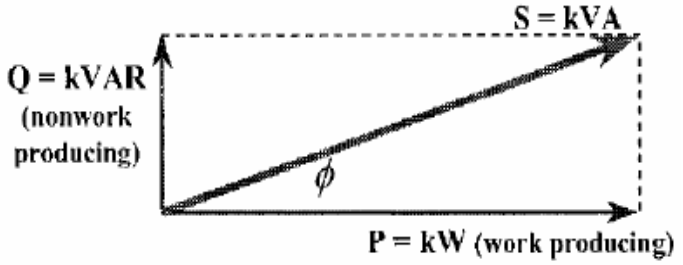

Figure 2.9: Power triangle with PF calculation.

The ideal power factor is unity PF means when the reactive power is disappeared and apparent and active power identically, but in real cases power factor values should be always above 0.85 and only fall below this number at high level of load. It's worth mentioning that PV-DG produce an active power with unity PF at the load side which leads to decrease the active power that drown from the network with the same reactive power, at that point the PF decreases to unacceptable levels during the peak operation of PV system. When PV power plant works with high penetration level, most active power demanded by the customers is supplied by the PV plant [37]. Fig. 2.10,11 represent the ac power profile along a day before and after of integration the PV-DG.

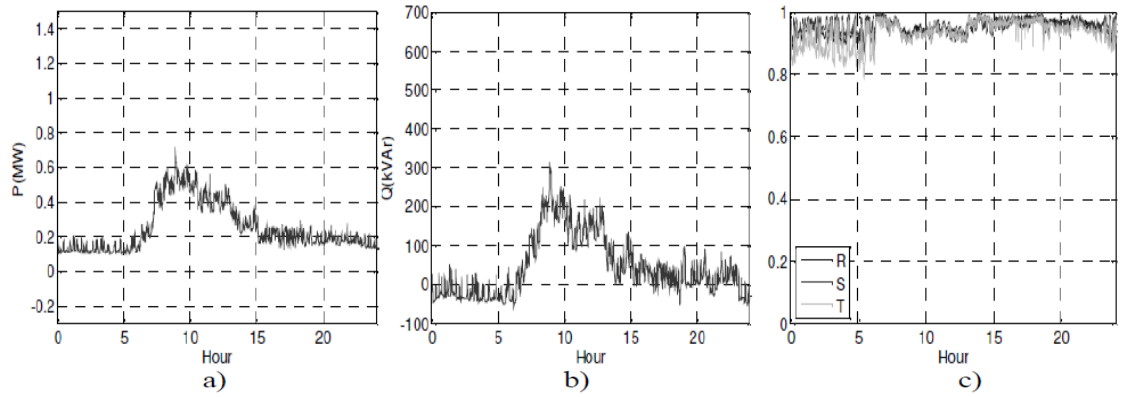

Figure 2.10: Power profile without PV-DG along 24 hours. a) Active power, b) Reactive power, c) Power factor [38].

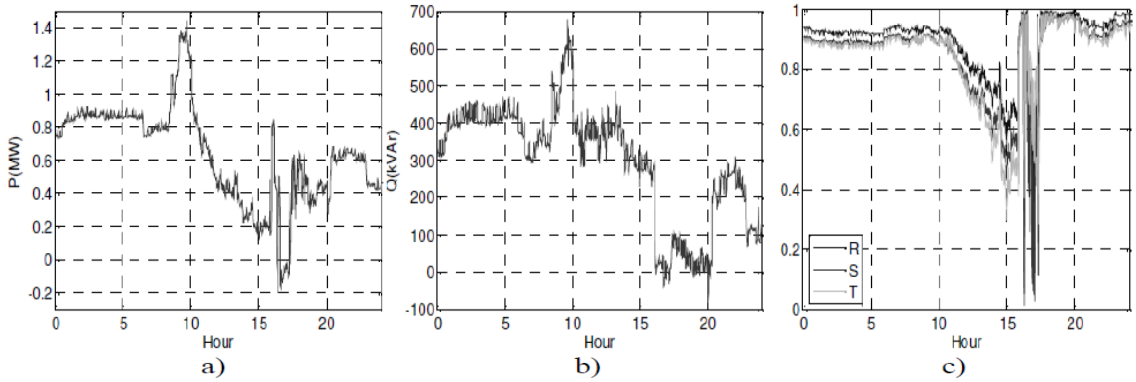

Figure 2.11: Power profile with PV-DG along 24 hours. a) Active power, b) Reactive power, c) Power factor [38].

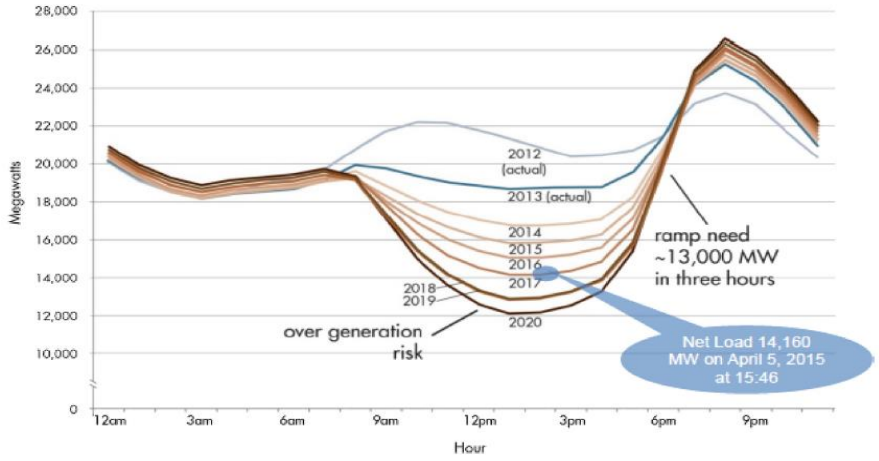

Figure 2.12: Active power profile with PV-DG along 24 hours [39].

2.6.4: Power Losses

DGs produce electrical power at the distribution power system phase means that the electrical consumption from the grid decreases because of the amount of energy that will be supplied by the DG system. Therefore, one of the main purposes of installing DG on a distribution system is to reduce power losses on the power system and it represent that DG bring the generation near the loads, and this claim is true until the reverse power flow occurs in the power system [40].

One of the problems in power systems that can be solved by the installation of DG is the power losses along the transmission conductors, in this study DG stands for reducing the power losses in the transmission lines and the power system components. The literature shows simulation results from specific case studies on the IEEE 33 bus standard system which illustrates that the power system losses was decreased from 5.78 MW to 1.58 MW or just 27.3% [41]. The methodology of loss reduction relay on the increase of using DG by strategic location and capacity. On the other hand, the Simulation indicates that the grid losses are related to the amounts and locations of the grid-tied PV systems. As the amount of PVs capacity increases, the variation of the grid losses reduces first and then increases.

2.6.5: Current Swing Issue Consideration

A current swings issue occurs at the instant that the PV power conditioning unit (PCU) disconnected from the power system. The current swings have impacts on the consumer and on the distribution network also. Switching off in periods of potential high generation impacts on the customers production and can possibly leave the utility liable for the damages incurred if the voltage is outside of acceptable limits.

At the distribution power networks level the current swings value can be measured at the secondary terminal of the transformer when there is a high PV penetration integrated with the network. And then this value compared to the current at the secondary terminal when none of the systems are generating. Thus, the net current swing is calculated by taking the generating current away from the non-generating current. As a result, when the current measured at different penetration levels of generation and compare them to the current without PV generation, it can be found that the current swings are increased as the penetration levels increase [42].

Current Swing phenomena happened at the moment when PV systems inverters are disconnected from the power system, this parameter is taking into consideration because of the protection equipment requirements of the inverters. However, the main issue associated with current swings is switching surges and it’s such appearance could affect the voltage stability of the system and possibly cause faults. As well, the current swings occurrence would be unpredictable as they are factor of dynamic generation and individual feeder demand levels [43].

2.6.6: Harmonics component and THD Consideration

The harmonics denote to the quality of the sinusoidal wave of both current and voltage. Harmonics occur at multiples of the fundamental frequency that produces by the switching power electronics devices and nonlinear loads, in the PV-DG the inverter converting the DC power from the PV to AC power which injects harmonics with different levels, it depends on the quality of that device which sometimes seem to be in acceptable range. However, when the number of harmonics component increase some issues occur in the distribution grid which is near the user [42, 43].

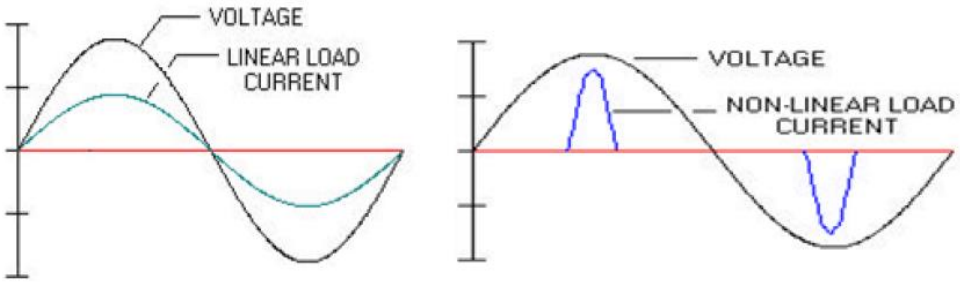

Figure 2.13: Voltage and Current waveform for linear and nonlinear loads [44].

Harmonics in the grid can be either on the voltage waveform or on the current waveform. Harmonics on the voltage waveform have more potential to cause damage on the network. But the harmonics are mainly negated due to harmonic filters on the output of the inverters, which can actually assist the network in absorbing harmful harmonics. However, many older style inverters have poor harmonic filtering and can contribute significant harmonics to the network [45].

Current harmonics are caused by inverters as they try to synchronize their output voltage with the system voltage. The inverters may need to supply extra current to certain parts of the waveform to make the voltages synchronized, thus introducing current harmonics. Then the voltage harmonics will be formed too, in addition to extra system losses in power system equipment like transformers. However, when similar converters are connected to the same feeder, they have the potential to make the harmonics on the feeder quite large, therefore a triple harmonic also causes excess current to flow in the system neutral wire which may be significantly underrated for this current to be flowing. This can cause damage to the network and will certainly result in extra system losses [46].

The existence of harmonic compensates in electrical power system can be rising some problems such as equipment overheating, reduced PFs, deteriorating performance of power system equipment and incorrect operation of protective relays. Moreover, the harmonics can be indicated by Total Harmonic Distortion (THD) or Individual Harmonic Distortion (IHD) [47].

- Total Harmonic Distortion (THD):

THD, also known as Harmonic Distortion Factor (HDF), is an important index that measures the level of harmonic distortion to voltage and current in electrical systems. It can be calculated as the ratio of the mean square root of all harmonics to the fundamental component. For an ideal system, THD is equal to zero. THD represented mathematically by:

$$THD = \frac{\sum_2^\infty {F_i}^2}{F_1} \quad (2.1)$$

Where, F_i is the amplitude of the i^{th} harmonics, and F_1 stands for the fundamental component.

- Individual Harmonic Distortion (IHD):

Individual Harmonic Distortion can be represented by the ratio of a given harmonic component to the fundamental one. This value is sometimes used to indicate the effect of each individual harmonic and examine its magnitude. IHD represented mathematically by:

$$IHD = \frac{F_i}{F_1} \quad (2.2)$$

Where F_i is the amplitude of the i^{th} harmonics, and F_1 stands for the fundamental component.

2.6.7: Protection and short circuit issue Consideration

Islanding protection technique which is the ability of DG inverter to isolate itself from the power system automatically when the centralized power plant is shut down and the grid voltage is maintained by the distributed generation connected to it, this scenario forming a first critical point in the protection system for the DG. Secondly when a short circuit fault occurs in the distribution network and the DG integrated with the power system, a large current will be generated. This current then will activate the protection devices and the short circuit will be isolated, to prevent any more damage to people or equipment in power system [48].

The connection of distributed generation (DG) to the electricity distribution networks has rehabilitated the traditional configuration unidirectional power flow and the short circuit capacity level. In some occasions, DG may also have extreme significant impact on the network short circuit level, in which may limit the connection of the DG to the network. However, the impact of PV penetration at a large scale into the electricity distribution networks, therefore a present of DG as a PV at the distribution system the short circuit capacity will be increased due to the existing of additional power source to the system, means that the highest fault current value which is a 3-phase to ground fault will be much higher than the nominal value without DG [49].

Based on the examination by Afifi et al in [49], the 3-phase to ground short circuit fault was tested for the IEEE-13 bus testing feeder in four different scenarios the first one is without PV-DG integration, the second and third were integration a 3 MW PV system on the bus 632 and bus 675 respectively, and final scenario was divided the PV system into two sub systems as follow 2x1.5MW PV arrays placed at buses 632 and 671. Fig 8 illustrates the results, that the fault current was increased by 2% after adding the PV-DG.

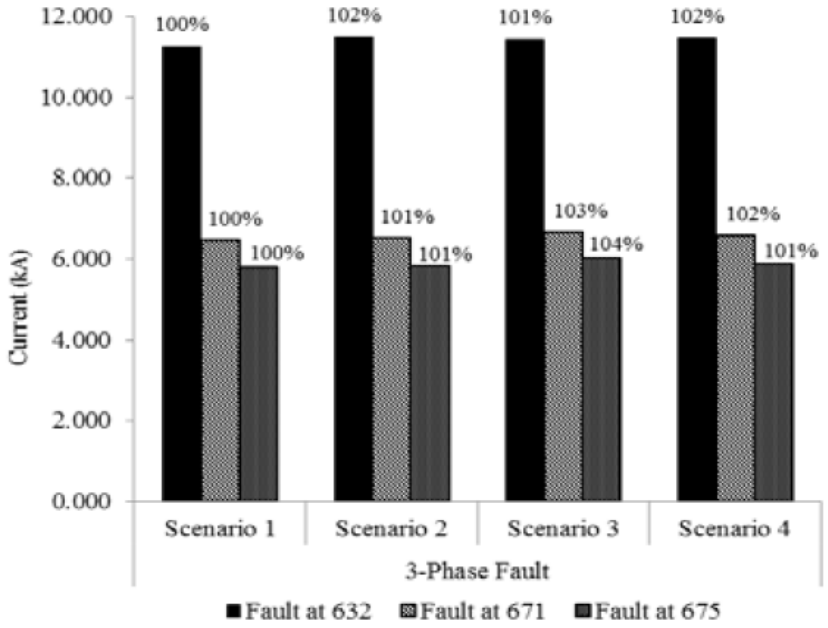

Figure 2.14: Short circuit currents in different scenarios for 3-Phase Faults [49].

2.7: PV Penetration levels on a distribution network.

Integrating the grid-tied PV systems to the electrical power system is recommended to assist and enhance the grid performance and the self-electricity generation and exploiting the available renewable energy sources, especially the solar energy in electricity generation. In the other hand, installing the PV systems must be constrained under certain conditions and standards to avoid the effect which could be happened if a large amount of these systems is installed to the grid.

The "PV penetration" of a power system is defined as the rated PV peak power produced by the grid-tie PV system connected with the distribution network divided by the peak load as an apparent power value. However, the penetration level in a distribution network differs from network parameters to another due to the differences in quality of the distribution network itself, the variation of peak demand and the network ability to withstand with this penetration level [50].

$$PV\ Penetration\ level\ (\%) = \frac{PV_{Peak\ power}}{Peak\ load_{(apparent\ power)}} \times 100\% \qquad (2.3)$$

The "PV hosting capacity" which is the maximum PV penetration at which no technical or legal constraints in the grid are violated. And based on the European standard EN-50160 which determines that a 3-5% overvoltage of a week is acceptable. Additionally, the PV system feed the grid with only a real power which will be affected on the PF at the PCC. Therefor the maximum allowed PV penetration level can be controlled regarding to the voltage and current limitation to the grid and the PF at PCC and then the other parameters such as the fluctuation, reverse power flow …etc, will come next and should be observed for each case separately [51].

As the PV penetration in distribution feeders increased, the power generation from PV systems will be increased too, at that point there is some negative impact appear in the distribution system operation, this section will focus on the most important phenomena and try to propose an optimal solution for each. However, power quality problems such a reverse power flow or voltage increases may occur because the increasing of active power feeding on the network, which leads to difficulties in any additional power generation plant connection [52].

The voltage variation problem can be seen within the whole grid levels, particularly in the distribution system the voltage level variations are relatively variable in distribution networks which is caused according to load variations, meanwhile to avoid voltage variations that exceeds the acceptable limits, many different regulation techniques are used depending on the network characteristics such as an automatic or manual tap changer transformers and voltage regulators at MV level. The importance of the regulation techniques is to guarantee the power quality requirements that should be supplied to consumers by distribution system operators [53].

2.7.1: Reverse Power flow

The reverse power flow phenomenon is another main effect of the high PV penetration level on the distribution feeders. In general, the power flow is usually unidirectional from the medium voltage system to the low voltage system. However, with a high PV penetration level the net energy production of the feeder is much higher than the energy demanded, especially at noon. And as a result, the direction of power flow is reversed as shown in fig 2.15, this reversing of power flow will cause an overloading of the distribution feeders and excessive power losses in addition to effect on the operation of automatic voltage regulators installed along distribution feeders [54].

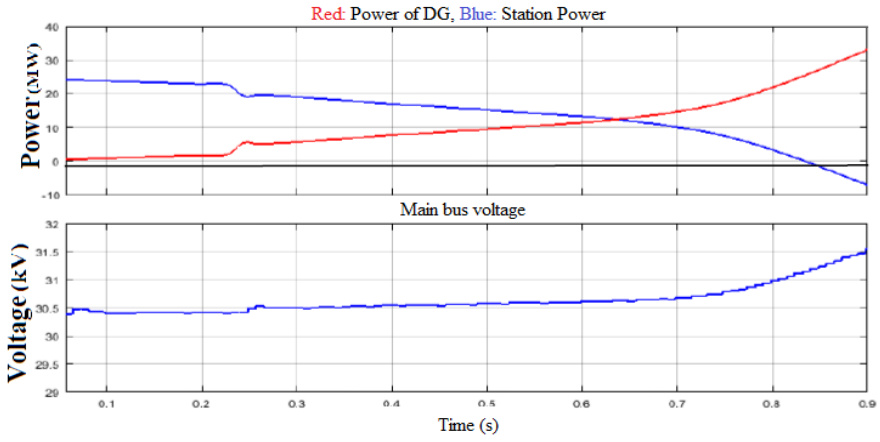

Figure 2.15: Reverse power flow effect and over voltage.

To perform active power regulation in grid integrated PV power plant, three approaches have been proposed [55]:

1. Using an ESS while maintaining the PV power plant operation point at the maximum power point.
2. Using a damp load banks to consume an excess energy production that produced by PV plant.
3. Change the strategy of the converter control to moderate the power extracted from the PV.

The reverse power flow can cause many draw backs of the distribution system as follows overvoltage on the distribution feeder, increasing short-circuit currents, in correct operation of control equipment and protection desensitization and potential breach of protection coordination. As a result, a reverse power flow direction relay was proposed to use in a large PV plant to prevent the reverse power flow occurrence in high voltage level as fig. 2.16 illustrates.

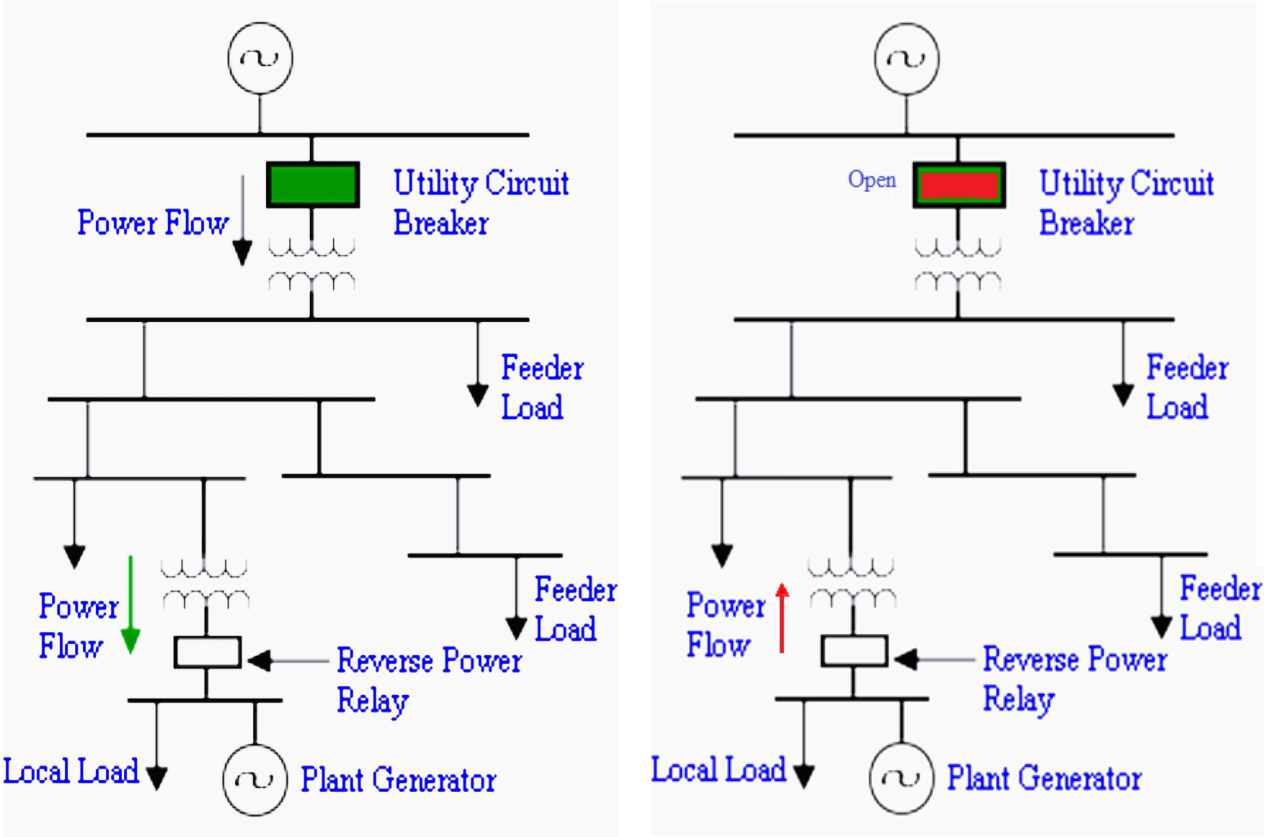

Figure 2.16: Reverse power flow relay operation configuration [54].

2.7.2: Enhancement of PV penetration level.

Regarding to the rabidly increasing of the PV penetration level on the distribution power system due to the development of this technology. Meanwhile the researchers are focusing on how to maximize the penetration level on the grid from this environmentally friendly technology, and how facilitate the integration of PV systems in the local distribution grid. Therefor Bucher et al in [56] raising a different method about how to maximize the PV hosting capacity of a grid. And it can be summarized as follows.

- Energy storage systems (ESS).
- Demand Side Management (DSM).
- Active Power Curtailment (APC) approach.
- Reactive Power Control (RPC) approach.
- Low voltage grid reinforcement.
- Different orientations such an (east-west oriented system) of PV systems.
- On Load Tap Change Transformer (OLTC).

Based on the up mentioned methods for enhancing the penetration level, DSM method mentioned with low potential specially with grid scale. APC is always a selected to mitigate problems in local distribution grids caused by PV. But it causes a losing of production during the hours with highest irradiation. The potential of RPC raises as a solution but not in grids where the lines are already heavily loaded. Different orientations of PV panels such east-west that help to lower the peak production during noon. However, the yearly PV electricity production is also reduced significantly. OLTC can solve the voltage problem only by reducing the overvoltage in the grid during peak hours. The use of ESS to integrate additional PV generation is studied in detail in this thesis. If all of the before mentioned methods are not sufficient to enhance the penetration level of DG to desired amount the best solution will be reinforcement the grid [57].

2.8: Energy Storage System (ESS).

In the electric power system, the generation must be equal to the demanding at every instant of time to keep the frequency constant. Nonetheless, with a high production of intermittent energy sources like PV system the task of keeping the system stable will become hard particularly at high penetration level of generation at the distribution stage [58].

Storing electrical energy in the Energy storage systems have many different technologies; they may come such as a mechanical, chemical and thermal. These forms of energy storage systems have been explored in [28], which dividing the energy storage technologies into two main categories:

- Low and medium power application scale which normally used in isolated areas. These two categories are preferred to be used where the energy stored as kinetic energy, compressed air, hydrogen, or even in super-capacitors type.
- Large scale power applications which used when the energy could be stored as potential energy, thermal energy, or chemical energy such a battery storage.

In addition, Storage technologies are characterized by several factors such as: storage capacity, available power, depth of discharge, discharge time, efficiency, durability (cycling capacity), self-discharge, mass and volume densities of energy, reliability, environmental aspect and other characteristics.

Fig. 2.17 illustrates the technical options for electrical energy storage technologies, as sited by [59] the compressed air energy storage and batteries would be an alternatives choice to pumped hydro. And that was refers to the energy conversion efficiency of pumped hydro which is 81% at max, but Batteries have an efficiency reach up to 85 %, however, the efficiency of compressed air energy storage is much lower (40% - 50 %) if no heat storage is used.

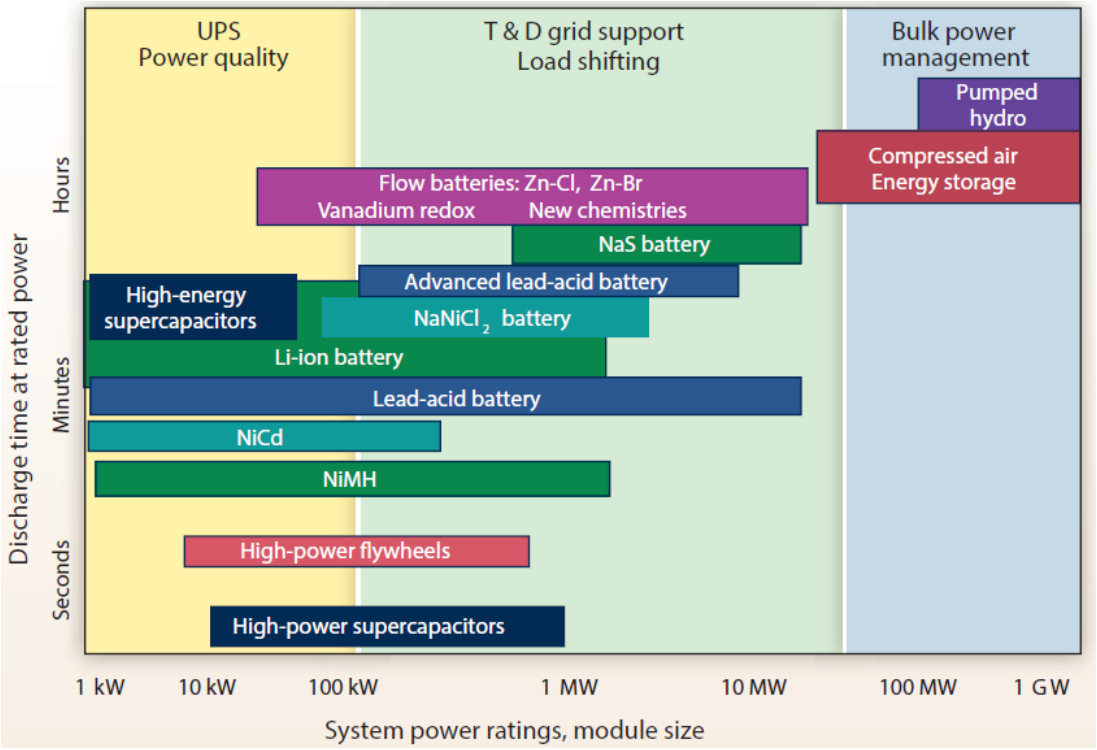

Figure 2.17: Different storage technologies for electrical energy [59].

Battery Energy Storage System (BESS) has a high efficiency ESS and in the intermediate rated power capacity which leads to make BESS is preferable for integration with the distribution generation systems. Fig. 2.18 illustrates that Lithium Ion (Li-Ion) batteries have the highest battery efficiency that what makes Binder et al in [60] to use it as an energy storage system but the main drawback of this type of batteries is the energy capacity until now for Li-Ion batteries can't be used in large scale in spite of its perfect efficiency. For this reason [14] support using Sodium–sulphide (NaS) batteries it has high capacity and acceptable efficiency range. Moreover, this battery system has developed for application in electrical power systems.

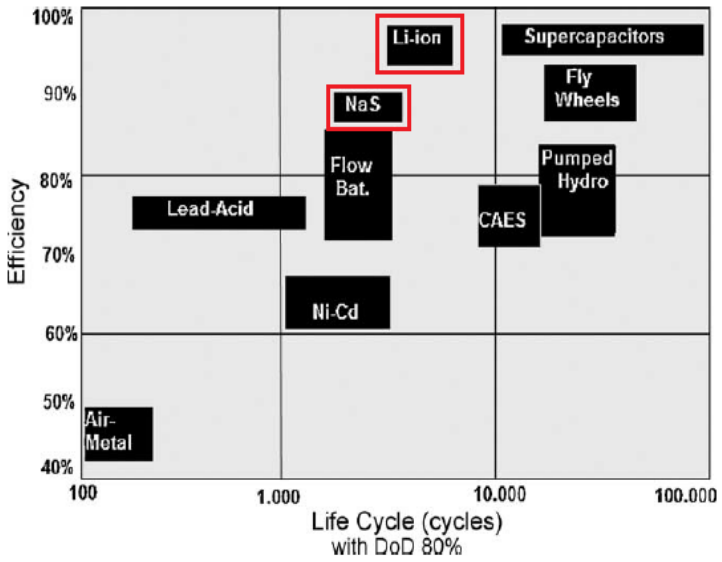

Figure 2.18: Battery efficiency and battery capacity based on its kind.

For a PV system operation point of view the Energy storage system can increase performance ratio of the PV system. ESS helps to reduce power injection to the grid during the peak times. Grid-integration of solar PV supported in reference [60] used to be a battery banks. But according to Zahedi et al in [28] PV panel is supported by a super capacitor and battery which is more efficient in technical point of view but the super capacitors still having some limits and less economical profitability as a large storage system. In this thesis, energy storage system as battery bank is proposed to integrate with grid connected photovoltaic system to reduce the PV impact and getting a backup source of the system.

2.9: Battery Energy Storage System (BESS) integrated with PV-DG.

There are many aims for integrating the DG with the electrical grid, such as reducing the transmission losses and the drop voltage at the end of the feeders. In contrast, the high penetration of intermittent source from renewable energy and increasing of the DG numbers at the same feeder may produce instability on the power system. A solution to this problem is the installation of energy storage systems (ESS) in the distribution grids. And in this thesis the BESS will be supported.

Battery energy storage system has shown potentials to mitigate the voltage rise issue in distribution networks especially at high PV penetration level [20]. Instead of restriction the surplus energy from PV, it can be redirected to the BESS, and it can be either self-consumed or injected back to the grid at a later time when necessary. This technique not only mitigates overvoltage, but also saves a considerable amount of energy, and shifting the peak generation to the later uses [61].

The voltage raises phenomena in the distribution network by the PV-DG is occur as a result of high level of PV generation. However, maximum tolerable PV feeding with the grid without violating voltage limits can determined regarding to the rating of cables or transformers and the distribution network itself. This limit of PV integration with the grid also known as “PV hosting capacity of a grid”. As in the case of high load peaks, batteries can be used to mitigate the effects of high PV generation, in addition to increase the hosting capacity to the electrical grid. In this case the battery is charged during peak PV feed-in and discharged in times of low PV generation and at night. The most critical time of the year is usually on weekends in summer [26].

The variable nature of power generation from intermittent sources such as solar PV systems is another drawback of the grid connected PV systems. As a result of this conditions, providing a reliable power supply is the solution. Integration of an energy storage technology causes the intermittent power sources have little effect on the power system operation. The important of using energy storage technology to enhance the performance of the grid and to maintain the continuity of the source in different radiation cases as shown in [60], in addition to that it supports a Li-Ion Batteries as a storage system, on the other hand the impact of PV system and the losses of the system in Islanding mode are reduced.

Moreover, the intermittent nature of power supplied from the PV generation and the voltage fluctuation phenomena make the BESS an essential component to keep the power balance between generation and consumption. Energy storage system and loads are able to operate either in grid-connected or islanded mode, with possibility of continuous power flow between them. In islanded mode the BESS unit is usually operates to feed as a grid forming unit that regulates ac bus, while the PV systems work as grid feeding units that inject all available power into the system [20]. But the amount of the required consumption when the PV and ESS connected to the grid is the main challenge of this case [14], to solve partially this problem an urgent loads separated from the system and it can be feeding by the PV integrated BESS.

However, the charging and discharging power cannot be calibrated to the power fluctuations without time delay so that an exact temporal mismatch between the BESS power and the excess power "PV production minus load demand" occurs under dynamic conditions. Reference [11] presents a mismatch loss amount of grid-integrated PV-BESS systems with response time-induced. It's worth mentioning that longer response times are accomplished by an increase in the grid feed-in and grid supply as well.

In addition, decentralized grid is integration of the renewable energy systems improves the uncertainties associated with variability, location and coordination of available DG capacities. Implementation of PV embedded generation reduces the substation transformer loss in peak generation in general, but with low consumption the loss increases due to reverse power flow, thus the distribution companies tariffs the surplus energy of the DG [11]. Which is justifying the 25% of the surplus energy from PV system production are taxes by the distribution companies.

From the PV system owner point of view these systems tried to minimize the "electricity bill" or, quite interchangeably, to maximize the PV system yield, although voltage regulation is not the primary objective of an PV system owner. However, under current utility practice, when overvoltage occurs due to high PV penetration in the distribution power system, PV shuts off which means a loss of revenue. Therefore, to avoid this problem and to maximize the ability of the grid to accept much higher penetration level an Energy Storage System (ESS) proposed to enhance the system voltage stability and shaving the peak generation from the PV system [62].

When the PV power rating is only a fraction of the generator ratings, the PV and generator will supply the total amount of power needed by demand loads. In a case of high PV generation and minimum load demand the energy storage system is start charging for the case of high demand and low generation without voltage rising on the feeder. This system can also be integrated such that the PV supplies all the power required by the loads connected to the bus, in such design the PV system will exclusively supply its rated power during the day, At night when the PV system is not supplying power, automatically, the required energy will be covered by energy storage system or it divided the demanding load among the grid and ESS for optimum economic dispatch.

According to Fig. 2.19, the aim of integrating BESS with the PV-DG is not only for mitigate all adverse effects of grid-tied PV systems with the distribution system. Therefore, the usage of BESS which integrated with PV grid tied can be classified according to the output energy duration of the BESS. In this thesis, the BESS is aiming to solve the overvoltage issue, the power fluctuation and power loss when a high penetration level of PV is connected with the distribution feeders.

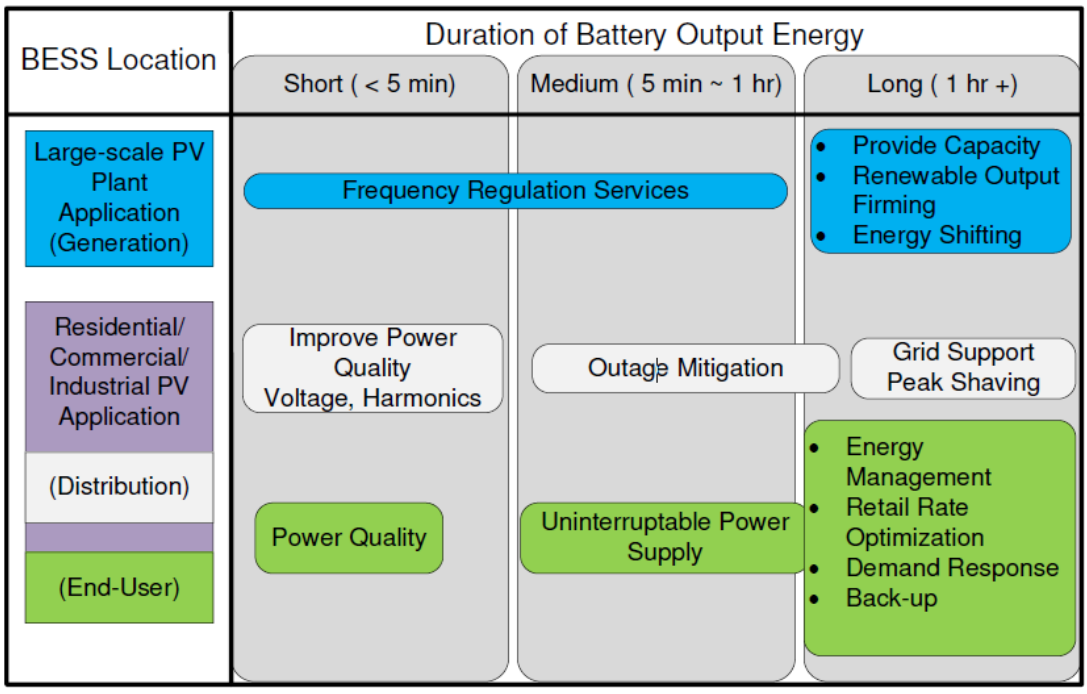

Figure 2. 19: BESS functions for PV applications [63].

For maximizing the PV penetration, a battery energy storage system will be tied to the system at optimum location. The BESS can be integrated with PV system for enhancement of penetration level as the BESS storing a real power that produced by the PVs at peak times which correct the power factor profile, during this circumstance leads to increase the stability at the PCC. It's worth mentioning that the integration of BESS in the PV-DG will not be represented as an independent source in the system and can't be replaced by the grid in normal scenarios, because of the main aim of BESS in this system is not to be a main source but to reduce the PV impact and enhance the PV operation performance on the grid at peak periods [62, 63]. Fig. 2.20 illustrates the load scale of BESS with the PV system.

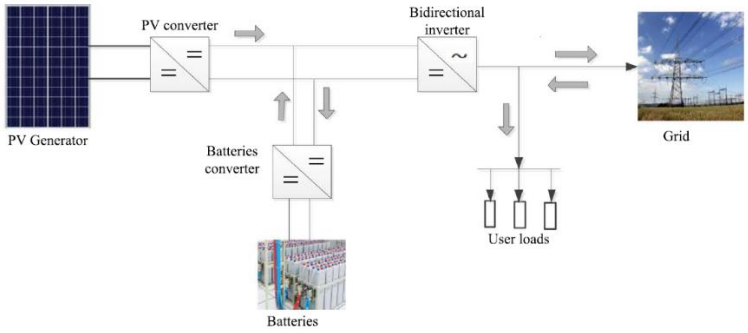

Figure 2.20: Power flow schematic diagram for small scale PV-BESS plant [64].

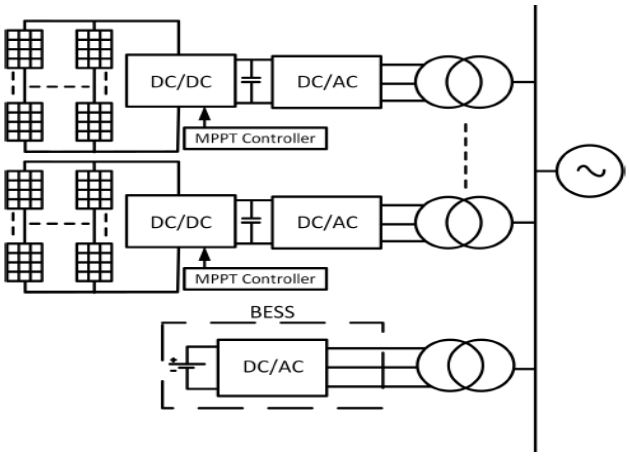

Figure 2.21: Schematic of a grid tied solar PV system with grid scale BESS [65].

For the grid scale BESS as illustrated in fig. 2.21 the situation will be much complicated and the number of batteries will be higher, fig. 2.22 shows the System components of a BESS as sited by [66] and the block diagram contains the most important component in the system which is the battery management system (BMS), that plays some rules such as maximizing the batteries capacity, preventing the usage of the battery outside its safe operating area, controlling the reactive power and estimating the batteries state of charge (SOC) level.

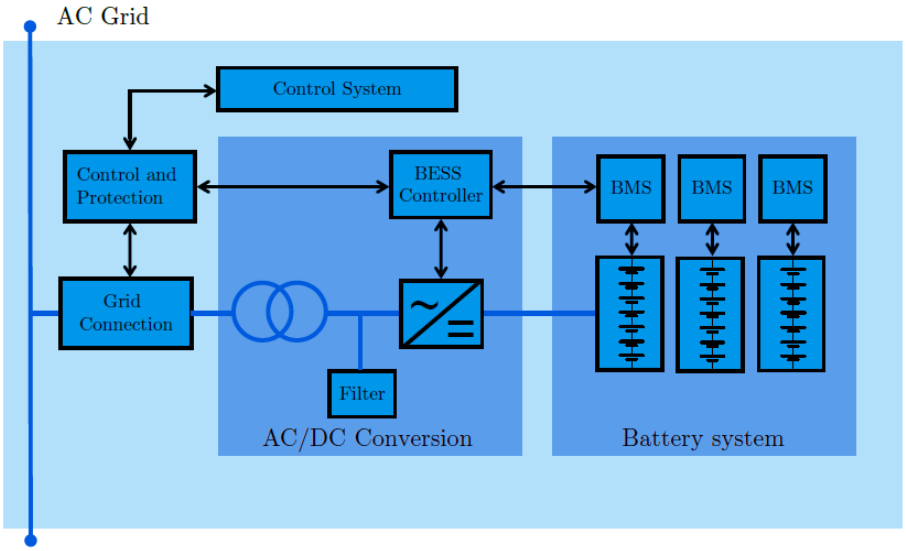

Figure 2. 22: System components of a Battery Energy Storage System (BESS) [66].

Capacity and sizing of BESS depending on the rated of the PV plant and the configuration of PV and BESS integration may be at the grid scale directly to the grid or small scale connected near the DC bus before the inverter. Fig 2.19, 20 demonstrate the both cases. However, the Ideal location of the BESS in the system is near the PV to maintain the minimum losses, optimum performance and less complication in the system. The capacity sizing issue is illustrated in [57], the optimum sizing of BESS in the PV-BESS integrated system, the optimization algorithm shows that the rated BESS capacity needed in these systems should be around 55% of the PV rated power.

During charging and discharging of the battery system, the electrical energy is converted between AC and DC by a four-quadrant inverter or as so-called charger/inverter. Therefore, an arbitrary combination of active and reactive power consumption or generation is possible in the system. The connection to the grid is established with a transformer. Table 2.1 represents the data of the PV-BESS in the Wolfswinkel project which shows the PV rated with a battery capacity of 500 kWh the BESS in the quarter Wolfswinkel, this project is one of the largest BESS in Switzerland [57].

Table 2.1: Data of Wolfs-winkle PV-BESS project.

Parameter	Value
PV Plant rated	960 kW_{peak}
Battery Capacity	500 kWh

Integration of the BESS is regulating the voltage at the PCC, additionally the peak shaving and transferring the demand from the extreme period will be the role of storage system. Fig. 2.23

illustrates the effect of integrating the storage system with the grid tied PV system. When overvoltage occurs on the PCC during PV production time, the battery will be charged with the excess PV power until the bus voltage drops to a normal range. Based on the BESS operation profile, the battery will discharge to support the bus voltage during a night time or when voltage sag occurs [57]. In the other hand the power demanded by the grid is decreased due to the contribution of the PV production.

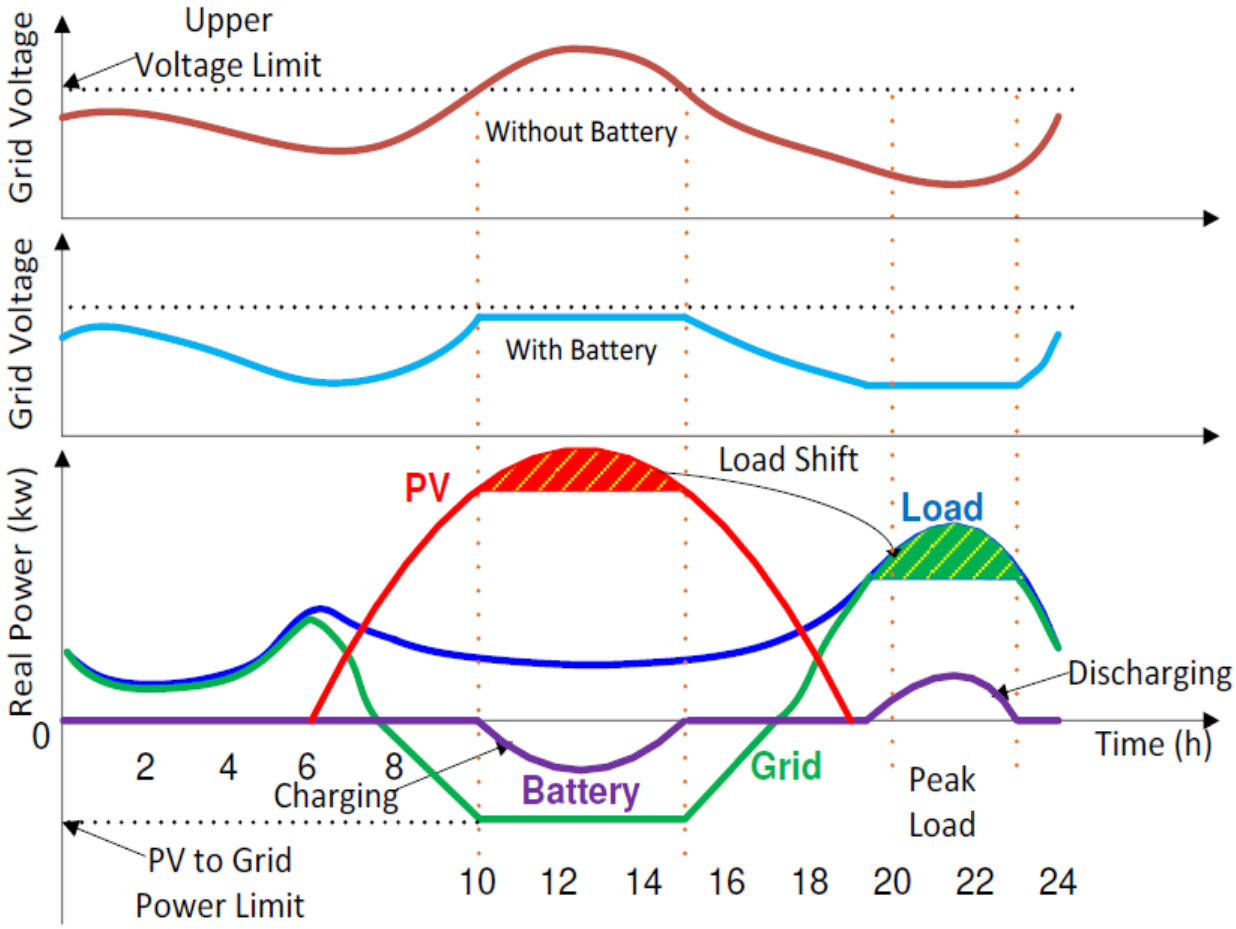

Figure 2.23: BESS operation daily profile with voltage effect [57].

2.10: Modeling and Power flow NRM

This section will explain the power system modeling for a distribution network feeder. For this purpose, a single line diagram for the distribution feeder has been considered then the single line diagram will be modeled using Electrical Transient Analyzer Programmed (ETAP) software. Load

flow study is carried out in ETAP using Newton Raphson method and it will be considered as a distribution analysis criterion. All of the physical and electrical parameters of the electrical power system will be taken into consideration, such a height of towers, spacing between transmission lines, resistance and reactance values of transmission lines, transformer and power grid ratings, these information collected and applied to obtain an exact grid model of the power system [67].

2.10.1: Newton-Raphson Solution Method

For a power system analysis technique, there are different solving approach of the obtained nonlinear system of equations. One of the important approaches known as the Newton-Raphson Method. This method begins with initial deductions of all unknowns such a voltage magnitude and angles at load buses and angles at generator buses. At that point, a Taylor Series is written, with the higher order terms ignored, for each of the power balance equations included in the system of equations. The result is a linear system of equations that can be expressed in the following matrix:

$$\begin{bmatrix} \Delta\theta \\ \Delta|\mathrm{V}| \end{bmatrix} = -\mathrm{J}^{-1} \begin{bmatrix} \Delta P \\ \Delta \mathrm{Q} \end{bmatrix} \tag{2.4}$$

$$\Delta P_i = P_i + \sum_{k=1}^{N} |\mathrm{V}|_i |\mathrm{V}|_k (G_{ik} \cos\theta_{ik} + B_{ik} \sin\theta_{ik}) \tag{2.5}$$

$$\Delta Q_i = -Q_i + \sum_{k=1}^{N} |\mathrm{V}|_i |\mathrm{V}|_k (G_{ik} \cos\theta_{ik} - B_{ik} \sin\theta_{ik}) \tag{2.6}$$

$$\mathrm{J} = \begin{bmatrix} \frac{\partial \Delta P}{\partial \theta} & \frac{\partial \Delta P}{\partial |\mathrm{V}|} \\ \frac{\partial \Delta Q}{\partial \theta} & \frac{\partial \Delta Q}{\partial |\mathrm{V}|} \end{bmatrix} \tag{2.7}$$

Where ΔP and ΔQ are the mismatch equations, J is Jacobian matrix which is the matrix of partial derivatives. In addition, the linearized system of equations is solved to determine the next guess (m + 1) of voltage magnitude and angles based on,

$$\theta^{m+1} = \theta^m + \Delta\theta \tag{2.8}$$

$$|\mathrm{V}|^{m+1} = |\mathrm{V}|^m + \Delta|\mathrm{V}| \tag{2.9}$$

This process continues until a condition of stopping point is met. A common stopping condition is to terminate if the norm of the mismatch equations is below a specified tolerance. Outline of solution of the power flow problem is:

1. Make an initial deduction of all unknown voltage magnitudes and angles. It is common to use a flatting starting point, which all voltage magnitudes are 1.0 p.u and its angles are set to be zero.
2. Solving the power balance equations using the most recent voltage angle and magnitude values.
3. Linearize the system around the most recent voltage angle and magnitude values.
4. Solve for the change in voltage angle and magnitude.
5. Update the voltage magnitude and angles.

Check the stopping conditions, if met then terminate, else go to step 2.

2.10.2 Modeling of Network

In the power flow analysis, the active power (P) and reactive power (Q) at each load bus are assumed to be known. For this reason, load buses are also known as PQ buses. For power grid buses, it is assumed that the real power generated P_G and the voltage magnitude |V| is also known. In electrical power systems a slack bus, defined as a V ∟θ bus, is used to balance P and Q in a system while performing load flow studies. The swing bus is used to provide for system losses by producing or consuming active and/or Q to and from the system. For the slack bus, it is assumed that the voltage magnitude |V| and voltage phase θ are known. Consequently, for each load bus, the voltage magnitude and angle are unidentified and should be solved; for each generator bus, the voltage angle must be solved for; there are no variables that must be solved for the Slack Bus. In a system of an N buses and R generator or power system network, there are 2 (N − 1) − (R − 1) unknowns.

In order to solve the 2(N − 1) − (R − 1) unknown parameters, there must be 2(N − 1) − (R − 1) equations that do not introduce any new unknown variables. The possible equations to use are power balance equations, which can be written for P and Q to each bus. The real power balance equation can be represented mathematically as follows:

$$0 = -P_i + \sum_{k=1}^{N} |V|_i |V|_k (G_{ik} \cos\theta_{ik} + B_{ik} \sin\theta_{ik}) \quad (2.10)$$

where P_i is the net injected power at bus i, G_{ik} is the real part of the element in the bus admittance matrix Y_{BUS} corresponding to the i^{th} row and k^{th} column, B_{ik} is the imaginary part of the element

in the Y_{BUS} corresponding to the i^{th} row and k^{th} column and θ_{ik} is the difference in voltage angle between the ith and kth buses. The reactive power balance equation is:

$$0 = -Q_i + \sum_{k=1}^{N} |V|_i |V|_k (G_{ik} \cos\theta_{ik} - B_{ik} \sin\theta_{ik}) \quad (2.11)$$

Equations included are the active and reactive power balance equations for each Load Bus and the active power balance equation for each generator bus. Only the active power balance equation is written for a generator bus because the net reactive power injected is not assumed to be known and therefore including the reactive power balance equation would result in an additional unknown variable. For similar reasons, there are no equations written for the slack bus.

Fig.2.2 illustrates a 3-phase line section between bus *x* and *y*, the line parameters are obtained by the technique developed by Carson and Lewis, considering the effects of self and mutual couplings of the unbalanced 3-phase line section, 4 x 4 matrix can be expressed as (2.12). By the application of Kron reduction method, to get the resultant matrix as represented in (2.13) [67].

$$[Z_{xy}^{abcn}] = \begin{bmatrix} Z_{xy}^{aa} & Z_{xy}^{ab} & Z_{xy}^{ac} & Z_{xy}^{an} \\ Z_{xy}^{ba} & Z_{xy}^{bb} & Z_{xy}^{bc} & Z_{xy}^{bn} \\ Z_{xy}^{ca} & Z_{xy}^{cb} & Z_{xy}^{cc} & Z_{xy}^{cn} \\ Z_{xy}^{na} & Z_{xy}^{nb} & Z_{xy}^{nc} & Z_{xy}^{nn} \end{bmatrix} \quad (2.12)$$

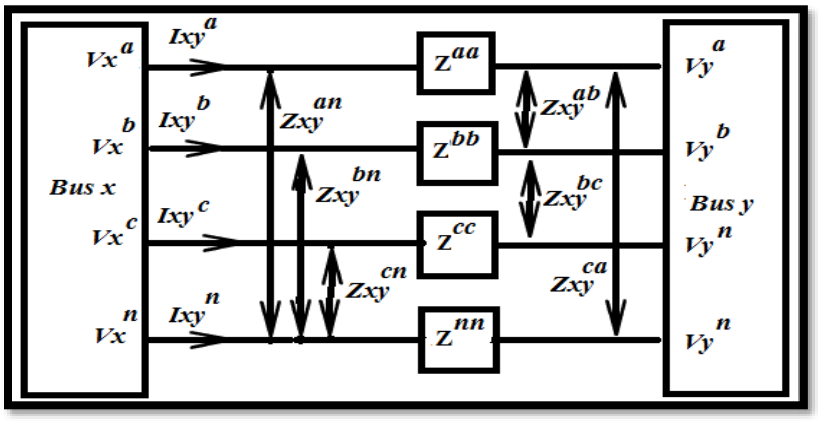

Figure 2. 24: Illustration of three phases, four wires line section.

$$\left[Z_{xy}^{abc}\right] = \begin{bmatrix} Z_{xy}^{aa-n} & Z_{xy}^{ab-n} & Z_{xy}^{ac-n} \\ Z_{xy}^{ba-n} & Z_{xy}^{bb-n} & Z_{xy}^{bc-n} \\ Z_{xy}^{ca-n} & Z_{xy}^{cb-n} & Z_{xy}^{cc-n} \end{bmatrix} \quad (2.13)$$

The relationships between bus voltages and branch currents for Fig.2.24 can be given as (2.14), (2.15).

$$\begin{bmatrix} V_y^a \\ V_y^b \\ V_y^c \end{bmatrix} = \begin{bmatrix} V_x^a \\ V_x^b \\ V_x^c \end{bmatrix} - \left[Z_{xy}^{abc}\right] \begin{bmatrix} I_{xy}^a \\ I_{xy}^b \\ I_{xy}^c \end{bmatrix} \quad (2.14)$$

Above equation (2.14) can be written as

$$\left[V_{xy}^{abc}\right] = \left[Z_{xy}^{abc}\right]\left[I_{xy}^{abc}\right] \quad (2.15)$$

2.10.3 Load Flow Data Requirement

1- Required data for a Bus:

The requirement data for the load flow solving approach for buses consist of:

- Rated voltage value in kV.
- %V and it's Angle especially when Initial Condition is set to the bus voltage.

2- Branch required data:

Branch data is entered into the branch managing editor, such transformer, transmission line, cable, impedance and reactor. The required data for load flow solving approach for branches consist of:

- Branch Z, R, X, or X/R values and units, tolerance, and temperature, if applicable
- Cables length and cross-sectional areas.
- transmission line length and unit and physical specifications
- Transformer rated kV and kVA/MVA, tap, and LTC settings
- Impedance base kV and base kVA/MVA

3- Power grid data:

Required data for load flow solving approach for the power grids includes the following:

- Operating mode such as Swing, Voltage Control, Var Control or even PF Control
- Rated voltage level in kV
- %V and its Angle especially for swing mode
- Voltage controlled mode: %V, MW loading, and var limits (Q_{max} & Q_{min}).
- Var controlled mode MW and Mvar loading, and var limits.
- PF controlled mode: MW loading and PF, and var limits

2.10.4 Load Modeling in Distribution system

A distribution system loads can be represented as 1-phase or 3- phase loads connected at the branches and laterals. These loads can be modeled as constant power (PQ), constant impedance, constant current or even any combination of the above. Table 2.2 summarizes the modeling equations of the load configurations [41].

The urgent need for modeling loads in the power system appear for energy scheduling, planning and grid operation. At the level of substation and beyond, modeling load is relatively simple. While load at the level of household is volatile, aggregation of loads at the level of substations and the grid is likely to be smooth and predictable. Despite significant differences from day to day, modeling load at substation is accurate provided contingencies do not arise. An overview of the load pattern at substation, the grid and the different types of forecast needed in general operation will be discussed in detail throughout the study.

Table 2.2: wye loads configuration model.

	Const. power (PQ)	Const. Impedance	Const. current
Y- configuration loads	$\begin{bmatrix} I_{L,a} \\ I_{L,a} \\ I_{L,a} \end{bmatrix} = \begin{bmatrix} \frac{(S_a)}{V_{an}} \\ \frac{(S_b)}{V_{bn}} \\ \frac{(S_c)}{V_{ac}} \end{bmatrix}$	$\begin{bmatrix} Z_a \\ Z_b \\ Z_c \end{bmatrix} = \begin{bmatrix} \frac{V_{an}{}^2}{S_b} \\ \frac{V_{bn}{}^2}{S_b} \\ \frac{V_{cn}{}^2}{S_c} \end{bmatrix}$	$\begin{bmatrix} I_{L,a} \\ I_{L,a} \\ I_{L,a} \end{bmatrix} = \begin{bmatrix} I_{L,a} < \delta_a - \theta_a \\ I_{L,b} < \delta_b - \theta_b \\ I_{L,c} < \delta_c - \theta_c \end{bmatrix}$ Where δ_{abc} are line-to- neutral voltage angles θ_{abc} power factor angles

Fig.2.25 Summaries the load flow approach using Newton Raphson method.

.

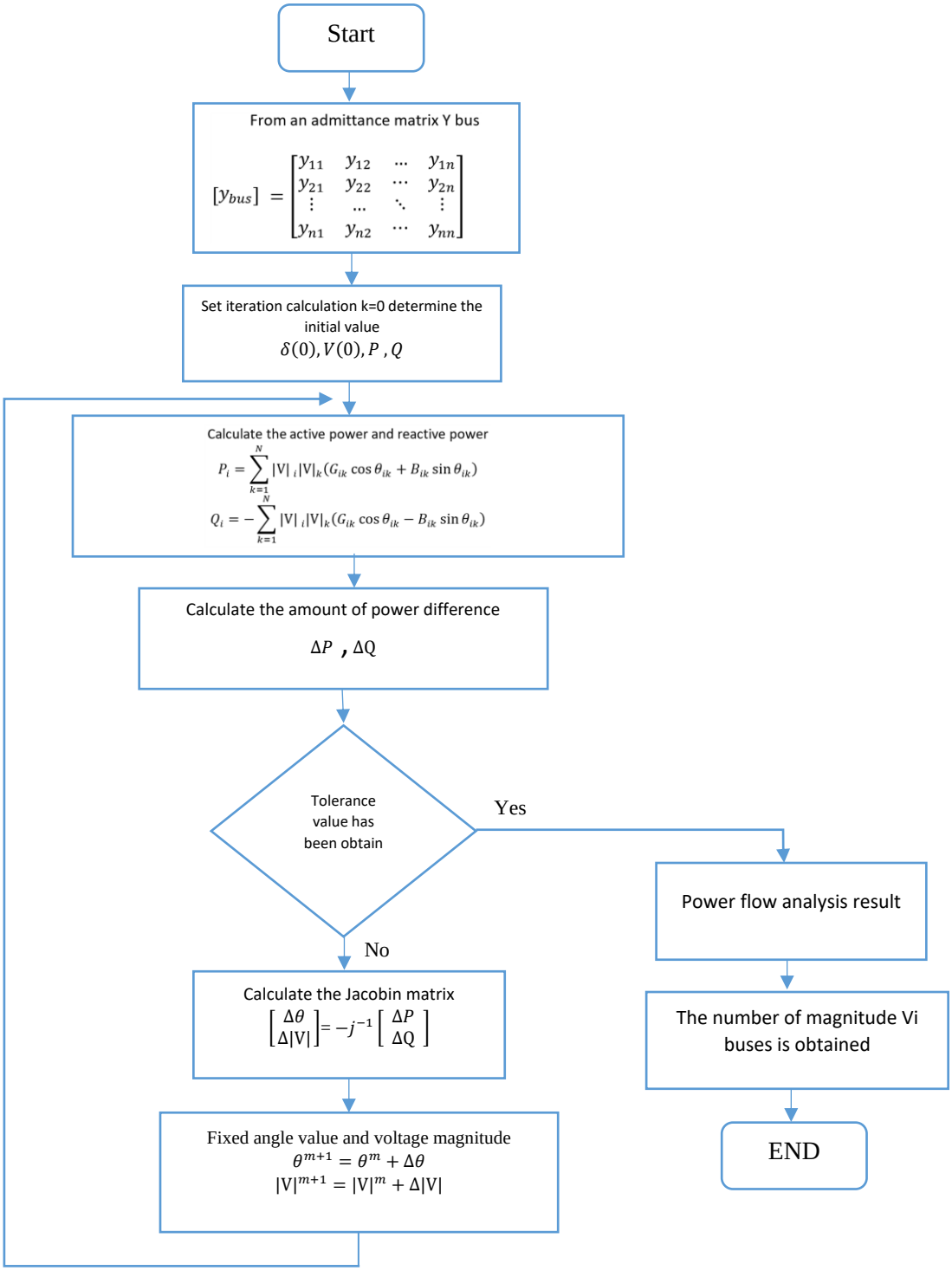

Figure 2. 25: Newton Raphson Approach flowchart of power flow determination.

2.11: International Standards for PV Integration.

Designing and installing a PV system and integrating with grid considering some factors and regulation. regarding to the operation and equipment that necessary to ensure compatible operation of PV systems and distribution networks can be found in the institute of electrical and electronics engineer's standards association (IEEE-SA) IEEE and European standards. Various factors must be considered when design and install PV systems to the distribution network. IEEE standard 929-2000 "Recommended practice for utility interface of photovoltaic systems". This specific IEEE standard contains information and restrictions of safety, grid operation, equipment protection and power quality parameters.

2.11.1: Voltage

Increasing penetration of distributed generation can cause a deviation in the voltage of distribution network as a consequence changes of the power flow in the feeders. In distribution power system the feasibility of voltage control with reactive power is limited as a result of the low X/R ratio. A solution proposed for this issue is based on the insertion of a controllable inductance in the feeder. In combination with reactive power support of the DGs the voltage can be controlled [68]. DVAR can be utilized and the table 2.3 explain issue.

Table 2.3: Voltage standards range.

Voltage Variation supplied ranges		
Germany /4015-2012 [69]	Spain 661/2007 [70]	France 2011 [71]
0.8Vn < V <1.1Vn	0.85Vn < V < 1.1Vn	0.9Vn < V < 1.1Vn

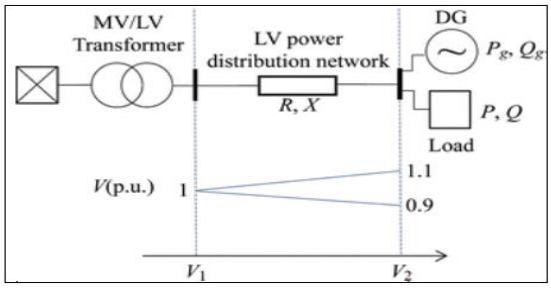

Figure 2.26: Voltage rise effects in radial weak distribution networks.

The standards for voltage fluctuations at the PCC of the PV plant facility to the power system should, for example, follow the requirement outlined in table.2.4.

Table 2.4: Voltage fluctuation limit [71].

Voltage change	**Maximum rate of occurrence**
+/-3% normal level	Once per hour
+5/-6% of normal level	Once per 8-hour
Exceeding +5/-6%	As agreed by utility

2.11.2: Power Factor

The dominate production of PV power plant is an active power due to the unity power factor operation, at the instant of rated production from PV plant, the PF range should be capable of 0.95 PF lagging and 0.95 PF leading. Automatic voltage regulation that is able to regulate the voltage at desired point which should be within +/-0.5 %. Moreover, the device may be more easily used for voltage regulation even when the PV is disconnected since it is directly controlled by the substation. In general consensus, it is believed that a PF requirement of +/- 0.95 at the point of interconnection is a reasonable requirement

2.11.3: Harmonics

IEEE Standard 519-2014 "Recommended Practices and Requirements for Harmonic Control in Electrical Power Systems" illustrates the limits of voltage and current harmonics at the point of common coupling between end-users and distribution utilities as shown in table 2.5. It's worth mentioning that the limits established by this standard are 5 % for the voltage and current THD on the distribution level. The limits for the maximum individual harmonic components are also determined and must be less than 3 % for voltage lower than 69 kV.

Table 2.5: IEEE 519-2014 voltage distribution standard [72].

Bus Voltage (V) at PCC	Individual Harmonics (%)	Total Harmonic Distortion THD (%)
$V \leq 1.0$ kV	5.0	8.0
1kV < V ≤ 69 kV	3.0	5.0
69kV ≤ V ≤ 161 kV	1.5	2.5
161 kV < V	1.0	1.5

2.11.4: Frequency

Frequency of the power system indicates one of the most important power quality factors. Consequently, it must be uniform throughout an integration with grid. To control the frequency of the system through maintaining a balance between the generation part of the grid and the load which is connected to the grid.

The frequency will fall when the demand exceeds the generation and it will rise when the generation exceeds the demand (light load). But with the increasing penetration of grid connected PV systems, frequency control becomes more difficult. Moreover, as a number of grid-tied PV systems increases, the impacts of frequency fluctuation will become more significant. Inverters can provide frequency control in short time, sometimes milliseconds, which is significantly faster than conventional generation. But the inverter may cause harmonics and inject it to the distribution

network which makes losses and disturbance in the voltage and current. Table 2.6 illustrates the frequency standard ranges [73].

Table 2.6: Frequency range versus time.

Frequency range (Hz)	Time (second)
>51.7	0
51.6 to 51.7	30
50.6 to 51.6	180
>49.4 to 50.6	Continuous operation
>48.4 to 49.4	180
>47.8 to 48.4	30

2.11.5: Short circuit capacity

Distributed generation that integrated with the grid has a high influencing on the short circuit capacity (SCC) of power systems. The behavior of short circuit level that caused by PV power generator is different from the one that generated by a classical synchronous generator (SG) during symmetrical or asymmetrical short circuits. The response of PV-DG systems to short circuits is controlled by the power electronic components used in the converters and their control algorithms.

The German grid code of the short circuit capacity level is distinguishing between nonrenewable generation power units with directly connected SG and renewable energy units such as PV or wind power. The regulations contain requirements with respect to the real and reactive power control and the power quality. Fig 2.27 shows the Fault requirements in the German grid code. It is required that the DG system remains connected to the power system not more than 150 ms if a voltage dip down to 0 [74]. And the current level is depending on the power system components specification.

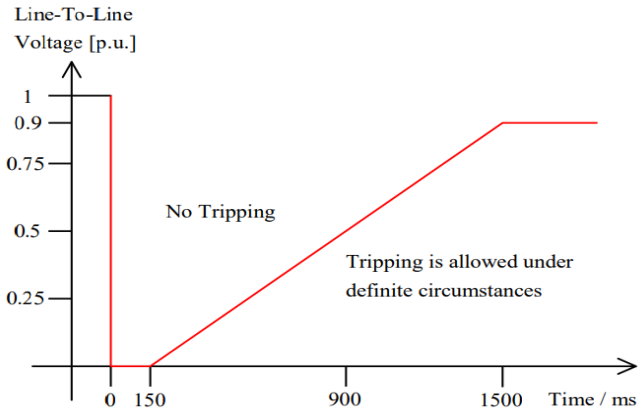

Figure 2. 27: German standard for the tripping time with voltage value [74].

3

Chapter Three

Case Study State of Art

3.1: Introduction.

3.2: Case study description.

3.3: Load profile generation and analysis.

3.4: Allocation factor method.

3.5: PV system description.

3.1: Introduction.

The main goal of an electric grid operation is to supply electric energy from generators to satisfy the electrical demand of loads, so the load profile should be taken into consideration. The grid operation is facing complicated conditions produced from a large number of non-linear constraints coming from operational limits in generators such as transmission networks, distribution networks, and customer units. The reliability of components in the grid also makes the grid operation complicated. Another source of complication is an uncertainty in loads. Once a high amount of distributed PV generation is added to the demand side as a negative load, the net load which is a summation of a regular load and a negative load becomes even more uncertain [75].

In electric power distribution, Feeder is "voltage power line transferring power from a distribution substation to the distribution transformers". In other words, electrical circuit in power system that carries power from power transformer or switch gear to distribution ones [76].

Meanwhile, The Palestinian Electrical Power System (PEPS) is a 33-kV medium distribution voltage that fed by Israel electrical company (IEC) at 161-kV at the transmission line, means that the PEPS have the control role only at the distribution level but not for the transmission lines. However, the PEPS is a distribution level network divided into two configurations: the first one is beginning from the transformation power transformer stations 33/11 KV through multiple of 11 KV feeders to many of distribution transformers that feeds end users grid by 0.4 KV electricity. And the second configuration is from 33kV power station to 0.4 kV power lines to end users. In this thesis the first configuration distribution system will be considered.

3.2: Case study description

Palestine Polytechnic University (PPU) PV grid tied system is one of the largest PV plant that integrated with the Hebron Electrical Power Distribution System (HEPDS), therefore in this thesis the PPU PV plant was selected as a case study. In this section, the distribution Medium Voltage (MV) PPU feeder will be described in addition to the all real parts specifications. Moreover, an accurate study of the influences and performance of the installed the PPU grid-tied PV systems on distribution network, to investigate the effect of different weather conditions on the power production of the PV modules in current situation and other proposed scenarios.

The PPU PV power plant is integrated with HEPDS which means that PV system and loads are part of Hebron Electrical Power Distribution System, HEPDS which is the distribution network of Hebron electrical Power company, which is supplied from 161 kV transmission line of IEC through an IEC power station which steps down the voltage level to reach (33 KV) then this transmitted power is received to the Main Power Control (MPC) station, fig. 3.1 shows the 161 kV line, IEC power station and MPC.

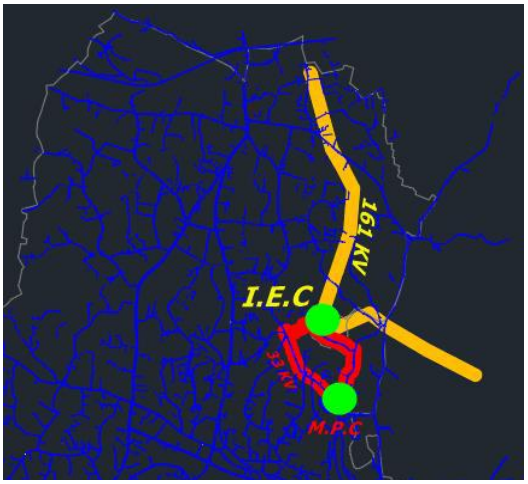

Figure 3.1: Electrical supplier path (161 KV) and MPC.

Medium Voltage lines comes out from the IEC power station into the MPC by underground cables, and then the network power connection is distributed in a radial configuration at medium voltage level of 33 kV, to seven substations inside the city borders which step the voltage down to (11-kV) level to build the distribution feeders.

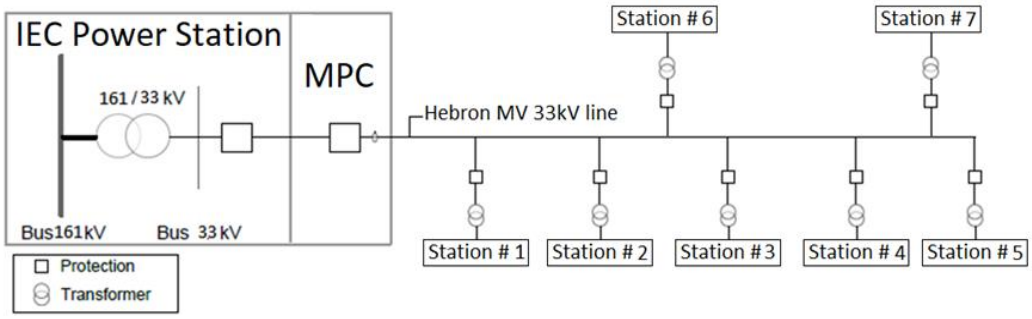

Figure 3.2: The single line diagram of 33kV line of HEPDS.

The PPU feeder is one of the MV feeder of the station #7, In a Fig. 3.2 the PPU feeder path on a real map is shown, and the satellite photo for the seventh station of the HEPDS which contains two 10 MVA Power transformer to step the voltage down from 33kV/11kV. However, fig 3.3 illustrates a photo of the both power transformers, and the path of the PPU feeder appears in fig. 3.4.

Figure 3.3: Substation #7 and Power Transformers.

Figure 3. 4: PPU feeder path from substation #7.

The first power transformer (Power Tr. 1) of the station #7 of HEPDS with a 10-MVA rating and ONAN cooling method and Dy11 vector group, furthermore it supplies two feeders and distribution serves transformer for the station which includes 42 distribution transformer in a wide range of (kVA), from (160-1000) kVA, table 3.1, shows the classification of these transformers rating.

Table 3.1: Distribution transformer rating classification.

No.	Transformer rating (kVA)	amount
1	1000	1
2	630	6
3	400	18
4	250	10
5	160	7
	Total	42

At the consumer side, distribution transformers transform the distribution voltage to the service level voltage directly used in households and industrial plants, usually around 400 V. Distribution Stations in HEPDS provide two types of customers, special for industrial loads and general for homes and commercial loads. However, these distribution transformers described by some electrical specifications and parameters, one of the most important parameters for the transformer is X/R ratio, which is simply the imaginary part of its impedance divided by the real part of its impedance, Z percentage of the rated voltage applied to the transformer, table 3.2 shows the X/R ratio for the feeder transformers.

Table 3.2: Transformers rating data.

Transformer rating (KVA)	**X/R**	**Z %**
160	1.5	4.4
250	2.5	4.4
400	4	4.4
630	6.3	4.5
1000	8	4.6

On the other hand, the majority of the transmission conductors of the MV system is underground cables single core 120-150 mm^2 Cu $15kV_{AC}$ XLPE and the rest of them is over headlines 50-120 mm^2 Al ACSR, connected with 12m height towers and 0.8m separation distance in flat configuration. Fig. 3.4 shows the cables and overhead line configuration. And table 3.3 represents the cables and overhead lines electrical parameters. Appendix A shows the lines, cables and Tr. data sheets

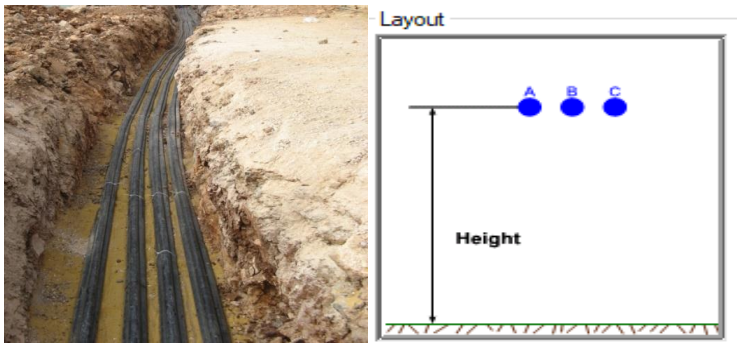

Figure 3.5: Underground Cables and over headlines configuration.

Table 3.3: Standard cables and overhead lines data.

Data Line Type	**Cross section (mm^2)**	**Resistance (Ω/km)**	**Reactance** (Ω/Km)	**Admittance (Ω^{-1} /km)**
Coyote	150	0.216	0.318	0
Dog	120	0.269	0.326	0
Rabbit	50	0.529	0.347	0
Nexans, single core XLPE	95	0.321	0.22	5.2*10−5

Fig. 3.6 represents a single line diagram (SLD) of the Power Tr.1of the station #7 and its feeders, the first power transformer supplies two main MV feeders with 11kV PPU and ZAL feeders in addition to distribution transformer with 400 kVA rating for the station serves. Each feeder supplies a number of distribution transformers which steps the voltage down to 0.4 kV to feed the customer's needs.

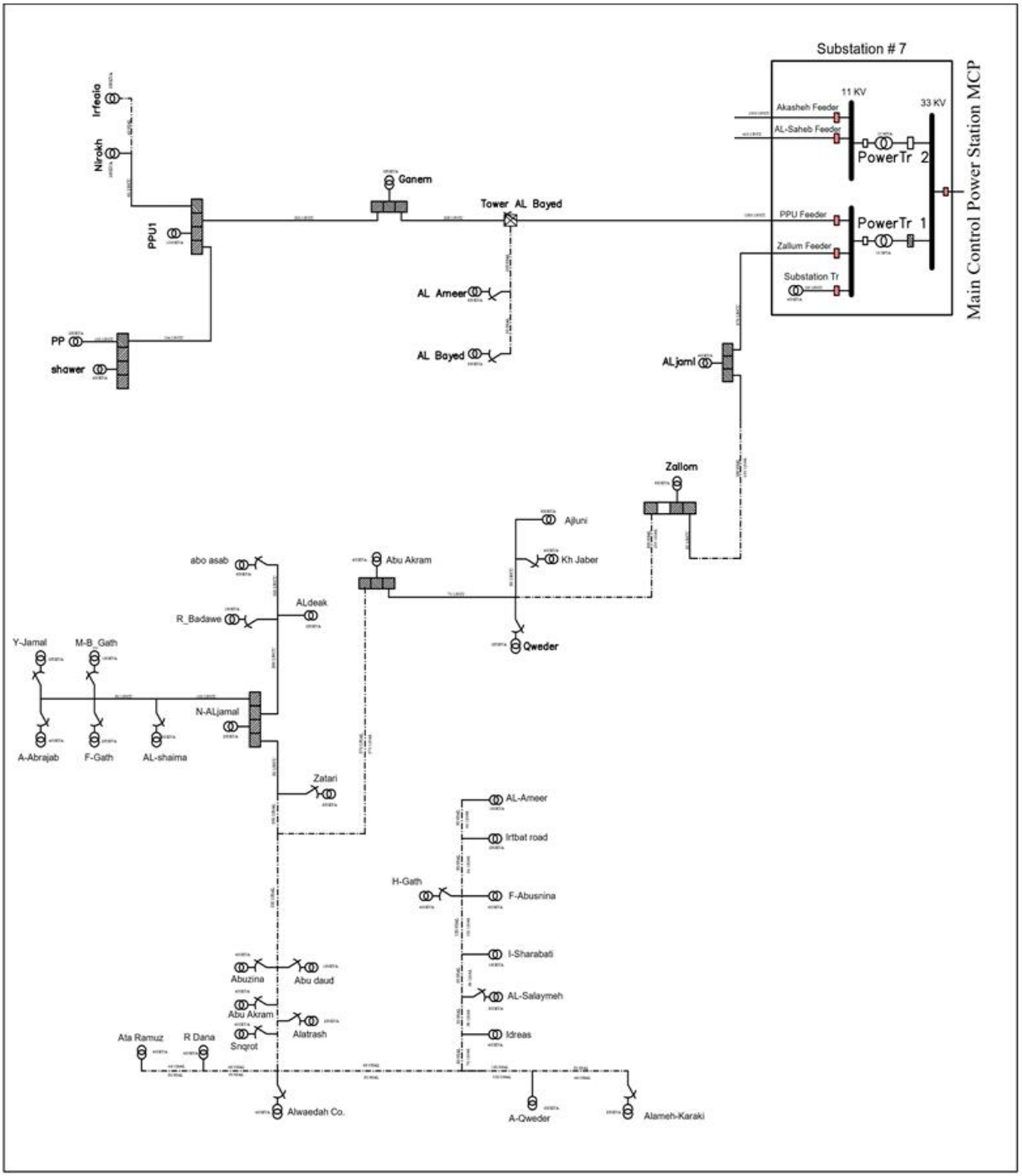

Figure 3.6: Single line diagram of the Station #7 and PPU & ZAL MV feeders.

3.3: Load Profile Generation and Analysis

The HEPDS is monitored by a Supervisory control and data acquisition system (SCADA), with a number of measurement devices to observe the main values of the MV distribution systems, which means that voltage, current, real and apparent power and power factor recording for each hour along a day for the MPC and each station of the HEPDS, However the current loading for each feeder also monitored, fig. 3.7 shows the measuring values for the station and feeders.

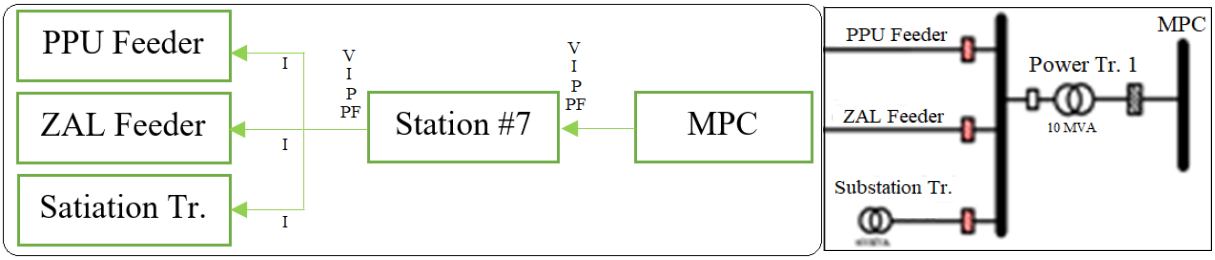

Figure 3.7: Metering system points of the HEPDS.

Fig. 3.8 represents the average daily voltage profile measured of the main MV bus that feeds PPU, ZAL and station transformer, the voltage varies between $\mp 0.4\%\, pu$ only at the MV main interconnection point. The main point can be observed from this profile is the voltage drop which concentrated at the mid days and over voltage period located at night, due to the PPU and ZAL feeders are day consumption loads since the majority of their users are industrial and commercial.

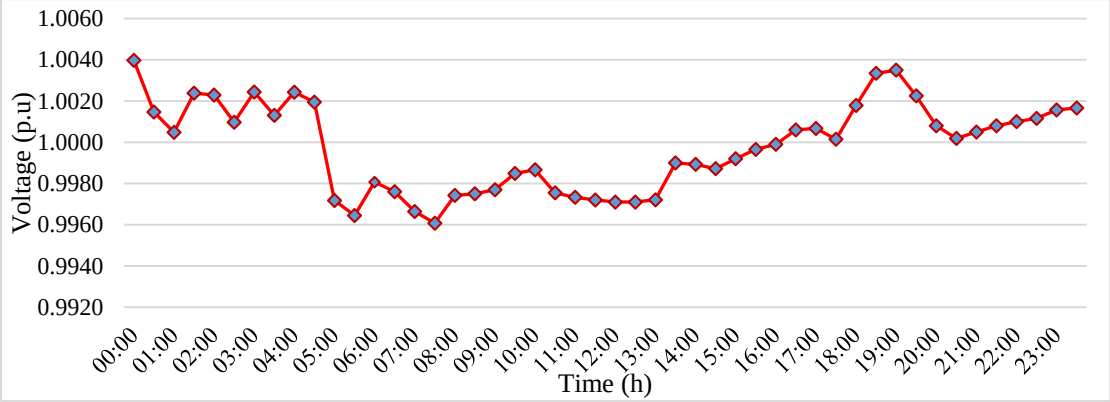

Figure 3. 8: Main Power Tr. 1 Voltage Average Daily Profile (p.u).

The monitoring system recording the data each 15 min a day, means the load is varying each 15 min and the DG production also, therefore the needs of demand profile is appeared. Generation of load profile can help the system monitor to observe the distribution system power flow and voltage analysis. The methodology of profile generation should be fast and allow the generation of a large number of realistic load profiles. Nowadays, when distribution systems are simulated, loads are normally represented with an aggregated or lumped load, but does not represent individual loads.

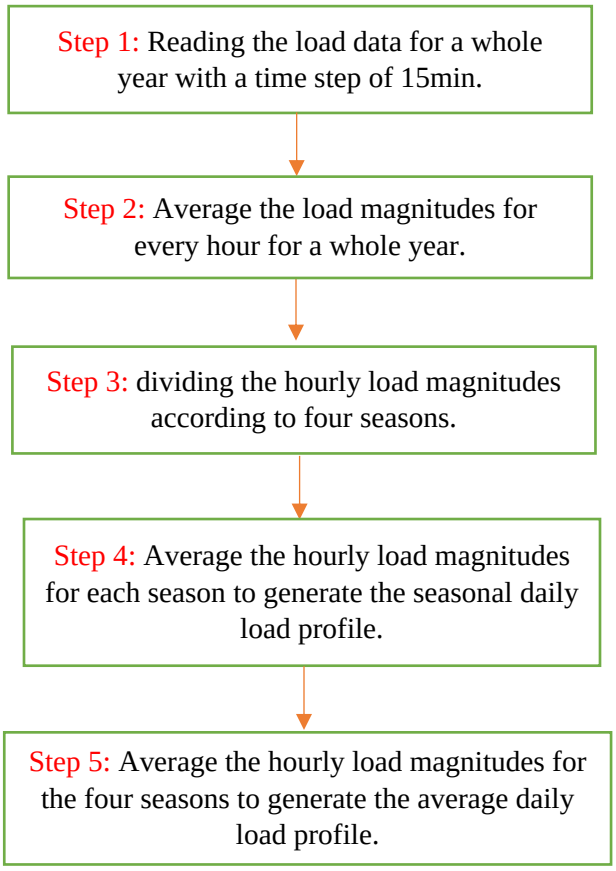

Figure 3.9: Block diagram of the load profile generation approach.

Fig. 3.10 illustrates the generated average daily load profile of the main power transformer #1 in the seventh station which includes the PPU feeder, ZAL feeder and station transformer loading. However, this value is the yearly average profile hour by hour, and the average profile is calculated by four profiles summer, autumn, spring and winter value along a year. This procedure was followed for performing all load profiles that taken from the HEPDS monitoring system fig. 3.9 specifies in details how the approach was followed, and this technique used not only for the main power transformer but also for the PPU feeder, ZAL feeder starting point and their distribution transformers and even for station serves transformer.

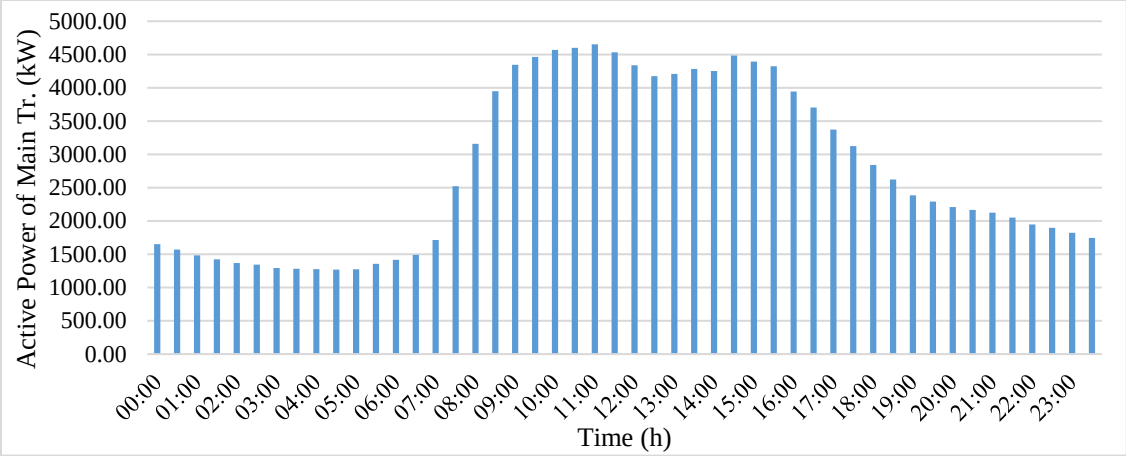

Figure 3.10: Active power of Main Power Tr. 1 average daily load profile.

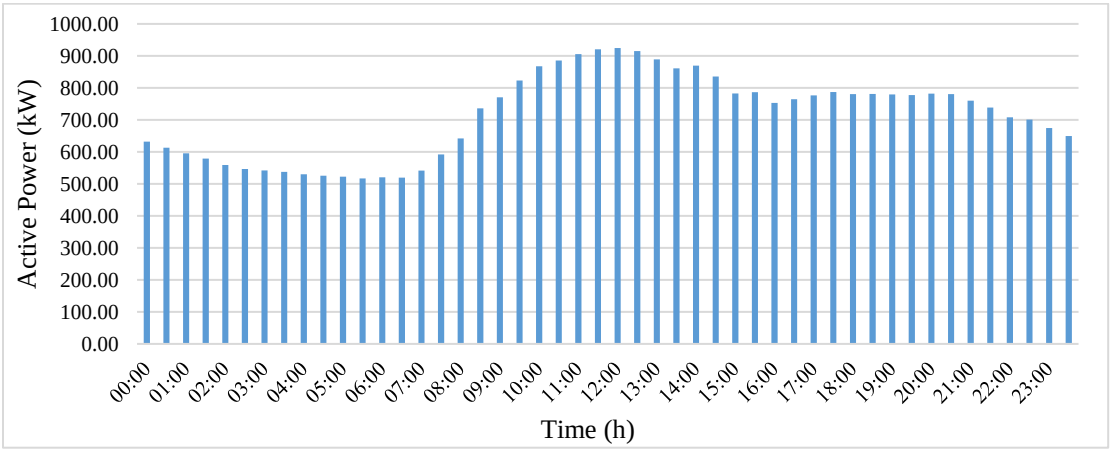

Figure 3.11: PPU feeder average daily load profile.

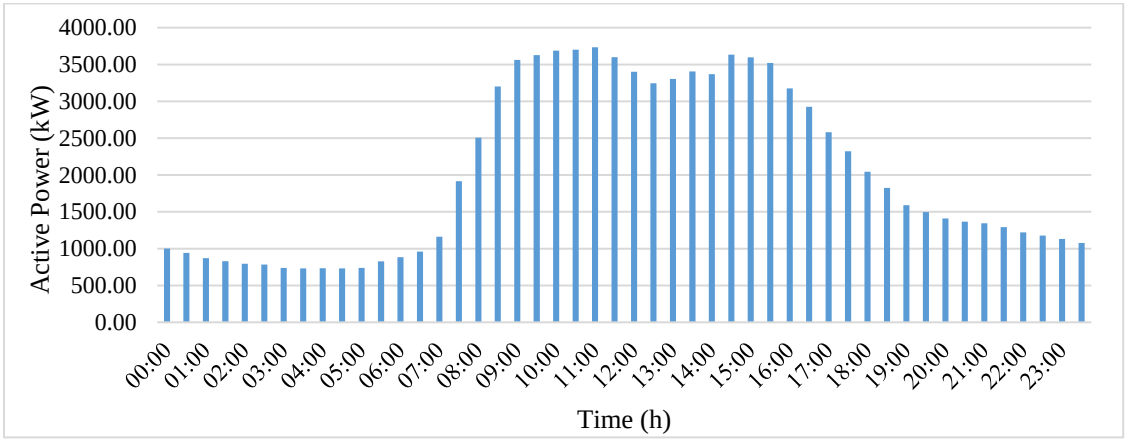

Figure 3.12: ZAL feeder average daily load profile.

The main observation is the number of domestic loads at the PPU feeder is much higher than the amount in ZAL feeder, so this is what makes the clear difference between their profiles. On other hand, the station serves transformer profile is random and can't be predicted since the consumption in the station depends on the maintenance and the weather condition as represented in fig.3.13.

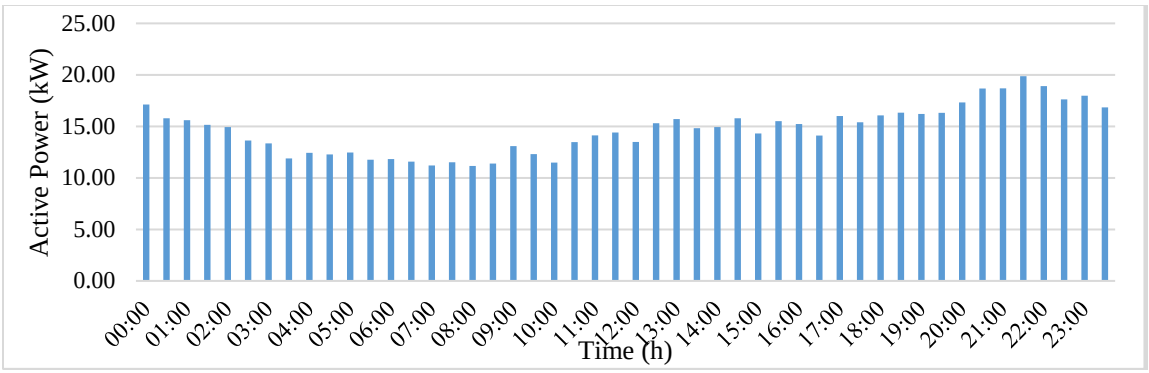

Figure 3.13: Station serves Transformer average daily load profile.

The second measured parameter by the SCADA monitoring system of the HEPDS is power factor, fig. 3.14 represents the power factor profile that build for the main power transformer, PPU feeder, ZAL feeder and station serves transformer and the procedure of determining the following values is such the procedure of the power profiles.

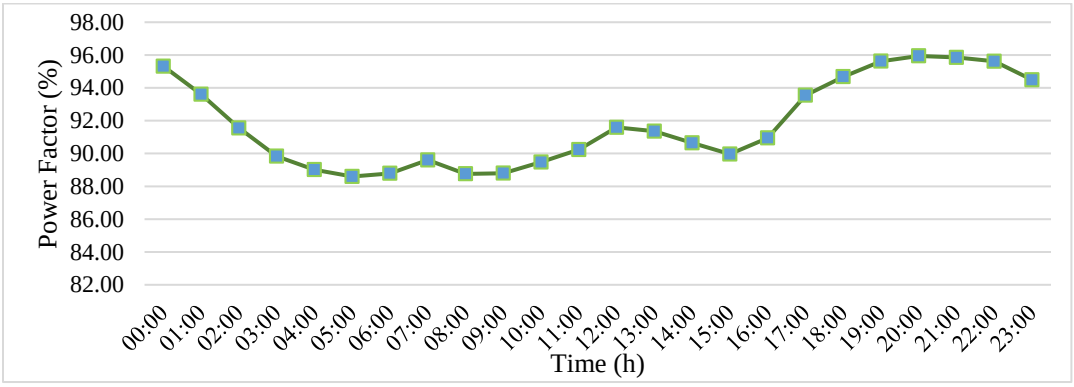

Figure 3.14: Main Power Tr.1 Average Daily PF Profile.

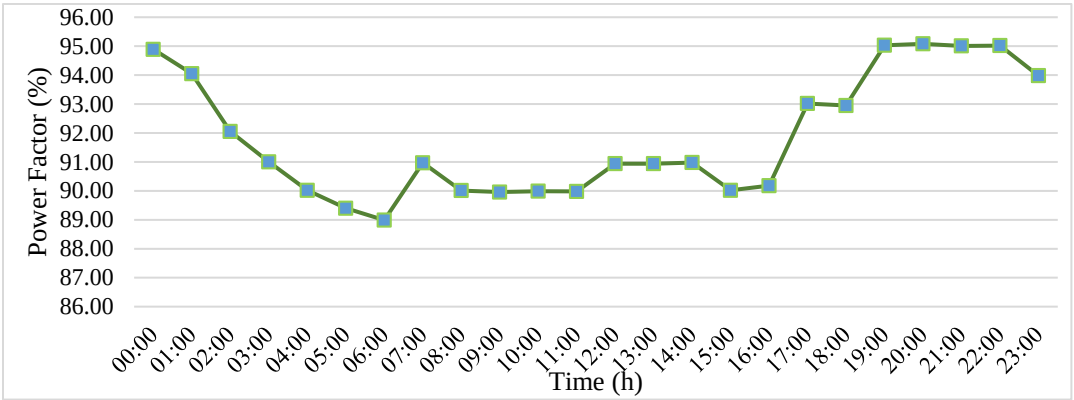

Figure 3. 15: PPU Feeder Average Daily PF Profile.

The power factor value of the main power transformer is located between 90-96% which is acceptable based on the IEEE standard which is mentioned in the chapter 2, and the most drop value of it is in the day time which reflects the concentration of the increasing of the demand during

the day for the feeders and decreasing the consumption in the night time. Fig.3. 15,16 represent the power factor profile for PPU and ZAL feeder respectively and its values located between 89-95% only which leads to the result that the power factor of the feeders and the interconnection point of the station #7 of the HEPDS is in acceptable range so far.

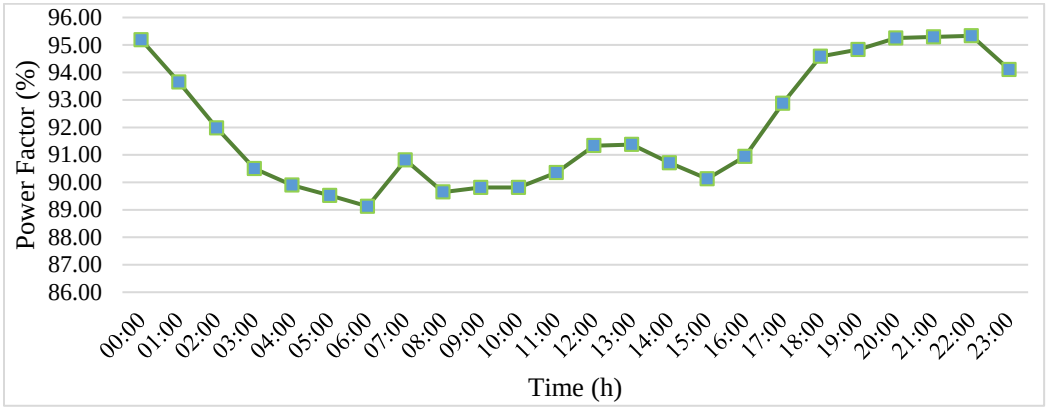

Figure 3.16: ZAL Feeder Average Daily PF Profile.

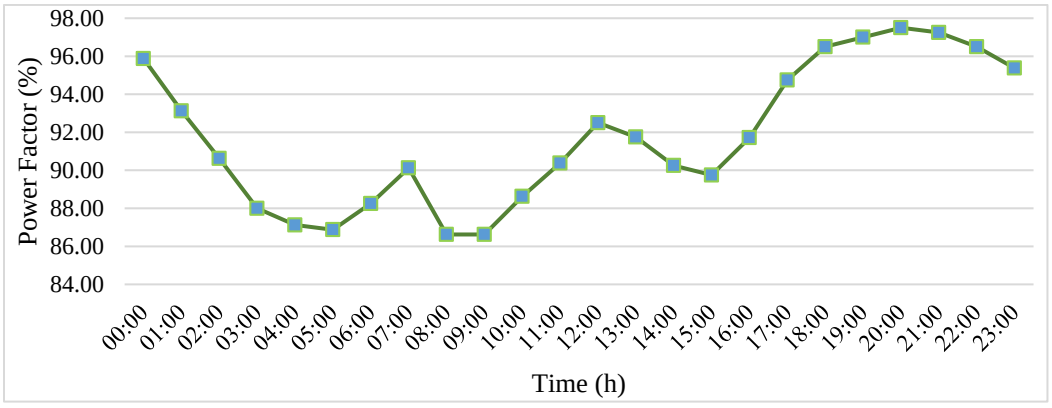

Figure 3.17: Station serves Tr. Feeder Average Daily PF Profile.

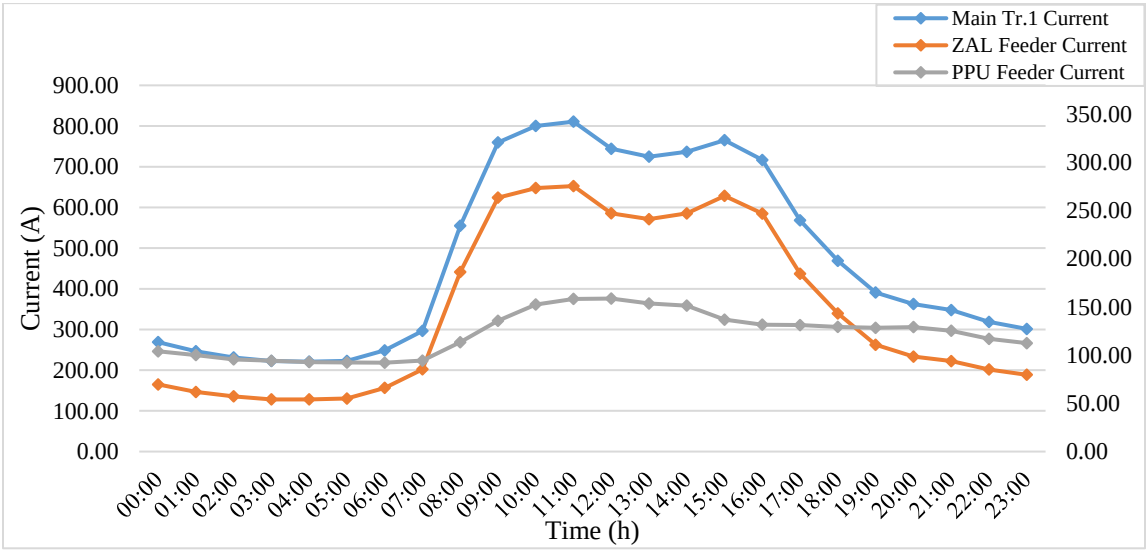

Figure 3.18: The Current Profile of the main power transformer and its feeders.

3.4: Allocation Factor

The metering system of the HEPDS is measuring the voltage, current, active power and power factor at the power transformer and on the starting point of the feeders but not at the distribution transformers, means that the loads of each distribution transformer is not specified by the monitoring system which is a challenge for the system analysis. Consequently, for modelling, analyzing and simulating the network and to determine the distribution transformer loading of the feeders and to get a distribution system with full of information, the allocation factor method was considered.

Allocating load based upon the metered readings in the substation requires the least amount of data. Most feeders will have metering in the substation that will, at minimum, give either the total three-phase maximum diversified kW or kVA demand and/or the maximum current per phase. Consequently, the kVA ratings of all distribution transformers are always known for a feeder. At the seventh station of HEPDS having the active power and power factor of the power transformer which means the distribution transformers loading can be determined.

The metered readings can be allocated to each transformer based upon the transformer rating. An "allocation factor" (AF) can be determined based upon the metered three-phase kW or kVA demand and the total connected distribution transformer kVA [77].

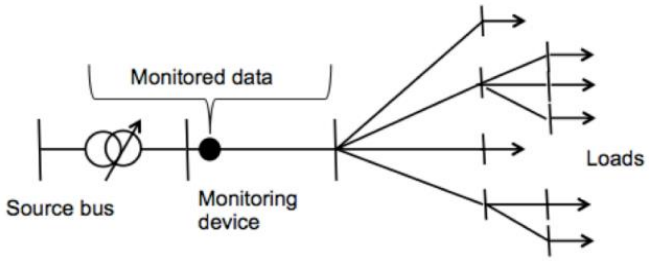

Figure 3.19: Allocation factor load principle.

$$Allocation\ Factor\ (AF) = \frac{Metered\ Demand}{kVA_{Total}} \quad (3.1)$$

Where: -

- Metered demand can be either kW or kVA.
- kVA_{Total} = sum of the kVA ratings of all distribution transformers.

The allocated load per transformer is then determined by:

$$Transformer\ demand\ = AF\ .kVA_{transformer}$$

The transformer demand will be either kW or kVA depending upon the metered quantity and the rating value. The load allocation to each distribution transformer can be done by measuring voltage and current at the substation and then computing the resulting kVA. The load allocation will now follow the same procedure as outlined above. With this data, the active and reactive power can also be allocated. Since the metered data at the substation will include losses, which means that the allocated load plus losses will equal the metered readings.

The calculated allocation factor for the Hebron Distribution Grid is 36.2%∠0.96 based on their data available. Consequently, the feeders that considered in this thesis is the PPU and ZAL feeders which fed by the power transformer 1 of the power station #7, the loading of each feeder on average hour per hour daily is 1428.57 kW for the PPU feeder and 4071.95 kW for ZAL feeder, but the distribution transformer loading is not specified and its rated value is known, therefore the AF is determine by the table 3.4, and the loading of the distribution transformer in the table 3.5,6.

Table 3.4: Power Tr. 1 feeders average daily Parameters.

PPU Feeder	
Real Power (kW):	1428.57
Power Factor (%):	92
Apparent power (kVA):	1552.79
Apparent power (kVA):	1428.6+608.47i
Allocation Factor (AF):	0.48 ∠23.07

ZAL Feeder	
Real Power (kW):	4071.95
Power Factor (%):	92
Apparent power (kVA):	4426.03
Apparent power (kVA)	4071.95+1734.64i
Allocation Factor (AF):	0.37 ∠ 23.07

Table 3.5: Distribution transformers loading of the ZAL Feeder.

No.	Transformer Name	Transformer rating (kVA)	Transformer loading (kVA)	No.	Transformer Name	Transformer rating (kVA)	Transformer loading (kVA)
1	Aljamal	400	136.2+58i	18	alatrash	250	85.1+36.25i
2	zallom	630	214.5+91.36i	19	abuzaina	400	136.2+58i
3	kh jaber	400	136.2+58i	20	abuakram	400	136.2+58i
4	ajluni	630	214.5+91.36i	21	snoqrot	400	136.2+58i
5	qweder	250	85.1+36.25i	22	rdana	400	136.2+58i
6	abuakram	400	136.2+58i	23	ataramoz	400	136.2+58i
7	aboasab	630	214.5+91.36i	24	alwaedah	400	136.2+58i
8	Rbadawe	160	54.46+23.2i	25	Hgath	400	136.2+58i
9	aldeak	250	85.1+36.25i	26	alameer	160	54.46+23.2i
10	Naljamal	250	85.1+36.25i	27	Irtbat	250	85.1+36.25i
11	alshaima	400	136.2+58i	28	Fabusnina	400	136.2+58i
12	Fgath	250	85.1+36.25i	29	Isharabati	160	54.46+23.2i
13	aburajab	400	136.2+58i	30	salaymeh	400	136.2+58i
14	yjamal	250	85.1+36.25i	31	Idrees	400	136.2+58i
15	mbgath	160	54.46+23.2i	32	Aqweder	630	214.5+91.36i
16	zatari	630	214.5+91.36i	33	alameh-k	250	85.1+36.25i
17	abdaud	160	54.46+23.2i		Total	6250	2127.88+906.29i

Table 3.6 Distribution transformers loading of the PPU Feeder.

No.	Transformer Name	Transformer rating (kVA)	Transformer loading (KVA)
1	Al ameer	630	278.208+118.503i
2	al bayed	160	70.656+30.096i
3	Ganem	400	176.64+75.24i
4	PPU1	1000	441.6+188.1i
5	Nirokh	160	70.656+30.096i
6	Irfeaia	250	110.4+47.025i
7	PP	250	110.4+47.025i
8	Shawar	400	176.64+75.24i
	Total	3250	1435.2+611.325i

The up mentioned table was the load based on the rated allocation factor but the AF is changing frequently along the day based on the load profile metering. Thus, the AF profile along a day on average for the PPU Feeder was calculated and represented in fig. 3.20, based on this AF profile the load profile for each distribution transformer that connected to the PPU feeder is specified. In this thesis the PPU PV system was taken into consideration, therefore fig. 3.21 illustrates the active, reactive and apparent power of the PPU 1000 kVA distribution transformer by the AF technique, and fig. 3.22 represent the power factor profile of the PPU load. In addition to that the load profile for the feeder loads are determined.

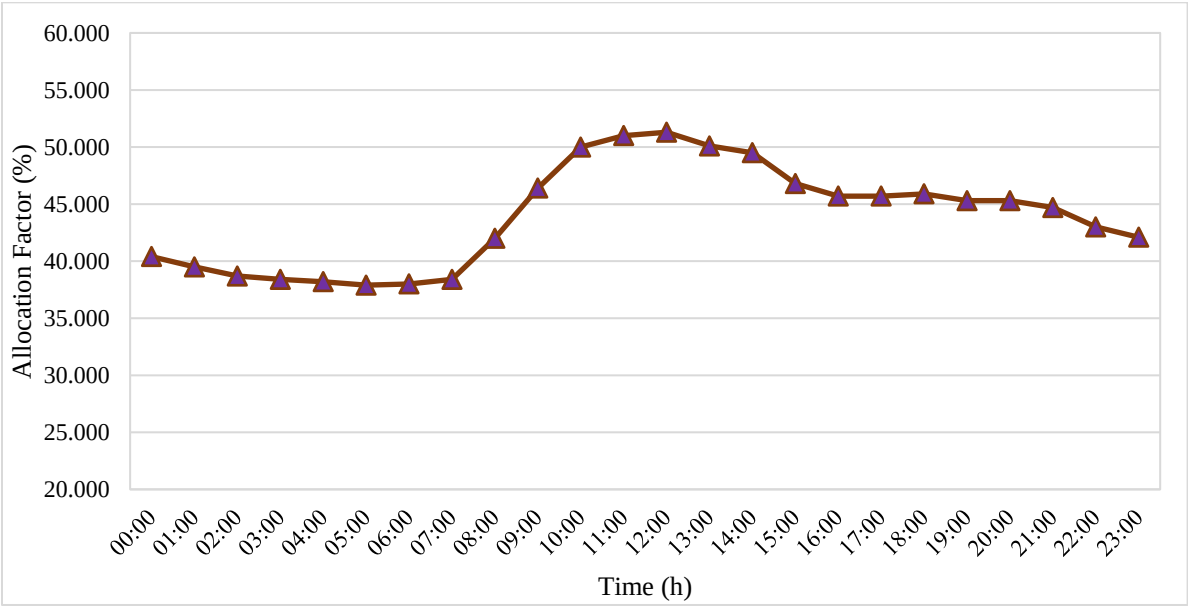

Figure 3. 20: PPU Distribution Feeder Allocation Factor Profile (%).

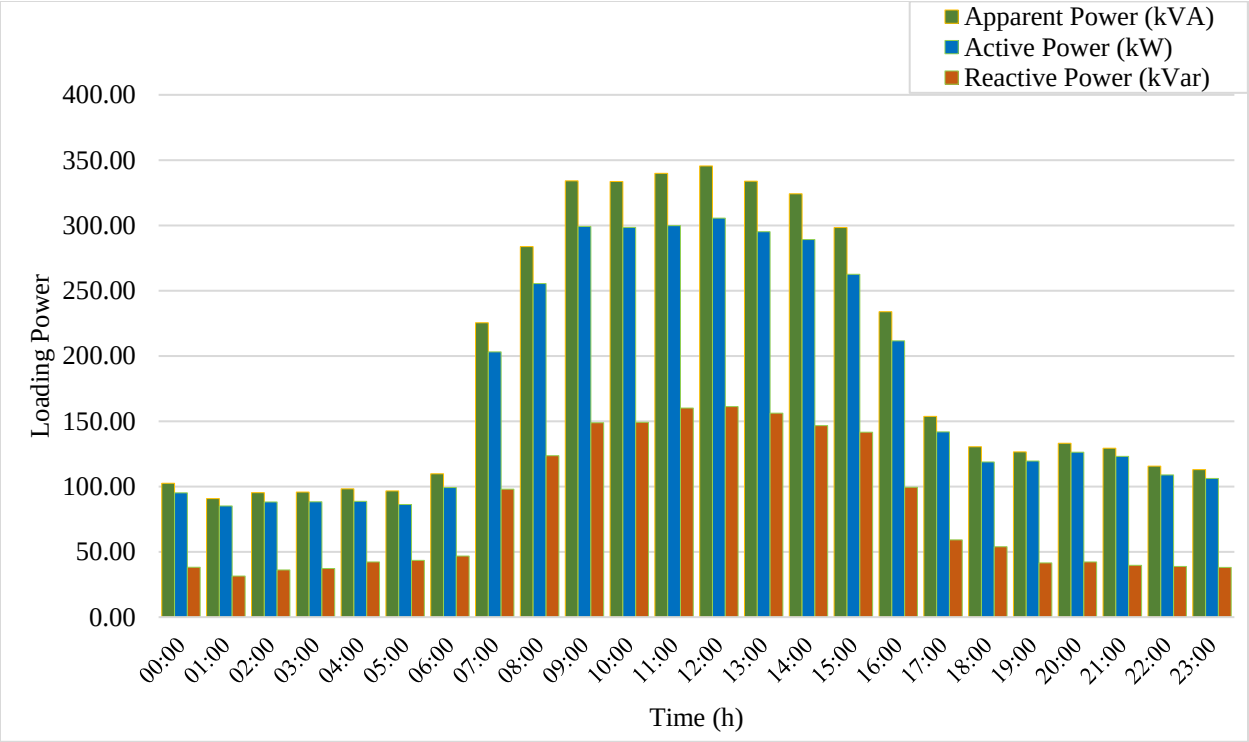

Figure 3. 21: Daily load profile of the PPU distribution transformer.

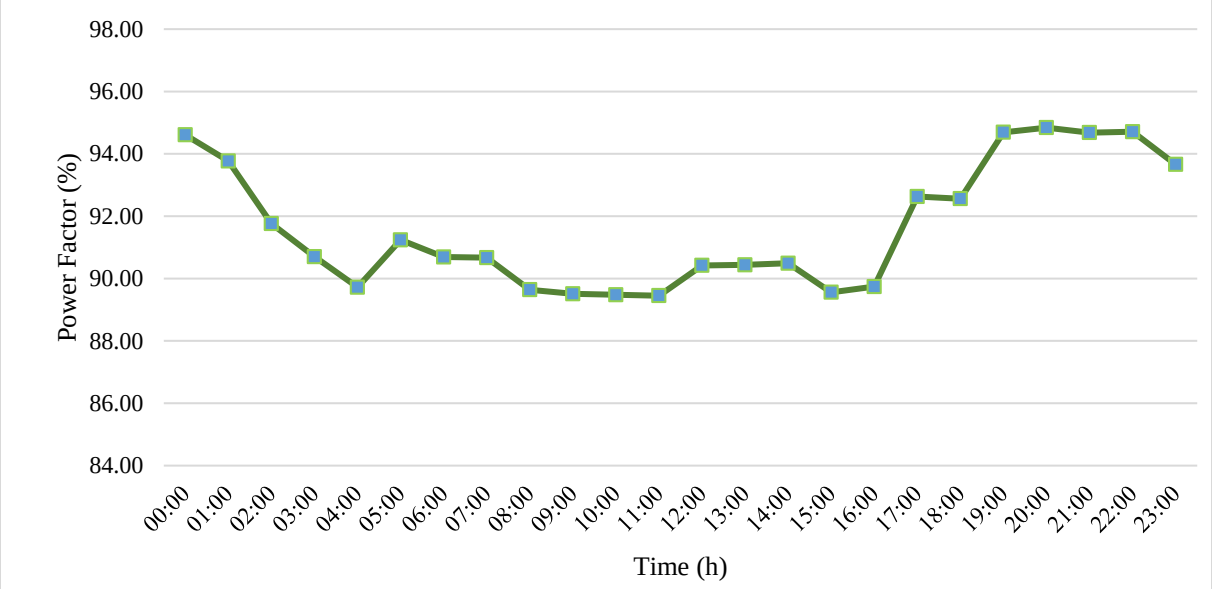

Figure 3. 22: Daily Power factor profile of the PPU distribution transformer.

The allocation factor method is not the only way for determining the loading of the distribution transformers along a feeder, but there are different methods such a diversity factor approach or even to measure the loading for each transformer by metering system. However, the main problem in majority of distribution system is the lacks of precise data about the loads, as a result, the needs of the up mentioned methods.

Each load determination approach used in the distribution system has its advantages and drawbacks, the diversity factor approach generates the load profile closed to the maximum demand pointes. On the other hand, using a metering system on each bus of the feeder is highly expansive method and the continues expansion in the distribution system stands as a major obstacle. In this thesis the allocation factor approach was used for generating a load profile for each distribution transformer.

One of the main problems in this system is the loading of the distribution transformer not measured. However, the AF was used to identify each loading value for each distribution transformer and to make a real validation for the generated load profiles, additionally the real justification of this approach considered through the PPU distribution transformer which is the only bus that has an hourly metering system that recording an importing and exporting power value as shown in fig.3.23. Besides the PPU distributed transformer connected with a PV power plant which feeding the PPU loads at the same instant by its required energy, therefore to determine the average daily PPU real load profile the eq 3.1 is applied hour by hour.

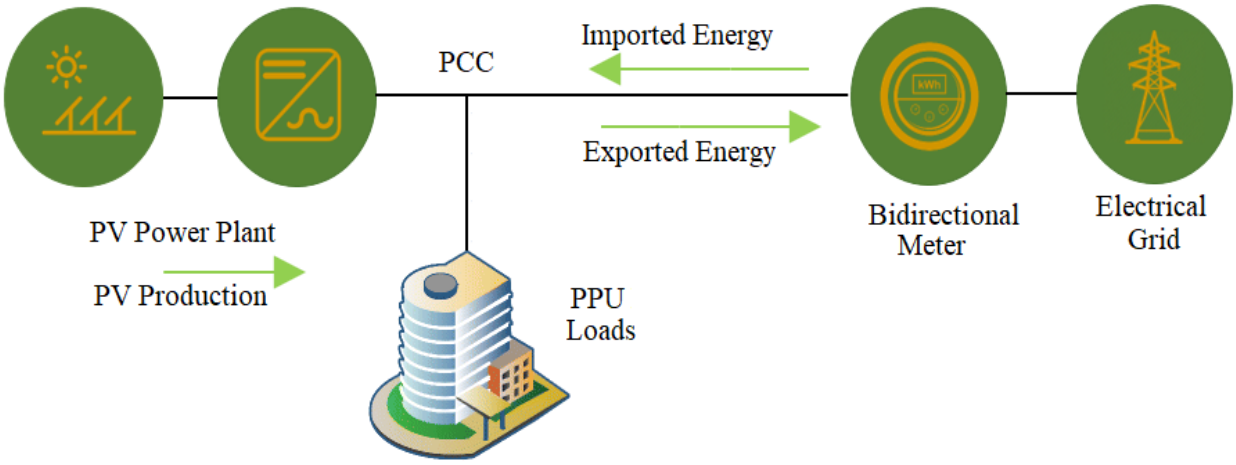

Figure 3.23: The Metering system configuration of the PPU distribution transformer.

PPU Load = Imported Energy + PV Production – Exported Energy *(3.1)*

Fig. 3.24 illustrates the PPU PV system average daily production based on the monitoring system for the eleven inverters of the 230.1 kWp PV plant, in addition to the average daily imported power from the grid that recorded at the PPU distribution transformer metering system.

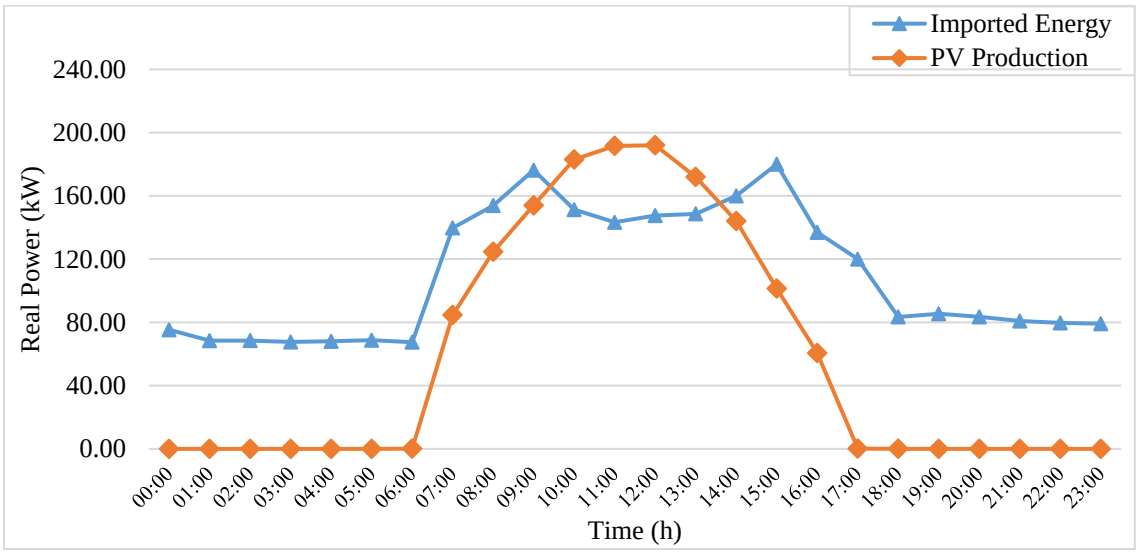

Figure 3.24: Active power profile for PV production and importing energy from grid.

For real validation issue of the allocation factor approach the comparison have been done between the measured active power profile and the active power profile generated by the AF approach as fig.3.25 illustrates. Therefore, the relative error between the real measured and the generated by the AF was varying between (3.1-12.54) and the average value during a whole day is 8.43%, with reference to this, it can be illustrated as 9.23% error during a night time and 6.83% during a midday time, these values in error are justified due to the high number of domestic users along the feeder that have a high consumption during a night which differs than the PPU demanding pattern.

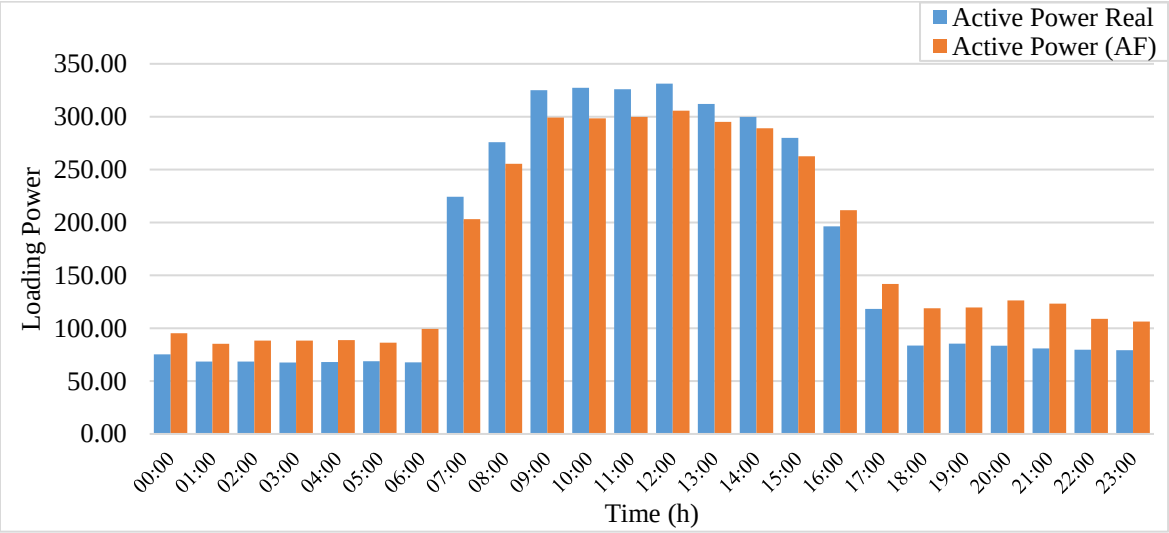

Figure 3.25: Average daily PPU load Profile in real case and AF determination.

3.5: Description of PPU_PV system

Palestine is situated between (29.15º – 33.15º) north latitude and (34.15º – 35.14º) longitude east. And the elevation ranges from 350m below the see level and exceeds 1000m above the Mediterranean Sea which is an ideal location for solar energy utilization. Palestine has about 3000 sun shine hours per year. The annual solar radiation on horizontal surface varies from 2.63 kWh/m^2 daily in December to 8.41 kWh/m^2 daily in June, with yearly average value of 5.4 kWh/m^2 [19]. Fig 3.27 represent the Palestinian solar Atlas.

Hebron is situated at 31.54° N latitude and 35.1° longitude. The daily average solar radiation varies between (2.7 to 8.2) kWh/ m^2 daily. Maximum amount of radiation is available during the months of June -July and minimum on December-January. Monthly global solar insolation and daily average bright sunshine hours in Hebron city are presented in the table 3.7. These values are a 22-year ago average solar insolation from the test reference years of METEONORM.

Table 3. 7: Monthly global solar insolation at Hebron.

Month	Solar insolation (kWh/m^2-day)	Month	Solar insolation (kWh/m^2-day)
January	2.69	July	7.95
February	3.20	August	7.70
March	4.95	September	6.27
April	6.20	October	4.35
May	7.27	November	3.50
June	8.20	December	2.75

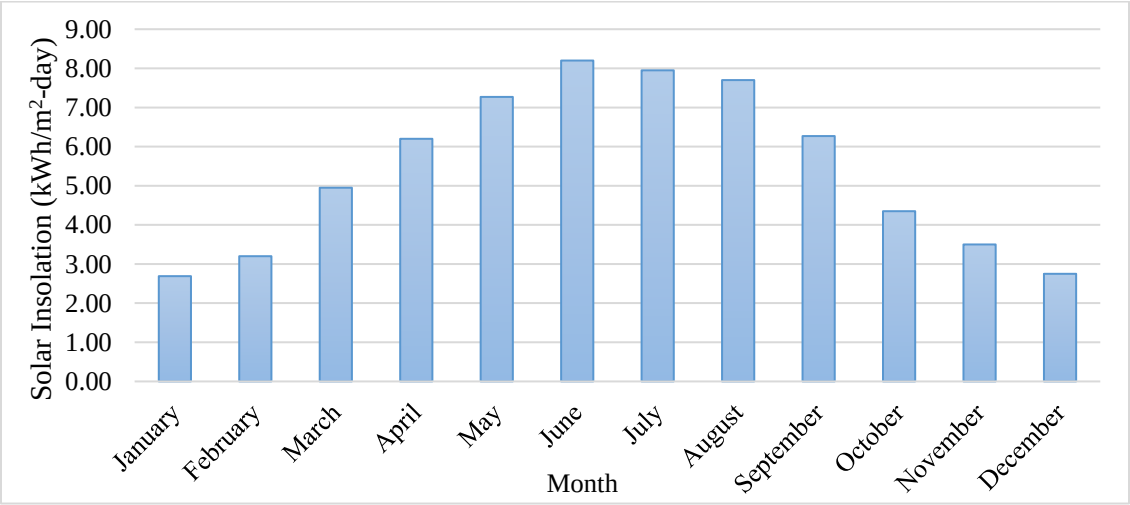

Figure 3.26: Column Diagram of Monthly Average Solar Potential in Hebron Area.

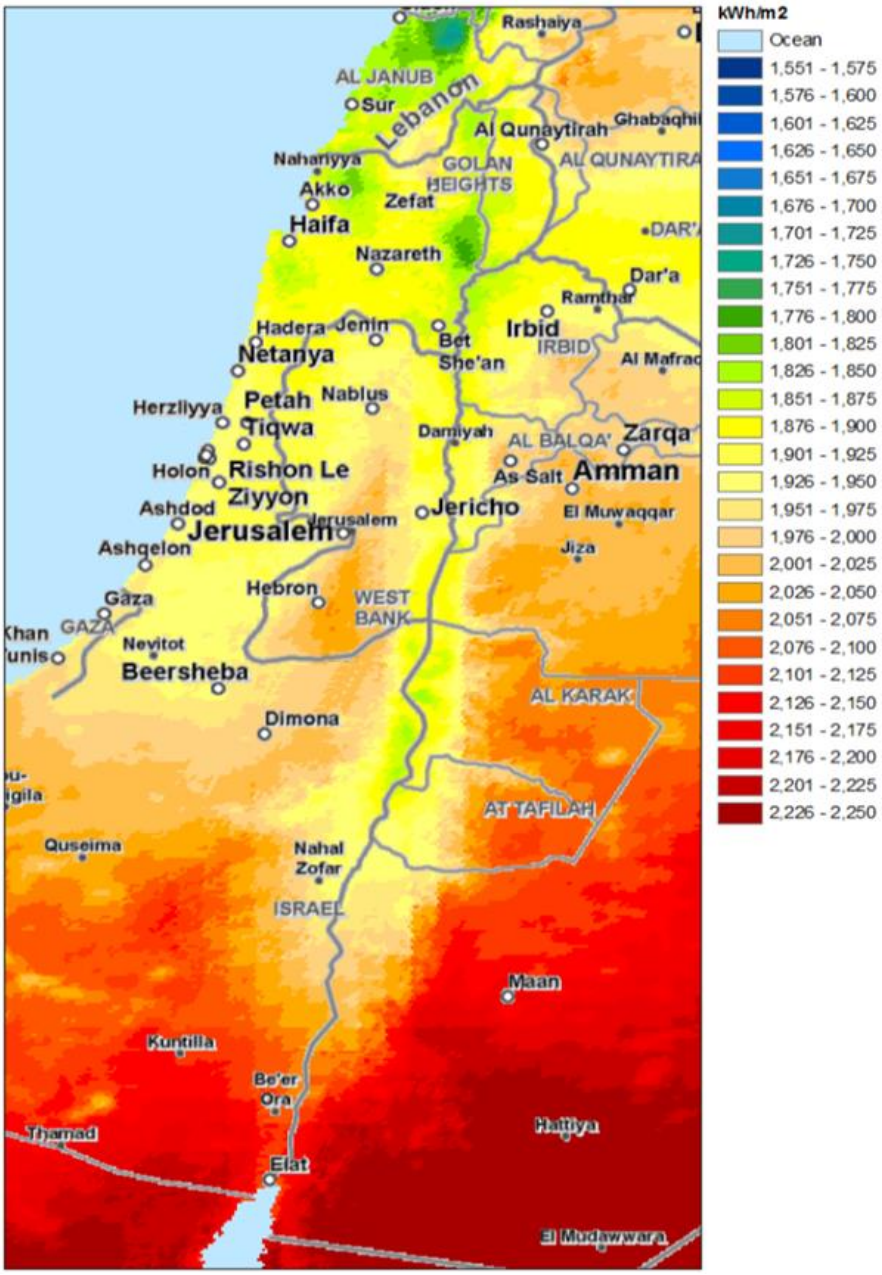

Figure 3.27: Solar Atlas for Palestine in kWh/m^{2,} Focus Solar Website, Regional Maps of Middle East, Map of Palestine.

PPU PV grid-connected plant is located on a roof top of the PPU campus at Hebron-Palestine. Fig.3.28 presents the real system placement, which is located at the end point of the MV 11kV PPU feeder which is 2900 m long from the station number 7 of the HEPDS grid, Its worth mentioning that the PPU load connected at the secondary side of a 11/0.4 kV 1000 kVA distribution transformer. Moreover, a 230 kW$_P$ PV system was built on the roof of the University buildings, the PV system contains 708 PV panels 325 W and 11 inverter 21 kW per each. Appendix D represents the data sheet of the PV panels and the inverters

Figure 3.28: Satellite photo of the PPU PV System.

Fig. 3.29 represents the single line diagram of the system configuration and the integration approach with the HEPDS, the SLD is for two inverters and the all inverters is the same, as a result the average daily generated power from this system which produced by the averaging of the daily production by the monitoring system of the whole inverters in system as illustrated in fig. 3.30.

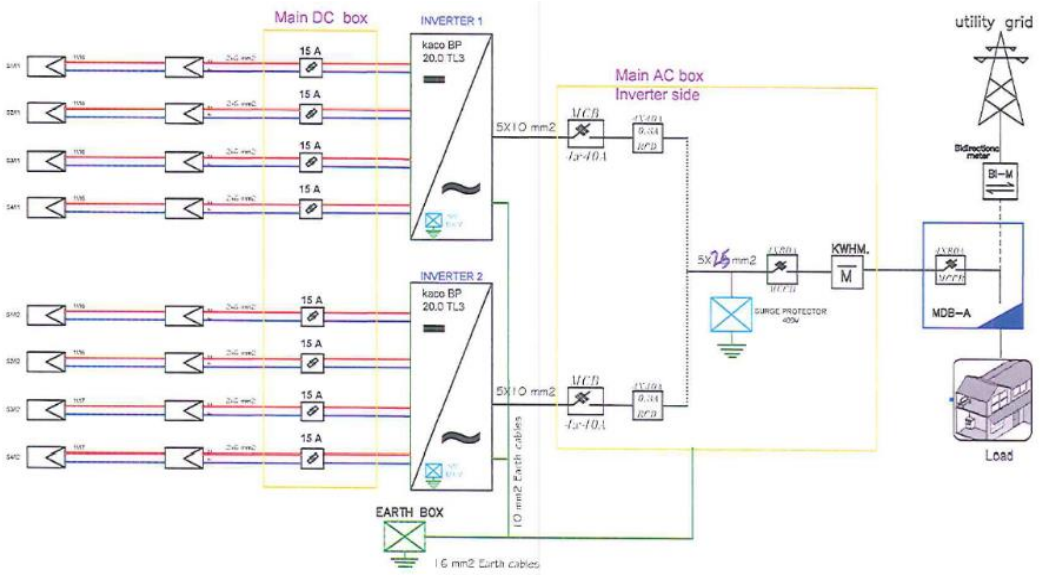

Figure 3. 29: Single line diagram of two inverter from the PPU PV plant.

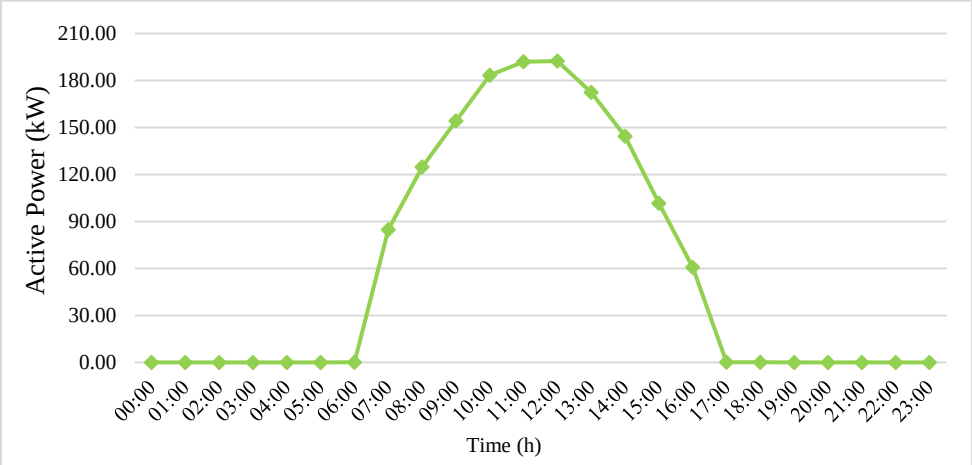

Figure 3. 30: PV system average daily generation.

4

Chapter Four

PV and BESS integration Impact at the Grid profiles

4.1: Introduction

In the new grid generation and the developed cities PV systems are mostly used for electricity production to reduce the dependency on the traditional sources but the power output from the sun can be fluctuations with a sudden time seconds-scale. PV generation penetration within residential and commercial feeders will change the network profiles and parameters. Climate fluctuations such as clouds, cause large power fluctuations at the output of the PV solar facility. Meanwhile, the using of software for analyzing the network with a numerical method became more commonly, because of its accuracy of measurements and the large number of parameters to observe. As a result, it will help the grid for planning and forecasting, and the ability to solve the problems.

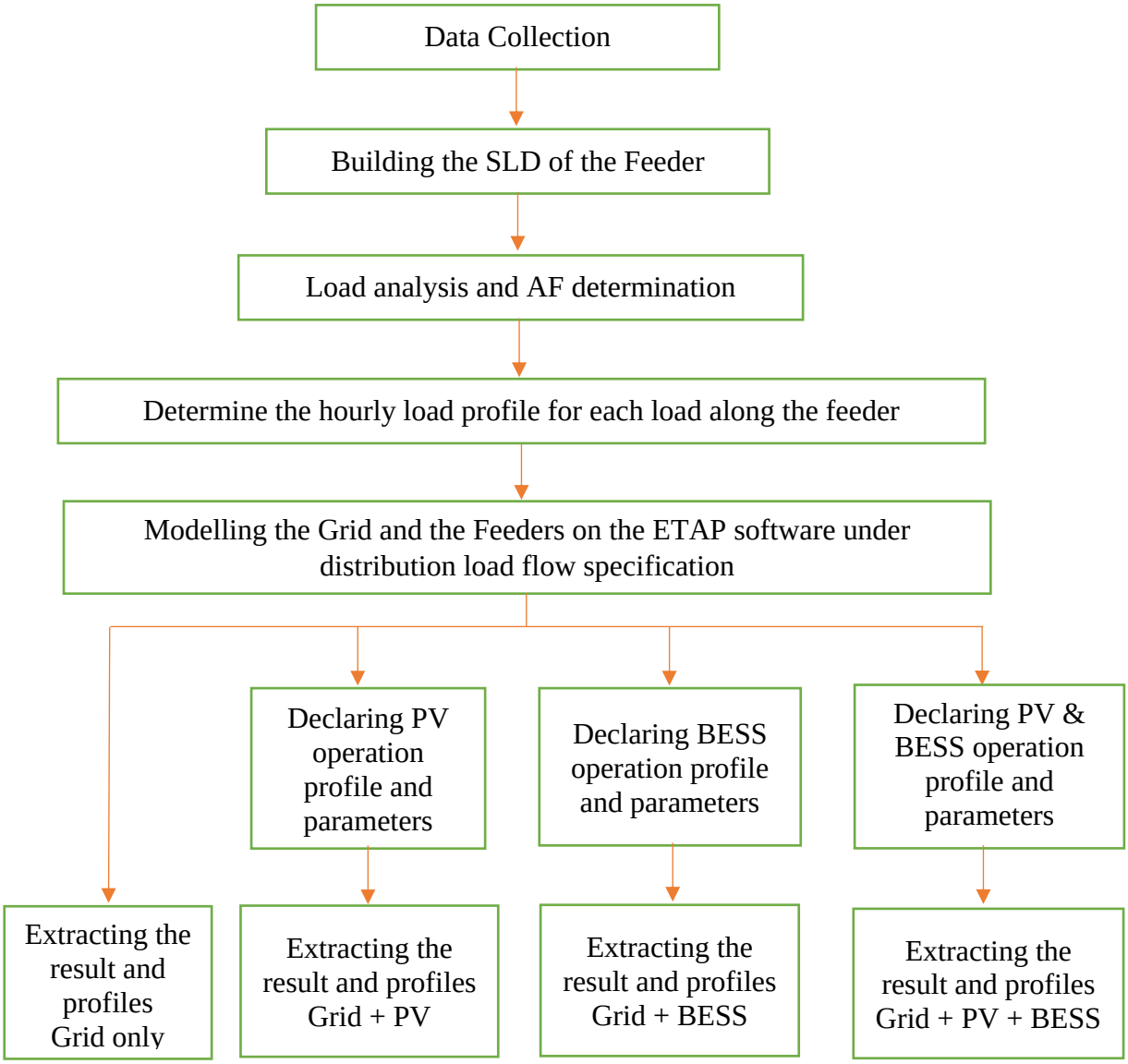

Figure 4.1: Methodology Block diagram.

4.2: Feeders ETAP Modelling

Modelling and simulation of a real power system network of the power Tr. 1 feeders PPU and ZAL feeder were considered, a single line diagram (SLD) is modelled using ETAP 16.0.0 software. All the physical and electrical parameters of the power system including height of towers, spacing between transmission lines, resistance and reactance values of transmission lines, transformer and interconnection point ratings etc. Then the distribution mode solver of load flow study, harmonics analysis and short circuit analysis are conducted using the same software and simulation results are analyzed. However, the grid feeders are built in the ETAP and then the integration of the photovoltaic system in addition to the Battery Energy Storage system (BESS).

Integration of photovoltaic (PV) systems with certain penetration level may introduce many of adverse impacts on a grid operation. Voltage rise, reverse power flow and voltage unbalance can be listed as some of the major impacts however the BESS will play its role in some cases to minimise this effect. In this thesis ETAP Electrical Transient Analyzer Program used under the calibration of distribution system power flow solver to design the integrated electrical network and distribution feeders, and which can provide many types of analysis such as the balanced load power flow unbalance load, in addition to analyse power systems, THD, short circuit analysis.

In this chapter modelling has been performed using the ETAP software based on the single-line diagram and the data of the Feeder. Load-flow analysis under steady-state condition has been done to simulate the condition before and after installing the 230 kW_P PV power plants which already built in PPU in addition to conducting a propose 126 kWh BESS to minimize the PV effect on the peak production. Load flow simulation has been undertaken by defining one bus as slack-bus with voltage of 1.0 p.u which is the interconnection point bus. It's worth mentioning that the PPU PV system connected with a low voltage bus near the load which mean that the generated energy may consumed by the load directly or send to the MV feeder, fig. 4.2 shows the single line diagram of the PPU feeder which conducted on ETAP.

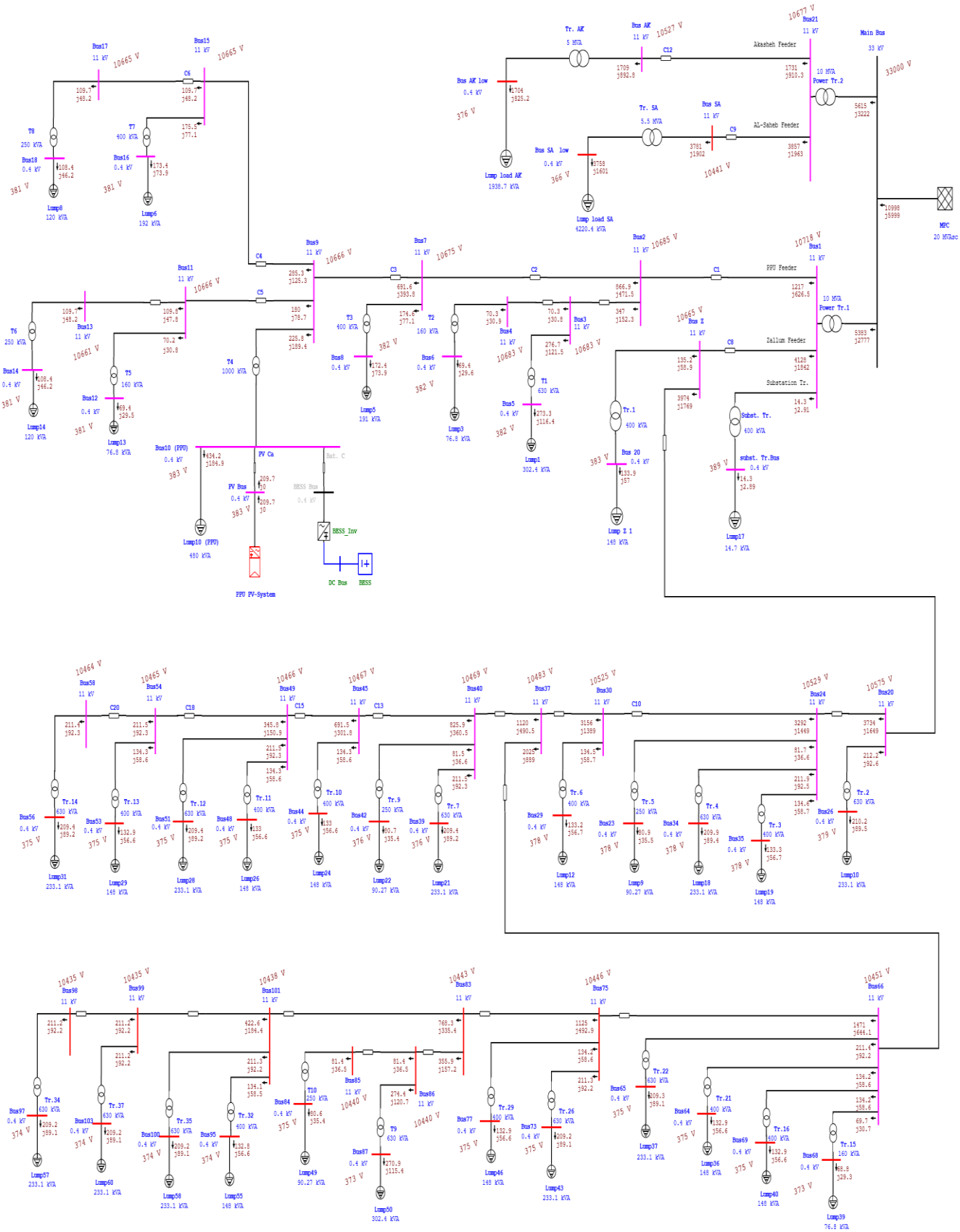

Figure 4.2: Single line diagram of the PPU & ZAL feeder on the ETAP.

The analysis of the feeders and the up-mentioned single line diagram will be conducted in four scenarios along a day as the load profile generated hour by hour:

- Grid only.
- Grid + PV system.
- Grid + BESS.
- Grid + PV + BESS.

The connection of the DG whatever it is on the electrical grid has direct impact on the operation and performance of the network, there are some changes to the characteristics of the network such as the voltage profile, powers and the power factor, harmonics components and the short circuit capacity. The output result from ETAP Modelling cases will be present on two main point on the grid feeders first on the main bus bar of the feeder, secondly on the PPU Point of common coupling (PCC) bus. Fig. 4.3 demonstrate the names of points that will be use on this chapter.

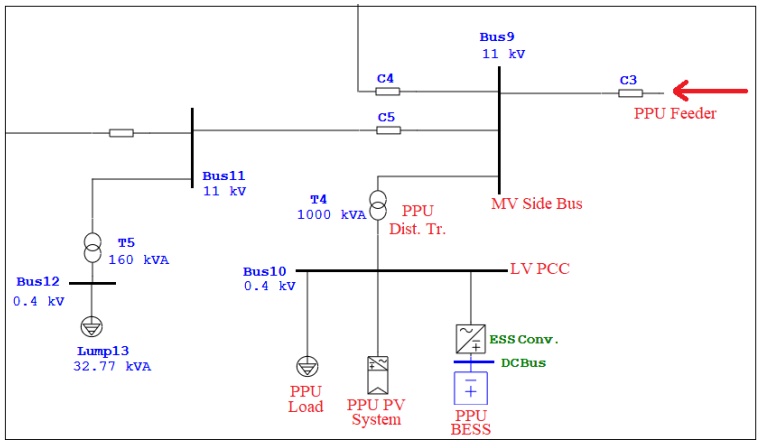

Figure 4.3: PPU load, PV system and BESS configuration.

At the beginning based on the load profile which is generated along 24 hours a day on average the operation average daily profile of the PV system and the operating modes, fig. 4.4 represent the average daily generated energy produced from the 230kW$_P$ PPU photovoltaic system in kW which is represented in chapter 3.

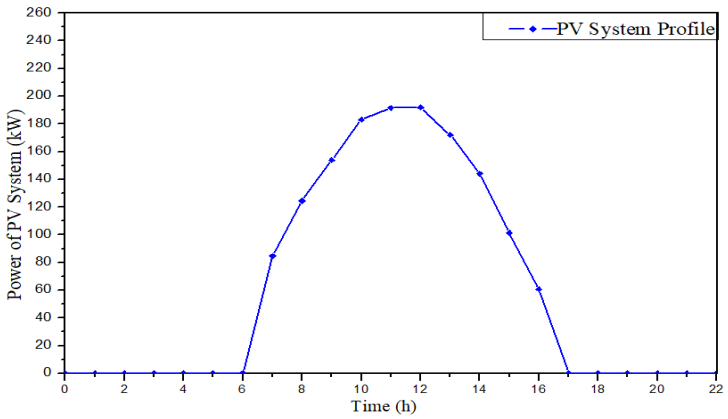

Figure 4.4: PPU PV system average daily load profile.

On the other hand, the operating profile of the charging and discharging system of the battery energy storage system build based on the PV system operation regarding to the aim of the BESS in the proposed method. The charging of the BESS will be along the minimum peak sun hours in the most yearly days to minimize the effect of the PV system on the grid quality parameters in addition to guarantee that the BESS will always charge by the PV system, consequently this is what will explain the operation profile in fig. 4.5 and the discharging period located the night time and when the domestic loads high.

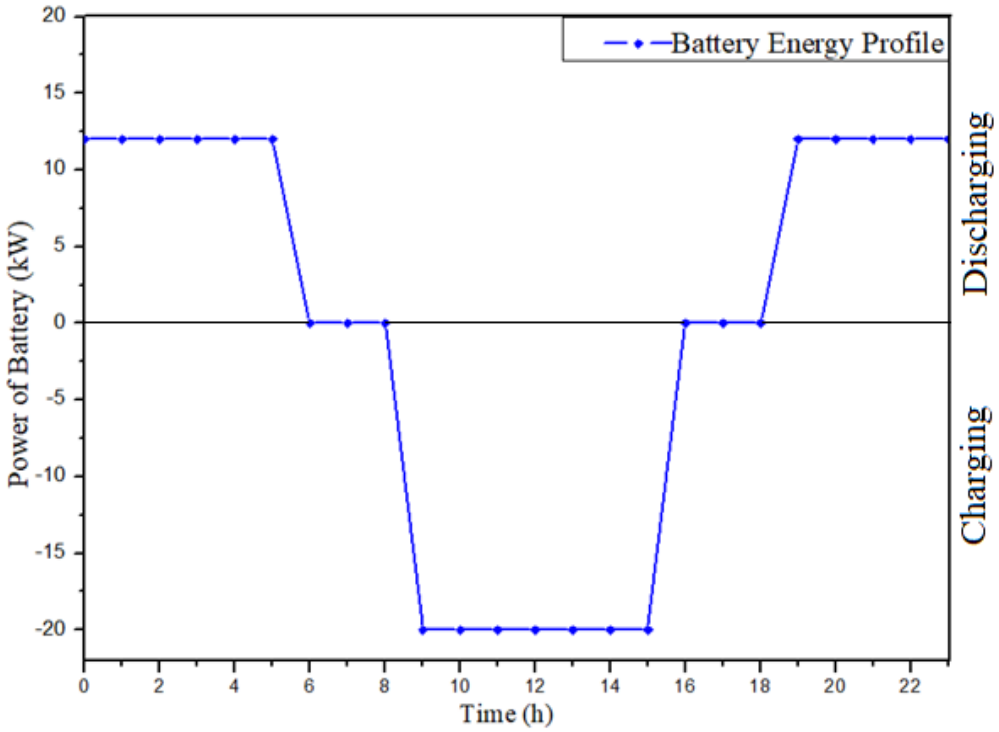

Figure 4.5: BESS energy flow profile.

This BESS based of [57] a residential/commercial building integrated a PV system and BESS, and the duration operating mode of battery out energy is much higher than 1 hour as mentioned before in chapter 2. Fig 2.19 for BESS application this operation mode will be for Grid support, enhancing and peak generation shaving, which leads to determination of the BESS capacity which is depend on the PV plant rating based on [57] the optimum BESS capacity of the PV-BESS plant is 55% of the PV rated power. In this thesis the PV plant rating was 230kW$_P$ therefore the BESS capacity is 126 kWh and the operation curve will be as in fig. 4.5 it was illustrated based on the Wolfs-Winkel project and the charging mode will be on the exact peak hours of the PV production for the yearly profile and discharging mode will be on the night period when there is no sun for PV operation.

4.3: Grid with PV system integration.

In this section the effect of integrating PV system with electrical network will be shown and discussed and all observed parameters will take into consideration in two main point, the main bus of the feeders and the second point is the PCC and the output result from the ETAP in **Appendix E.**

4.3.1: Main bus profile results.

4.3.1.1: Voltage Profile.

The literature indicates clearly that integrated DG could impact the voltage of the distribution grid, From the selected feeder, the voltage profile was simulated at the main bus and the voltage was increased slightly at the main MV bus after adding PV, and the voltage profile at the main bus increases by 0.03% only due to the low PV contribution of the feeder demand, which still within the IEEE standard. Fig. 4.6,7 shows the voltage profile of the main bus and the present of voltage drop with and without PV.

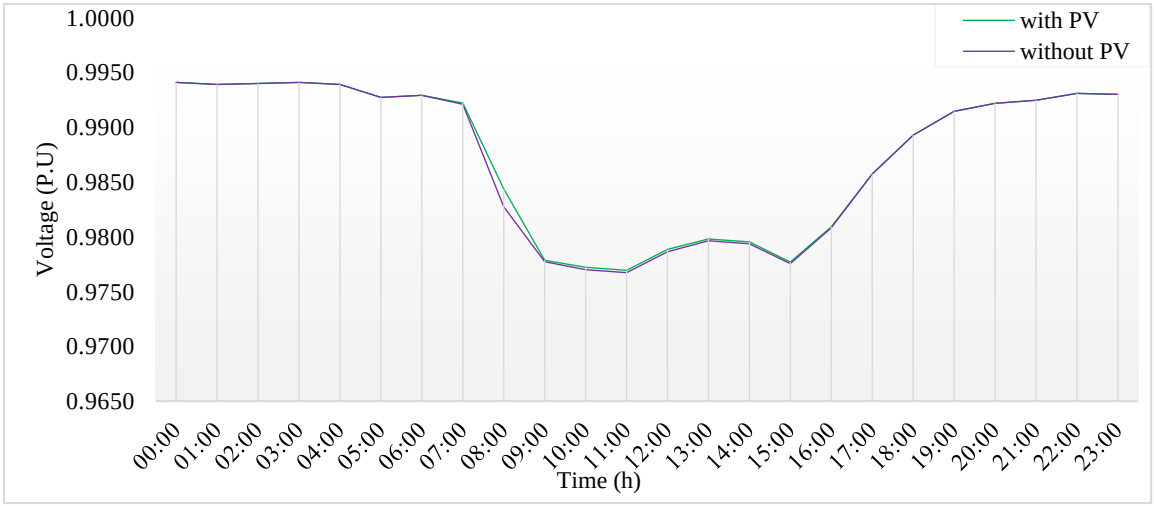

Figure 4.6: Voltage profile at the main bus of the feeder.

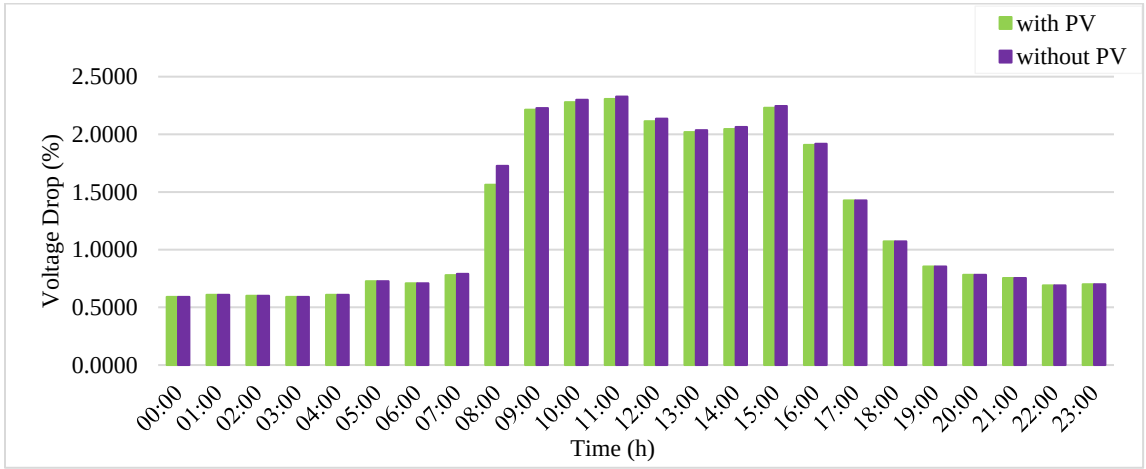

Figure 4.7: Voltage drop per hour at the main bus of the PPU feeder.

4.3.1.2: Power and Power factor results.

The production of solar energy should be as high as possible at the mid-day, depending on radiation value and ambient temperature. Household load demand is comparatively high during this time, and real power generation from PV sources is high too, means that the demanded real power from the feeder will decreases but the reactive power will be the same. Therefore, it may exceed the load level at the PV connection point at this time, and voltage rise may be observed especially at high penetration level. After the PV system installed at the feeder the real power drown from the grid was decreased and the power factor was getting worse. Fig. 4.8,9,10,11 shows the powers and the power factor at the main bus of the feeder.

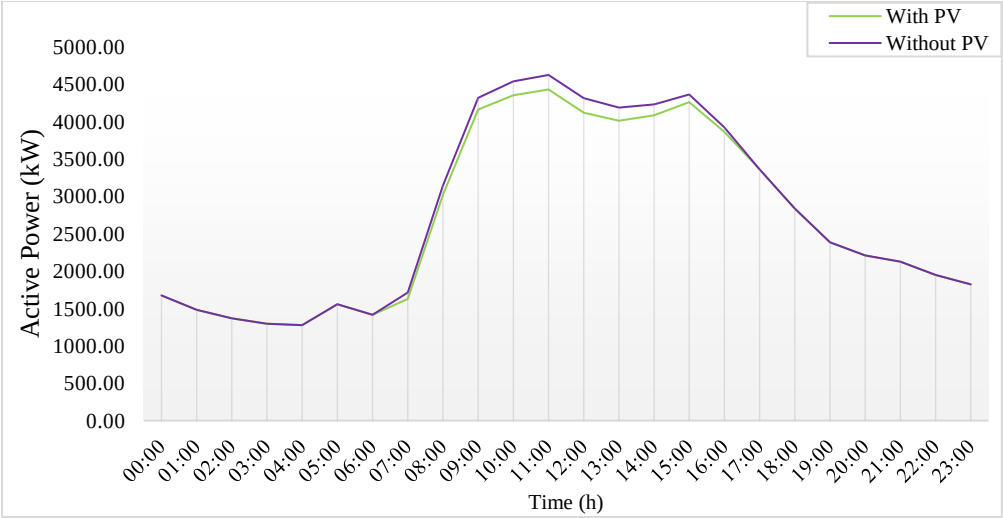

Figure 4.8: Active power at the main bus with and without PV.

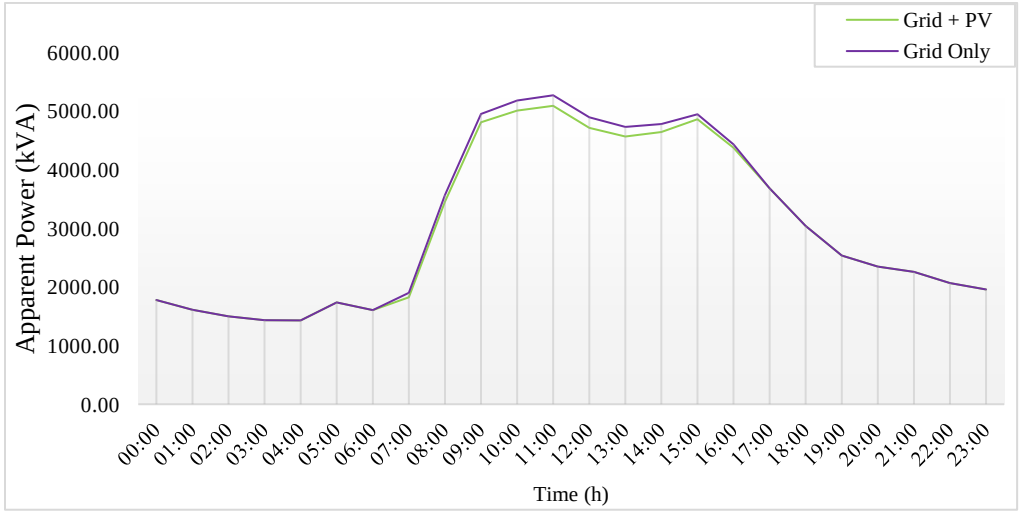

Figure 4.9: Apparent power at the main bus with and without PV.

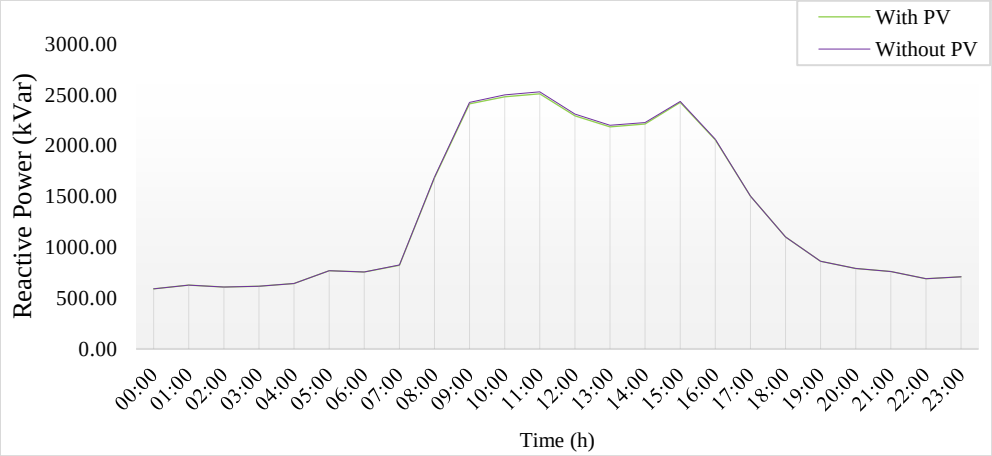

Figure 4.10: Reactive power at the main bus with and without PV.

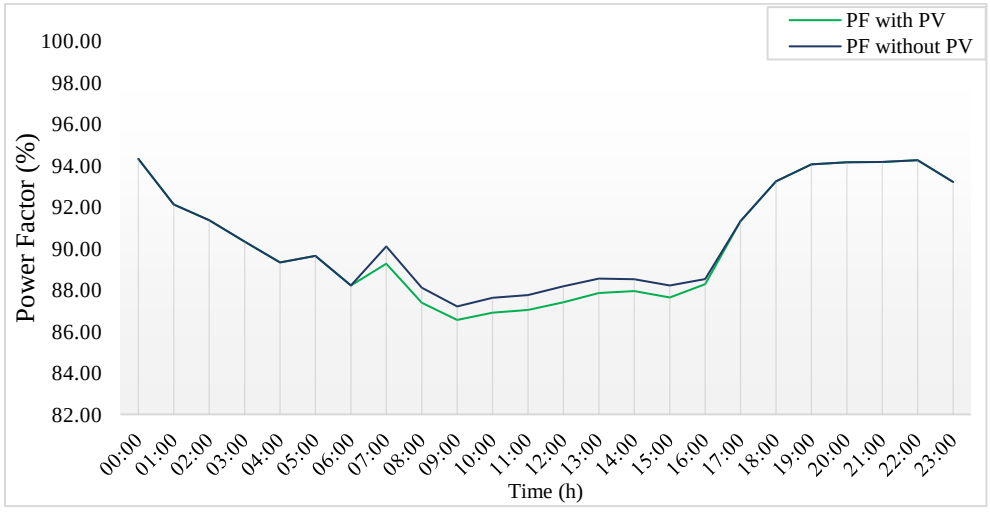

Figure 4.11: Power Factor (PF) at the main bus with and without PV.

4.3.1.3: Active & Reactive Power loss at the PPU feeder.

In normal case the power flows from the interconnection point to the distribution feeders, distribution transformers and to reach the loads at the end. During this path there are a voltage drop and loss in the transmission cables in the form of power loss, it is directly proportional with the length of the feeder. It's worth mentioning, that in the AC system the power loss along the line divided into two main types of losses active power produced by the resistance, and reactive power formed by the reactance of the lines and cables. Fig. 4.12,13 represent the active and reactive power loss profile along the PPU feeder in the case of installing and absence of the PV system.

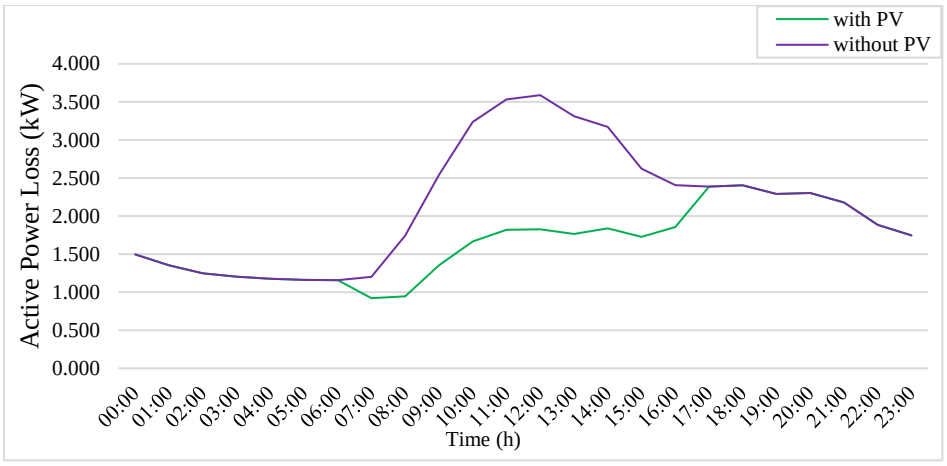

Figure 4.12: Real Power loss in the PPU feeder in kW.

However, integrating the PV-DG with the electrical network will lead to decreases this loss especially at the peak generation time of the PV, and regarding the PV inverters are calibrated with a unity power factor the production of the system will be pure active power, therefore the near load will be feed by the system and the real power loss was decreases clearly after adding the PV system. But the loss of the reactive power along the feeder slaitly decreases. So, the active power demanded by the customers is supplied by the PV plant, which reducing the demand of active power from the grid.

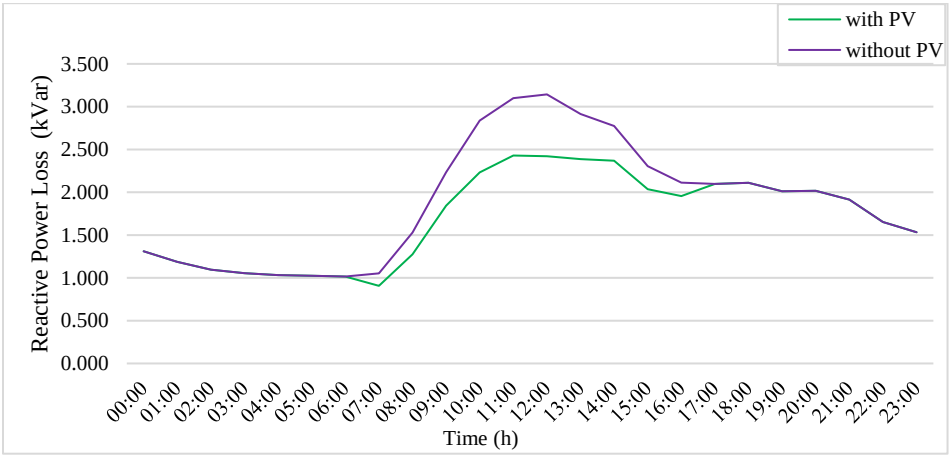

Figure 4.13: Reactive Power loss in the PPU feeder in kVar.

4.3.2: PCC bus profile results.

4.3.2.1: Voltage Profile.

The PPU PV system was connected with the grid through a 1000 kVA distribution transformer and tied at the low voltage side, integrating DG could impact the voltage profile at the distribution grid particularly on the Point of Common Cabling (PCC) of the feeder, the voltage profile was simulated at the LV bus and the voltage was increased clearly at the PCC bus, and the voltage level at the bus increases by 0.45% at the PCC with only 14.7% of PV penetration level of the feeder with, which still within the IEEE standard.

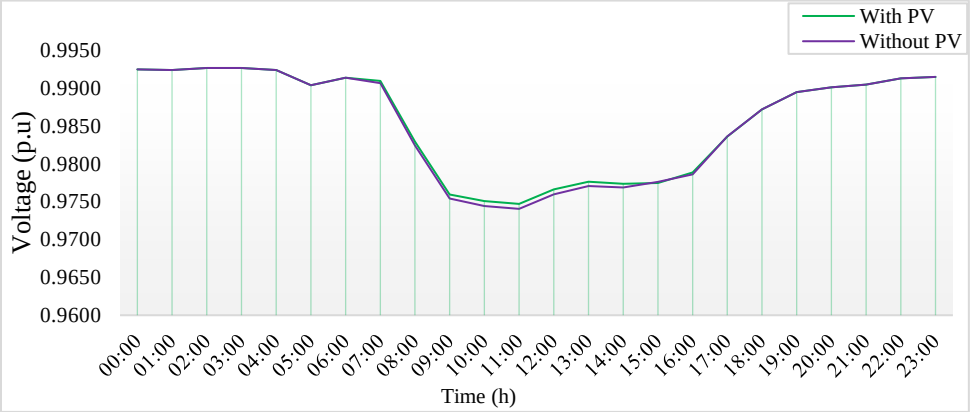

Figure 4.14: Voltage profile at the MV side of the distribution transformer with and without PV.

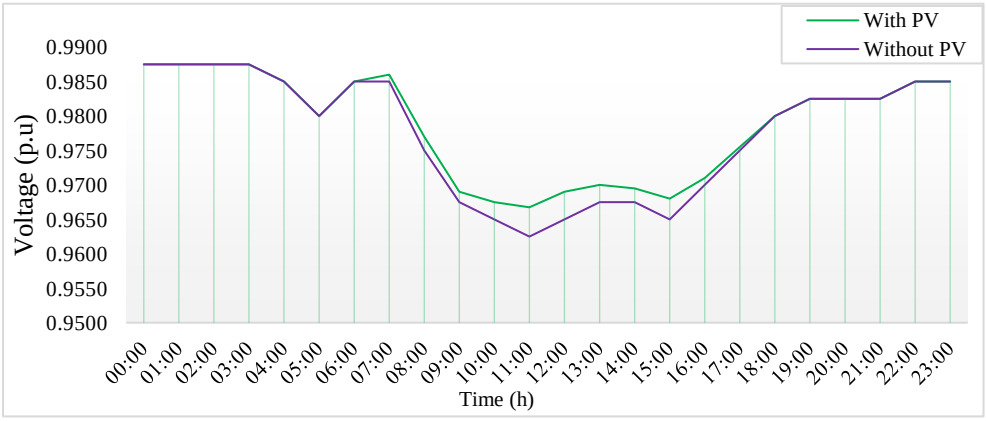

Figure 4.15: Voltage profile at the PCC LV side of distribution transformer with and without PV.

Fig. 4.15 shows the voltage profile of the PCC low voltage side bus of the distribution transformer and the voltage raising was clearly appear particularly at the peak time, besides fig. 4.14 represent the voltage profile at the MV bus side of the distribution transformer and the observation was the effect of PV generation at the MV level of the feeder is much lower than the LV level. and voltage drop at the PCC are clearly decreases after adding the PV plant as fig. 4.16 represent.

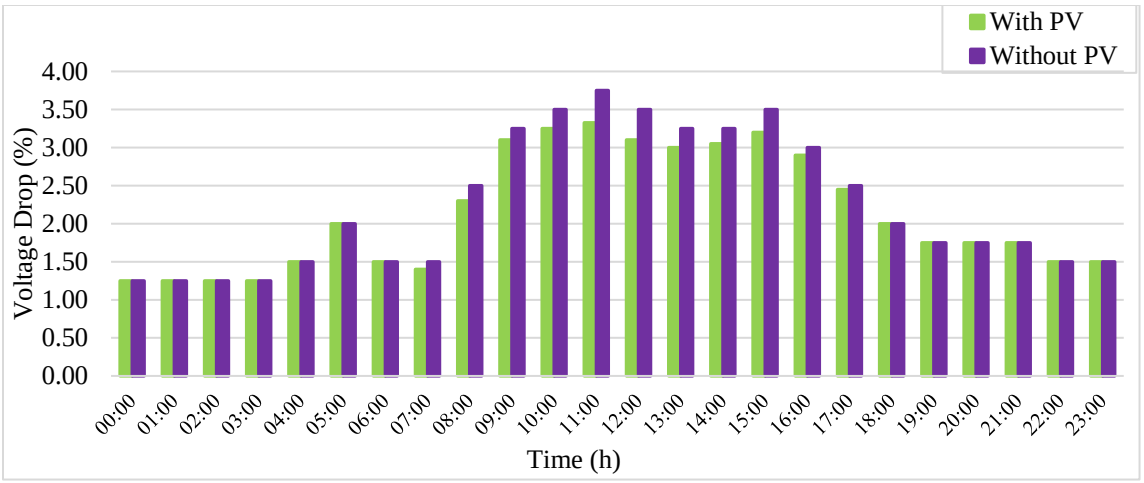

Figure 4.16: Voltage drop per hour at the PCC of the PPU feeder.

4.3.2.2: Power and current Profile.

The production of solar energy should be as high as possible in the middle of the day, depending on climatic conditions and temperature. Also, the peak load of the PPU is at the middle of the day, which mean that the energy demand was high at the noon and which is perfect to PV plant production. Therefore, the active power profile will be changed from the feeder side.

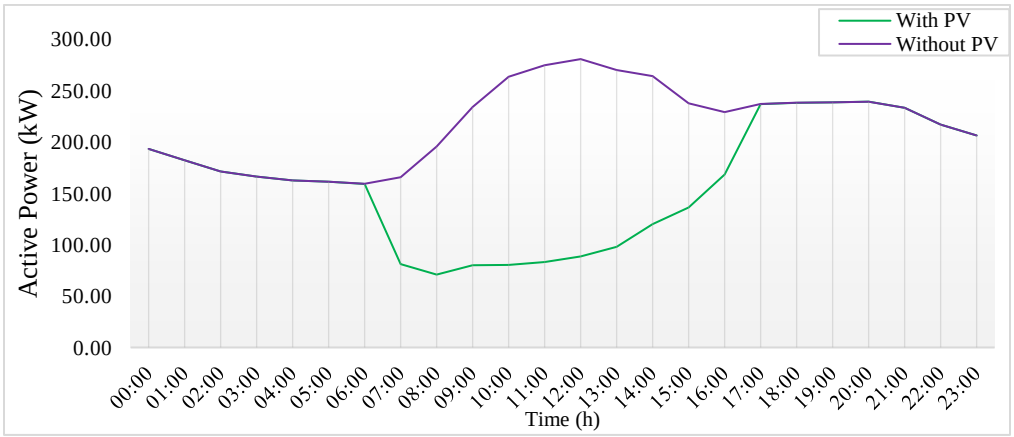

Figure 4.17: Active Power Consumed from the PCC Grid Side.

PV power plant integration to a distribution network will contribute to generate the active power with the grid. So, the active power supplied from the utilities will be decreased. However, to accomplish the optimum performance of the PV power conditioning units the operation will be at unity power factor to maximize the active power generated. A higher rate of reactive power supply is not preferred by the utility because; in case of high rate of reactive power to the grid, the distribution transformers will operate at a very low power factor, so transformers efficiency decreases as their operating power factor decreases, as a result, the overall losses in distribution transformers will increase which reducing the overall system efficiency.

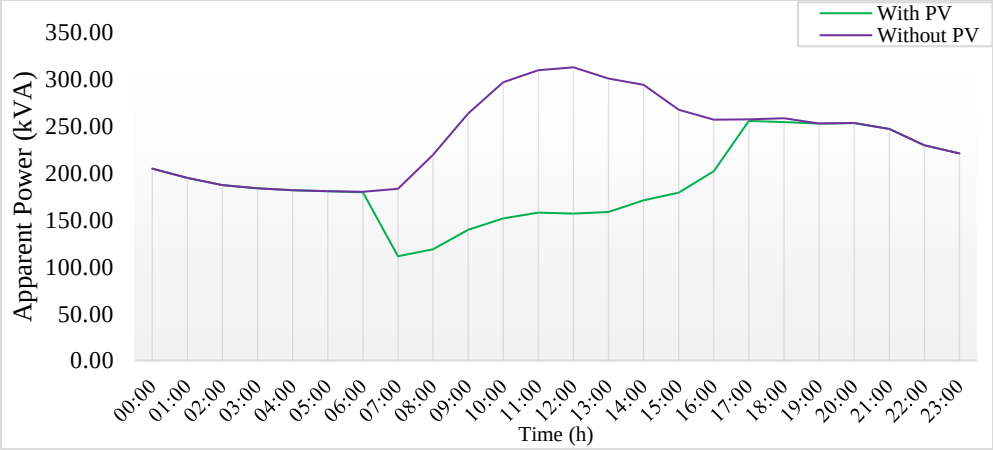

Figure 4.18: Apparent Power Consumed from the PCC Grid Side.

From fig. 4.17,18 after integrating the PV plant to the distribution feeder, the active power consumption from the grid side was decreases gradually because of the active power generated from the PV plant, besides the apparent power will decrease as a result, and the power factor too. But the reactive power that needed from the grid side will be the same because of the inverters of the PV plant will operate at unity power factor.

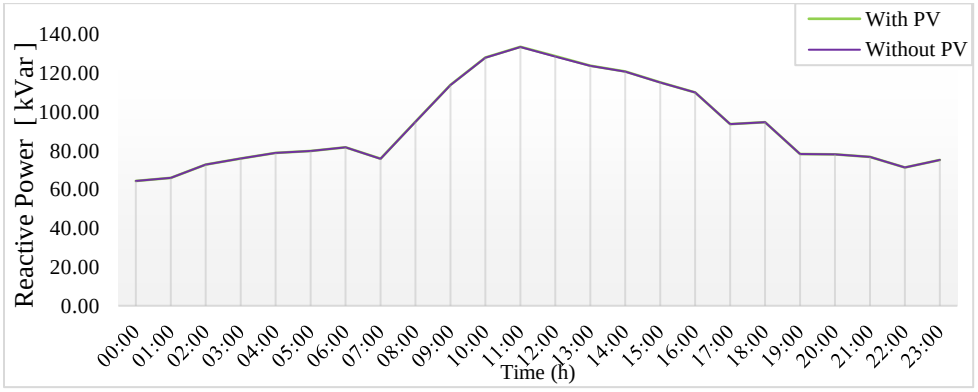

Figure 4.19: Reactive Power Consumed from the PCC Grid Side.

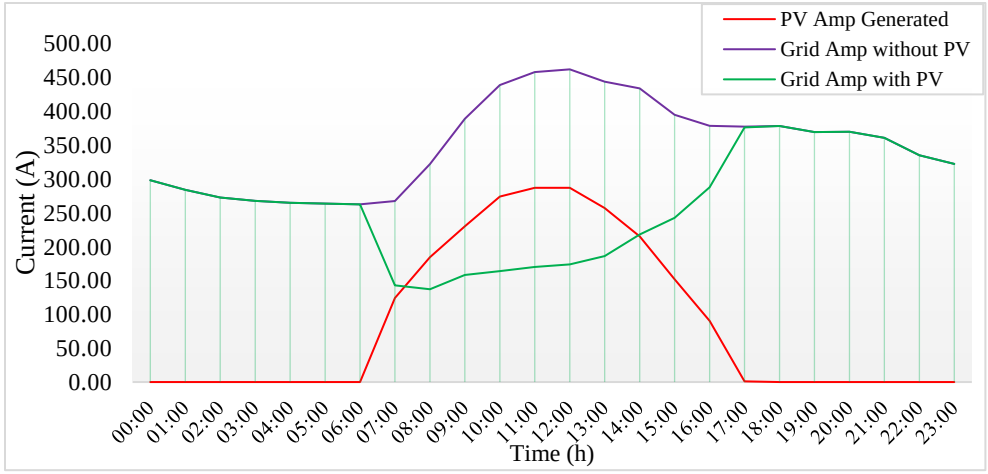

Figure 4.20: Current profile at the PCC (Amp).

4.3.2.3: Power factor Profile.

The PV power plant reduce the active power consumption from the electrical grid and the reactive power demanding remains constant, besides of the PV inverters which operated at unity power factor, at high PV penetration power the conditions got worst, and as can be observed in fig. 4.21 the power factor decreases to unacceptable levels during PV system operation. When PV system works with high power the most active power demanded by the customers is supplied by the PV plant, reducing the demand of active power from the grid and reactive power demand is the same, so it causes a low power factor measured at the PCC.

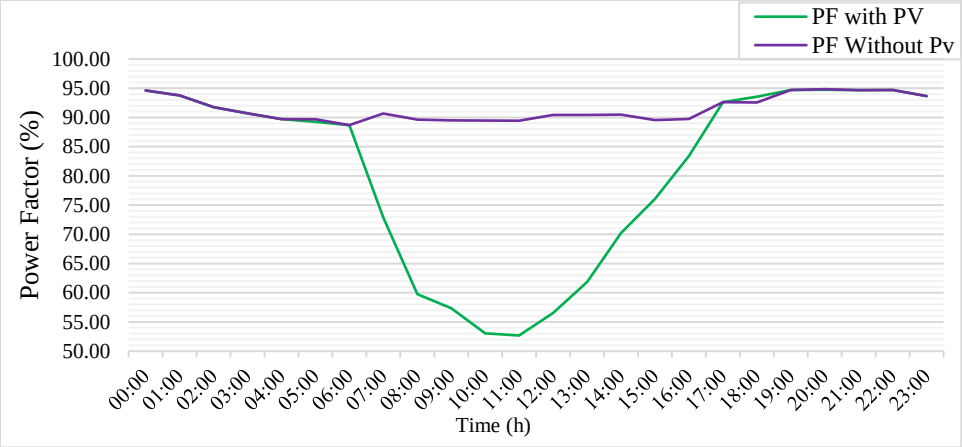

Figure 4.21: Power factor at PCC the low voltage side of the PPU distribution transformer.

PPU-PV system connected on the LV side of the distribution transformer and the excess energy will export to the MV grid and from fig. 4. 21,22 the effect of the PV on the PCC is much higher than the MV bus of distribution transformer, since at LV the PV system facing the PPU load only but at the MV side the whole feeder is the load, therefor At the peak generation from the PV system the power factor goes down gradually at the LV side of the PPU distribution transformer and reach to extreme values like 53%. On the other hand, at the MV side of the distribution transformer the effect of the power factor wasn't exceed 82% at the peak generation point.

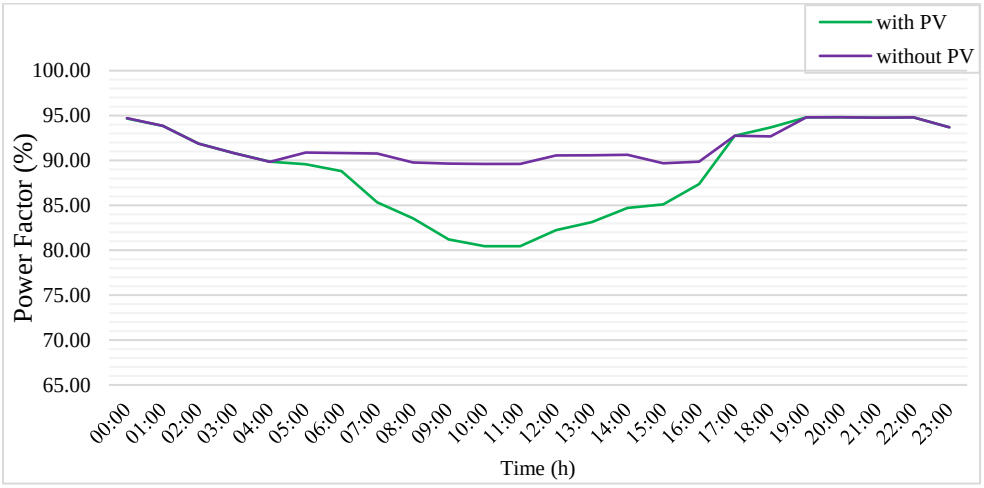

Figure 4.22: Power factor at the Medium voltage side of the PPU distribution transformer.

4.4: Grid with BESS integration.

In this section a special case study will be observed which an effect of integrating BESS with electrical network only without any other DG the all results will be shown and discussed and all observed parameters will be taken in consideration in two main points, the main bus of the feeders and the second point is the PCC and the output result from the ETAP in **Appendix E.**

4.4.1: Main bus profile results.

4.4.1.1: Voltage Profile.

Integration of DG could impact the voltage of the distribution grid, the BESS integrated with the grid only at the selected feeder in the same rating which is 126kWh and with operation profile of charging during a day and discharging during the night, this condition will have approximately no effect at the main bus feeder which is demanded by 4.5 MW, as voltage profile at the main bus illustrate the voltage was approximately not changed at the main MV bus after adding BESS. Fig. 4.23,24 shows the voltage profile of the main bus and the voltage drop with and without BESS.

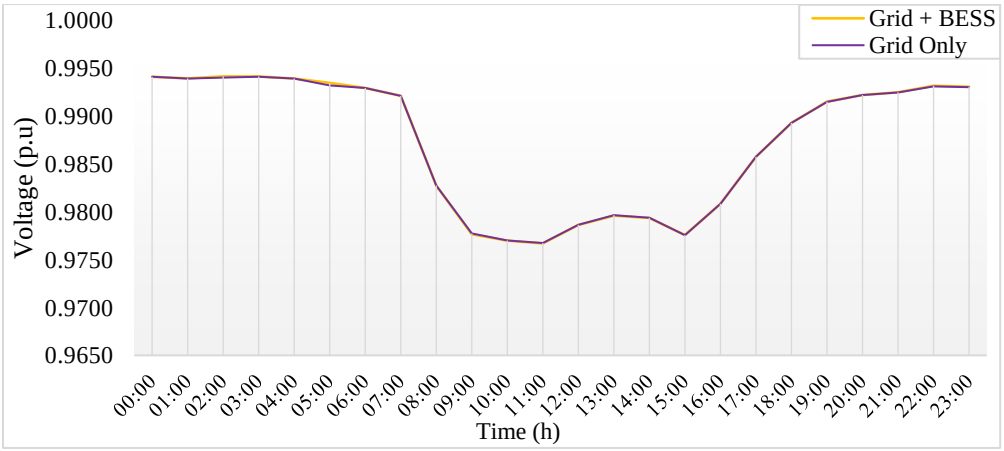

Figure 4.23: Voltage profile at the main bus of the feeder.

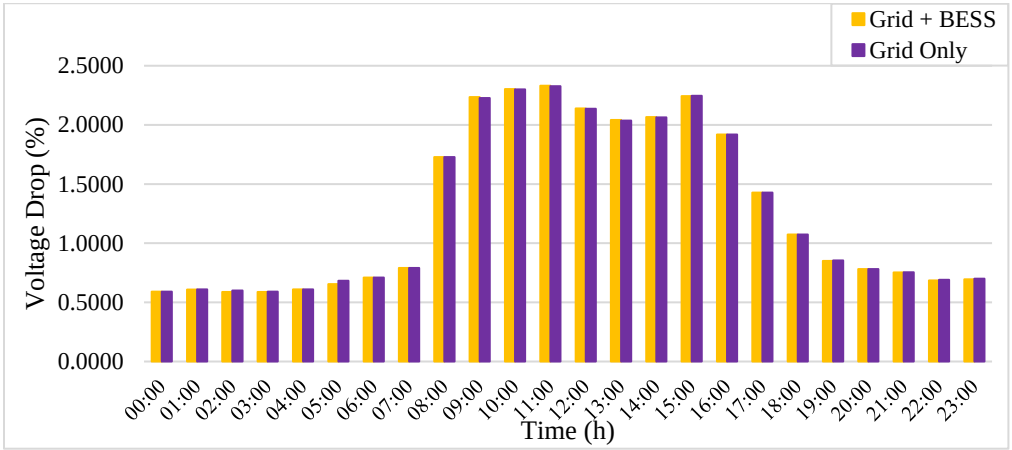

Figure 4.24: Voltage drop per hour at the main bus of the feeder.

4.4.1.2: Power and Power factor results.

The charging of the BESS which consume the energy as high as possible during the mid-day, to shift the power to the later use during a day. Household load demand is comparatively high during this time, which raising the problem that the BESS with the grid only configuration increases the real power demand at the peak load because of that the storage system have a special operation curve may be change in the circumstances of each case, the PCU with operate at unity power factor Fig.4. 25,26,27 show the three powers profile at the main bus with and without integrating the storage system, and the power factor at the main bus of the feeder illustrated in fig. 4.28.

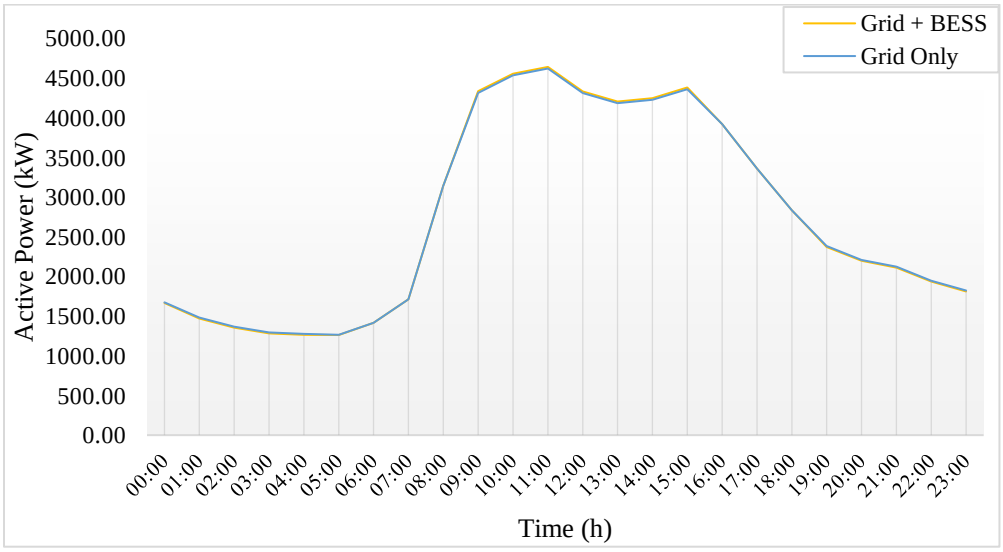

Figure 4.25: Active power at the main bus with and without BESS.

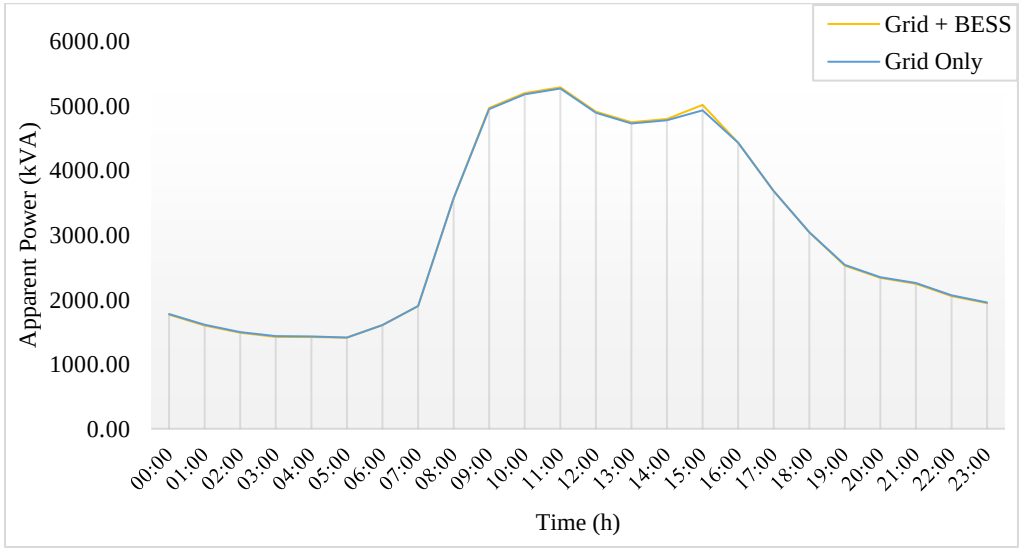

Figure 4.26: Apparent power at the main bus with and without BESS.

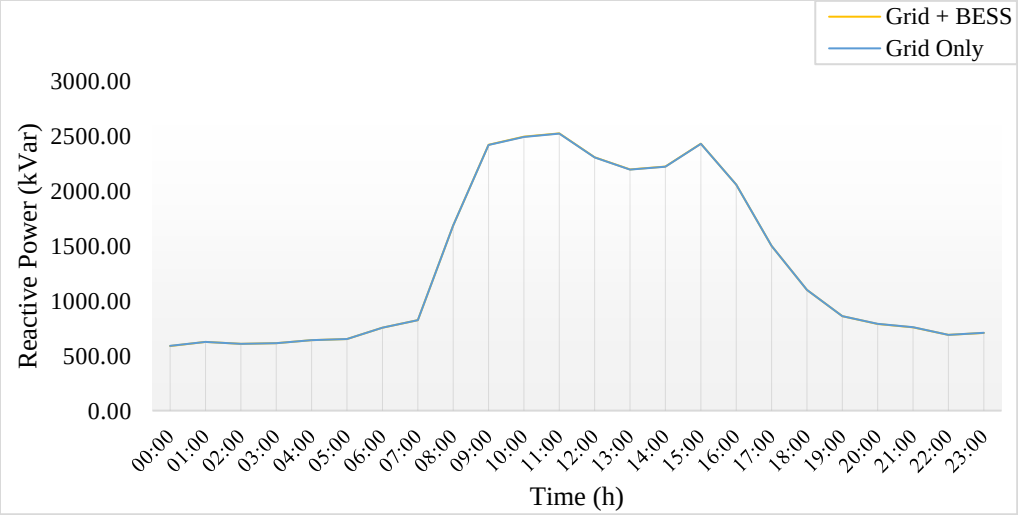

Figure 4.27: Reactive power at the main bus with and without BESS.

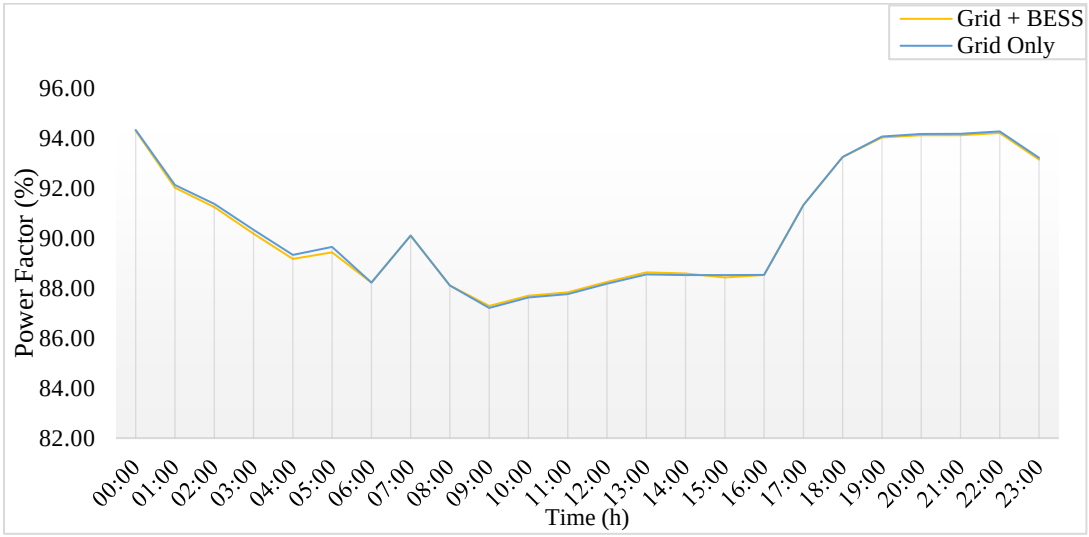

Figure 4.28: power factor at the main bus with and without BESS.

4.4.1.3: Active & Reactive Power loss at the PPU feeder.

In normal case the power flows from the main bus system to the distribution feeders, distribution transformers and to reach the loads at the end. During this path there are a voltage drop and losses in the transmission cables in the form of power loss, it is directly proportional with the length of the feeder. And the duration of the loading demand.

However, the power system losses along the line will appear in two main types of losses, active power from the resistance, and reactive power by the reactance of the lines and cables. Fig. 4.29,30 represent the active and reactive power loss profile along the PPU feeder in the case of storage system only integration with the grid and the absence of the BESS. However, integrating of BESS with the electrical network will lead to increase this loss in the charging mode of operation and decreasing it during discharging mode. In other words, the losses will be shifted from the period of production to the period of the consumption, consequently the overall losses amount approximately stay constant.

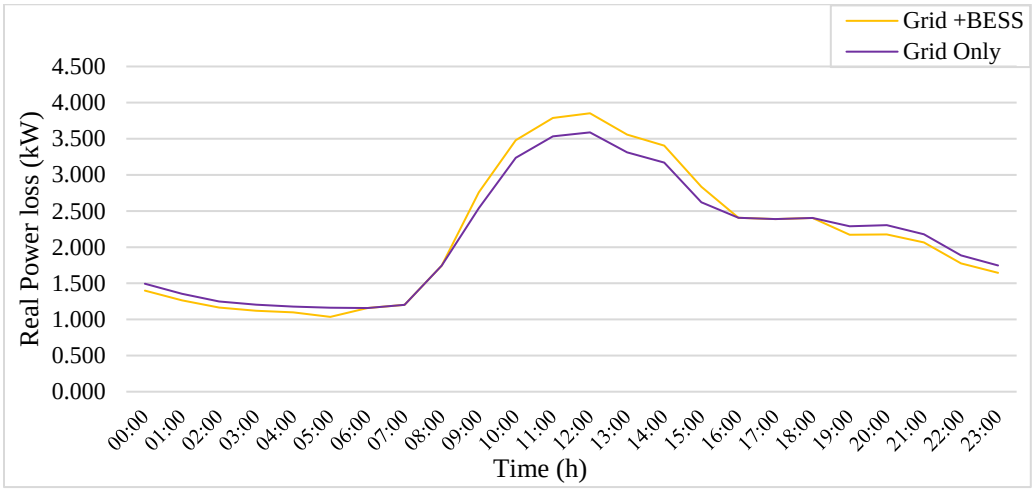

Figure 4.29: Real Power loss in the PPU feeder in kW.

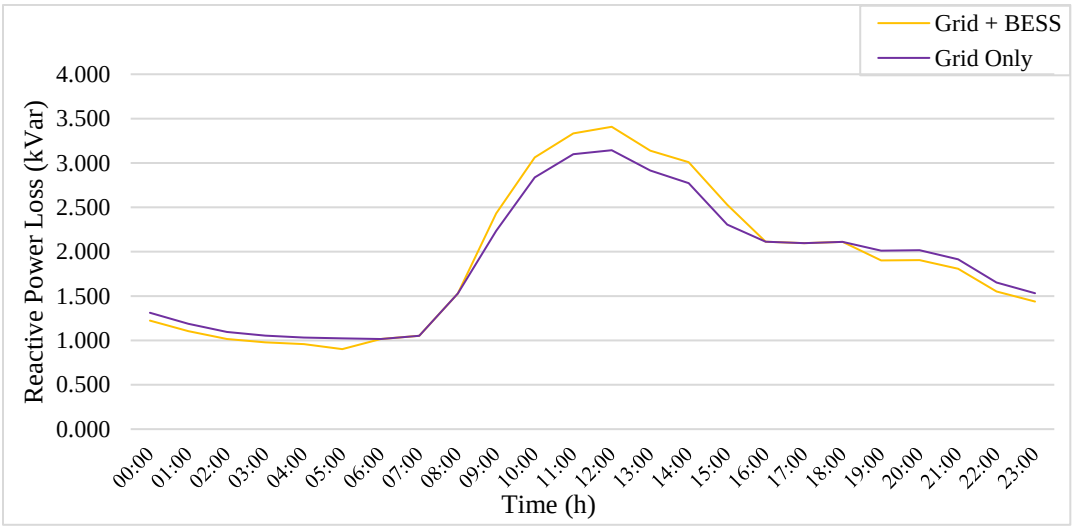

Figure 4.30: Reactive Power loss in the PPU feeder in kVar.

4.4.2: PCC bus profile results.

4.4.2.1: Voltage Profile.

The proposed BESS at the PCC was connected with the grid through a 1000 kVA distribution transformer and tied at the low voltage side, integrating BESS could have an obvious impact the voltage profile at the distribution grid particularly on the Point of Common Cabling of the feeder, the voltage profile was simulated at the LV bus and the voltage was decreases during the peak charging period and increases during the BESS work as a DG during the night, the voltage level at the PCC was decreases by 0.203% during charging and overvoltage 0.228% during energy production by the BESS. Fig. 4.31,32 illustrate the voltage and voltage drop profiles.

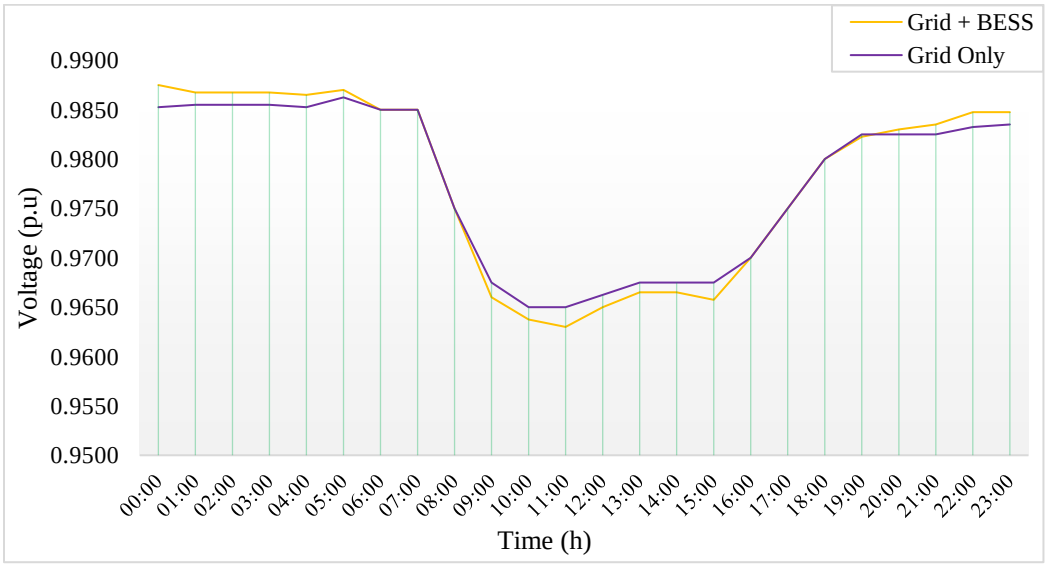

Figure 4.31: Voltage profile at the LV side of the distribution transformer with and without BESS.

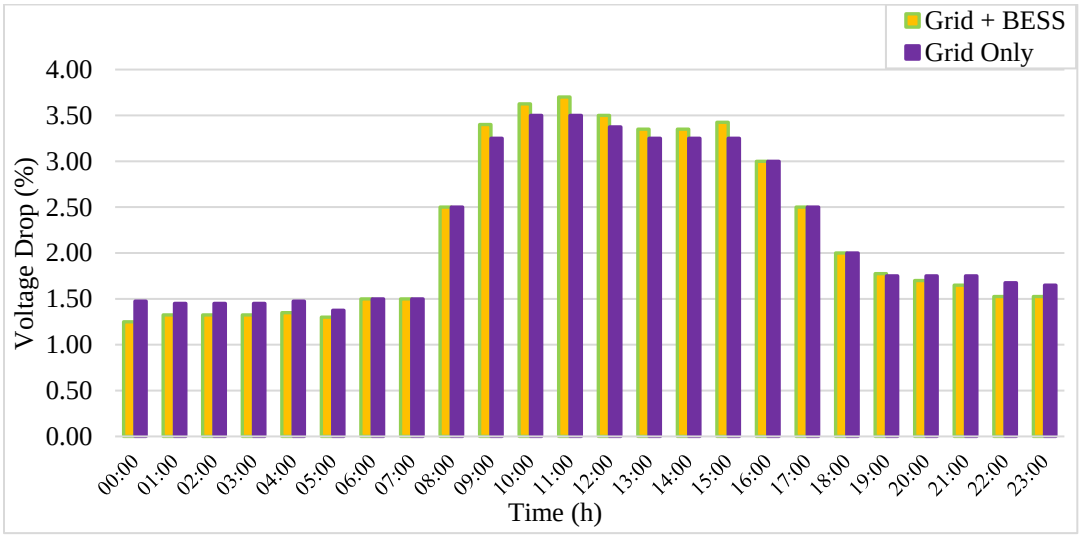

Figure 4.32: Voltage drop per hour at the PCC bus of the feeder.

4.4.2.2: Power and current Profile.

The load profile of the power demanded from the electrical grid by PPU load having a high concentration at the middle of the day, which means that the energy demand was high at the noon and moreover the charging period of the BESS is also at noon which Leads to increase the active power demanded by grid at that time, but the produced energy during a night period will decrease the demand by the grid and the over voltage back. Due to the unity power factor operation of the PCU of the BESS in both modes charging and discharging the contribution in a power profile will be appeared in a real and apparent power but the reactive power profile will be the same. The following figures illustrate the power profiles.

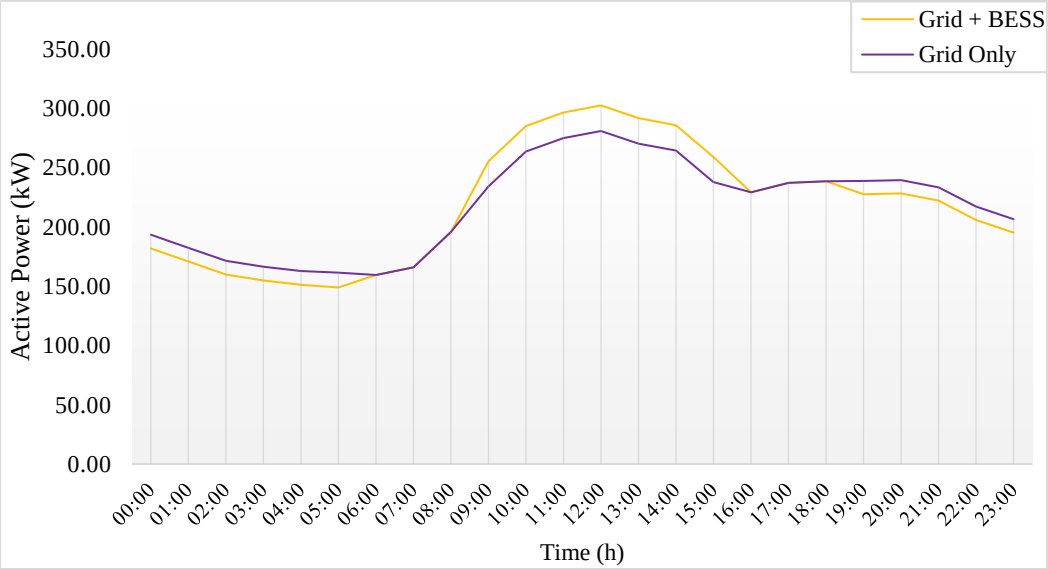

Figure 4.33: Active Power Consumed from the PCC Grid Side.

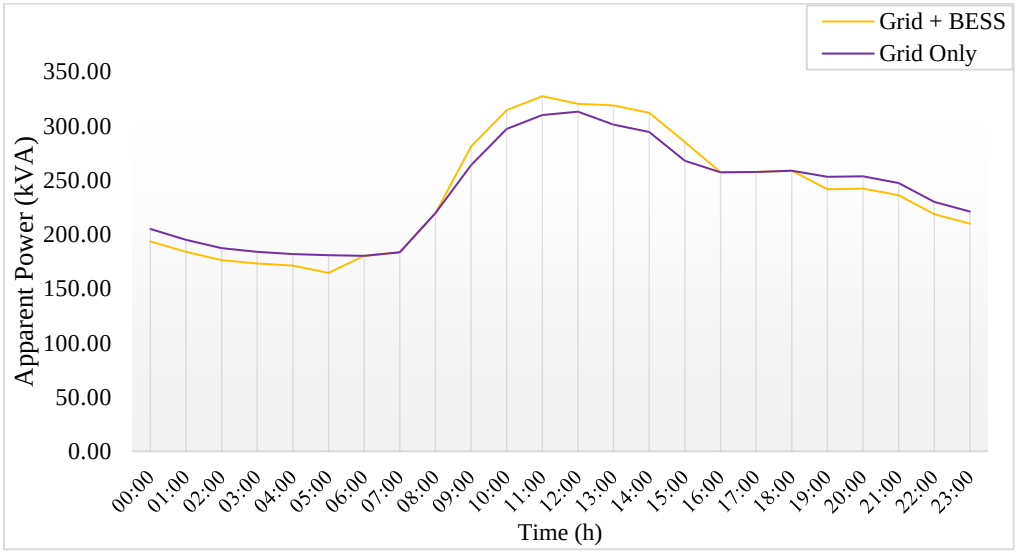

Figure 4.34: Apparent Power Consumed from the PCC Grid Side.

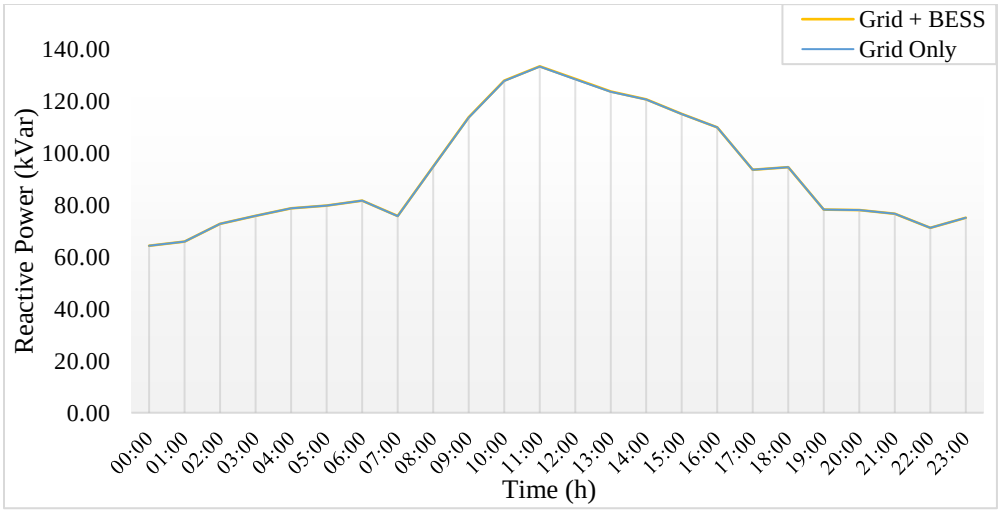

Figure 4.35: reactive Power Consumed from the PCC Grid Side.

The current profile is the reflection of the power flow at the PCC, original profile which is the grid only case which represent the conventional demand by the load along a day. And the BESS PCU was working as a charger at the charging mode period when the power flows to the storage system, and work as an inverter during a period of discharging mode. However, the demand power will increase at the charging mode and decrease at the discharging mode. See fig. 4.36.

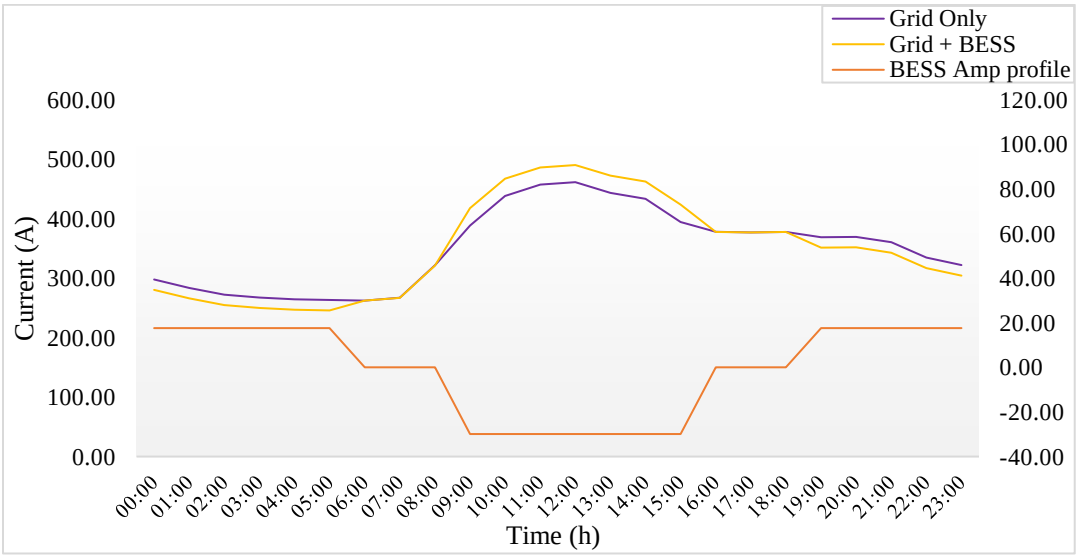

Figure 4.36: Current profile at the PCC (Amp).

4.4.2.3: Power factor Profile.

The BESS reduce the active power consumption from the electrical grid in one case and increasing it in another one. At the same moment the reactive power demand remains constant, besides the PCU operates at unity power factor which enhance the PF at the PCC in charging mode, and got decrease in an energy production mode, moreover it's obvious that the effect of the BESS operation on the PCC which is LV, is much higher than the MV bus of distribution transformer. Fig.4.37 represents the LV side profile with and without BESS, and fig.4.38 shows the MV side.

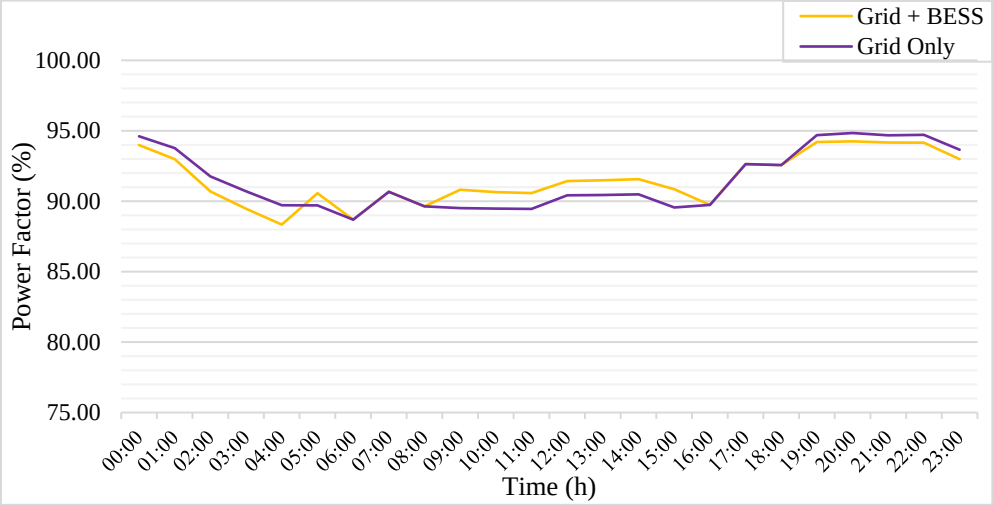

Figure 4.37: Power factor at PCC the low voltage side of the PPU distribution transformer.

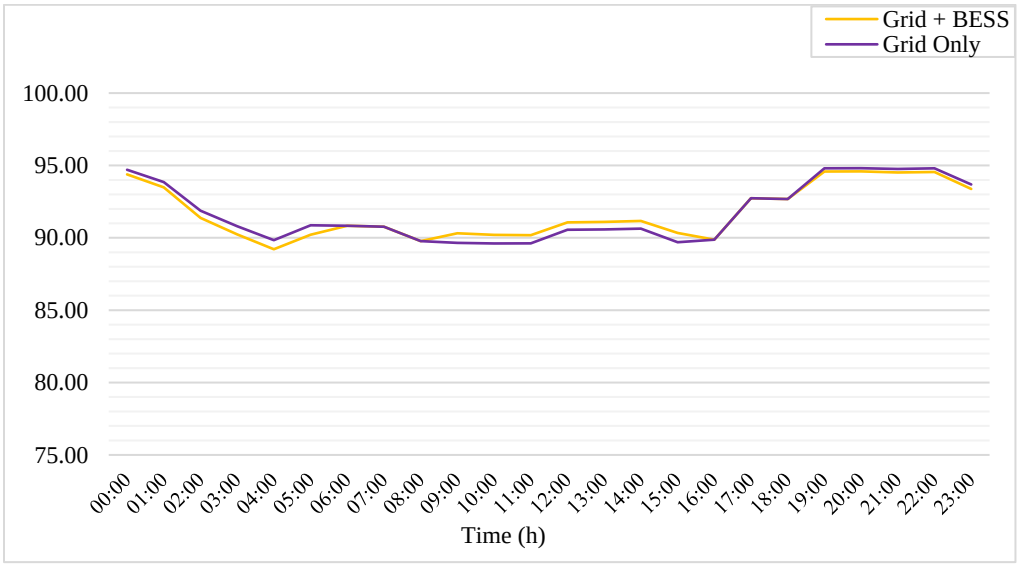

Figure 4.38: Power factor at the Medium voltage side of the PPU distribution transformer.

4.5: PV-BESS with grid integration.

In this section the BESS will integrated with the PV system to enhance the performance of the system and minimizing the impact of integrating PV system with electrical network and the hour by hour simulation result will be shown and discussed and all observed parameters will be taken in consideration in two main point, the main bus of the feeders and the second point is the PCC.

4.5.1: Main bus profile results.

4.5.1.1: Voltage Profile.

The literature indicates clearly that integrated PV-DG could impact the voltage profile of the distribution grid, the voltage profile was simulated at the main bus and the voltage was increased slightly at the main bus because of the penetration level of the PV at the main bus of the station is 3.62%, and the voltage level at the main bus increases by 0.03% at the MV level after installing the PV system and it was decreases by 0.005% by adding the BESS. Fig. 4. 39,40 shows results.

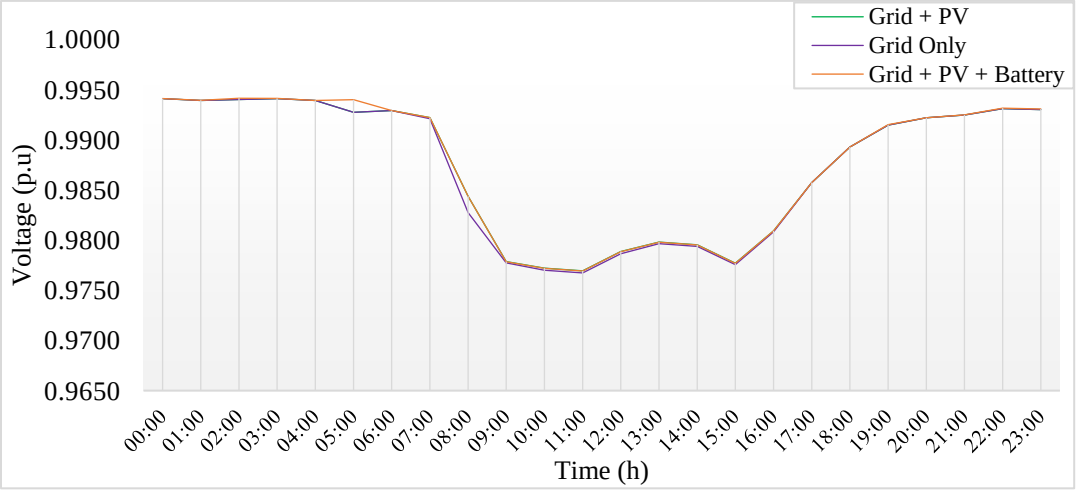

Figure 4.39: Voltage Profile at the main bus in 3 cases.

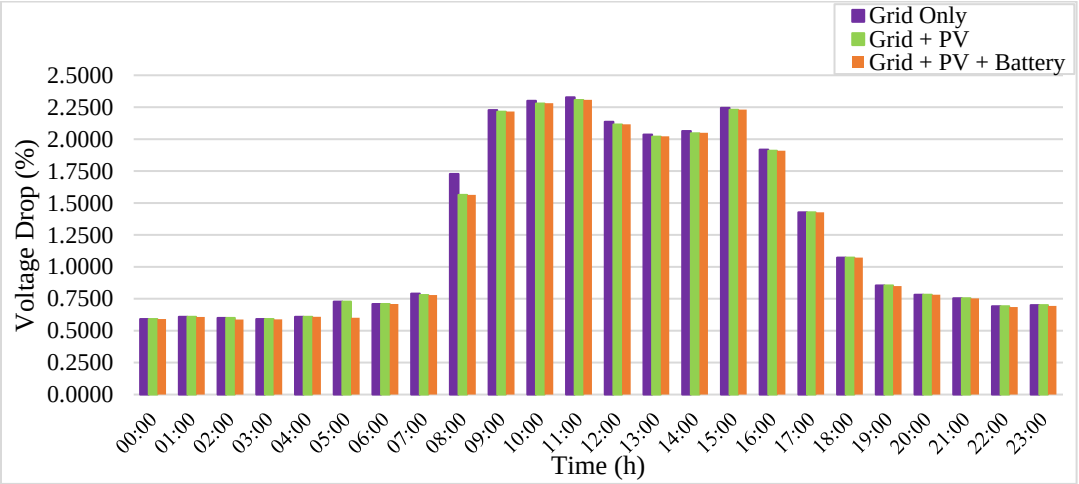

Figure 4.40: Voltage drop per hour at the main bus of the 3 cases.

4.5.1.2: Power and Power factor results.

The PV system production profile has the highest contribution in the middle of the day at peak sun hours, at that point the energy production that consumed from the interconnection point will be decreased, but after integrating the BESS with the system part of the generated energy by PV will moved to the storage system, therefore the active power at the starting point of the feeder will be much higher than the BESS absence case. Fig. 4.41-44 illustrate the active power, apparent power, reactive power and power factor profile respectively. However, reactive power profile was constant due to the unity power factor of the converters in the DG and the power factor was enhanced slightly at the interconnection point by adding the BESS.

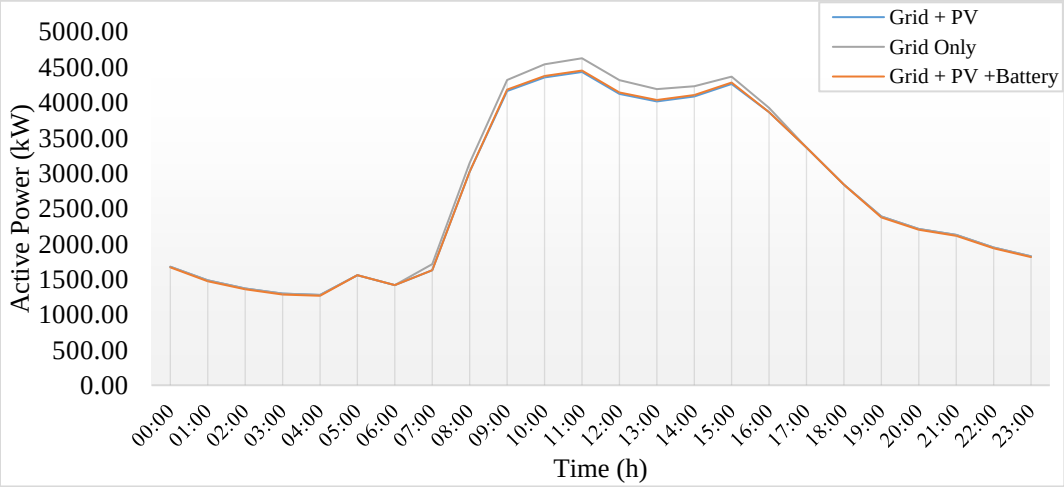

Figure 4.41: Active Power profile at the main MV bus in different cases.

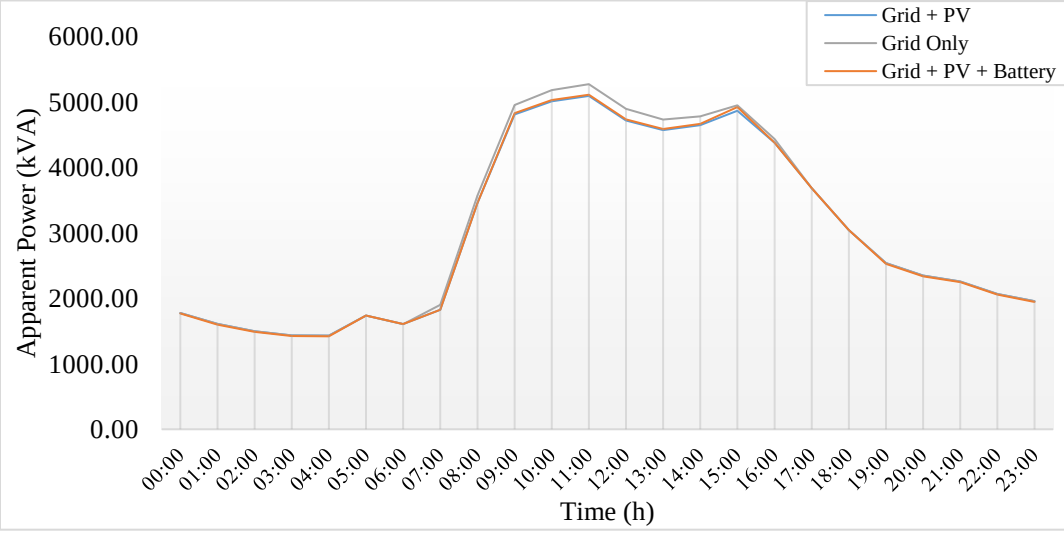

Figure 4.42: Apparent Power profile at the main MV bus in different cases.

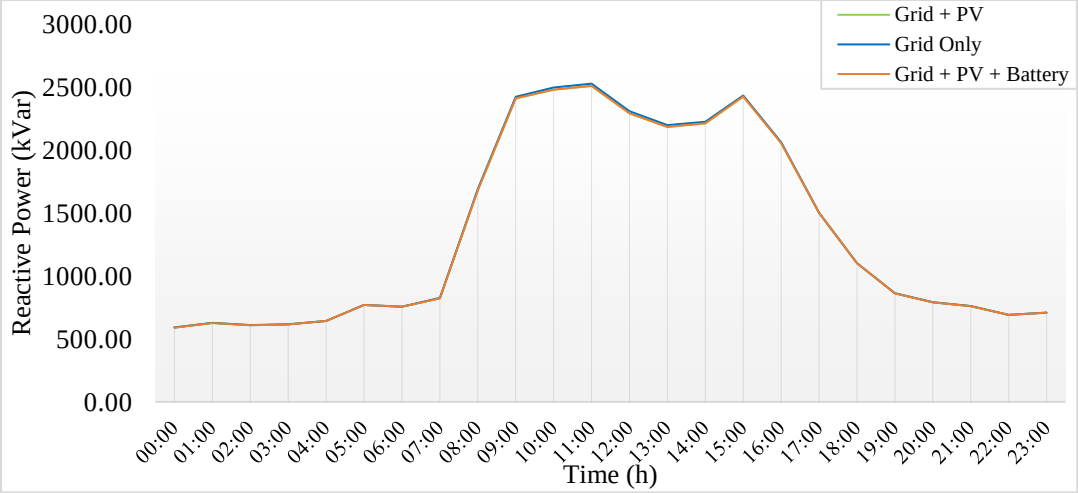

Figure 4.43: Reactive Power profile at the main MV bus in different cases.

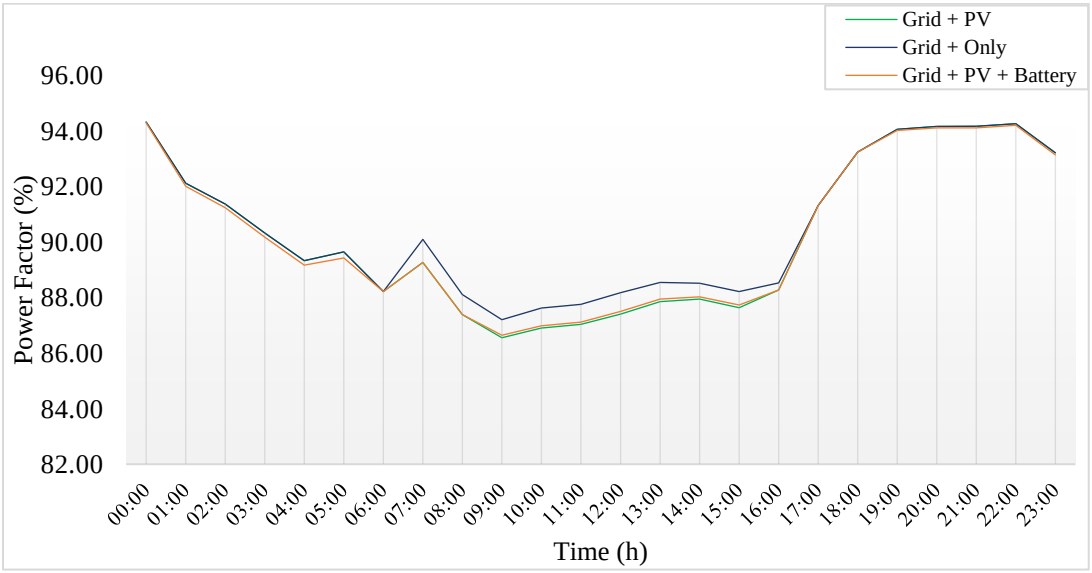

Figure 4.44: Power factor profile at the main bus in different cases.

4.5.1.3: Active & Reactive Power loss at the PPU feeder.

The load flow of the feeder flows from the step-down high voltage power station along the feeder up to reach the loads, as a result at this path of the power transmission will lead to drop the power as the distance increases because of the resistance and the reactance of the lines and cables will increase. However, in the AC system the power loss along the line divided into two main types active power produced by the resistance, and reactive power formed by the reactance of the lines and cables. Fig. 4.45,46 represent the active and reactive power loss hourly profile along the PPU feeder in the case of installing and absence of the PV system.

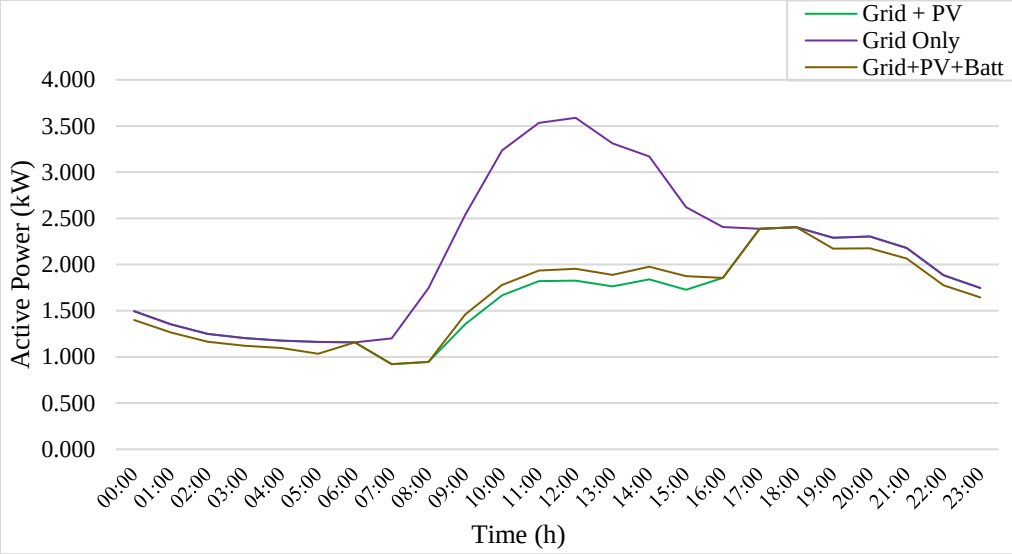

Figure 4.45: Active power losses profile in the feeder.

Its clearly that the daily real power losses was decreased after adding the PV system, but the losses of the reactive power along the feeder slaitly decreased. when the BESS integrated with the grid tied PV system, the total amount of loss was the same but it was shifted in the profile as an increasing during a day time and decreaseing in a night period. The peak value of the hour by hour profile was 3.5 kW at max but the average daily amount of loss without PV nor BESS was the accumelated value of losses 1429.5 kW and 634.7 kVar power consumption of the whole feeder. Table 4.1 illustrats the summery of the losses amount during three scenarios.

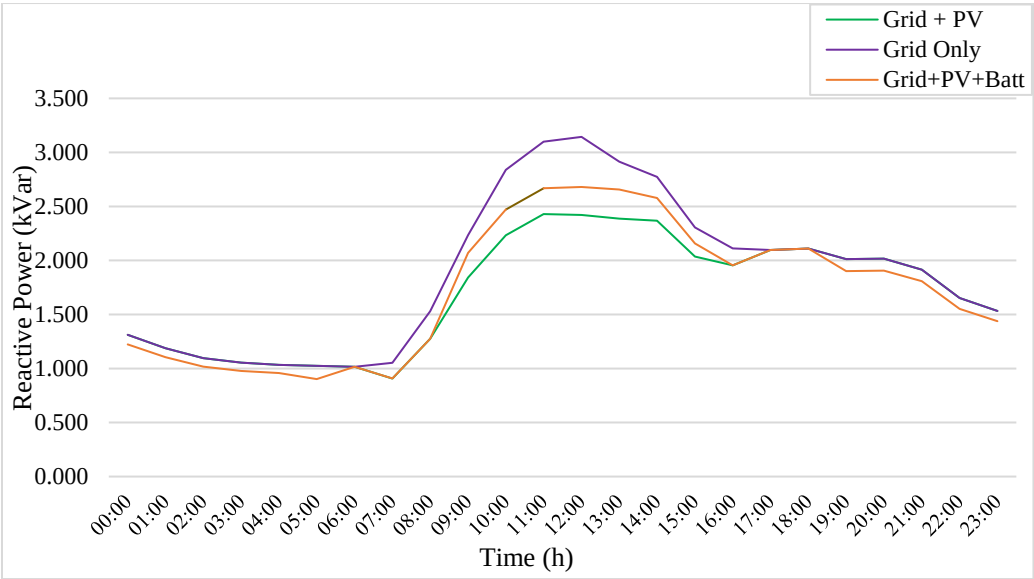

Figure 4.46: Reactive power losses profile in the feeder.

Table 4.2: The losses value for the PPU feeder.

#	Scenario	Active power loss (kW)	Ractive power loss (kVar)	Active power loss (%)	Ractive power loss (%)
1	Grid only	36.35	30.06	2.54	4.73
2	Grid + PV only	24.71	25.91	1.73	4.08
3	Grid + PV + BESS	24.45	26.42	1.71	4.16

From the table it can be observed that in normal case the rael power losses was the domenatnt along the feeder but after integrating the PV and BESS the reactive became higher than the real due to reducing in the real power demanded from the feeder, in the other hand when the BESS integrated with the PV system the covered load power by the PV is reduced because of the charging of the storage system and losses amount approximately remains constant but with shifting profile and the concentration of the losses reduction not on the day time only, but also in a night time as represented above.

4.5.2: PCC bus profile results.

4.5.2.1: Voltage Profile.

The integrated PV-DG could affect clearly on the voltage profile of the LV distribution grid particularly on the Point of Common Cabling (PCC) of the feeder, the voltage profile was built at the PCC bus in steady state situation then the PV system and BESS were connected, it's worth mentioning that the voltage was increased clearly at the PCC bus with PV integration only, and the voltage level at the bus increases by 0.45% at the PCC with only 14.7% of PV penetration level of the feeder. But after the BESS Enter the operation the voltage was decreased than with PV only which means that BESS reduces the over voltage situation at the peak operation time of the PVs.

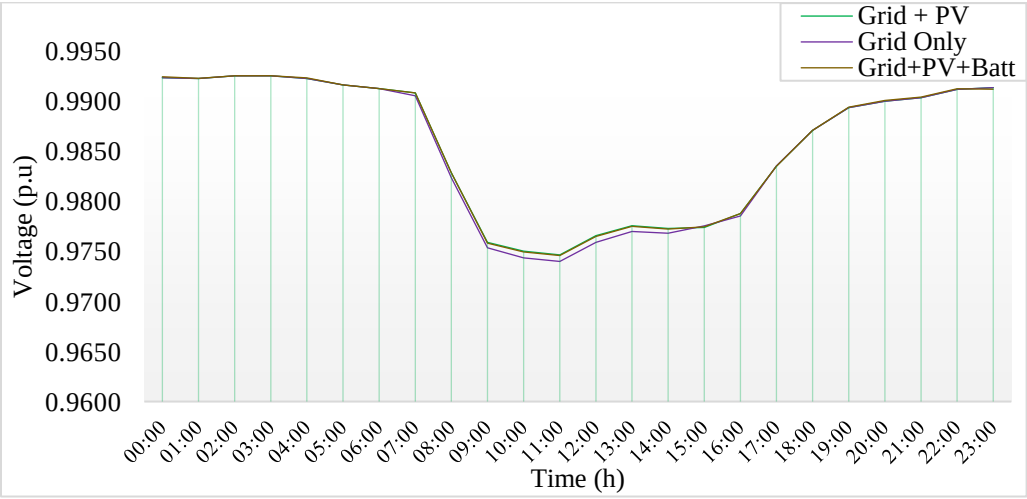

Figure 4.47: Voltage profile at the MV side of the PPU distribution transformer.

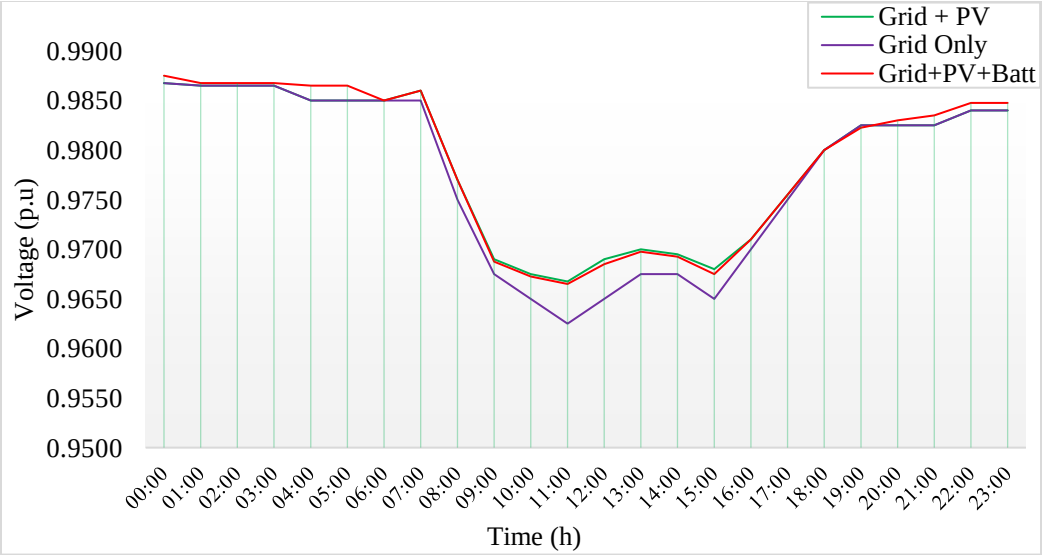

Figure 4.48: Voltage profile at the LV side of the PPU distribution transformer.

Fig. 4.48 shows the voltage profile of the PCC low voltage side bus of the distribution transformer, but the voltage profile at the MV bus side of the distribution transformer illustrated at fig.4.47, the voltage increases with integrating the PV but this over voltage was minimized by BESS integration, which means the effect of PV generation at the MV level of the feeder is much lower than the LV level. And voltage drop at the PCC is clearly decreased after adding the PV plant as fig. 4.49 represents.

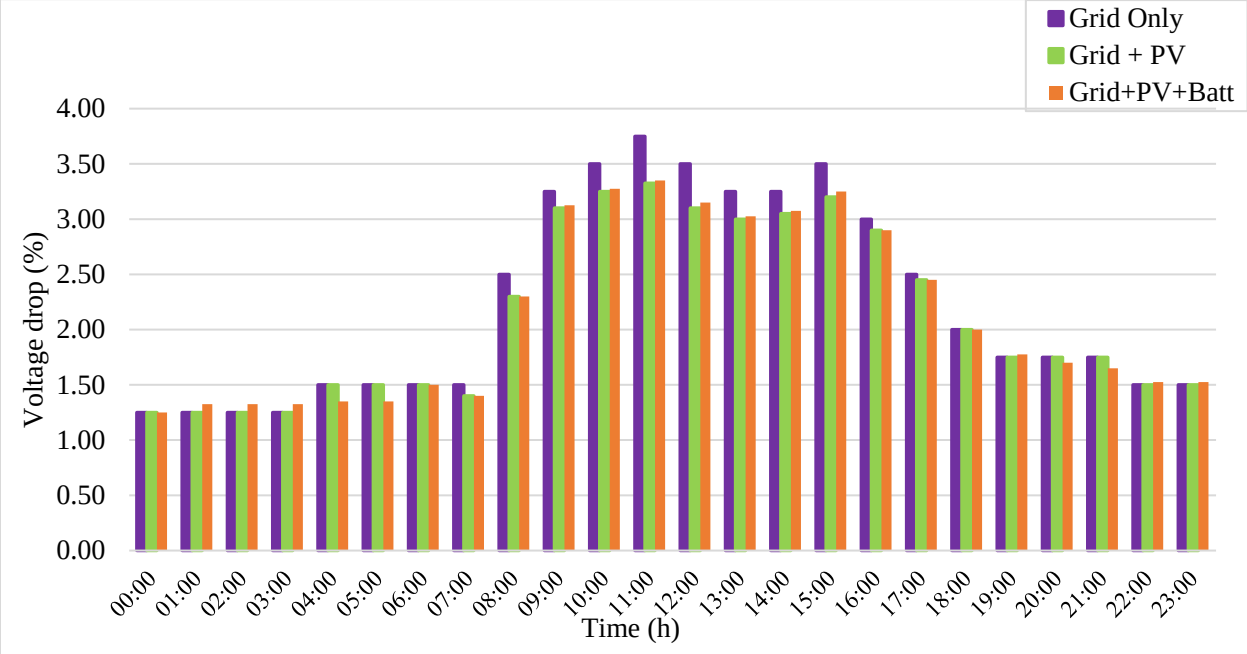

Figure 4.49: Voltage drop percent at the PCC with different cases.

4.5.2.2: Power and Current Profiles.

The production of photovoltaic power plant should be the highest at the middle of the day, regarding to the radiation level and temperature variation. Also, the PPU profile consumption concentrated at the mid-day, Connection the PV plant to a distribution network Contributes to generate the active power with the grid. So, the active power supplied from the utilities will decrease. However, to enhance the performance of the PV operation and minimize it's impact of the grid, the BESS used for shifting the produced power from the day time to the night time, resident of BESS will justify the reduction of the night active and by default apparent demand of the PPU load as appear in fig. 4.50,51.

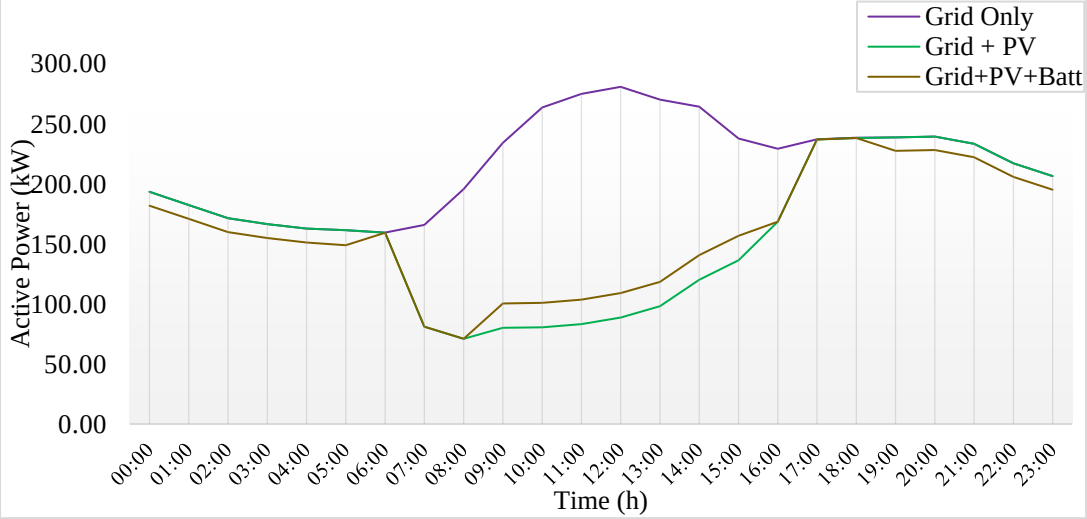

Figure 4.50: Active power consumption from the grid along a day for the cases.

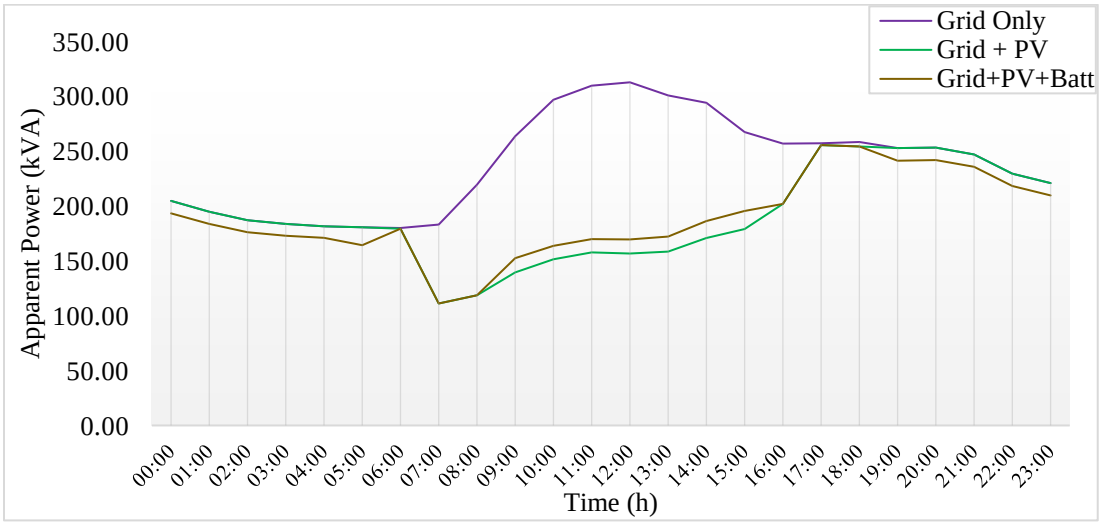

Figure 4.51: Apparent power consumption from the grid along a day for the cases.

Fig. 4.52 illustrates the reactive power profile which remains the same in all cases, due to the unity PF which the PV and BESS power conditioning unit operation, to guarantee the high performance and efficiency from the distributed generation. And fig 4.53 represents the current profiles for the PV system production and grid consumption current without any DGs, with PV only and with PV-BESS.

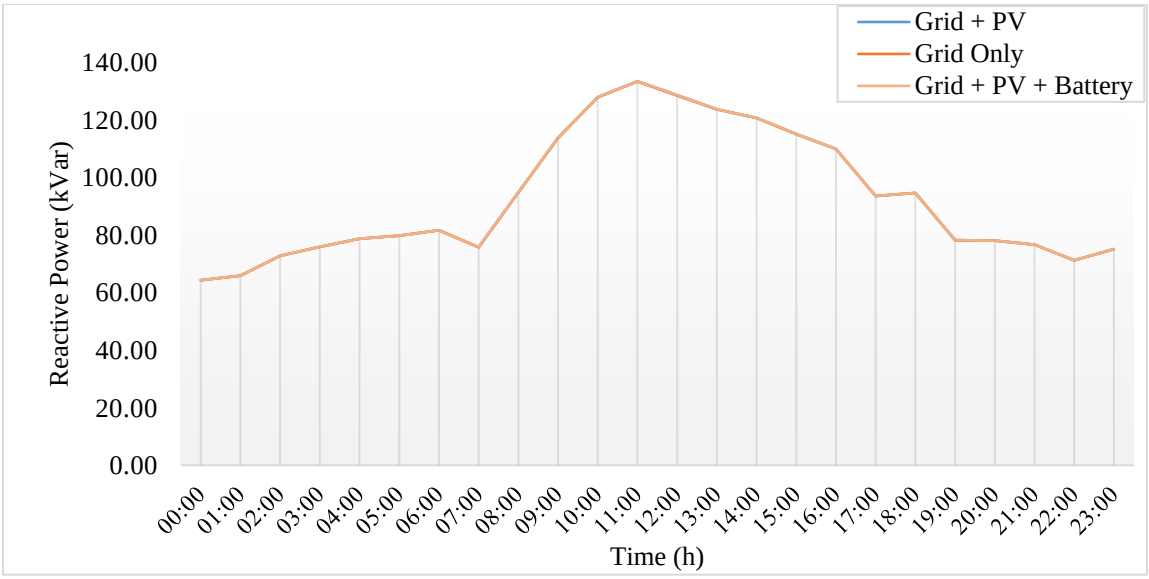

Figure 4.52: Reactive power consumption from the grid along a day for the cases.

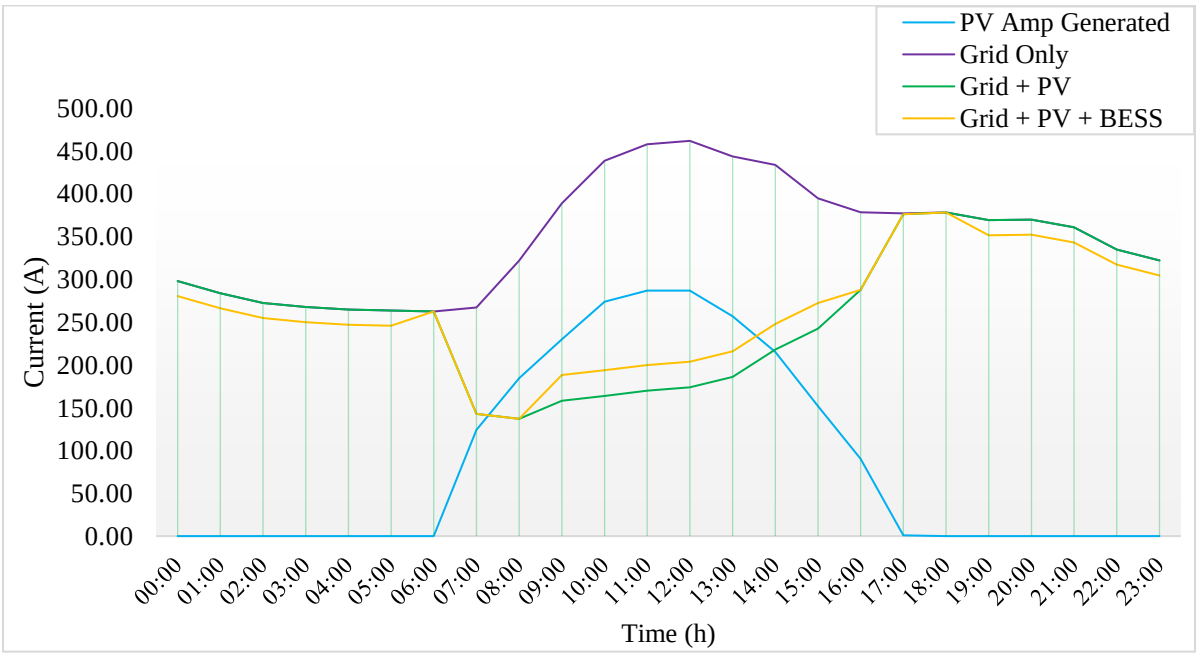

Figure 4.53: Current profiles consumption from the grid along a day for the cases.

4.5.2.3: Power factor Profile.

The PV-DG generate an active power and feed it to the load directly which reduce the real power demanded from the grid, besides of no changing in reactive demand which leads to decrease the power factor to extreme conditions during PV system operation. However, unity PF operation of the DG converters is required to prevent the increasing of reactive power in the grid; in case of high rate of reactive power to the grid, the distribution transformers will operate at a low PF.

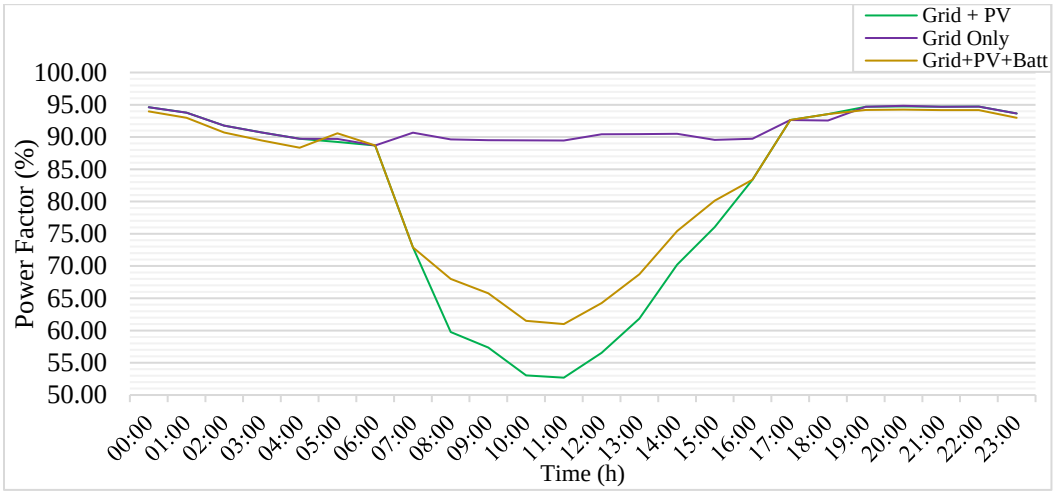

Figure 4.54: Power Factor Profile at the LV side PCC along a day for the cases.

Thus, as appear in fig. 4.54,55, it's obvious that the effect of the PPU-PV system on the LV side of the distribution transformer at the PCC is much higher than the MV. At the peak generation period of the PV system the power factor goes down gradually at the LV side of the PPU distribution transformer and reach to extreme values like 53% but the BESS enhance this value up to 63%. On the other hand, at the MV side the effect of the power factor wasn't exceed 81% at the peak generation point and the BESS enhance this value up to 83%.

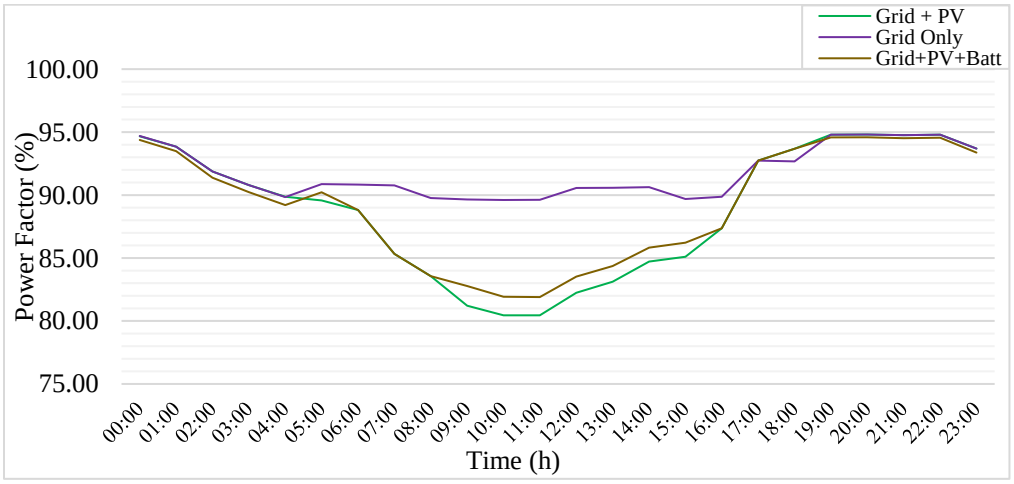

Figure 4.55: Power Factor Profile at the MV side PCC along a day for the cases.

4.6: Critical scenarios analysis for PV & BESS with grid integration.

In this section the extreme scenarios of distributed generation operation are examined at the PPU feeder with PV only and PV-BESS DG configuration. The selected scenarios are: the maximum load and minimum generation point, and the minimum load and maximum generation point.

4.6.1: Maximum load with lower Generation of the PV& PV-BESS DG.

Integration of the DG with the electrical network changing the voltage profile at the whole buses in the feeder not only at the PCC, even if it has the maximum effect in the system. However, this effect depends on the loading amount and the production power level of the DG, fig.4.56 illustrates the voltage buses profile of the PPU feeder in the case of highest load demand point and lowest generation production of the PV system, and fig.4.57 shows the PV-BESS integration case.

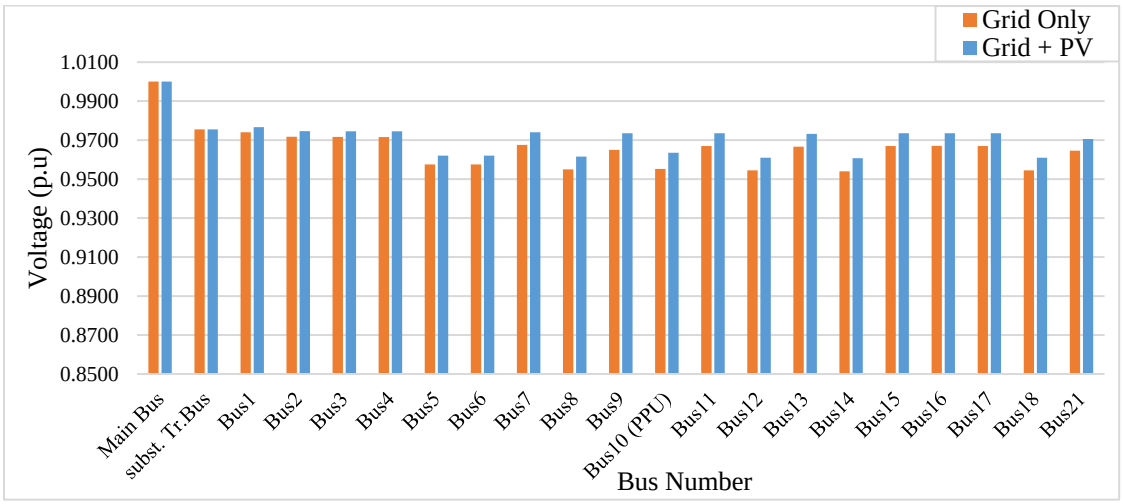

Figure 4.56: Voltage profile for the PPU buses at maximum load and minimum generation of PV only.

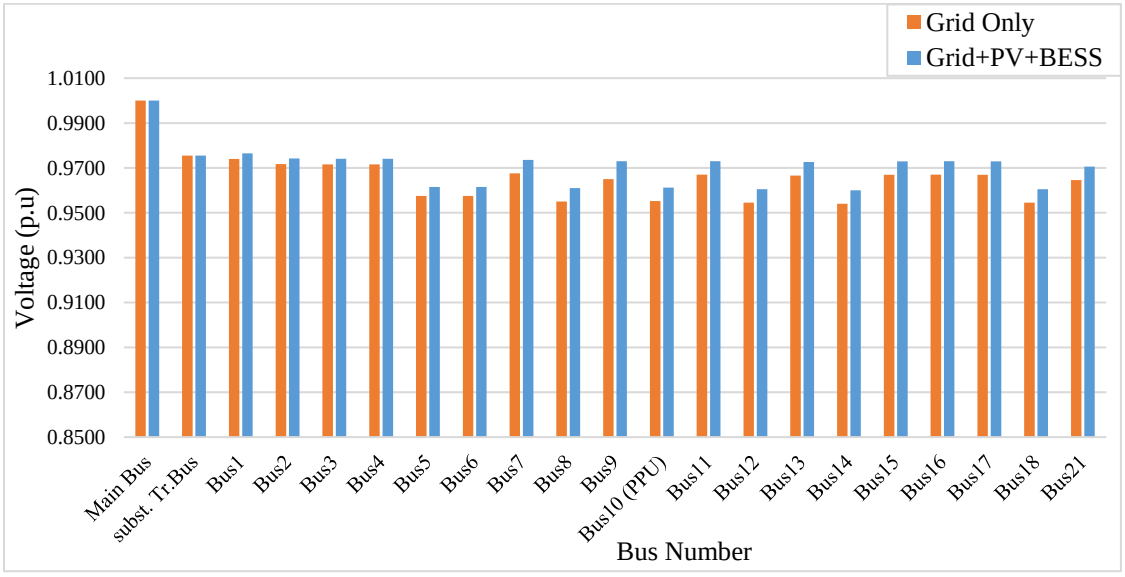

Figure 4.57: Voltage profile for the PPU buses at maximum load and minimum generation of PV&BESS.

4.6.2: Minimum load with highest Generation of the PV & PV-BESS DG.

In the minimum load demand and high PV production case, the effects at the voltage profile of the whole buses in the feeder is much higher than the previous case. Fig.4.58 illustrates the effect of integrating the PV system only with the PPU feeder in the case of minimum loading and highest production. For the PV-BESS integration case the voltage buses profile shown in fig.4.59 “To be more precise” table 4.2 illustrates the observations at the PPU LV bus in the whole scenarios.

Table 4. 3: voltage raising at the PCC percent of PPU feeder.

DG configuration	Voltage raising percent at the PCC	
	Max. load with Min. generation	Min. load with Max. generation
PV	0.825%	1.525%
PV+BESS	0.600 %	1.200%

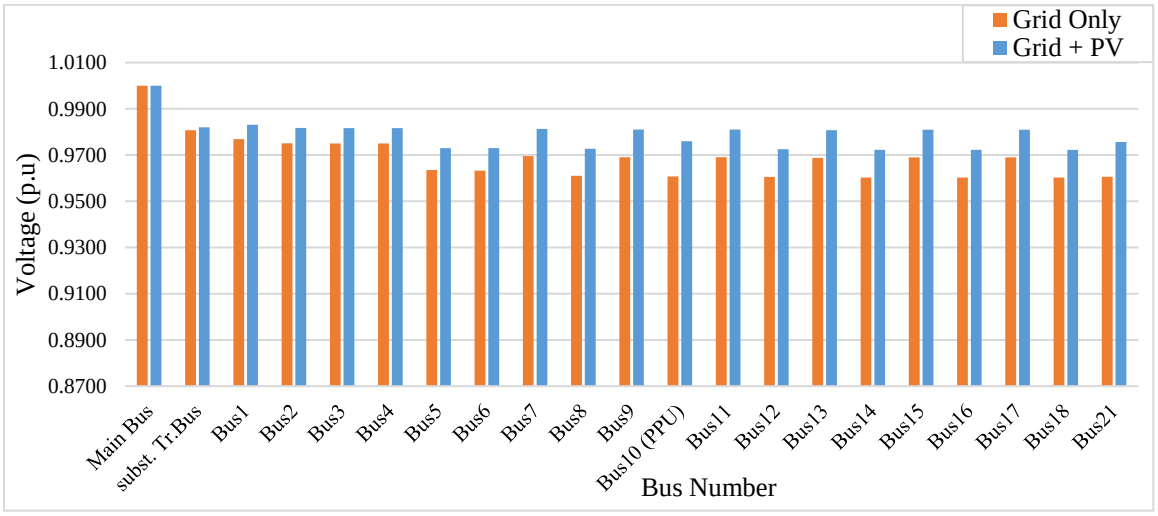

Figure 4.58: Voltage profile for the PPU buses at minimum load and maximum generation of PV only.

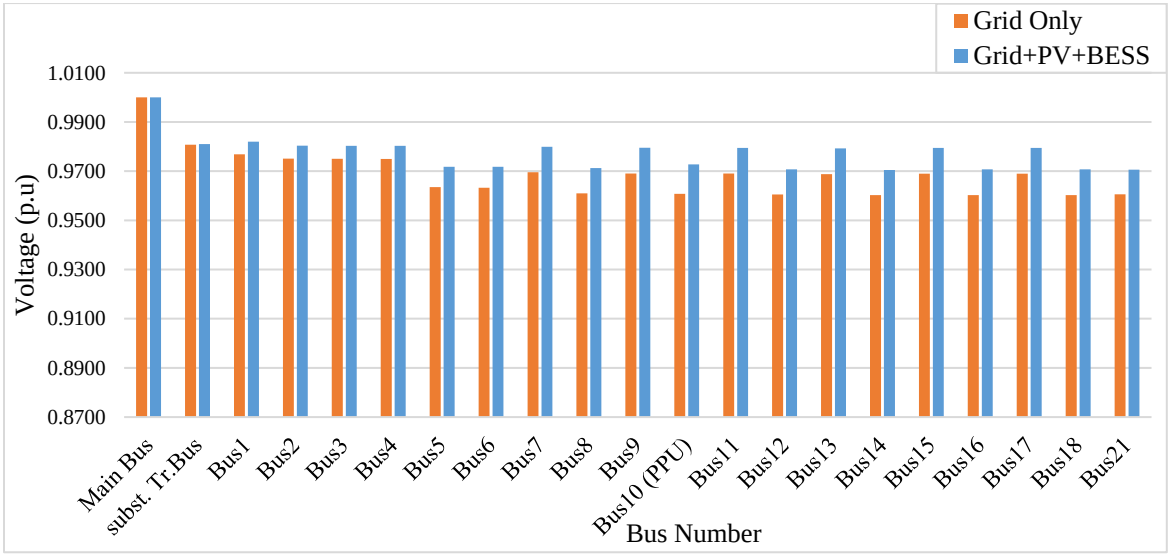

Figure 4.59: Voltage profile for the PPU buses at minimum load and maximum generation of PV & BESS.

4.7: Harmonics analysis PV & BESS with grid integration.

A harmonic analysis for a single line diagram of the PPU feeder which modeled used ETAP software. Here harmonic components are modelled to create harmonic current for harmonic distortion in grid feeder. After enabling an effective harmonic analysis, the system was tested under different scenarios and load conditions. However, in this section the harmonic components and the total harmonics distortion of the system in three scenarios: grid only configuration, grid integrated with PV system only and PV-BESS integrated with the grid were modeled. To observe the magnitude of harmonic distortion in the network, at different points from main bus feeder up to PCC, the results will be the harmonic components and wave form on the main MV bus which is the interconnection point 33kV source, bus 1 the main bus of the PPU feeder 11kV, bus 9 the MV side of the PPU distribution transformer finally bus 10 (PPU) is the LV PCC.

As a reference the harmonics source was detected from the power quality analyzer which applied by the distribution company at the PPU transformer was approximately closed with the 12-pulse harmonic source which Proposed by IEEE 519 standard and All the buses are designed in accordance to the IEEE 519 standards to check for the harmonic distortion. So, the harmonics analysis in the ETAP software considered this situation as a reference.

4.7.1: Grid only system harmonics analysis.

The harmonics spectrum for the first 50th harmonic components and voltage waveforms of the main four buses after Harmonic load flow analysis was illustrated in fig 4.60,61 respectively. It can be seen that, 5th component of the LV PPU PCC bus 10 the dominate component in this case.

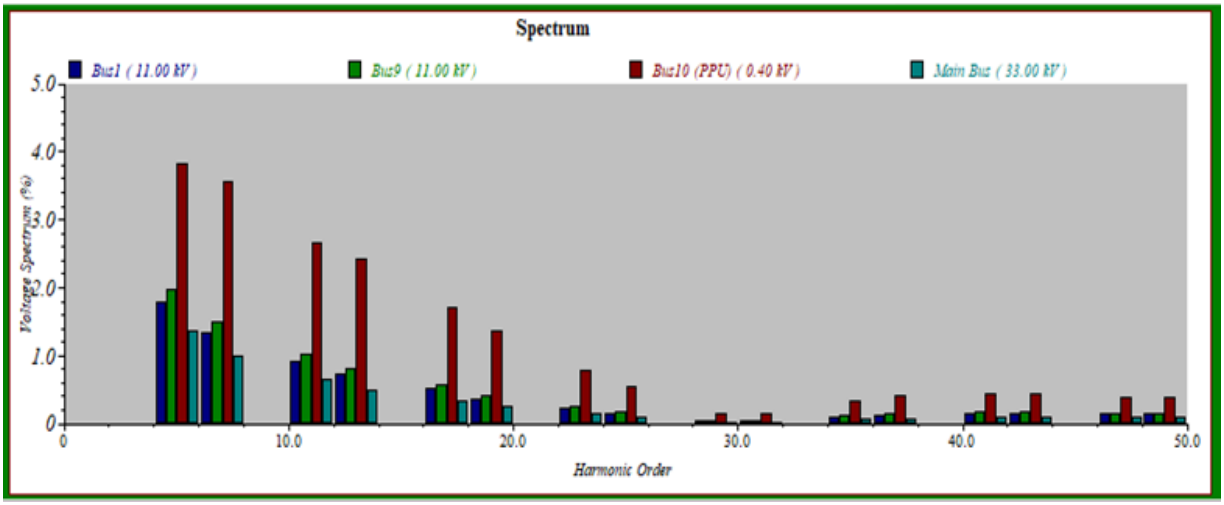

Figure 4.60: First 50th harmonics component at the four points along the grid only system.

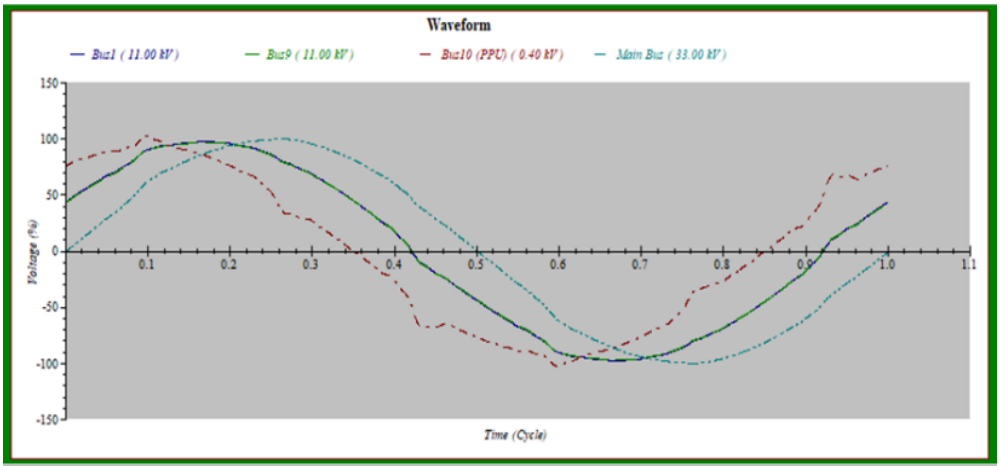

Figure 4.61: Harmonic Load Flow Plots for four buses, grid only.

4.7.2: Grid + PV system only harmonics analysis.

The harmonics spectrum for the first 50th harmonic components and voltage waveforms of the main four buses after Harmonic load flow analysis was illustrated in fig 4.62,63 respectively. It can be seen that, 11th and 13th harmonic components of the LV PPU PCC bus 10 the dominate component after integrating the PV Inverters with the system, but the percentage was less than 3.8% the LV bus and 1.5% for the MV, means that the harmonic components still stands under the standard deadlines as mentioned in chapter two which is 5% for the LV bus and 3% for MV. Additionally, bus bar 10 a PPU LV PCC is the most distorted bus because of the PV inverters integrated with, so this bus represents the harmonic sources to the system.

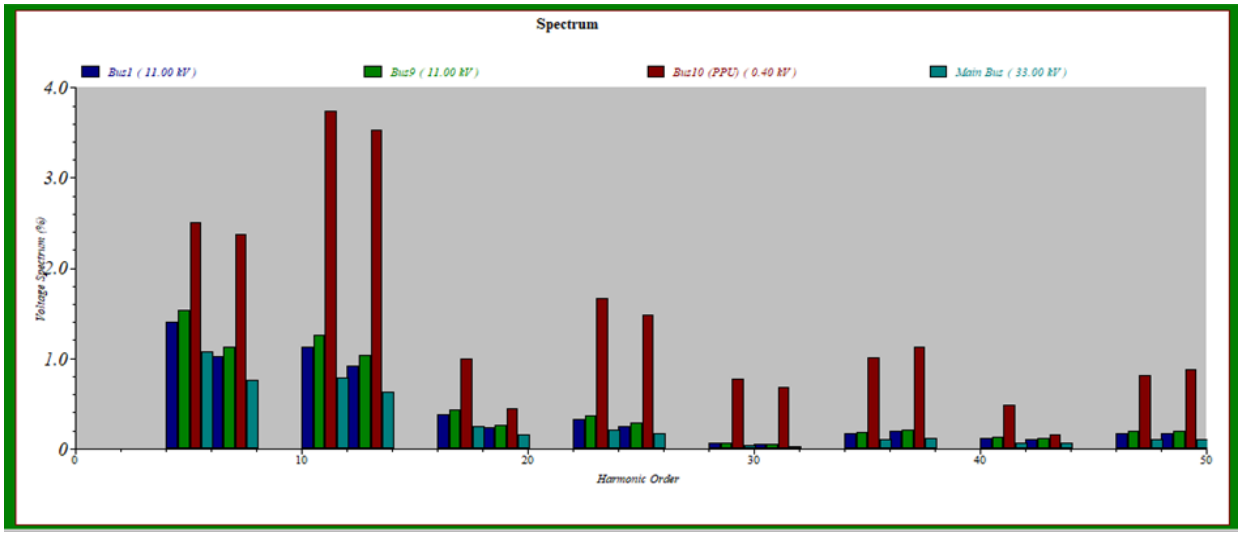

Figure 4.62: First 50th harmonics component at the four points along the grid + PV system.

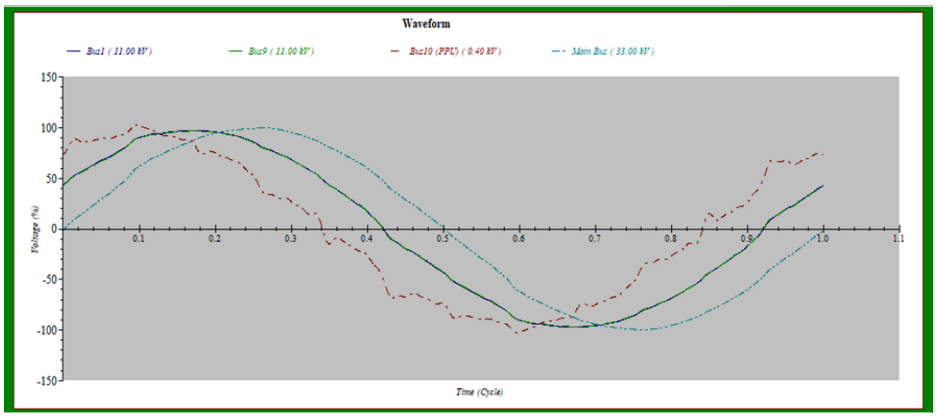

Figure 4.63: Harmonic Load Flow Plots for four buses, grid and PV only.

4.7.3: Grid + PV + BESS harmonics analysis.

The harmonics spectrum for the first 50th harmonic components and voltage waveforms of the main four buses after Harmonic load flow analysis was illustrated in fig 4.64,65 respectively. It can be seen that, 5th and 7th harmonic components of the LV PPU PCC bus 10 are back dominate component again after integrating the BESS charger/inverters with PV Inverters with the system at the same bus, but the percentage was decreased to 3.5% LV bus, due to the peak harmonics production of the PV was faced by the consumption of the storage system.

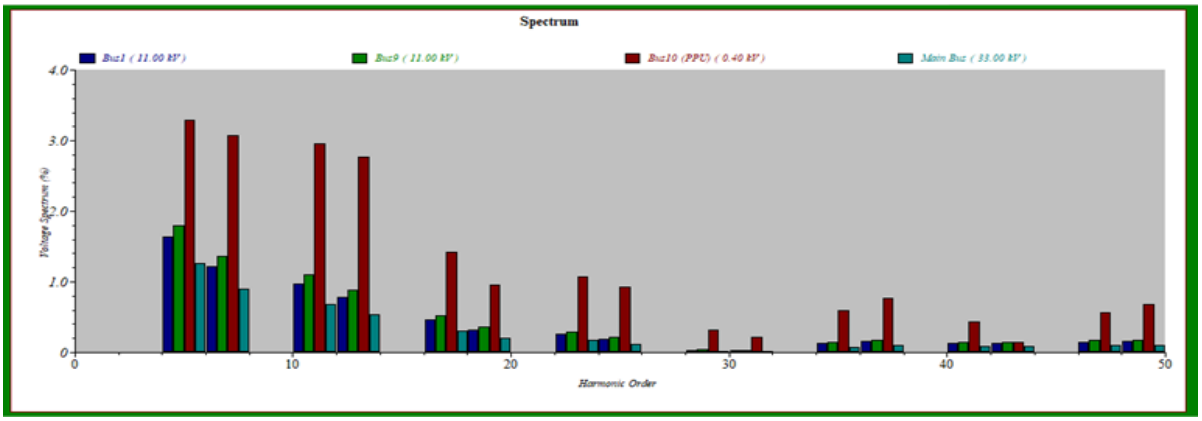

Figure 4.64: First 50th harmonics component at the four points along the grid + PV + BESS system.

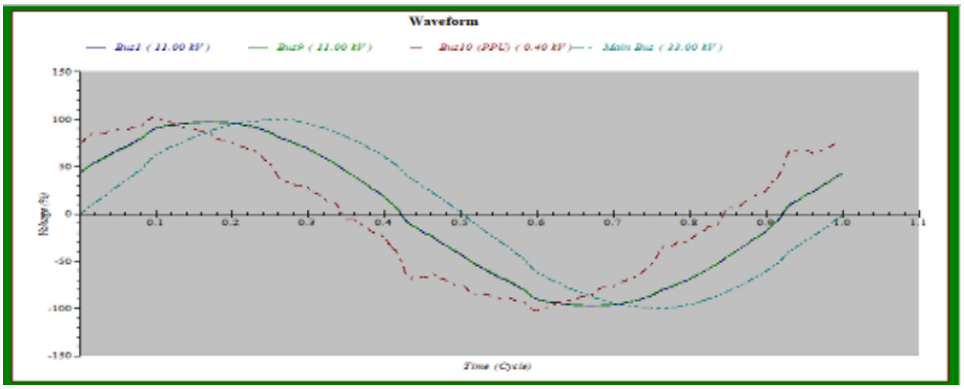

Figure 4.65: Harmonic Load Flow Plots for four buses, grid and PV only.

4.7.4: Total Harmonics Distortion (THD) profile analysis.

Total Harmonic Distortion (THD), also known as Harmonic Distortion Factor, is the most popular index to measure the level of harmonic distortion to voltage and current. It is a measure that shows the ratio of the mean-square-root of all harmonics to the fundamental component. For an ideal system, THD is equal to zero. In this section the total harmonics distortion hour by hour daily profile of the system in the three cases as follows electrical grid only, grid with PV system only and the electrical grid with PV and BESS integration.

To check the harmonic distortion or effect of harmonic source on the power network, Harmonic load flow needs to be performed. The harmonic load flow is performed with a daily load profile and average daily conditions to observe the THD profile for the cases at along the feeder from the interconnection point, main bus feeder and the LV PCC near the PV system with different voltage levels. Fig 4.66 illustrates the steady state THD average daily profile at the main bus of the PPU feeder 11kV and its clearly that the THD increased after integrating the PV system with the electrical grid and decreases with the BESS integration.

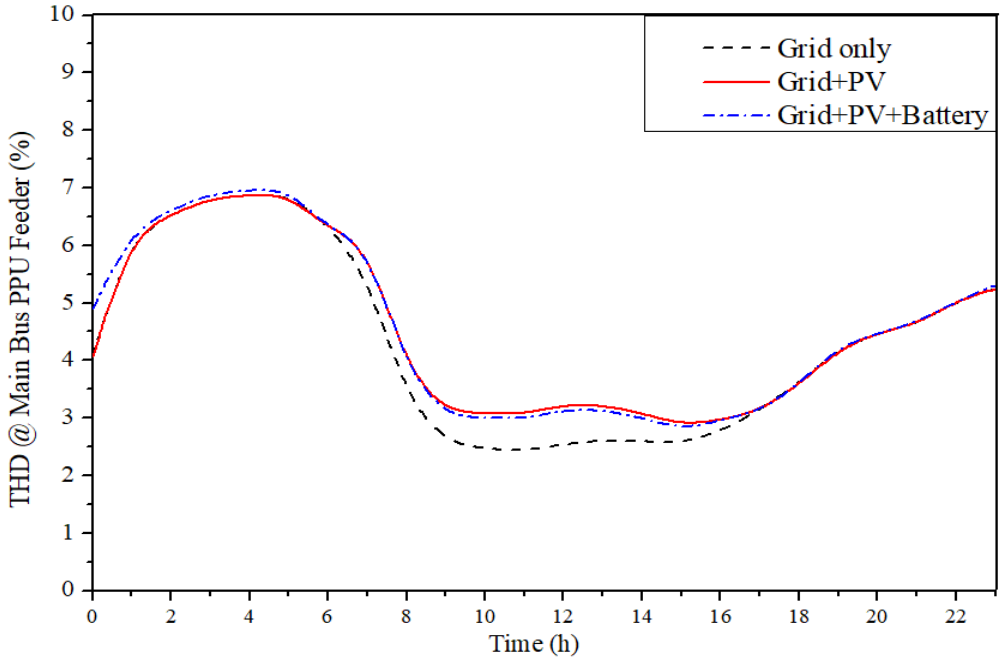

Figure 4.66: THD daily profile at the main bus of PPU feeder.

Fig. 4.67 shows that in the reference profile of the 11kV grid system only the THD, In general having a high concentration in the light load in the system, on the other hand integrating the PV system was increasing the THD present in the peak time production period but the integration of BESS minimized the THD increasing which contribute to reduce the impact of the PV system on the electrical grid. However, and regarding to fig 4.68 the THD that produced by the PV system was much higher at the 400 V LV side of the PPU distribution transformer near the PV inverters connection and the BESS clearly eliminated the THD magnitude particularly at the peak time.

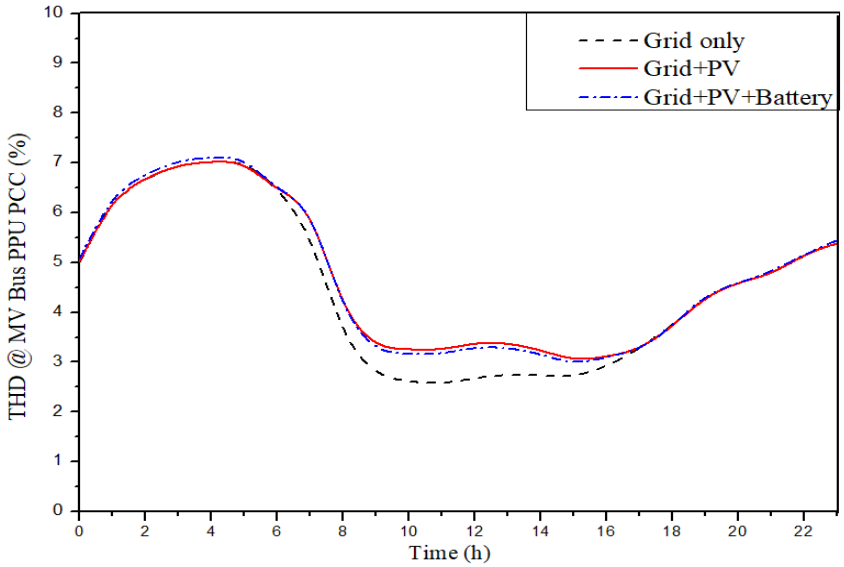

Figure 4.67: THD daily profile at the MV side of the PPU distribution transformer.

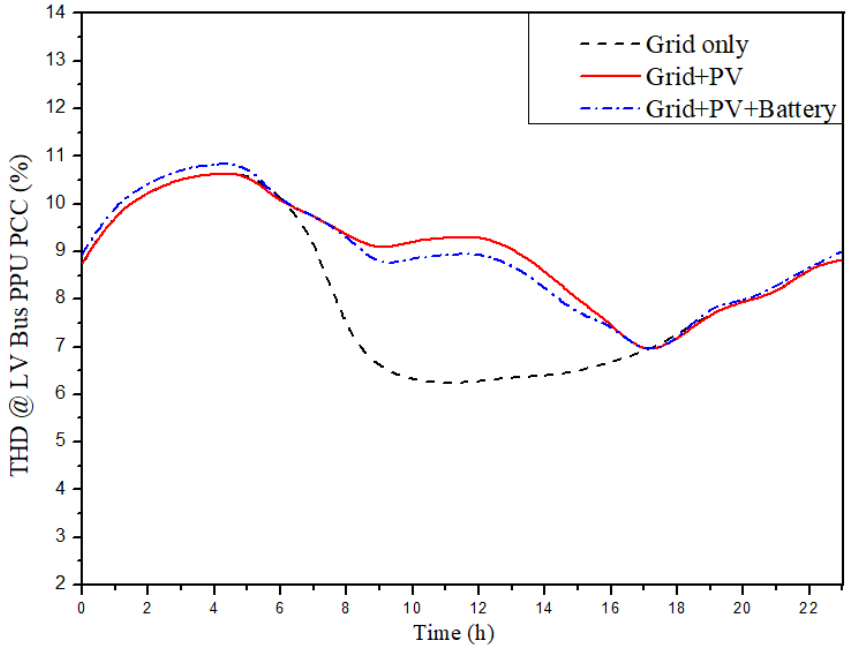

Figure 4.68: THD daily profile at the LV side of the PPU distribution transformer.

4.8: Short Circuit analysis PV & BESS with grid integration.

Short circuits studies are the most required in a power system in order to sufficiently size the devices, so that they are capable to handle the short circuit currents. The fault analysis may occur in different forms of faults such as three-phase, single-line to ground, line to line and double-line to ground, but the dominant is always the three phases to ground fault. These studies also help to adequately design the protection system, prerequisite for relay co-ordination and arc flash Studies.

Integration of the DG may also have extreme significant impact on the network short circuit level, in which may limit the connection of the DG to the network. However, the impact of PV penetration at a large scale into the electricity distribution networks, at severe network conditions (i.e. weak network), and location of fault occurrence remains uncertain. This leads to the importance of examining the short circuit level to assure the validity of connecting such DG to ensure smooth network operation and reliability.

This section examines the impact of PV and BESS on short circuit level of PPU feeder using ETAP software. Comprehensive results comparison is presented between the different cases for the grid only, grid and PV system only and grid and PV-BESS. due to the three phases to ground fault having the maximum current level fault configuration, this configuration only will be considered. Fig. 4.69 shows the proposed location for the fault study.

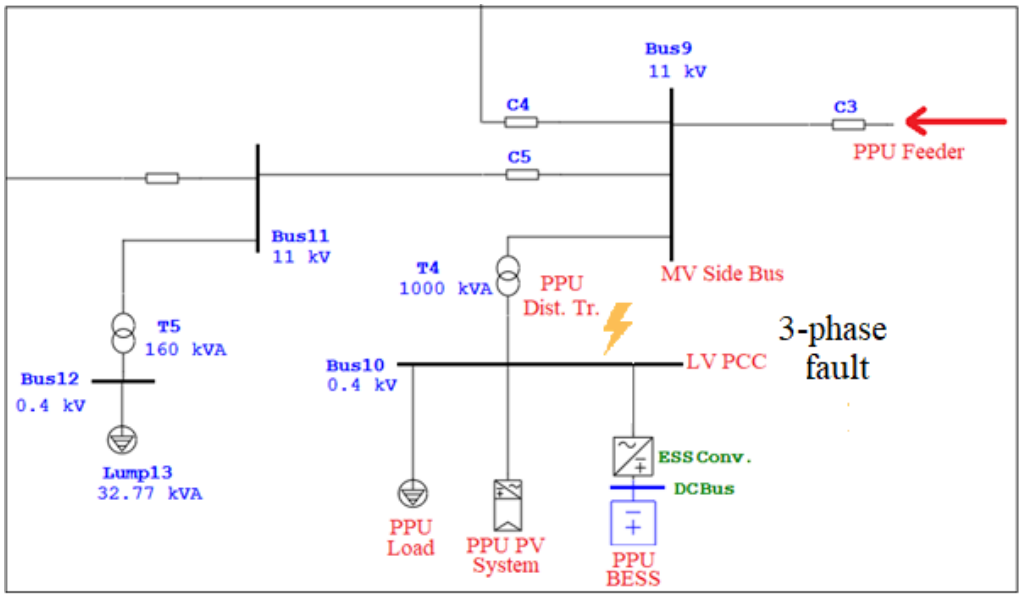

Figure 4.69: The proposed location for the fault.

4.8.1: Grid alone short circuit analysis.

The three phases to ground short circuit analysis was simulated at the ETAP software in addition to propose the fault was occur at the LV side of the PPU distribution transformer before integration and DG to the system and fig.4.70 shows the short circuit current in form of AC and DC component and the dominant was 24.66kA and the total envelope was illustrated at fig.4.71.

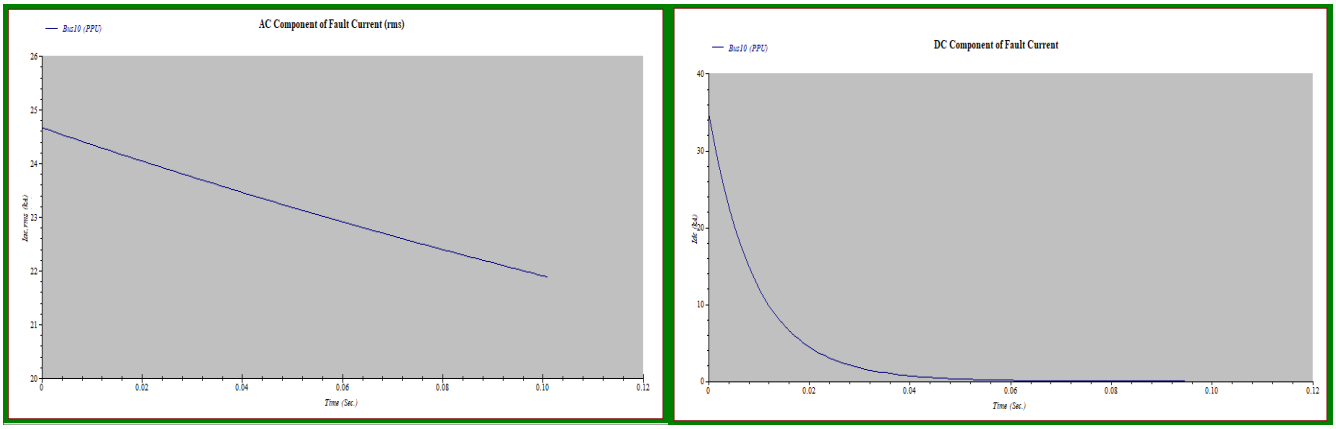

Figure 4.70: AC component and DC component fault current.

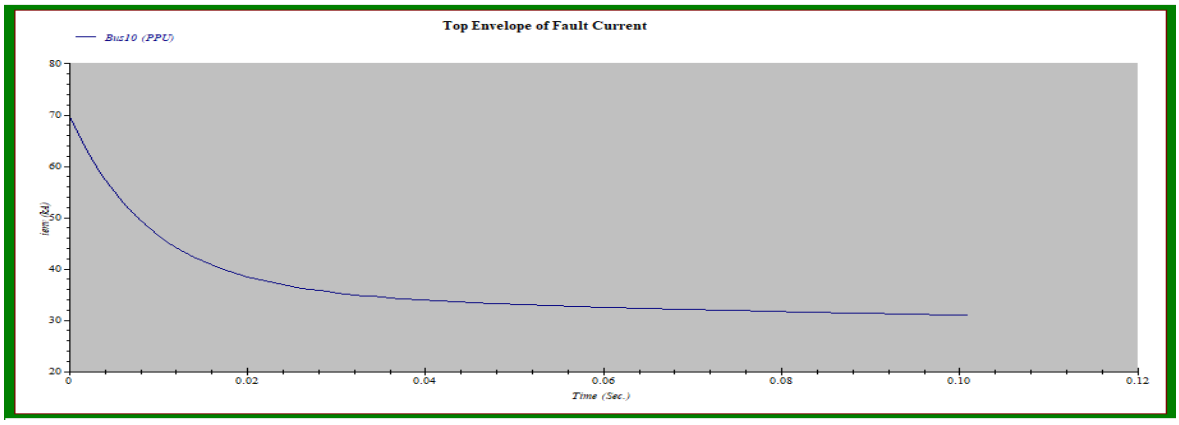

Figure 4.71: The top envelope of fault current for the three phases to ground fault.

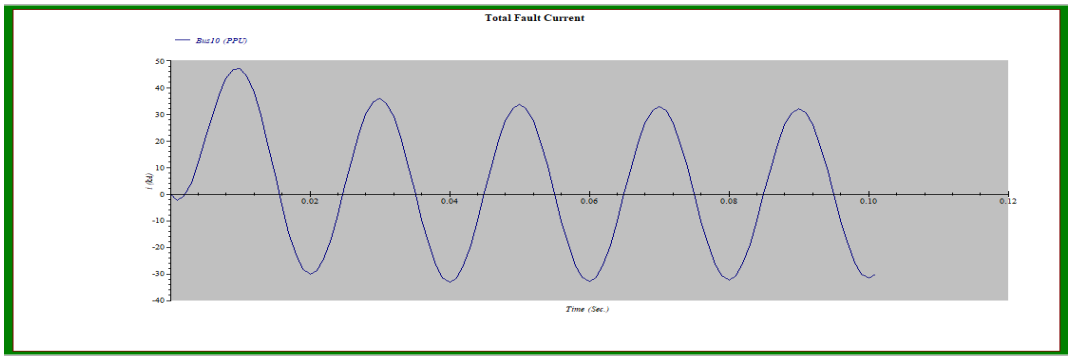

Figure 4.72: The total fault current wave form.

4.8.2: Grid with PV system integration short circuit analysis.

The three phases to ground short circuit analysis was simulated at the ETAP software in addition to propose the fault was occur at the LV side of the PPU distribution transformer with PV system integration to the electrical network, fig.4.73 shows the short circuit current in form of AC and DC component and the dominant was much higher than in the previous scenario 25.136kA which prove that the DG integration will increase the short circuit level in the system, and the total envelope was illustrated at fig.4.74.

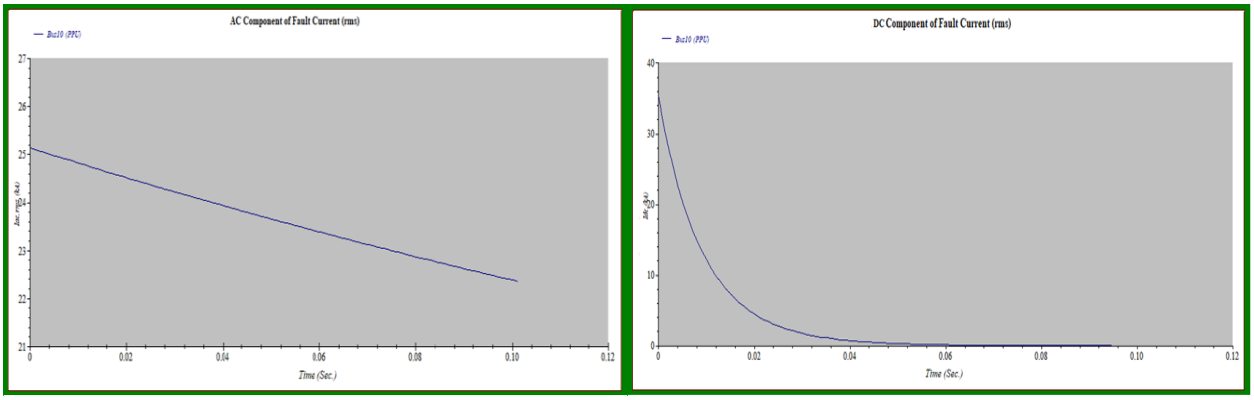

Figure 4.73: AC component and DC component fault current.

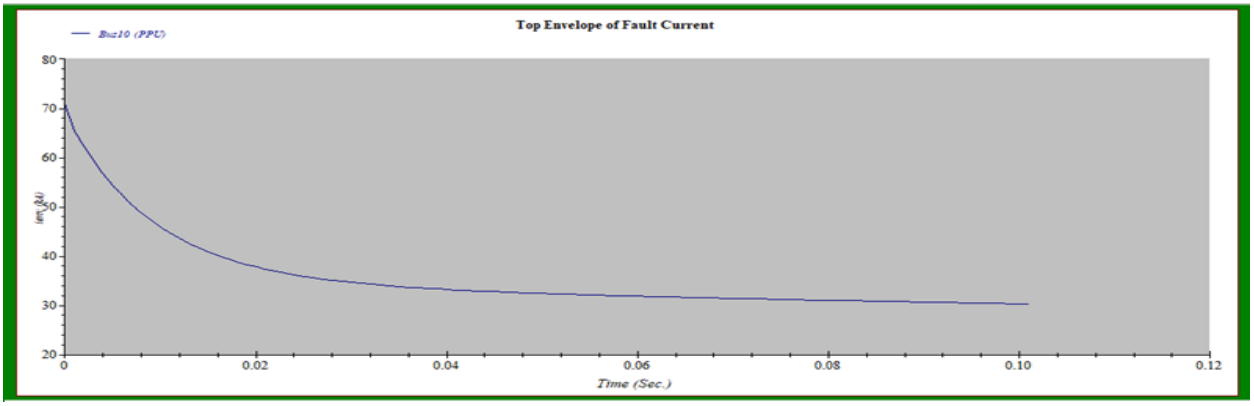

Figure 4.74: The top envelope of fault current for the three phases to ground fault.

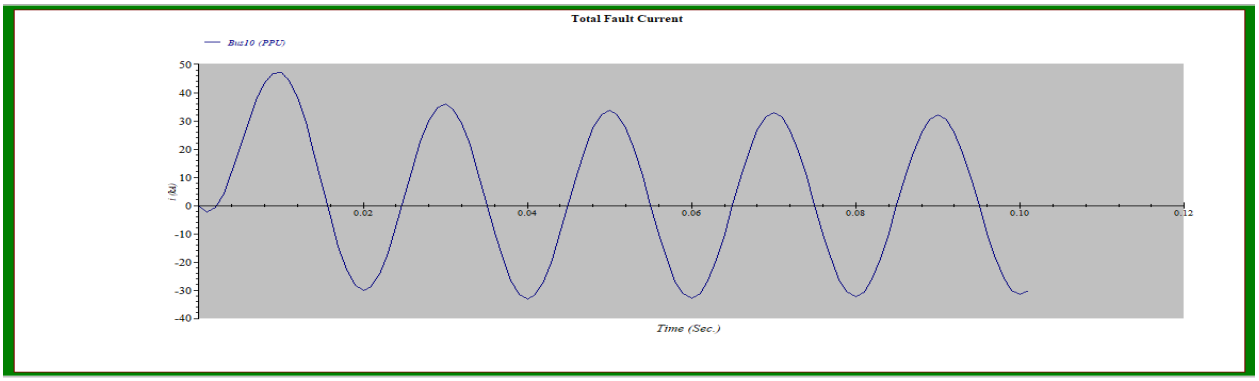

Figure 4.75: The total fault current wave form.

4.8.3: Grid with PV-BESS integration short circuit analysis.

The three phases to ground short circuit analysis was simulated at the ETAP software in addition to propose the fault was occur at the LV side of the PPU distribution transformer with PV system and BESS integration to the electrical network, fig.4.76 shows the short circuit current in form of AC and DC component and the dominant was much higher than in the previous scenario 25.2kA which prove that the storage system with DG integration will slightly decrease the short circuit level in the system, and the total envelope was illustrated at fig.4.77.

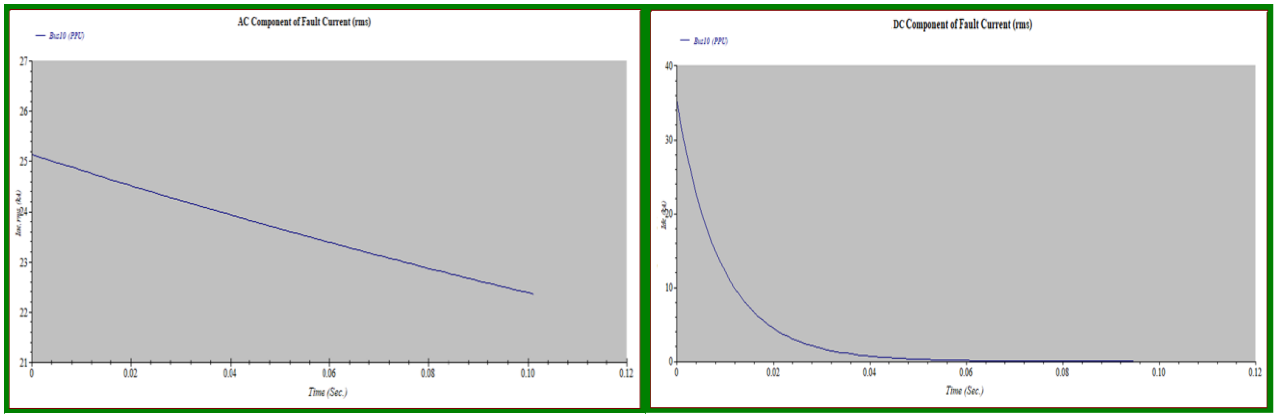

Figure 4. 76 AC component and DC component fault current.

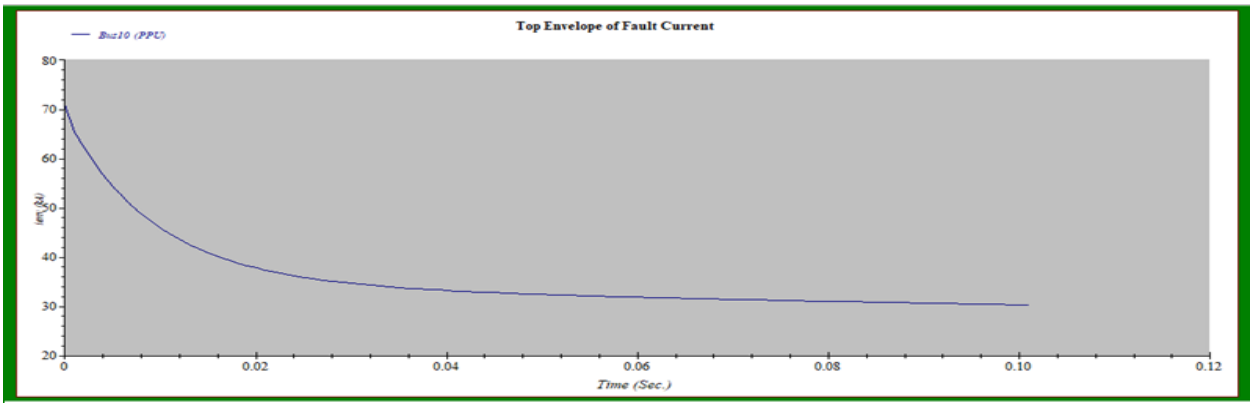

Figure 4.77: The top envelope of fault current for the three phases to ground fault.

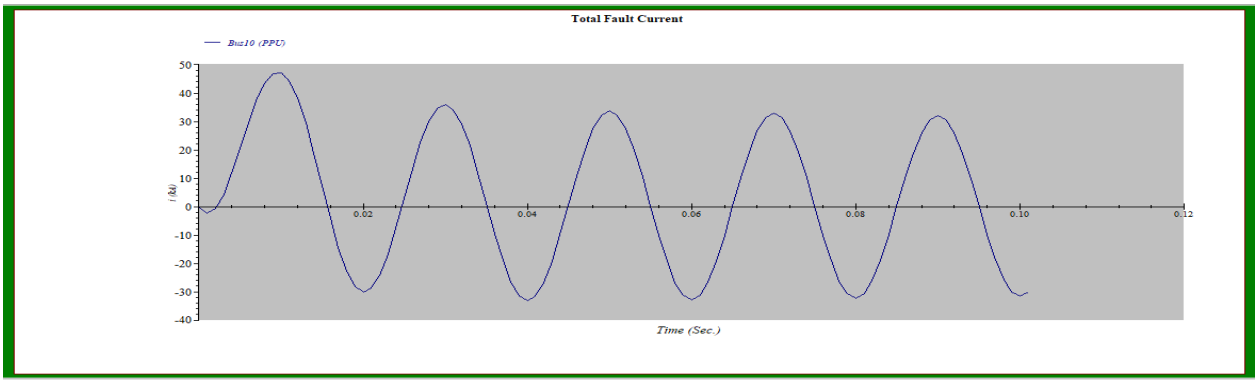

Figure 4.78: The total fault current wave form.

5

Chapter Five

PV Penetration level and enhancement using BESS

5.1: Introduction

Electric power network in a conventional configuration was designed with a radial nature unidirectional power flow. Power is generated at large power plants away from the users, then it transmitted through transmission lines at high voltages to the distribution networks that service the end users. This structure of power flow starts to change after the distribution generation system appeared. But the high penetration of the DG creates some issues to the modern grid.

The rabid increasing of the development in the DGs especially the PV technology which is integrated with the distribution system at the same rate, but the main issue in this case is the penetration level that allowed to be integrated with the electrical network which is limited by the grid parameters and component capacity to prevent the reverse power flow. However, the problem occurs when the power flows from the DG back to the substation and could feed power back into the grid. Reverse power flow has been identified to cause problems such as: Overvoltage on the distribution feeder, increasing short circuit currents and Protection desensitization. In this chapter the PV penetration level and how to maximize it will be under consideration.

5.2: PV Penetration level.

The amount of electrical energy that the grid tied PV system shared of the total demand feeder is a PV penetration level of a distribution network, eq. 2.3 illustrates the mathematical equation to specify the penetration level. However, the penetration level in a distribution network depends on network parameters and quality of the distribution network itself, the maximum PV penetration level on the distribution network or PV hosting capacity regarding to technical concentrations of the grid, based on the European standard EN-50160 which determines that a 3-5% overvoltage is acceptable. Additionally, the PV system feed the grid with only a real power which will effect on the PF at the PCC.

One main goal of this thesis is Determination of maximum PV penetration level accepted by the network and this aim can be achieved regarding to the Technical Rules for the Assessment of Network Disturbances method which can be used to integrate PV into the LV DG. Additionally, the BESS are proposed to improve Hosting Capacity for the feeder.

The power flow study is an important tool involving numerical analysis applied to a power system. Unlike traditional circuit analysis, a power flow study usually uses simplified notations such as a single line diagram and per-unit system and focuses on various forms of power such an active, reactive and apparent power, rather than voltage and current. It analyzes the power systems in normal steady-state operation. In this chapter the different scenarios will be conducted on the ETAP software for the integration of the PV system with the grid and BESS, fig.5.1 shows the block diagram of the working approach.

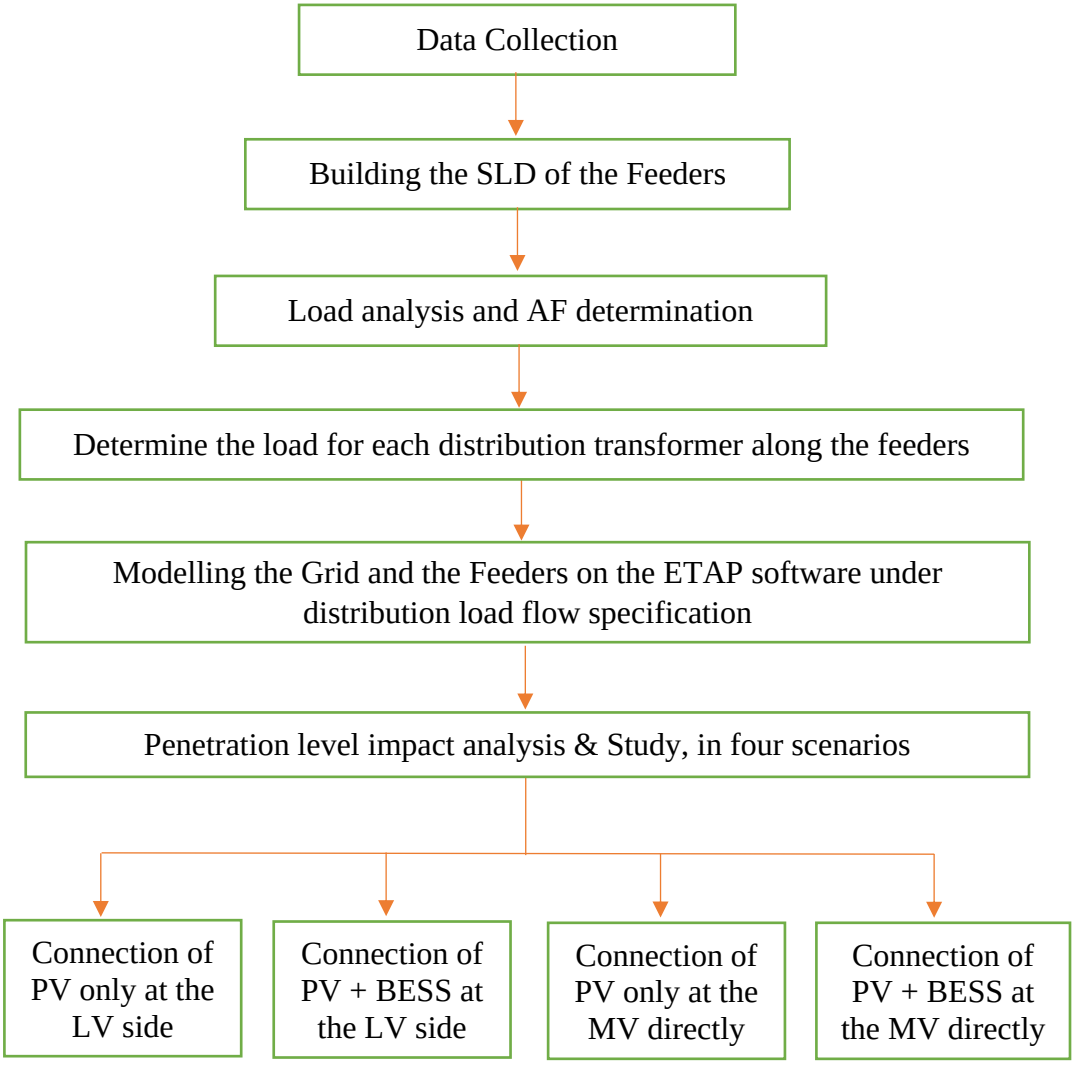

Figure 5.1: Methodology Block diagram.

5.3: Maximizing PV Penetration assessment.

One main goal of this thesis is to determine the maximum amount of PV generation that can be integrated in the PPU feeder from the Hebron distribution system and maximizing the PV hosting capacity by the BESS integration method. Furthermore, the current PV penetration level on the PPU feeder according to the penetration level eq. 2.3 is 13.4% with a 233 kW_{DC}, and regarding to [57] the optimum capacity of the storage system which integrated with the PV system to enhance the PV penetration level and performance should be 55% of the PV rated power. In current state the PV plant rating was 230kW_P therefore the BESS capacity is 126 kWh.

In this chapter a set of PV penetration level scenarios are considered, in which the PV penetration varies according to table 5.1 from 0 % to 100 %. The set of 11 scenarios was generated once by adding successively additional PV systems at the PCC in the grid. In a second step, battery storage system connected to the PV systems compatible with the penetration level for the same aim.

Table 5.1: Penetration level with PV and BESS capacity.

#	Penetration level (%)	PV rated (kW_{DC})	PV output (kW_{AC})	BESS Capacity (kWh)
1	0	-	-	-
2	13.4	231.0	210.0	127.1
3	15	260.6	234.5	143.3
4	20	347.5	312.8	191.1
5	25	433.7	390.3	238.5
6	35	608.0	547.2	334.4
7	45	782.0	703.7	430.1
8	50	870.3	783.3	478.7
9	60	1042.3	938.1	573.3
10	75	1303.0	1173.0	716.7
11	100	1734.3	1564.0	953.9

The examination of the PV penetration level and BESS integration impact on the electrical network is one of the main objectives of this chapter, the study will be along 11 cases of penetration level to observing the changing on the active power, reactive power, apparent power, power factor, voltage, THD and short circuit capacity level. However, the study will be described according the comparison cases as follows, and fig. 5.2 shows the connection placement of the PV and BESS in different situations:

- ❖ The PV Penetration level before and after integration of BESS with the PV system while the PCC is at the PPU low voltage bus (load bus).
- ❖ The PV Penetration level before and after integration of BESS with the PV system while the PCC is at independent Medium Voltage bus.
- ❖ Comparison between integrating the PV system in different penetration level at the medium voltage and low voltage bus system.
- ❖ Comparison between integrating the PV-BESS system in different penetration levels at the medium voltage and low voltage bus system.

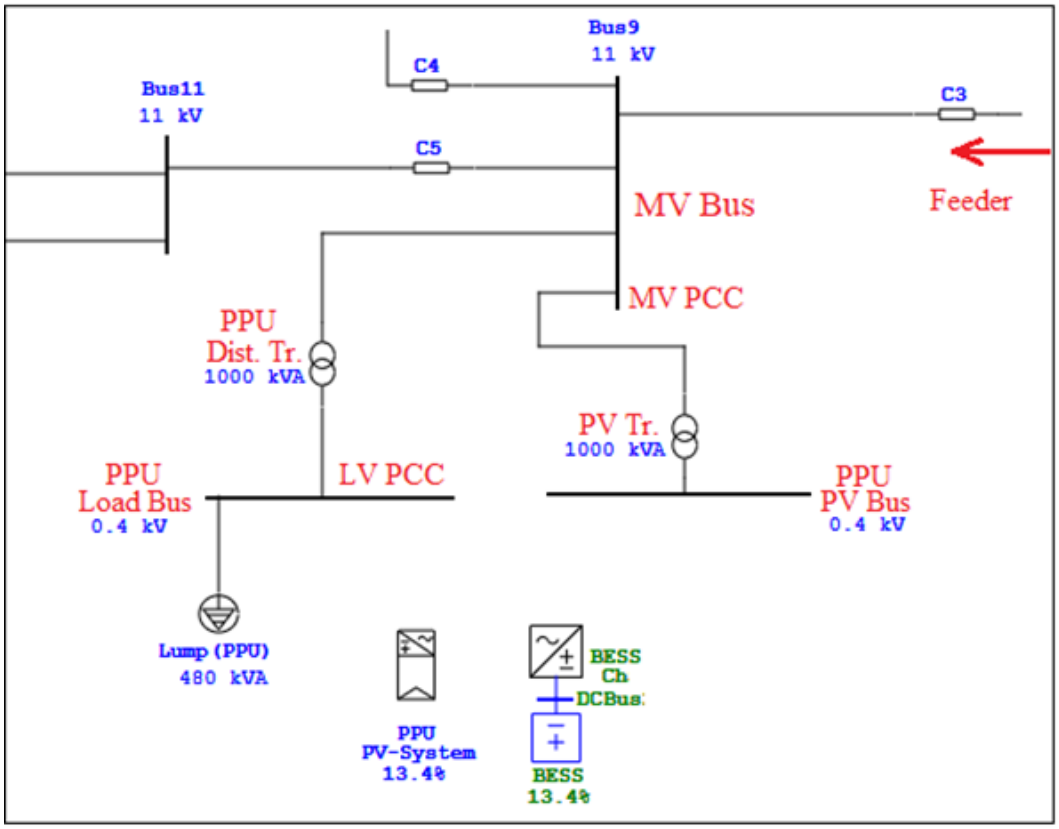

Figure 5.2: The single line diagram of the network and PV and BESS integration in MV and LV bus.

5.4: PV Penetration level and BESS Integration.

To maximize the PV hosting capacity of the electrical grid BESS approach was proposed, In this section the different proposed PV penetration level will examined with the electrical grid in two different scenarios, the first one is at the LV load bus, the second one is at the MV voltage bus directly to the MV feeder fig. 5.3 represents the SLD description.

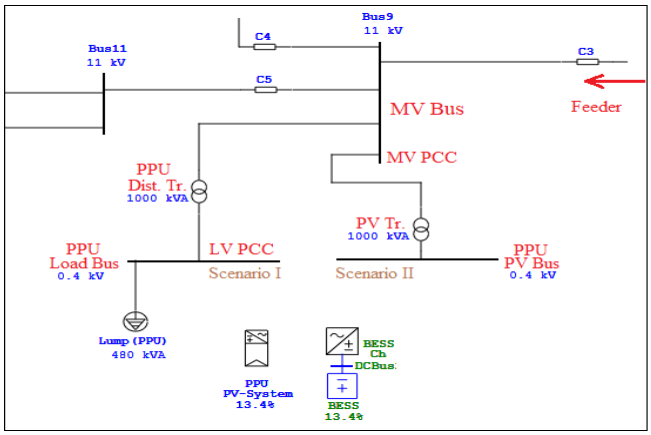

Figure 5.3: SLD of the two proposed approach.

The peak production of the PV system in different penetration level will be considered and its clearly that the PV production increases by increasing the penetration level and the consumption from the feeder side declines at the same point. On the other hand, the instant production of the PV-BESS is less than the PV without BESS which decreases the contribution of the PV system at the peak production and allow the DG to shift its peak energy generation from the peak time. Fig.5.4 represents the produced power at different penetration levels with and without BESS integration, and the power demanded from the interconnection point for the same cases illustrated in fig.5.5.

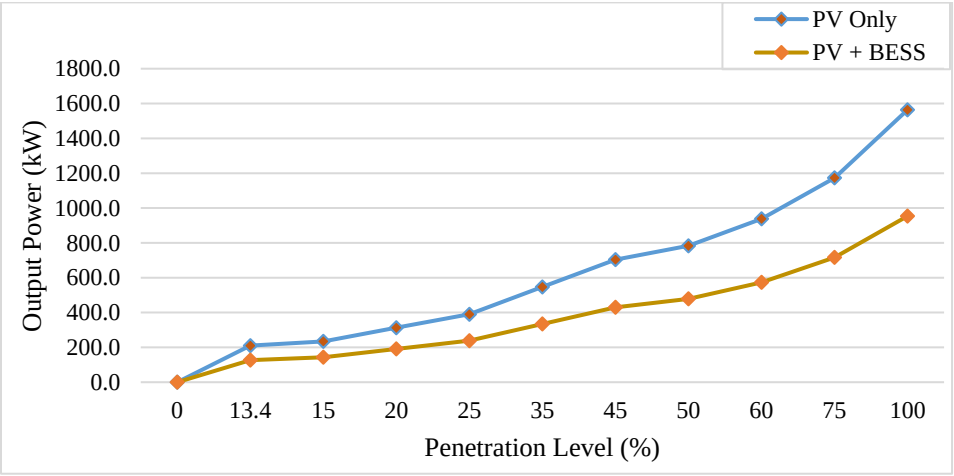

Figure 5.4: Output power of the system with and without BESS.

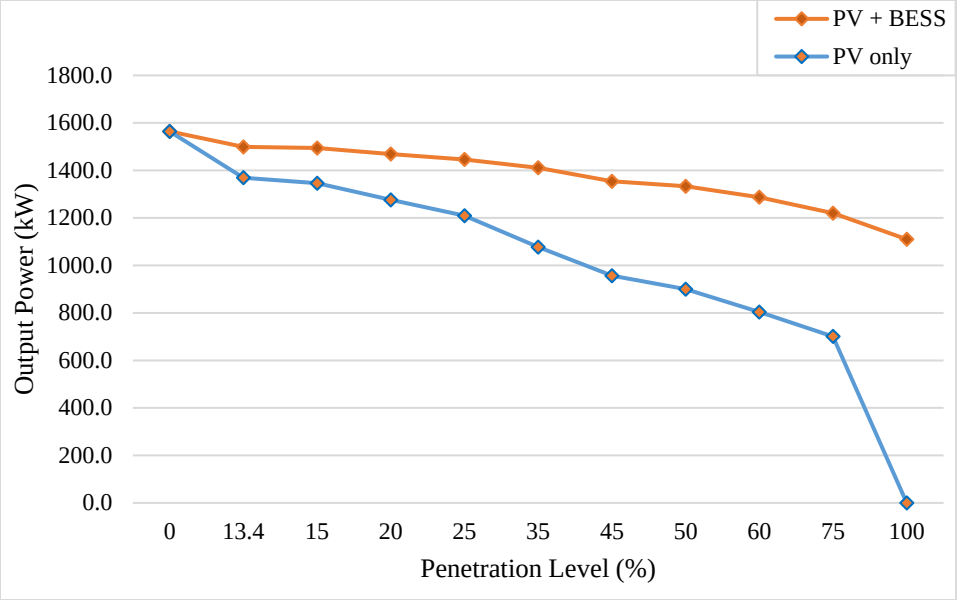

Figure 5.5: Power consumption from the main feeder with and without BESS.

It's worth mentioning that, due to the decreasing of the demand of the interconnection point, the power losses along the feeder decreases at the low penetration levels, but at the instant that the high penetration level and the PV plant begin to be the dominant power source of the feeder, the power loses will return back to be increased. Fig. 5.6 illustrates the power losses profile. On the other side BESS reducing the effect of the PV system only means that the power losses along the feeder stay high comparing with the PV without BESS.

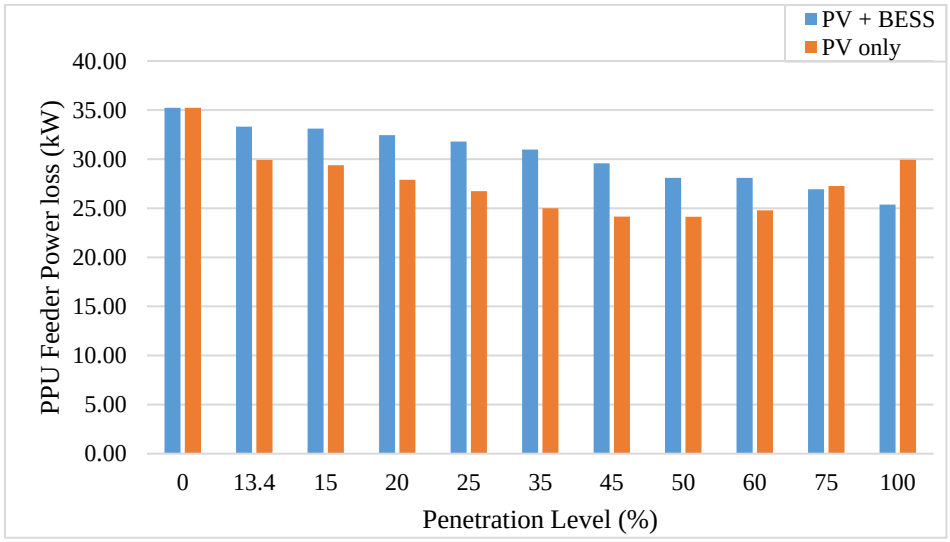

Figure 5.6: Power losses along the feeder with and without BESS.

5.4.1: PV Penetration level with and without BESS at LV.

In this section the study will be in a LV PCC scenario that has two cases, therefor the 11-penetration levels of the PV system will be considered and integrated with the LV PCC the power, PF, power losses, voltage, harmonics and short circuit capacity will be observed and then the BESS integrated with the system in the same circumstances to make an exact comparison between the PV system only and the PV-BESS configuration.

5.4.1.1: Voltage profile issue.

Integration of the PV systems with the electrical network have a direct impact on the voltage level on the PCC in addition to the voltage level on the main buses of the system particularly at the high penetration level of PV system. On the other hand, integration of BESS has advantage to minimize this over voltage even in high penetration level, so this is to justify the storage system use. In this case the observation of integration BESS with the PV system in different penetration levels will be done in three main point of the feeder, at the LV PCC in fig.5.7, at the MV side of the PPU distribution transformer at fig 5.8, and the voltage level at the main bus of the feeder at interconnection point shown in fig 5.9.

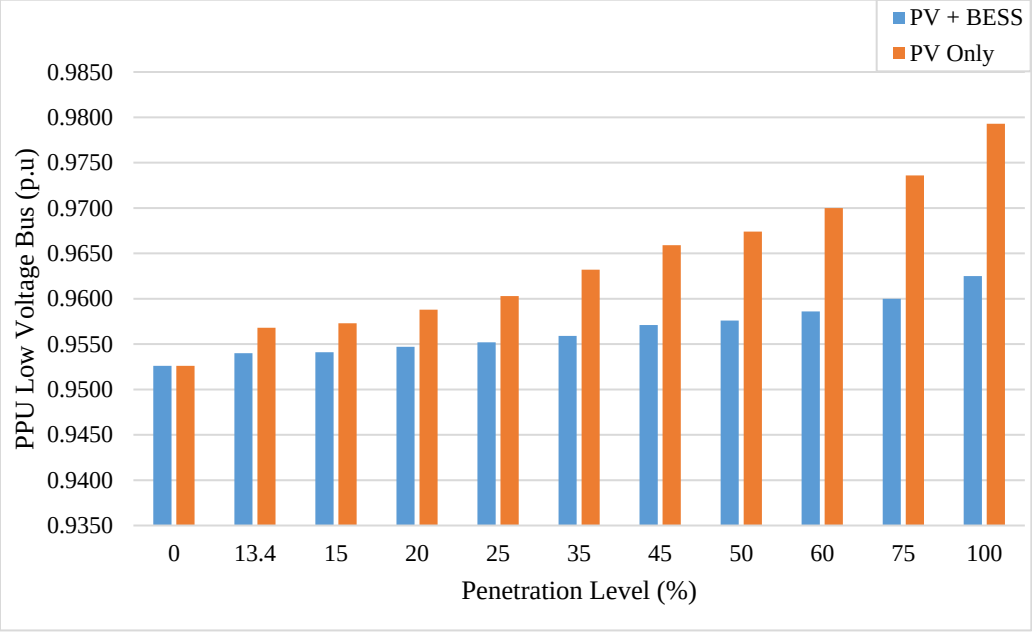

Figure 5.7: PPU low voltage bus value with and without BESS.

However, the over voltage at the LV PCC between 0-100% penetration level is 2.8% with PV only case and 1.3% after integrating BESS, but at the MV main bus the voltage over did not exceed 0.12% without BESS and the effect at the main bus with storage system is very low. Consequently, the effect of increasing the penetration level at the LV PCC is much higher than the effect at the interconnection point at the starting point of the feeder.

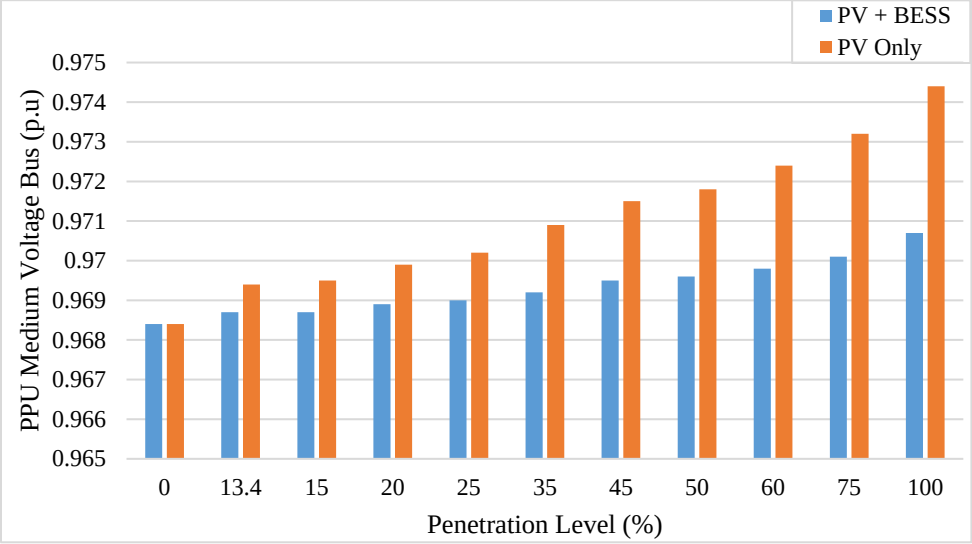

Figure 5.8: Medium voltage side bus value with and without BESS.

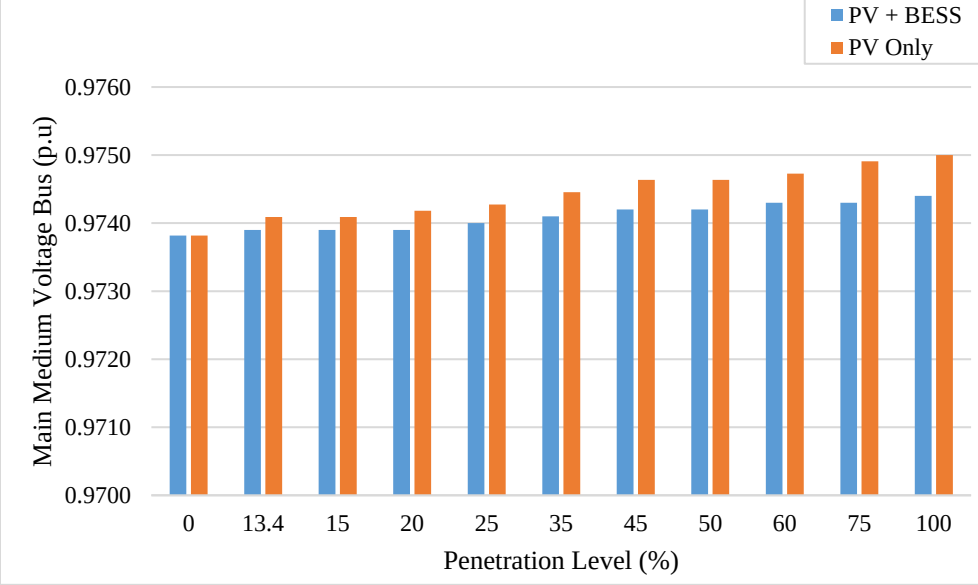

Figure 5.9: Main voltage bus value with and without BESS.

5.4.1.2: Power factor and power flow indication issue.

Steady-state power flow analysis is used to examine the power factor variation for a variety of distributed generation penetration. Based on the power flow analysis, the PV system produces the active power to the grid and at high penetration level the power factor will indicate the power flow direction, in case of preventing the reverse power flow at the critical points. When PV system works with high power values, most active power demanded by the customers is supplied by the PV plant, reducing the demand of active power from the grid. However reactive power demand is the same, therefore the power factor will be worst. Fig 5.10 illustrates the PF variation along different penetration levels on the feeder at the low voltage PCC and PPU distribution transformer view, it's clear that after 25% of penetration the power flow starts to be transmitted to the MV feeder in the most cases, in other words after 25% always there are exporting energy to the MV feeder. In contrast when BESS integrated with the system the percent of penetration get to be more than 75%.

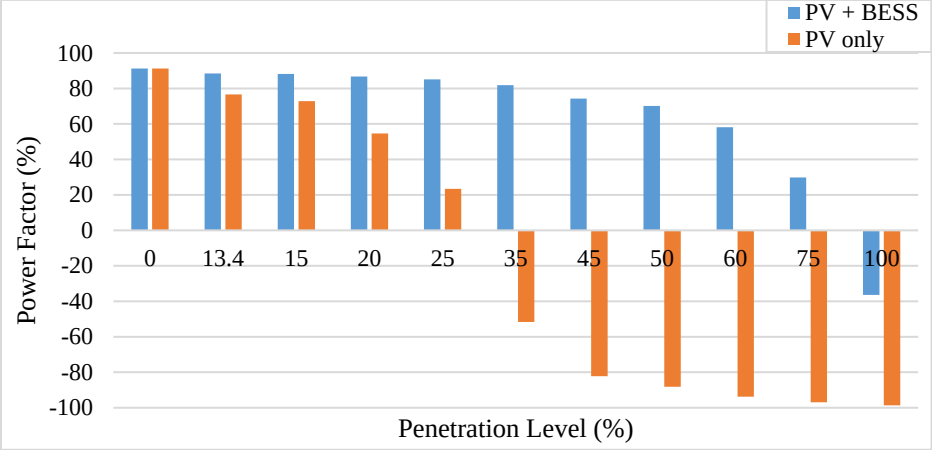

Figure 5.10: Power factor at the LV bus with and without BESS.

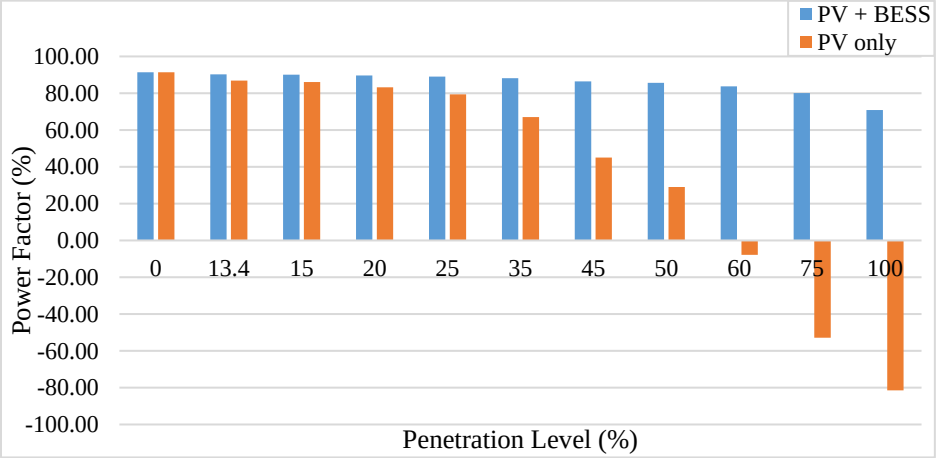

Figure 5.11: PF at the MV side of the distribution PPU transformer bus with and without BESS.

In the PV plant when a Penetration level becomes 100%, a significant reverse energy flow observed to the source that raises the voltages on the buses. The source bus appears as a reactive power source only, the heating on the network elements reduce the effectiveness of network. But when the BESS integrated with the system the condition will be changed and the reactive power will be regulated, fig 5.11 shows the PF at the MV feeder in the side of the PPU distribution transformer which indicates that the critical penetration level will be less than 60%. At the main bus of the feeder the whole demanded real power will covered by the PV at 100% and the reverse power to the transmission will be at the boundary point, but not with the PV-BESS configuration. See fig. 5.12.

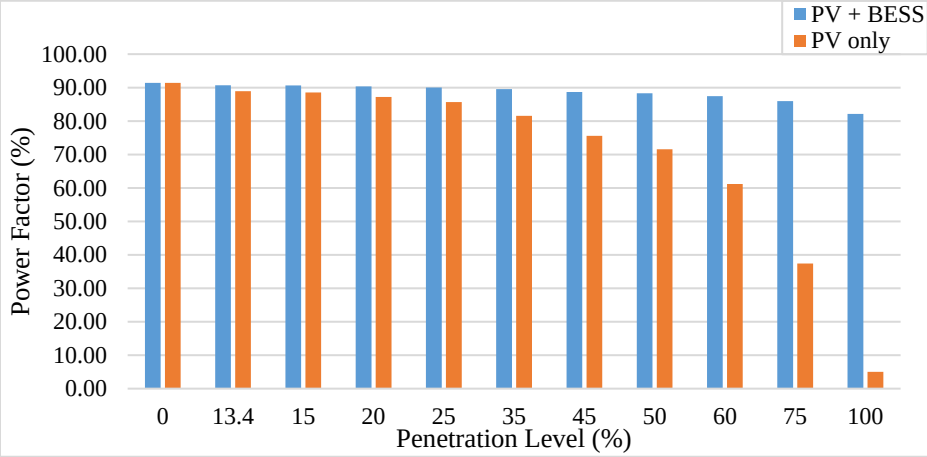

Figure 5.12: PF at the feeder starting point with and without BESS.

5.4.1.3: Total Harmonic Distortion & shot circuit capacity issue.

To check the harmonic distortion or effect of harmonic source on the power network, Harmonic load flow needs to be performed. Meanwhile, harmonic load flow is performed to the PPU feeder. Total harmonic distortion at the PCC gradually increases after integrating the PV system as the penetration level raises, since PV system connected with a LV bus, and regarding to the IEEE-THD standard, the THD limit is 8% and the system will exceed this limit after the 25% of penetration which justifies the limitation role of distribution company. However, the integration of the BESS increases the limited penetration levels up to 75% at the same condition. Fig. 5.13 illustrates the THD in a different penetration level at the LV PCC. From the main bus point of view the THD reference will be at 0% penetration which is 2.7%, and due to the decreasing of power demanded by the source the distortion also decreases but not at the PCC. Means that the allowable penetration level is increasing by BESS due to the regulation of the harmonic at the main bus. As in fig. 5.14

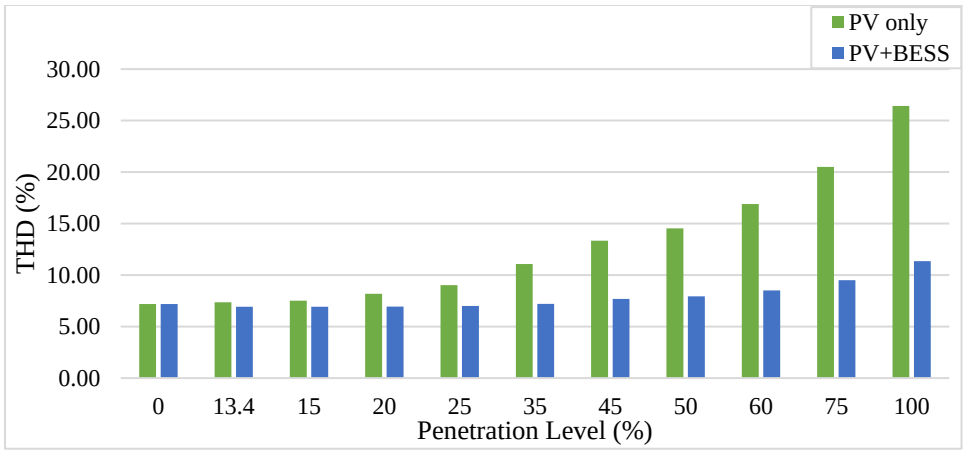

Figure 5.13: THD in different penetration level with and without BESS LV of PPU Dist. Tr.

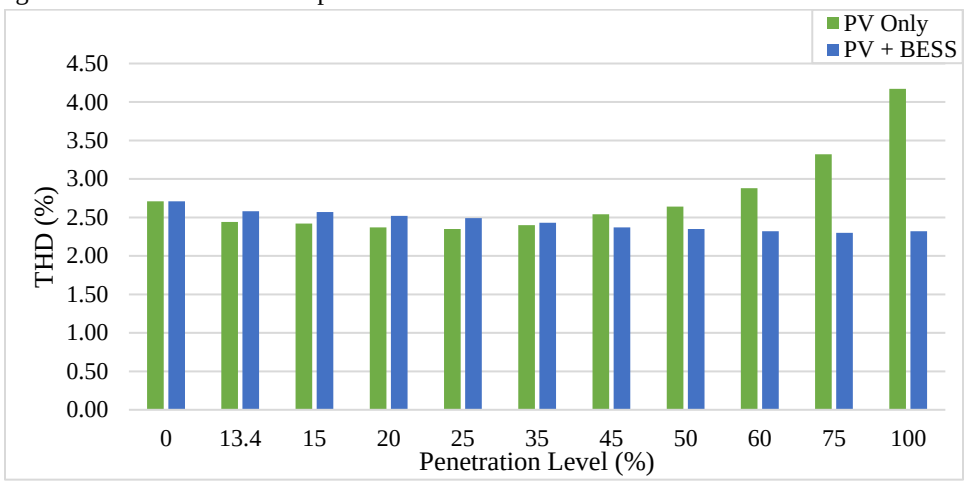

Figure 5.14: THD in different penetration level with and without BESS main bus.

BESS used to enhance the performance of the grid and maximizing the PV penetration level, this is a very interesting solution for grid operators to reduce the primary power reserve. But the technical drawback of storage system is the short circuit level, which increases after the BESS integrated as in fig. 5.15, the observation is clearly that level of SC capacity increase.

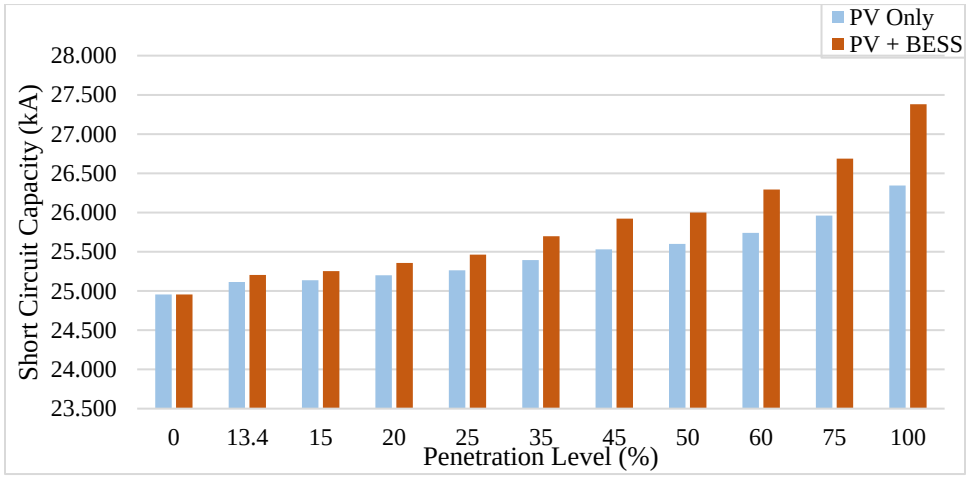

Figure 5.15: Short circuit capacity at different penetration level with and without BESS.

5.4.2: PV Penetration level with and without BESS at MV.

The previous section was discussing the impact of PV penetration on the grid at a LV load bus PCC, whereas this section will discuss the second scenario which is the integration of PV system and the PV-BESS directly to the MV feeder. MV connection approach proposed due to the clear impact of the PV system that appear at the LV PCC. However, the 11-penetration levels of the PV system integrated with the MV feeder with and without BESS, then power, PF, losses, voltage, harmonics and short circuit capacity, will be observed as follows:

5.4.2.1: Voltage profile issue.

The maximum penetration level of the PV system that allowed to be integrated with the electrical network can be limited by the overvoltage issue at the PCC, in this case the effect of PV is directly to the MV bus feeder and it will be extreme particularly at high penetration levels. While BESS which integrated with the system, was contribute to minimize the high penetration effect and maximize the hosting capacity. The observation of integration BESS with the PV system in different penetration level will be done in three main point of the feeder: at the LV bus directly the LV side of the step up PV transformer in fig.5.16, at the MV side of the step up PV transformer in fig 5.17, and the voltage level at the main bus of the feeder at interconnection point fig 5.18.

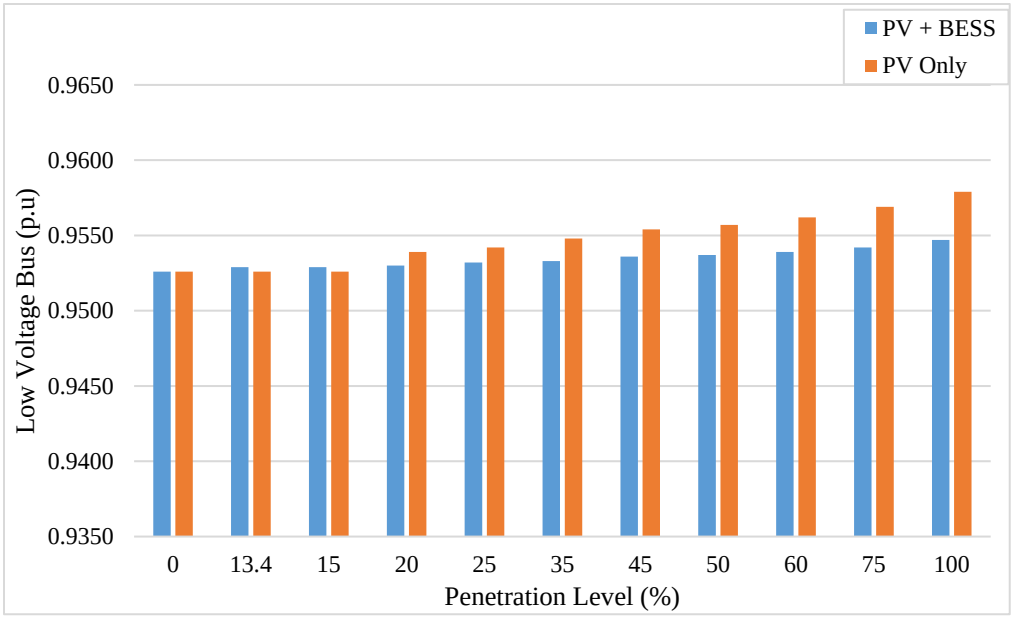

Figure 5.16: Low voltage PV bus voltage value with different penetration level.

However, the over voltage at the LV side of the step-up PV transformer, and penetration level between 0-100% penetration level is 0.53% with PV only case and 0.21% after integrating BESS means that the voltage variation at the LV bus is pretty low not like a load bus case. While at the MV main bus of the feeder the over voltage did not exceed 0.05% without BESS and the effect at the main bus with storage system is very low. Consequently, the effect of increasing the penetration level at the MV PCC at after the step-up PV transformer is much higher than the effect at the interconnection point at the starting point of the feeder.

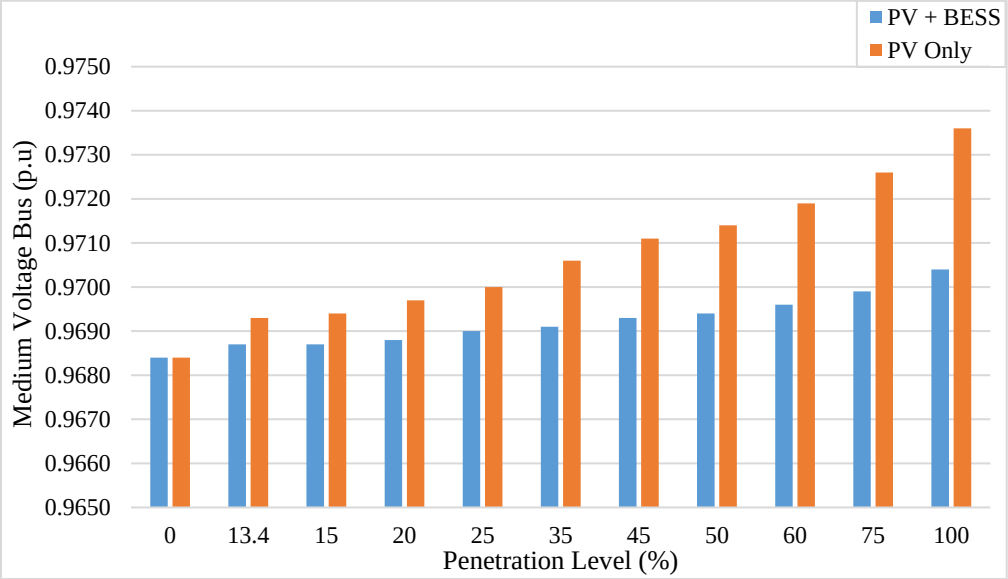

Figure 5.17: Medium voltage PV bus voltage value with different penetration level.

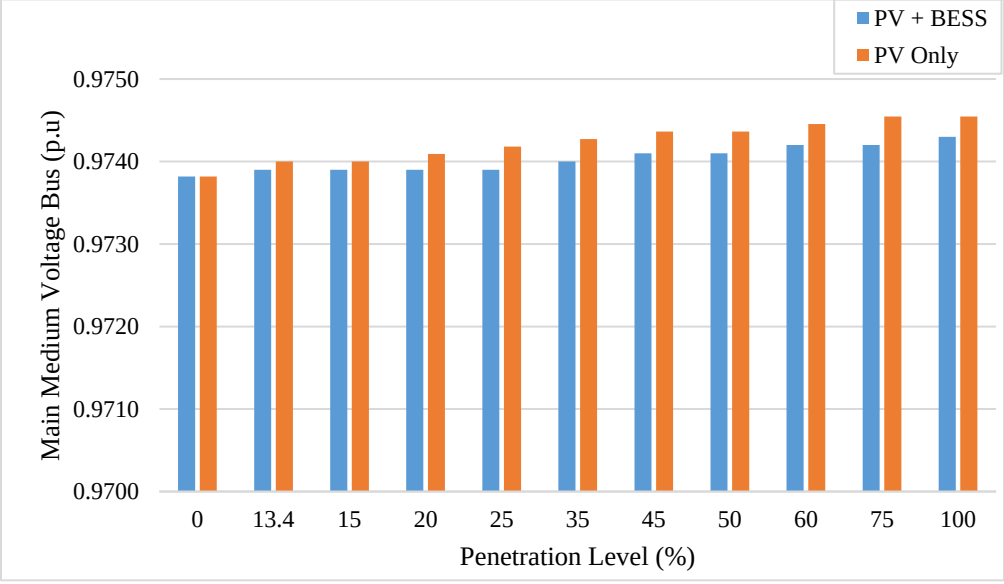

Figure 5.18: Main bus voltage value with different penetration level.

5.4.2.2: Power factor and power flow indication issue.

Steady-state power flow analysis is used to examine the power factor variation for a variety of distributed generation penetration. PV plant feed the electrical network by an active power only, when a high penetration of PV which directly tied with grid leads to the majority active power of the system covered by the PV plant and reduced its demand from the starting feeder point. However, PF will indicate the power flow direction in the grid due to the constant demand of the reactive power.

Fig 5.19 illustrates the PF variation along different penetration level on the feeder at the MV side of the PV step-up transformer, it's clear that the critical penetration level of the PV system is less than 60%, while integration of the BESS with the PV system prevent that point. Moreover, 100% penetration level at the main MV bus of the feeder is critical point due to the reverse power flow to the transmission line. But when BESS integrated with the system the percent of penetration reach 100% with a PF = 0.7, means the hosting capacity increased to this feeder, see fig. 5.20.

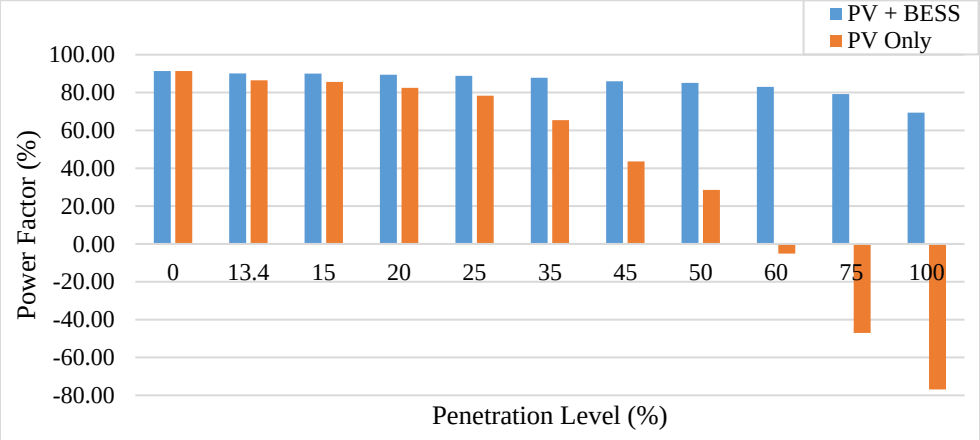

Figure 5.19: PF with different penetration level at the MV side step-up Tr. of PV bus.

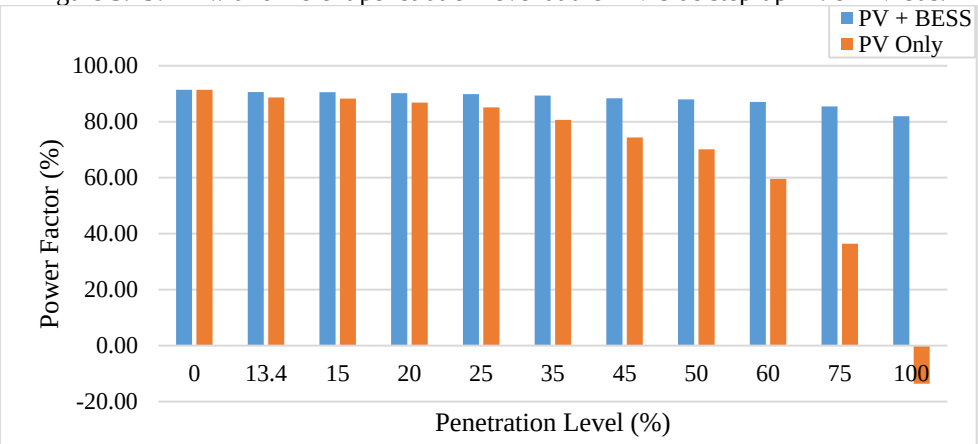

Figure 5.20: PF with different penetration level at the main bus of the PPU feeder.

5.4.2.3: Total Harmonic Distortion & shot circuit capacity issue.

Total Harmonic Distortion is an indication to the harmonic distortion level in the electrical network, Harmonic load flow needs to be performed. In this section a harmonic load flow is performed to the PPU feeder. Total harmonic distortion was observed at three main buses: the LV side of the step-up PV transformer, MV side of the step-up PV transformer and the THD at the main MV bus in the feeder.

Regarding to IEEE Standard 519-2014 as mentioned in chapter two which recommend that THD limit is 8% for LV bus and 5% for MV bus, fig 5.21 illustrates the THD profile along the PV penetration level increased and it's indicates that the penetration level should not exceed 15% with the PV only system due to the THD level, but when the storage system integrated at the same bus the boundary point of penetration increased up to 35%.

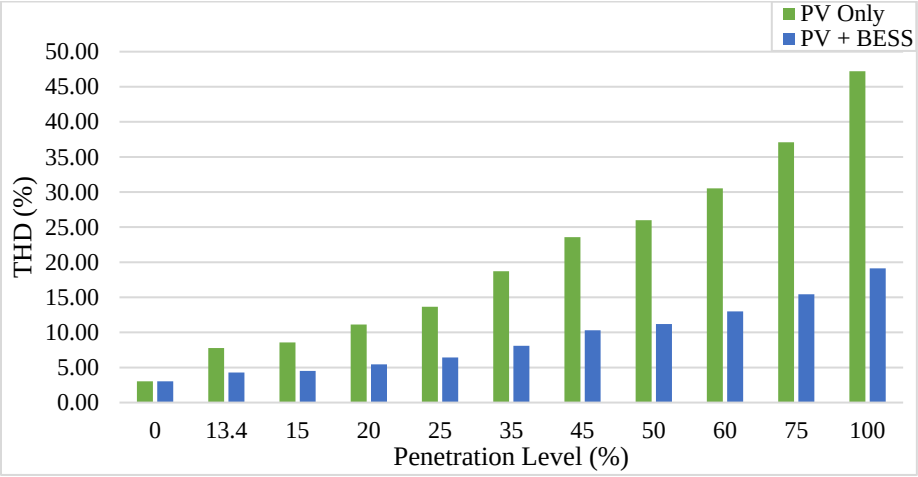

Figure 5.21: THD in different penetration level with and without BESS at LV PV bus.

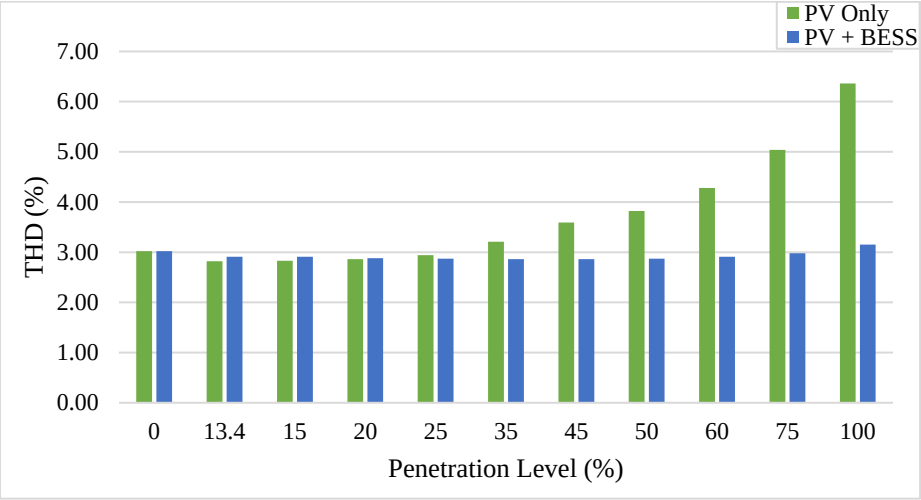

Figure 5.22: THD in different penetration level with and without BESS MV side of PV bus.

The MV side of the step-up PV transformer THD is illustrated in fig. 5.22 and its obvious the penetration level of the PV system could not be exceeding 75%, unlike the integration BESS case which still less than the standard limit even at 100% penetration level. At the main MV bus of the feeder point of view only the 100% is critical due to the reverse power phenomena but with the storage system the total hosting capacity of the PV for the feeder increased. As in fig 5.23.

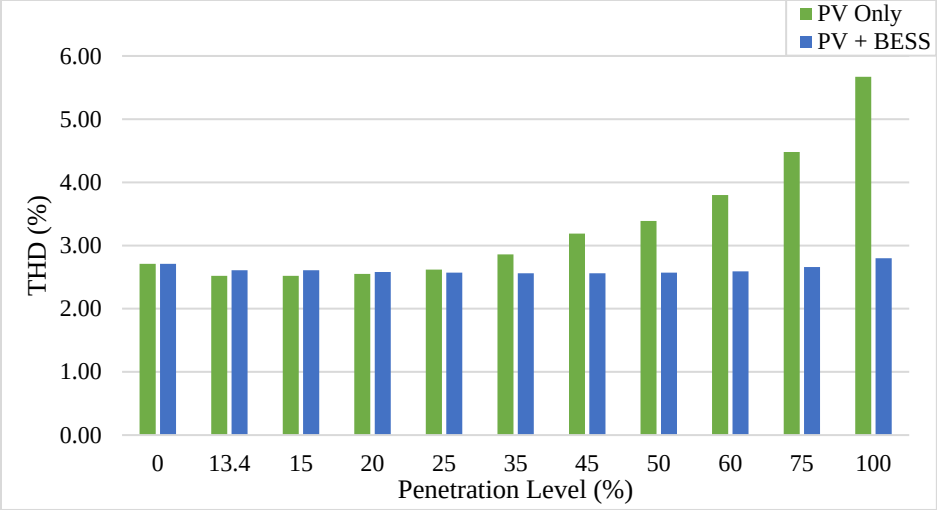

Figure 5.23: THD in different penetration level with and without BESS main bus.

One of the main aims of integrating BESS is to maximize the PV penetration level and enhance the performance of the grid, whereas integrating another power source on the MV feeder will increase the short circuit level when the electrical fault occurs. Fig 5.24, shows the short circuit level test at the MV side of the PV transformer when the extreme fault happened which is a 3 phase to ground fault test. The observation is short circuit level increases as the PV penetration increases and the condition get to be worst with the energy storage system.

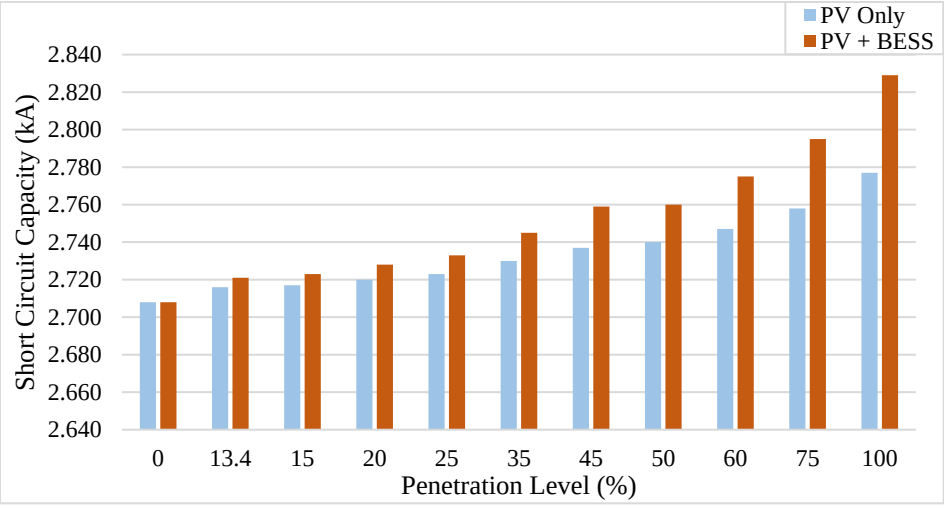

Figure 5.24: Short circuit capacity at different penetration level with and without BESS.

5.5: Medium and Low Voltage PCC comparison of PV Penetration level.

This section illustrates two scenarios of PV penetration which aims to investigate the difference effect between integration the PV-DGs at the medium voltage feeder directly and on the low voltage load buses. Furthermore, the observation was built upon two cases as follows:

5.5.1: PV penetration level at MV and LV PCC.

Meanwhile, an 11-penetration level of the PV system will be considered and integrated with the LV load bus and then with MV feeder directly. Voltage, PF, power losses, and harmonics were observed at the same circumstances to make an exact comparison between the PV system integration at the LV and MV bus.

5.5.1.1: Voltage profile issue.

The main limitation of integration PV system with the electrical network can be the overvoltage issue at the PCC, in this case the effect of PV production will be extreme when its integrated directly to the LV load bus particularly at high penetration levels. While integration of the PV system with the MV feeder has the less changing of voltage magnitude clearly, and it depends on the penetration level and the distance of the MV PCC from the starting point of the feeder. Fig. 5.25, shows the difference between integration the PV system with different penetration levels at the LV buses of the PV plant and the variation reached to 2.5% which indicates that the integration of PV at LV bus without load enhance the undervoltage phenomena at PCC.

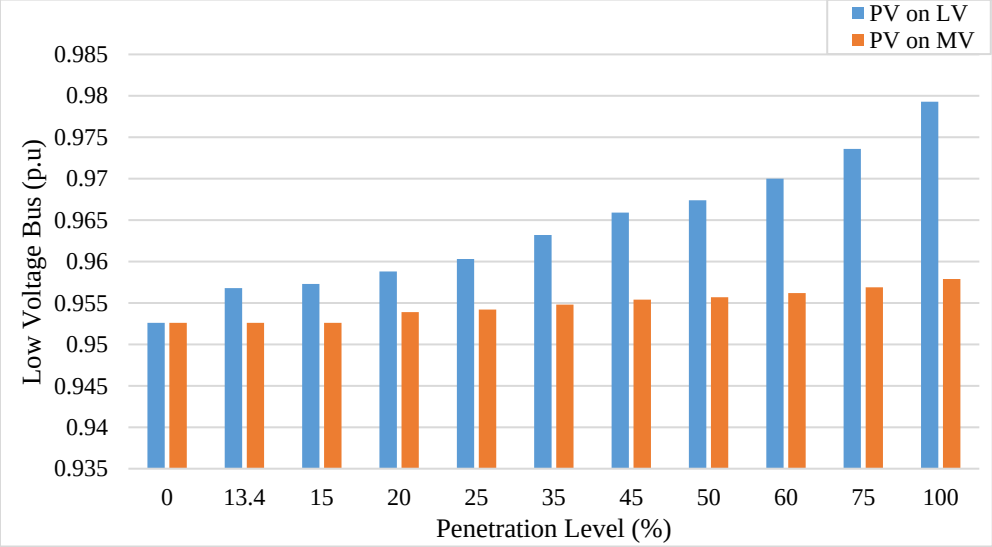

Figure 5.25: Low voltage bus voltage profile with LV PV integration and MV one.

The observation of integration PV system on the LV load bus is much higher than integrating it with the MV voltage bus. However, the over voltage at the MV side of the step-up PV transformer and PPU distribution transformer “Bus 9” along penetration level between 0-100% penetration level is 0.61% with PV at LV bus case and 0.5% with PV at MV directly, as illustrated in fig. 5.26. From the other side the effect of the main bus feeder is very low in the two cases as fig. 5.27 shows.

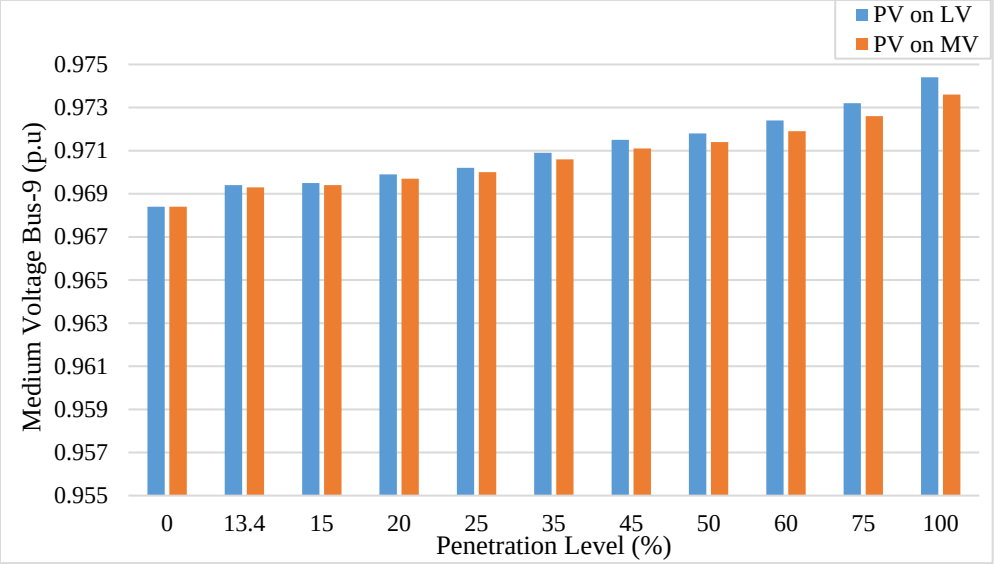

Figure 5.26: MV side of the PPU distribution Tr. And PV step up Tr.

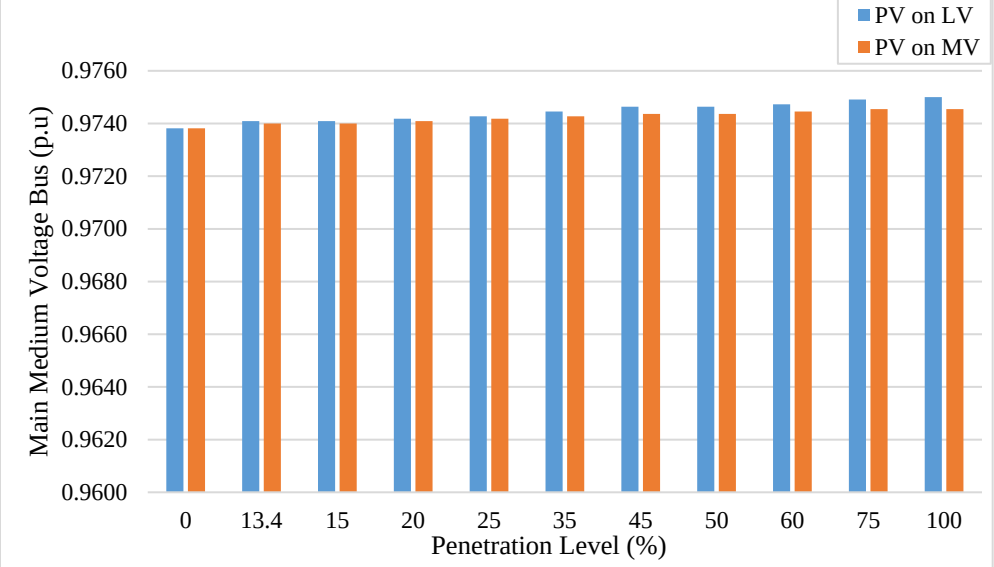

Figure 5.27: Main bus feeder voltage profile with all penetration level.

5.5.1.2: Power factor profile and power losses issue.

Power factor illustrates the power flow direction along the observed bus in the feeder, regarding to the constant value of the reactive power required by the system the effect on the PF varies clearly with different penetration levels. Fig. 5.28 represents comparison between the PF variation at the LV PCC in two different cases which is the LV side of the PPU distribution transformer with the load, and at the LV side of the step-up PV transformer without any loads. Therefore, without load the power factor will be controlled by the PV inverter, but with the load integration at the PCC the demand and PV penetration could control the PF profile, and the upper limit of the power flow is less than 35%.

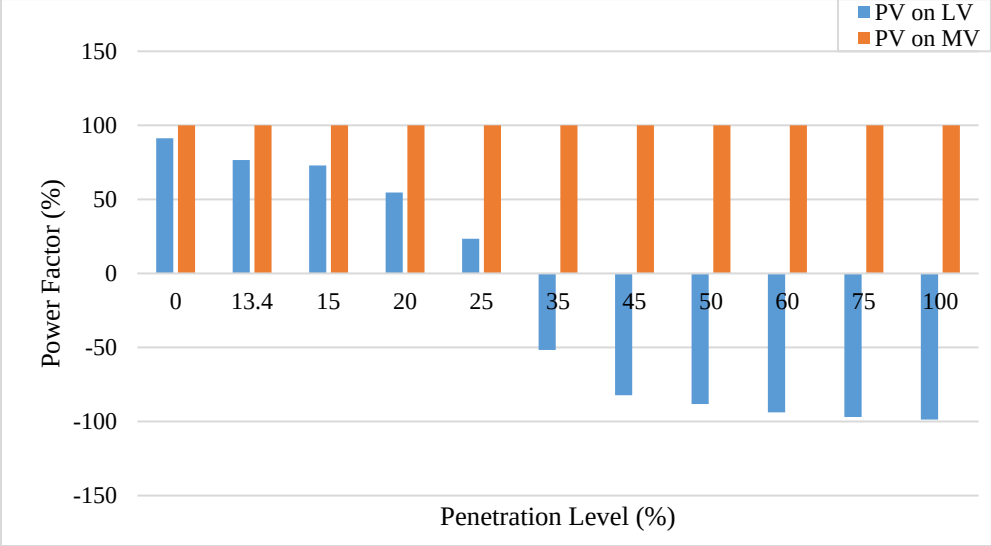

Figure 5.28: PF at the LV side of the Distribution transformer and the step-up PV Tr.

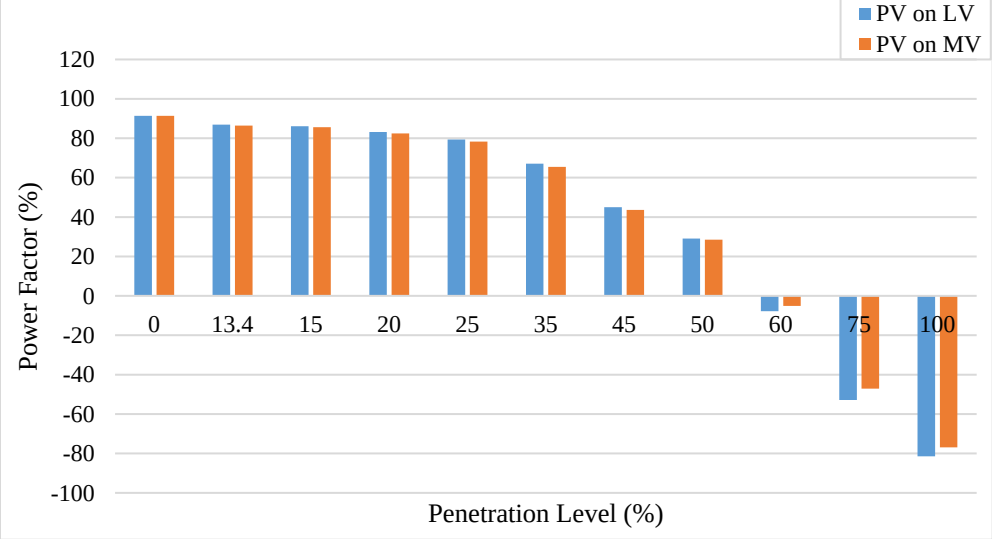

Figure 5.29: PF at the MV side of the Distribution transformer and PV step-up Tr.

Fig 5.29 illustrates the PF variation along different penetration level on the feeder at the MV side of the PV step-up transformer and the PPU distribution transformer, it's clearly that the critical penetration level of the PV system is less than 60%. While at the starting point of the feeder the critical point will reach the 100% penetration, and the effects of integration PV system at the MV and LV are closed to each other.

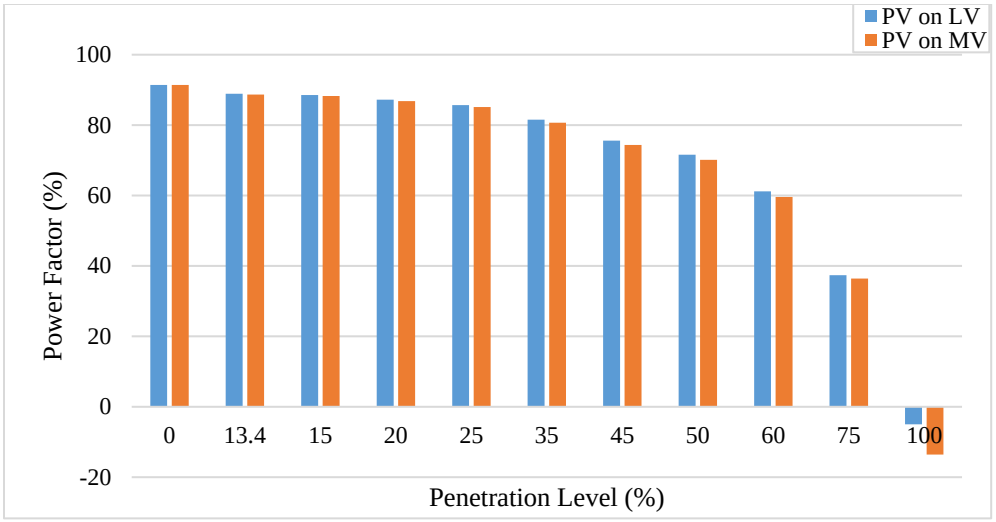

Figure 5.30: PF at the starting point of the feeder with PV only integration.

As the PV penetration level increases with the feeder the power losses decrease also but not with a high penetration level, due to fact that PV system will be the large feeding source in the system which increase the losses again along the feeder. On the other hand, with the MV directly integration case, the losses along the feeder starts to increase again earlier than LV PCC due to the residence of the load in the LV bus which directly consume its required demand from the PV system. as appears in Fig 5.31.

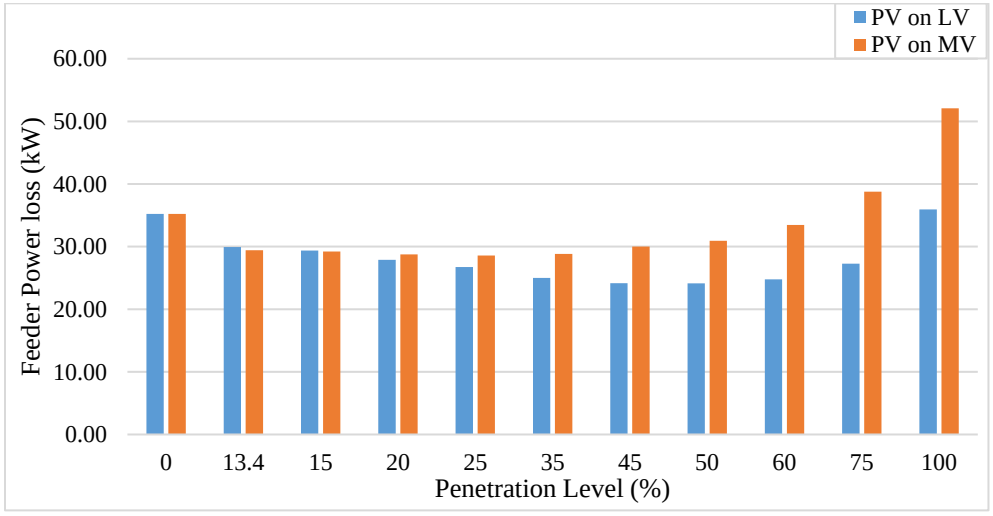

Figure 5.31: Power losses along the feeder when the PV integrated at LV and MV.

5.5.1.3: Total Harmonic Distortion level issue.

Regarding to IEEE Standard recommend to the THD limit which is 8% for LV bus and 5% for MV bus, fig 5.32 illustrates the THD profile along the PV penetration level increased and it indicates that the penetration level should not exceed 20% when the PV integrated at the LV PCC and 15% when the PV directly connected on the MV. On the other hand, with integration of PV at LV PCC the THD at the starting point of the feeder and bus-9 stay within the standard, in MV directly connected case the limitation of THD is around 75% of penetration. As in fig. 5.33,34.

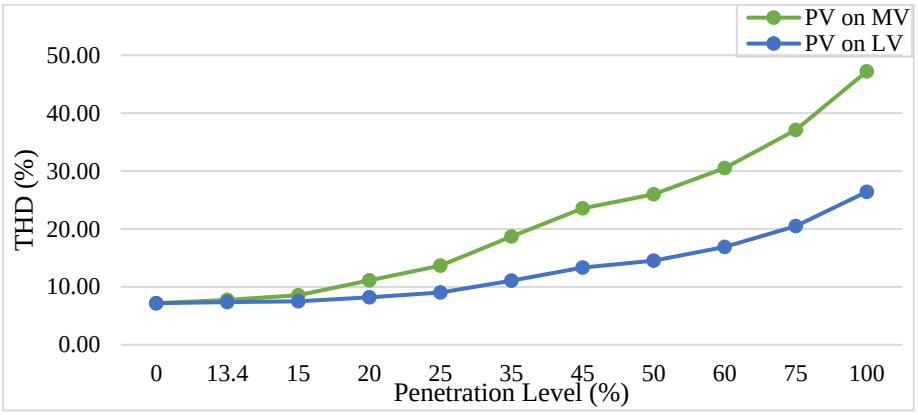

Figure 5. 32: THD at the LV buses of PV integration point with and without load at that bus.

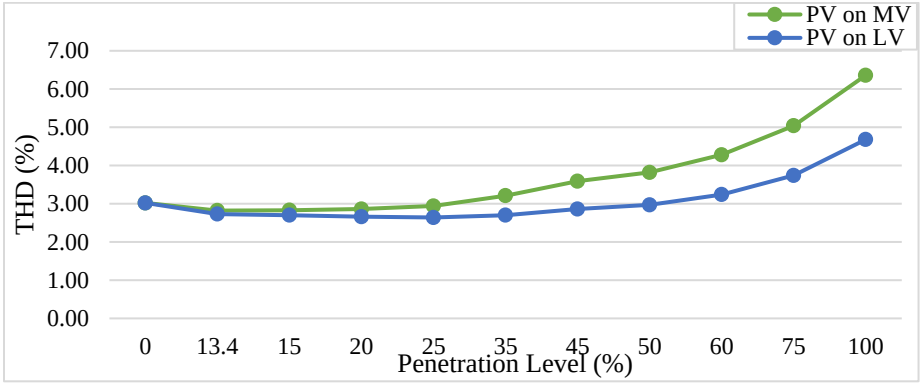

Figure 5.33: THD at the bus-9 MV side of the step-up PV transformer.

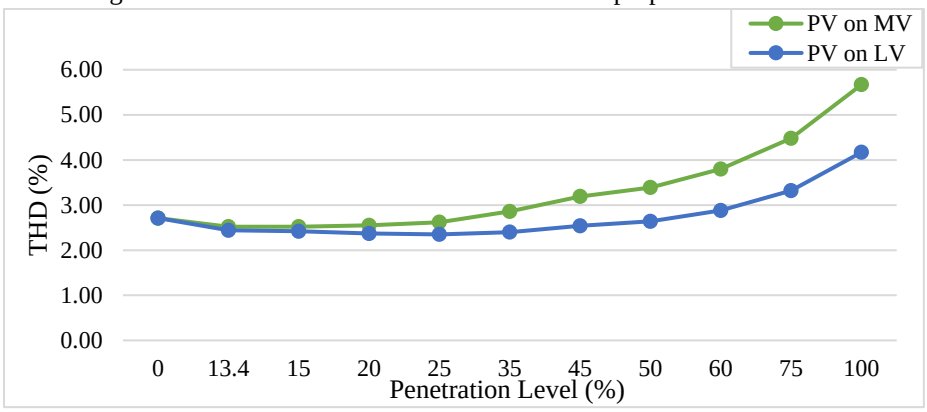

Figure 5.34: THD in different penetration when PV integrated at the MV and LV bus of the feeder.

5.5.2: PV penetration level at MV and LV PCC after integrating BESS.

In this section, an 11-penetration level of the PV system will be considered with BESS integration in two cases the LV load bus integration and MV feeder directly. Voltage, PF, power losses, and harmonics were observed at the same circumstances to make an exact comparison between the PV system integration at the LV and MV bus.

5.5.2.1: Voltage profile issue.

One of the main aims of integration storage system with the PV-DG is to mitigate the over voltage issue at the PCC, in this case the effect of integration PV-BESS with the grid in two proposed location, firstly is the LV PPU load bus, secondly integrated directly at the MV PPU feeder. However, the observation of this cases will be examined at three points: at the starting point of the feeder, at the MV side of the step-up PV transformer and at the LV side of the distribution transformer (LV PCC). Fig.5.35 illustrates the difference between integration the PV-BESS system with different penetration levels at the LV buses in the two cases, which is clarifies that the variation of voltage reached to 0.8% only, and that indicates the low variation of voltage profile in the two cases when the PV-BESS integrated.

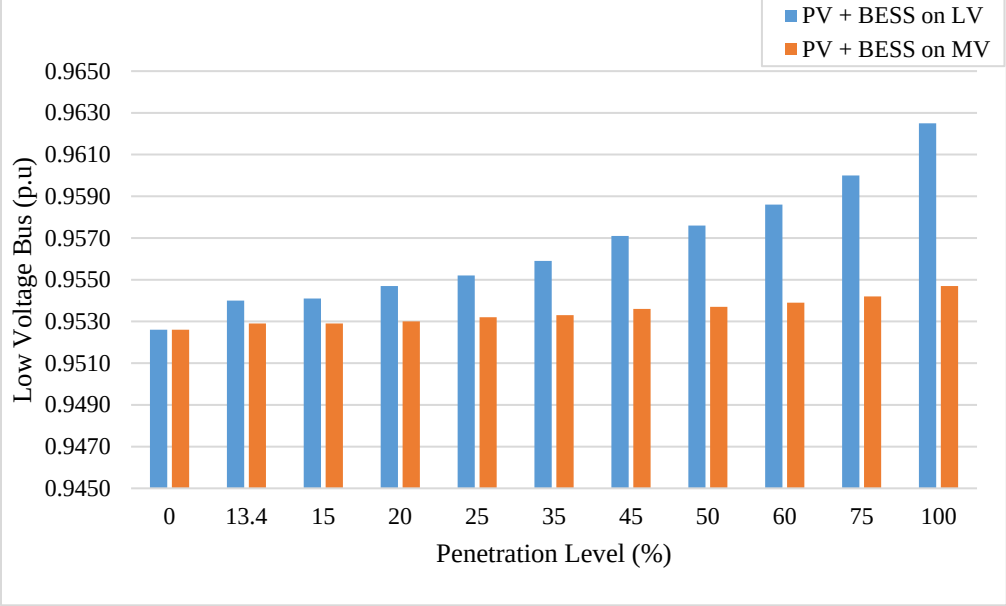

Figure 5.35: Low voltage bus voltage profile at LV PV-BESS integration and MV one.

The observation for integration PV-BESS system on the LV load bus is slightly higher than integrating it with the MV voltage bus which refers to the residence of the BESS that regulate the voltage at the PCC and reduce the impact of PV to the grid. However, the over voltage at the MV side of the step-up PV transformer and PPU distribution transformer “Bus 9” along penetration levels between 0-100% is 0.23% with PV at LV integration case and 0.20% with PV at MV directly as illustrated at fig. 5.36. From the other side the effect of the main bus feeder is very low less than 0.1% in the two cases as fig. 5.37 shows.

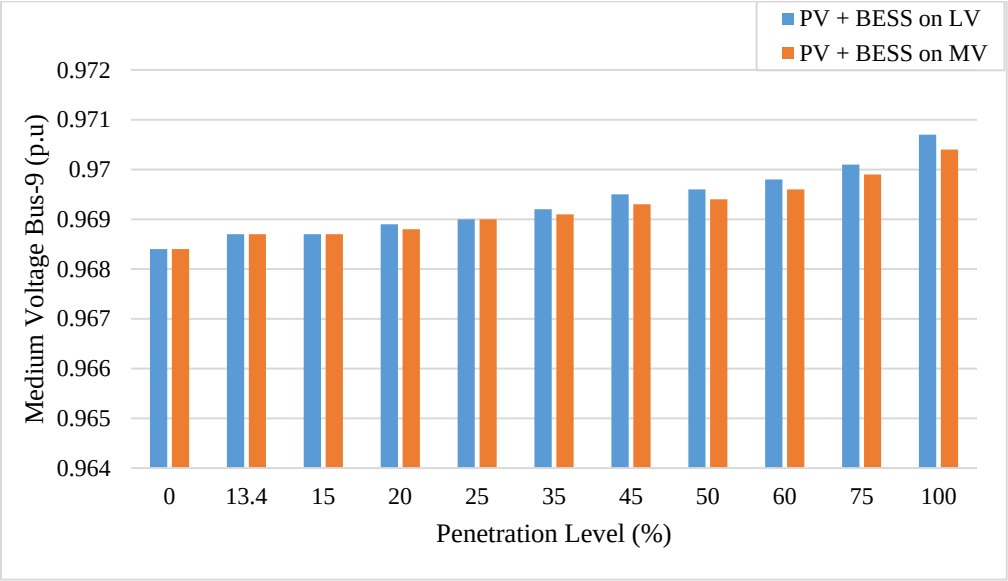

Figure 5.36: MV side of the PPU distribution Tr. And PV step up Tr.

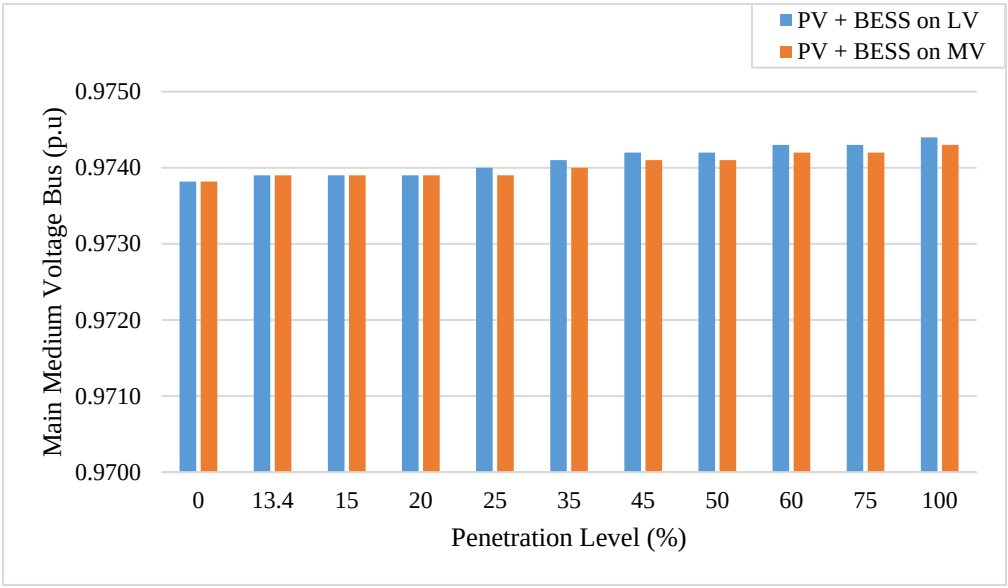

Figure 5.37: Main bus feeder voltage profile with all penetration level.

5.5.2.2: Power factor profile and power losses issue.

Power factor is one of the indication factors for the power flow direction in power system, regarding to the constant value of the reactive power required by the system loads the effect on the PF varies clearly with different penetration levels. Fig. 5.38 represents a comparison between the PF variation at the LV PCC in two different cases which is the LV side of the PPU distribution transformer with the load, and at the LV side of the step-up PV transformer without any loads. Therefore, without load the power factor will be controlled by the PV inverter, but with the load integration at the PCC the demand and PV penetration could control the PF profile, and the power starts to export to the feeder in peak generation around 100% penetration level and its referred to the BESS residence.

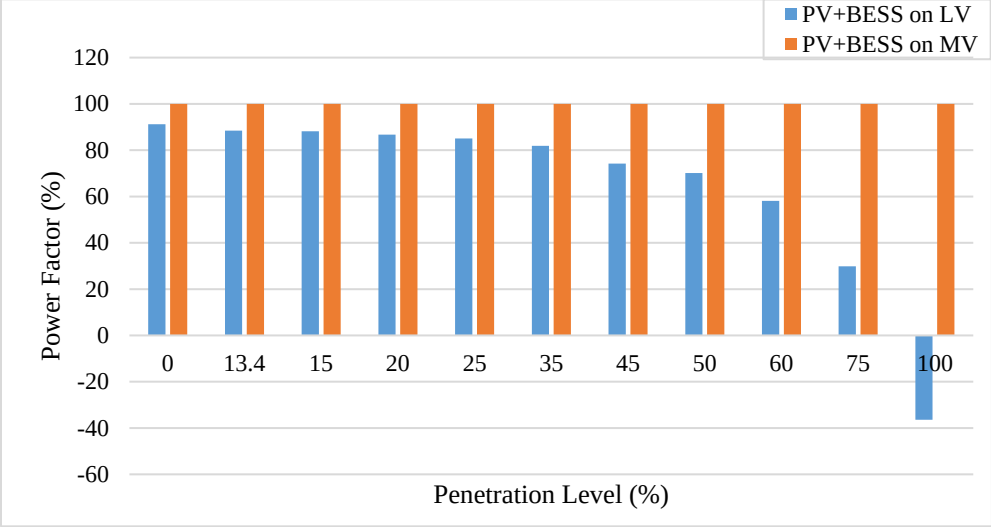

Figure 5.38: PF at the LV side of the Distribution Tr. and the step-up PV Tr. In PV-BESS integration.

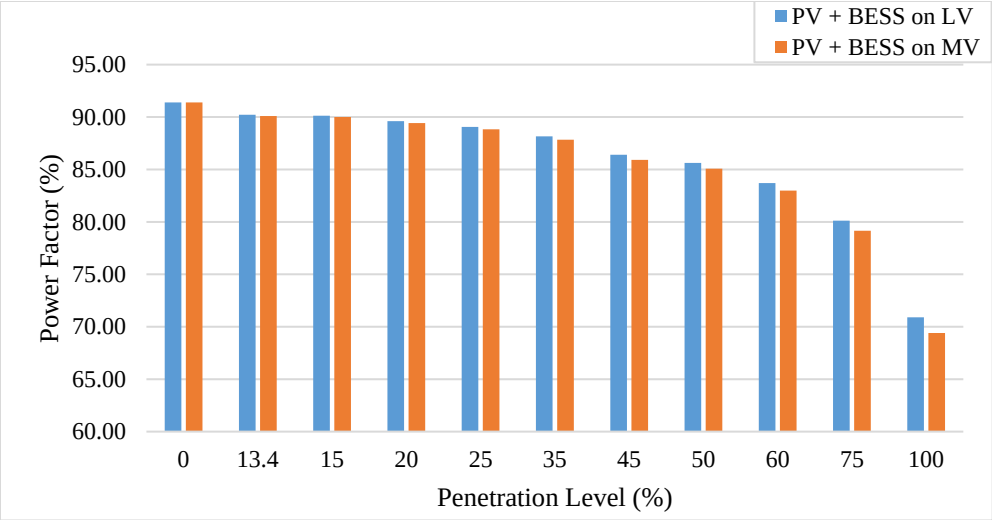

Figure 5.39: PF at the MV side of the Distribution Tr. and PV step-up Tr. In PV-BESS integration.

Fig 5.39 and 5.40 illustrate the PF variation along different penetration level on the feeder at the MV side of the PV step-up transformer and the PPU distribution transformer, it's clearly that the variation of PF is not so high even in case of LV or MV PV-BESS integration, which refers to the BESS integration.

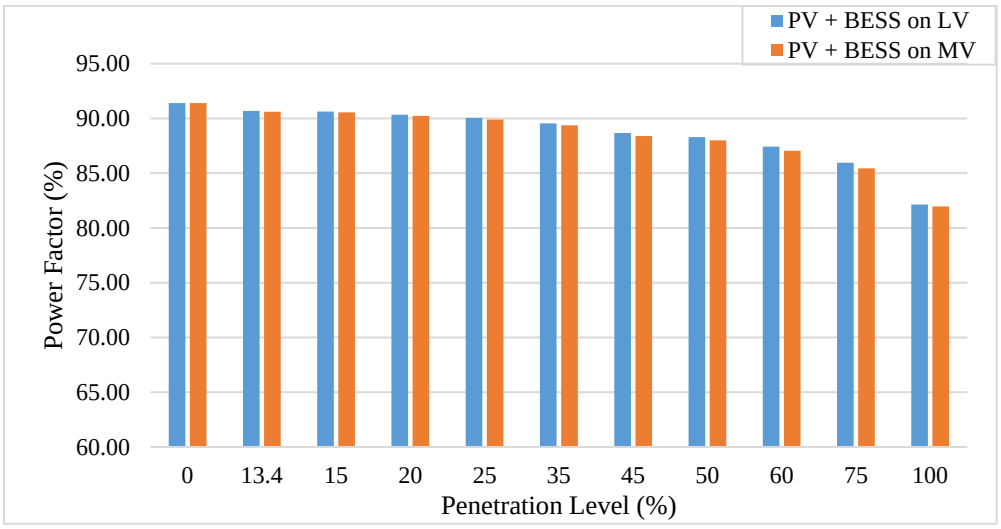

Figure 5.40: PF at the starting point of the feeder with PV-BESS integration.

As the PV-BESS penetration level increases with the feeder, the active power losses are decrease also. But due to the charging mode of the BESS, the contribution of the PV system on the feeder is less than the case of the absence of the storage system which effects on the losses profile along the feeder. On the other hand, with the MV directly integration case the losses along the feeder start to increase again much earlier than LV PCC due to the residence of the PPU load in the LV bus which directly consume its required demand from the PV system. as appears in Fig 5.41.

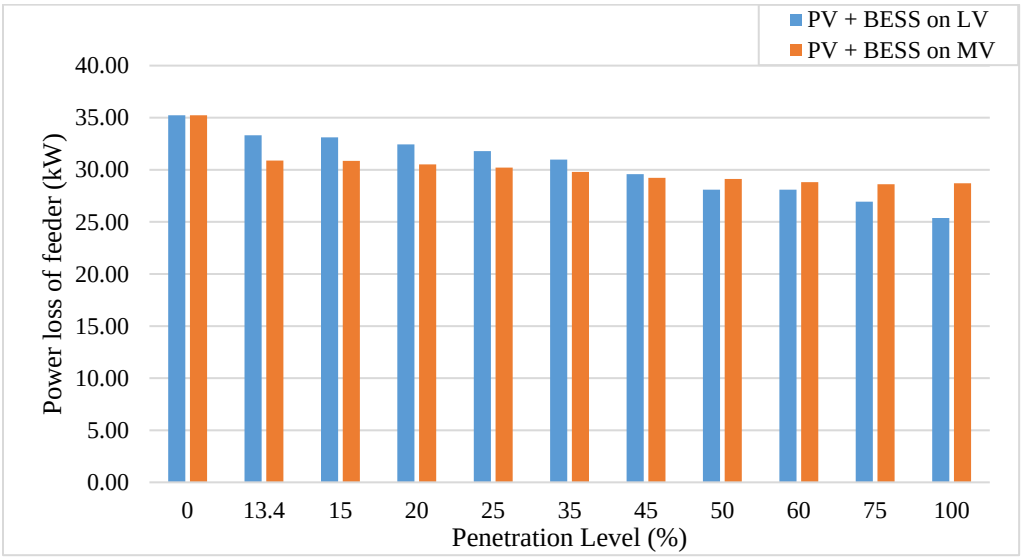

Figure 5.41: Power losses along the feeder when the PV-BESS integrated at LV and MV.

5.5.1.3: Total Harmonic Distortion issue.

Regarding to the IEEE Standard recommend to the THD limitation which is less than 8% for LV bus and 5% for MV bus, fig 5.42 illustrates the THD profile along the PV penetration levels increased and it's indicates that THD at the MV bus-9 decreased as the penetration level increased in the case of LV load bus connection due to the deceasing of the energy demand by the feeder as the PV penetration increased with BESS, but in the case of MV integration directly the variation of THD is low due to the residence of the storage system. At the starting point of the feeder the variation of the THD along the penetration level variating from 0-100% is less than 0.09% which indicates the low effect on the starting point of the feeder as shown in fig. 5.43. On the other hand, with integration of PV-BESS at LV PCC and at MV directly, the THD at the starting point of the feeder and bus-9 stay within the standard.

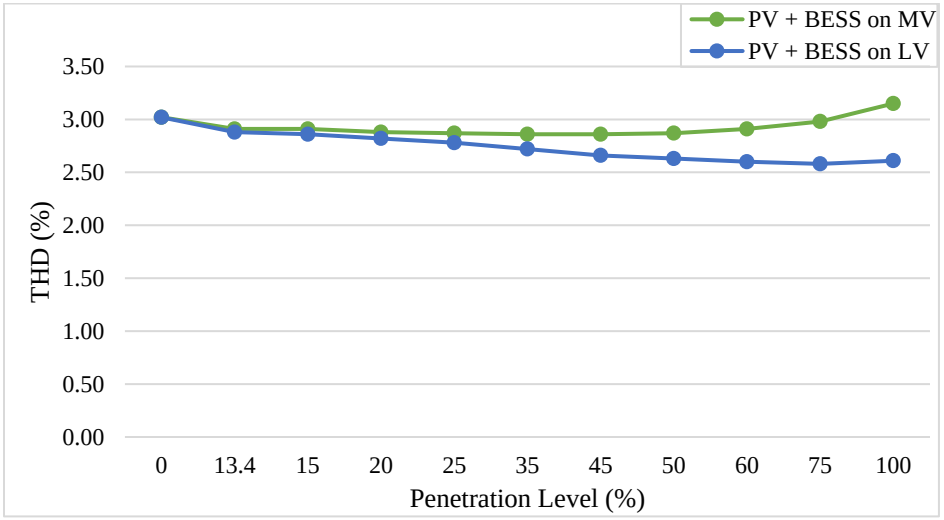

Figure 5.42: THD at the MV side of Distribution Tr. And step-up PV Tr.

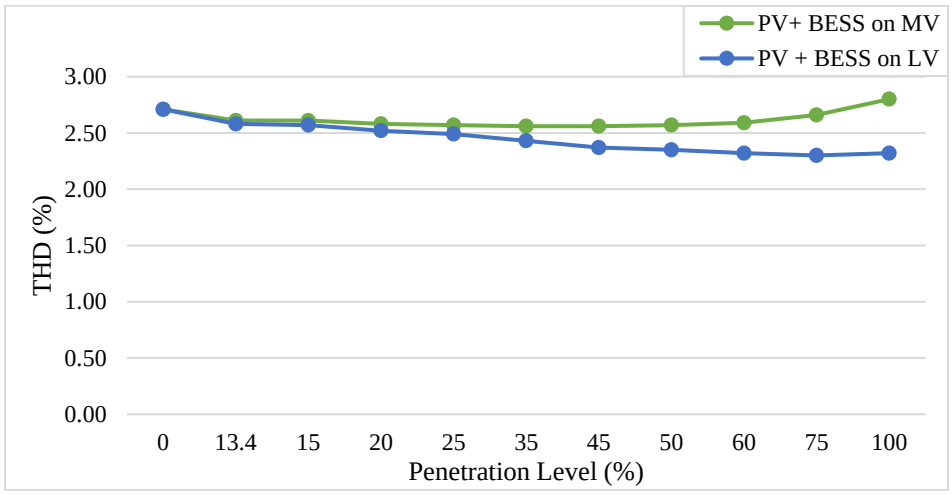

Figure 5.43: THD at the Main bus of the system when PV-BESS LV and MV integration.

6

Chapter Six

Conclusion and proposed Future work

6.1: Conclusion.

6.2: Future Work.

6.1: Conclusion.

PV power plant supported as a main renewable source in this study, but according to uncontrolled conditions which are the changeable weather states and the high penetration levels, some critical issues have been caused for the grid, and they were counted and mentioned in a detailed way in this thesis; However, due to the previous studies in the same field, that clarify the fact of the existence of more than one solution to deal with the system problems, the most helpful and recommended one is the usage of BESS. The usage of BESS helped to achieve the main purposes of this thesis which are firstly, to reduce the impact of PV on the system, and secondly to maximize the penetration levels of PV.

It is obvious that, modern grid with different distributed generators, especially renewables, is a really substantial grid that has great benefits even for environment, power quality, reliability, and for stakeholders since it supports the bidirectionality in power flow. In this thesis the analysis of the system are divided into two areas the first one which focused on integrating PV & BESS in three cases, that are to integrate the PV system alone with the grid to study its effects on the system's parameters, integrate the BESS alone with the grid, and using the PV with BESS as a compound system. The second orientation was about the effect of integration BESS with the grid-tied PV system to maximize the penetration level of the PV-DG with the distribution system in different configurations.

The 230kW_p PPU current PV system represents a 13.4% penetration level on a peak demand of the PPU feeder, in the PPU distribution transformer it contributes a 23%, but in the interconnection point of the seventh power station point of view it represents a 3.62% of its peak demanding. However, the effect of the integrating this PV plant and with proposed 126kWh BESS are considered, and the observation was focused on the main bus and the PCC, all results illustrated as an average daily profile for the whole cases. Integration of the PV and PV-BESS with the feeder from the side of voltage issue had an effect at the main bus which is pretty low; due to the low contribution on it, but at the PCC on average the effect of PV only case the voltage rises 0.45% and with PV-BESS the ratio is not exceed 0.21%.

On the other hand PV system feeds the distribution network by the active power only which reduce the active power demand with the same level of reactive power which justifies the effect on the PF, at the MV side of the PV distribution transformer the PF reaches 81% at peak point with PV integration and with the PV-BESS configuration the PF level was not exceeds 84%. At LV PCC

PF with the PV only connection reach 53% at peak production and it did not exceed the 63% with the PV-BESS integration.

In addition, that the transmission losses of the PPU feeder get less by 49% real power loss and 23% reactive power losses at peak point after integration of PV power plan, but it's worth mentioning that the active power losses is less than the reactive one because of the real power that consumed from the PV plant not from the feeder side. However, after integration the battery storage system with the grid-tie PV power plant the losses were increased during a day time; due to the decreasing of PV contribution for the feeder demand, when the BESS charging, and during a night time the BESS discharging which reduces the losses along the feeder.

Battery energy storage system is proposed to be integrated with the grid tied PV system in order to maximize the penetration level of PV-DG, this research used the ETAP software to test the short circuit level after integration PV only to the system and integrating with the BESS and the results show that the integration of PV increases the short circuit level and BESS with the system increases the extreme conditions. On the other side, the THD increased after integrating the PV system during a day time, but when the BESS integrated with the system the THD decreased during a day; due to the charging time of the storage system which decreases the contribution of PV to the feeder, but increases the THD during a discharging period of the storage system, which leads to the integration of the BESS alone with distribution system is not preferred except for demand side management and regarding to time of used economical dispatch period.

The main limitation of integrating PV system with the electrical network can be the overvoltage issue at the PCC, and after integrating the BESS with the grid tied PV system the voltage rising issue is minimized with the penetration level increases. And the observation was showing the fact that the integration of the PV system with the MV feeder has the less changing of voltage magnitude clearly compared with the LV level, it depends on the penetration level. The effect of the PV system on the electrical feeder was minimized by integration of BESS, and the PV hosting capacity was maximized clearly.

The information obtained using the proposed approach would be beneficial to implement mitigation actions against adverse impacts of PV penetration including fluctuations caused by sudden variations in PV output to the voltage level at resident load bus and line loss.

6.2: Future Work.

In this thesis different PV grid integration approaches were discussed and evaluated. Further research should go in to all directions. However, the study should be brought into a larger context looking not only at the distribution system but at the overall power system. This section elaborates further research ideas for looking at the whole picture of power system in the case of integration distributed generation as follows:

- Based on the research presented above, the future work may focus on developing the method to design hybrid PV and BESS. To maximize the PV hosting capacity in the distribution system and to reduce the PV plant impact on the electrical network.

- Analysis and study the case of determination the optimum location of the PV distribution generation using optimization location methods in electrical power system, trial and error or PSO methodology.

- Determine the optimum location of the BESS that integrated with PV distribution generation using optimization location methods in electrical power system, to ensure that the lowest power losses along the feeder case are reached.

- Study the case that 100% penetration level if it can be reached in with different DG system, due to severe impacts on the electrical network. These impacts such as power quality, reverse power flow and frequency stability issues.

References

[1] G. Masson, S. Orlandi, and M. Rekinger, "Global market outlook for photovoltaics 2014-2018," *Eur. Photovolt. Ind. Assoc.*, vol. 60, p. 12, 2014.

[2] A. Guichi, A. Talha, E. M. Berkouk, and S. Mekhilef, "Energy management and performance evaluation of grid connected PV-battery hybrid system with inherent control scheme," *Sustain. cities Soc.*, vol. 41, pp. 490–504, 2018.

[3] V. S. G. S. VSGS, "Weissbuch Smart Grid," *Ostermundigen CH*, 2013.

[4] V. Campos-Guzman, M. S. García-Cáscales, N. Espinosa, and A. Urbina, "Life cycle analysis with multi-criteria decision making: a review of approaches for the sustainability evaluation of renewable energy technologies," *Renew. Sustain. Energy Rev.*, vol. 104, pp. 343–366, 2019.

[5] A. S. Dagoumas and N. E. Koltsaklis, "Review of models for integrating renewable energy in the generation expansion planning," *Appl. Energy*, vol. 242, pp. 1573–1587, 2019.

[6] J. H. R. Enslin and H. Alatrash, "Distribution Network Impacts of High Penetration of Distributed Photovoltaic Systems," in *21 International Conference on Electricity Distribution, Frankfurt, 6-9 June 2011*, 2011.

[7] R. Tonkoski, D. Turcotte, and T. H. M. El-Fouly, "Impact of high PV penetration on voltage profiles in residential neighborhoods," *IEEE Trans. Sustain. Energy*, vol. 3, no. 3, pp. 518–527, 2012.

[8] Y. Yang, H. Li, A. Aichhorn, J. Zheng, and M. Greenleaf, "Sizing strategy of distributed battery storage system with high penetration of photovoltaic for voltage regulation and peak load shaving," *IEEE Trans. Smart Grid*, vol. 5, no. 2, pp. 982–991, 2014.

[9] H. A. Abdel-Ghany, A. M. Azmy, N. I. Elkalashy, and E. M. Rashad, "Optimizing DG penetration in distribution networks concerning protection schemes and technical impact," *Electr. Power Syst. Res.*, vol. 128, pp. 113–122, 2015.

[10] M. Karimi, H. Mokhlis, K. Naidu, S. Uddin, and A. H. A. Bakar, "Photovoltaic penetration issues and impacts in distribution network–A review," *Renew. Sustain. Energy Rev.*, vol. 53, pp. 594–605, 2016.

[11] N. Jayasekara, M. A. S. Masoum, and P. J. Wolfs, "Optimal operation of distributed energy storage systems to improve distribution network load and generation hosting capability," *IEEE Trans. Sustain. Energy*, vol. 7, no. 1, pp. 250–261, 2015.

[12] J. Weniger, T. Tjaden, J. Bergner, and V. Quaschning, "Dynamic mismatch losses of grid-connected PV-battery systems in residential buildings," *J. Energy Storage*, vol. 13, pp. 244–254, 2017.

[13] A. Nagarajan and R. Ayyanar, "Design and strategy for the deployment of energy storage systems in a distribution feeder with penetration of renewable resources," *IEEE Trans. Sustain. Energy*, vol. 6, no. 3, pp. 1085–1092, 2015.

[14] O. M. Toledo, D. Oliveira Filho, and A. S. A. C. Diniz, "Distributed photovoltaic generation and energy storage systems: A review," *Renew. Sustain. Energy Rev.*, vol. 14, no. 1, pp. 506–511, 2010.

[15] A. N. Azmi, I. N. Dahlberg, M. L. Kolhe, and A. G. Imenes, "Impact of increasing penetration of photovoltaic (PV) systems on distribution feeders," in *2015 International Conference on Smart*

Grid and Clean Energy Technologies (ICSGCE), 2015, pp. 70–74.

[16] K. Jadeja, “Major technical issues with increased PV penetration on the existing electrical grid.” Murdoch University, 2012.

[17] H. Kuang, S. Li, and Z. Wu, “Discussion on advantages and disadvantages of distributed generation connected to the grid,” in *2011 International Conference on Electrical and Control Engineering*, 2011, pp. 170–173.

[18] M. Heydari, S. M. Hosseini, and S. A. Gholamian, “Optimal placement and sizing of capacitor and distributed generation with harmonic and resonance considerations using discrete particle swarm optimization,” *Int. J. Intell. Syst. Appl.*, vol. 5, no. 7, p. 42, 2013.

[19] A. Juaidi, F. G. Montoya, I. H. Ibrik, and F. Manzano-Agugliaro, “An overview of renewable energy potential in Palestine,” *Renew. Sustain. Energy Rev.*, vol. 65, pp. 943–960, 2016.

[20] D. Wu, F. Tang, T. Dragicevic, J. C. Vasquez, and J. M. Guerrero, “Autonomous active power control for islanded ac microgrids with photovoltaic generation and energy storage system,” *IEEE Trans. energy Convers.*, vol. 29, no. 4, pp. 882–892, 2014.

[21] O. De Groote and F. Verboven, “Subsidies and time discounting in new technology adoption: Evidence from solar photovoltaic systems,” *Am. Econ. Rev.*, vol. 109, no. 6, pp. 2137–2172, 2019.

[22] D. M. Tobnaghi, “A Review on impacts of Grid-connected PV system on Distribution Networks,” *Int. J. Electr. Comput. Eng.*, vol. 10, no. 1, pp. 137–152, 2016.

[23] Y. Sawle, S. C. Gupta, and A. K. Bohre, “Review of hybrid renewable energy systems with comparative analysis of off-grid hybrid system,” *Renew. Sustain. Energy Rev.*, vol. 81, pp. 2217–2235, 2018.

[24] N. M. Kumar, M. S. P. Subathra, and J. E. Moses, “On-Grid Solar Photovoltaic System: Components, Design Considerations, and Case Study,” in *2018 4th International Conference on Electrical Energy Systems (ICEES)*, 2018, pp. 616–619.

[25] T. E. Hoff, R. Perez, and R. M. Margolis, “Maximizing the value of customer-sited PV systems using storage and controls,” *Sol. Energy*, vol. 81, no. 7, pp. 940–945, 2007.

[26] B. Ansari, D. Shi, R. Sharma, and M. G. Simoes, “Economic analysis, optimal sizing and management of energy storage for PV grid integration,” in *Transmission and Distribution Conference and Exposition (T&D), 2016 IEEE/PES*, 2016, pp. 1–5.

[27] H. Kanchev, D. Lu, F. Colas, V. Lazarov, and B. Francois, “Energy management and operational planning of a microgrid with a PV-based active generator for smart grid applications,” *IEEE Trans. Ind. Electron.*, vol. 58, no. 10, pp. 4583–4592, 2011.

[28] A. Zahedi, “Maximizing solar PV energy penetration using energy storage technology,” *Renew. Sustain. Energy Rev.*, vol. 15, no. 1, pp. 866–870, 2011.

[29] S. Conti, S. Raiti, G. Tina, and U. Vagliasindi, “Study of the impact of PV generation on voltage profile in LV distribution networks,” in *Power Tech Proceedings, 2001 IEEE Porto*, 2001, vol. 4, pp. 6-pp.

[30] R. Albarracín and H. Amarís Duarte, “Power quality in distribution power networks with photovoltaic energy sources,” 2009.

[31] W. Yan *et al.*, “Operation strategies in distribution systems with high level PV Penetration,” in *ISES Solar World Congress*, 2011, pp. 2–6.

[32] E. Demirok, D. Sera, R. Teodorescu, P. Rodriguez, and U. Borup, “Clustered PV inverters in LV networks: An overview of impacts and comparison of voltage control strategies,” in *Electrical Power & Energy Conference (EPEC), 2009 IEEE*, 2009, pp. 1–6.

[33] M. Al-Maghalseh, S. Odeh, and A. Saleh, “Optimal sizing and allocation of DGs for real power loss reduction and voltage profile improvement in radial LV networks,” in *2017 14th International Conference on Smart Cities: Improving Quality of Life Using ICT & IoT (HONET-ICT)*, 2017, pp. 21–25.

[34] C. L. T. Borges and D. M. Falcao, “Optimal distributed generation allocation for reliability, losses, and voltage improvement,” *Int. J. Electr. Power Energy Syst.*, vol. 28, no. 6, pp. 413–420, 2006.

[35] T. E. Kim and J. E. Kim, “A method for determining the introduction limit of distributed generation system in distribution system,” in *Power Engineering Society Summer Meeting, 2001*, 2001, vol. 1, pp. 456–461.

[36] P. McNutt, J. Hambrick, M. Keesee, and D. Brown, “Impact of SolarSmart subdivisions on SMUD’s distribution system,” National Renewable Energy Lab.(NREL), Golden, CO (United States), 2009.

[37] P. González, E. Romero-Cadaval, E. González, and M. A. Guerrero, “Impact of grid connected photovoltaic system in the power quality of a distribution network,” in *Doctoral Conference on Computing, Electrical and Industrial Systems*, 2011, pp. 466–473.

[38] Y. Ueda, K. Kurokawa, T. Tanabe, K. Kitamura, and H. Sugihara, “Analysis results of output power loss due to the grid voltage rise in grid-connected photovoltaic power generation systems,” *IEEE Trans. Ind. Electron.*, vol. 55, no. 7, pp. 2744–2751, 2008.

[39] S. M. Schoenung and J. O. Keller, “Commercial potential for renewable hydrogen in California,” *Int. J. Hydrogen Energy*, vol. 42, no. 19, pp. 13321–13328, 2017.

[40] N. Iqteit, A. B. Arsoy, and B. Çakır, “Load Profile-Based Power Loss Estimation for Distribution Networks,” *Electrica*, vol. 18, no. 2, pp. 275–283, 2018.

[41] A. Hasibuan, S. Masri, and W. Othman, “Effect of distributed generation installation on power loss using genetic algorithm method,” in *IOP Conference Series: Materials Science and Engineering*, 2018, vol. 308, no. 1, p. 12034.

[42] H. Sadiq, S. A. H. Raza, U. Hameed, A. K. Janjua, and K. Imran, “Impact Analysis of PV Penetration on Radial Distribution Feeder of National University of Science and Technology (NUST),” in *2018 International Conference on Power Generation Systems and Renewable Energy Technologies (PGSRET)*, 2018, pp. 1–5.

[43] S. J. Lewis, “Analysis and management of the impacts of a high penetration of photovoltaic systems in an electricity distribution network,” in *2011 IEEE PES Innovative Smart Grid Technologies*, 2011, pp. 1–7.

[44] N. A. Bhuiyan, “Power System Harmonic Analysis using ETAP.” Brunel University, 2011.

[45] S. Kulkarni and S. Sontakke, “Power system analysis of a microgrid using ETAP,” *Int. J. Innov. Sci. Mod. Eng.*, vol. 3, no. 5, 2015.

[46] M. Hussain, D. Hussain, M. Khan, and S. Shah, “Solar Grid Integration Issue: Overvoltage Dilemma,” *Available SSRN 2984567*, 2017.

[47] Y. Pang and Y. Xu, “Analysis and treatment of harmonic in power network with railway based on

ETAP software," in *2016 IEEE PES Asia-Pacific Power and Energy Engineering Conference (APPEEC)*, 2016, pp. 1424–1429.

[48] M. Q. Duong, N. T. N. Tran, G. N. Sava, and M. Scripcariu, "The impacts of distributed generation penetration into the power system," in *2017 International Conference on Electromechanical and Power Systems (SIELMEN)*, 2017, pp. 295–301.

[49] S. N. Afifi, M. K. Darwish, and G. A. Taylor, "Impact of photovoltaic penetration on short circuit levels in distribution networks," in *International Conference on Renewable Energy and Power Quality Conference*, 2014, vol. 17, pp. 1958–1966.

[50] R. A. Kordkheili, B. Bak-Jensen, R. Jayakrishnan, and P. Mahat, "Determining maximum photovoltaic penetration in a distribution grid considering grid operation limits," in *2014 IEEE PES General Meeting| Conference & Exposition*, 2014, pp. 1–5.

[51] C. Bucher, "Analysis and simulation of distribution grids with photovoltaics." ETH Zurich, 2014.

[52] K. A. Baharin, N. A. Isa, C. K. Gan, and M. Shamshiri, "High PV Penetration Impact on European-based LV Residential Network.," *Telkomnika*, vol. 16, no. 4, 2018.

[53] S. Kandil, H. E. Farag, L. S. Hilaire, and E. Janssen, "A power quality monitor system for quantifying the effects of photovoltaic penetration on the grid," in *2015 IEEE 28th Canadian Conference on Electrical and Computer Engineering (CCECE)*, 2015, pp. 237–241.

[54] D. P. LaPlante, J. L. Truong, and T. S. Chojnowski, "Reverse Power Mitigation System For Photovoltaic Energy Resources," 2015.

[55] G. M. Tina and G. Celsa, "Active and reactive power regulation in grid-connected PV systems," in *2015 50th International Universities Power Engineering Conference (UPEC)*, 2015, pp. 1–6.

[56] C. Bucher, G. Andersson, and L. Küng, "Increasing the PV hosting capacity of distribution power grids–a comparison of seven methods," in *28th European Photovoltaic Solar Energy Conference and Exhibition (PVSEC), Paris*, 2013, pp. 4231–4235.

[57] H. Vollenweider, "Grid integration of PV systems and local storage in distribution networks," *Swiss Fed. Inst. Technol. Zurich*, pp. 93–9994, 2014.

[58] Z. Wang, C. Gu, and F. Li, "Flexible operation of shared energy storage at households to facilitate PV penetration," *Renew. energy*, vol. 116, pp. 438–446, 2018.

[59] B. Dunn, H. Kamath, and J.-M. Tarascon, "Electrical energy storage for the grid: a battery of choices," *Science (80-.).*, vol. 334, no. 6058, pp. 928–935, 2011.

[60] J. Binder *et al.*, "Sol-Ion PV Storage System: Field Trial Results, Spread of Operating Conditions and Performance Evaluation Based On Field Data," in *27th European Photovoltaic Solar Energy Conference and Exhibition*, 2012.

[61] R. Martins, H. Hesse, J. Jungbauer, T. Vorbuchner, and P. Musilek, "Optimal component sizing for peak shaving in battery energy storage system for industrial applications," *Energies*, vol. 11, no. 8, p. 2048, 2018.

[62] O. Erdinc, "Economic impacts of small-scale own generating and storage units, and electric vehicles under different demand response strategies for smart households," *Appl. Energy*, vol. 126, pp. 142–150, 2014.

[63] Y. Yang, "Optimization of Battery Energy Storage Systems for PV Grid Integration Based on Sizing Strategy," 2014.

[64] C. Lupangu and R. C. Bansal, “A review of technical issues on the development of solar photovoltaic systems,” *Renew. Sustain. Energy Rev.*, vol. 73, pp. 950–965, 2017.

[65] IEEE, *T. W. o. contributor, \Solar has become America’s fastest-growing, nonpartisan energy source," Mar 2017.* .

[66] C. Williams, J. Binder, M. Danzer, F. Sehnke, and M. Felder, “Battery charge control schemes for increased grid compatibility of decentralized PV systems,” in *Proceedings of the 28th European Photovoltaic Solar Energy Conference, Paris, France*, 2013, vol. 30, p. 145154.

[67] V. Raveendran and S. Tomar, “Modeling, Simulation, Analysis and Optimisation of a Power System Network-Case Study,” *Int. J. Sci. Eng. Res.*, vol. 3, no. 6, 2012.

[68] M. Tonso, J. Moren, S. W. H. de Haan, and J. A. Ferreira, “Variable inductor for voltage control in distribution networks,” in *Power Electronics and Applications, 2005 European Conference on*, 2005, pp. 10-pp.

[69] B.-I. Crăciun, T. Kerekes, D. Séra, and R. Teodorescu, “Overview of recent grid codes for PV power integration,” in *Optimization of Electrical and Electronic Equipment (OPTIM), 2012 13th International Conference on*, 2012, pp. 959–965.

[70] J. R. Abbad, “Electricity market participation of wind farms: the success story of the Spanish pragmatism,” *Energy Policy*, vol. 38, no. 7, pp. 3174–3179, 2010.

[71] A. Fediaevsky, J.-J. Bénet, M. L. Boschiroli, J. Rivière, and J. Hars, “La tuberculose bovine en France en 2011, poursuite de la réduction du nombre de foyers,” *ANSES Bull Epidemiol*, vol. 54, pp. 4–12, 2011.

[72] P. Thakur, “Nonlinear Load Distribution and Drives Configuration Selection for Harmonic Mitigation as Per IEEE 519-2014 Standard,” in *2018 IEEE International Conference on Power Electronics, Drives and Energy Systems (PEDES)*, 2018, pp. 1–6.

[73] H. Golpîra, H. Seifi, A. R. Messina, and M.-R. Haghifam, “Maximum penetration level of micro-grids in large-scale power systems: frequency stability viewpoint,” *IEEE Trans. Power Syst.*, vol. 31, no. 6, pp. 5163–5171, 2016.

[74] T. Neumann and I. Erlich, “Short circuit current contribution of a photovoltaic power plant,” *IFAC Proc. Vol.*, vol. 45, no. 21, pp. 343–348, 2012.

[75] Q. Zheng, J. Li, X. Ai, J. Wen, and J. Fang, “Overivew of grid codes for photovoltaic integration,” in *2017 IEEE Conference on Energy Internet and Energy System Integration (EI2)*, 2017, pp. 1–6.

[76] A. Barnes, H. Nagarajan, E. Yamangil, R. Bent, and S. Backhaus, “Resilient design of large-scale distribution feeders with networked microgrids,” *Electr. Power Syst. Res.*, vol. 171, pp. 150–157, 2019.

[77] S. Jia *et al.*, “Application of Load Allocation Algorithm to Low Voltage Distribution Network,” in *2018 China International Conference on Electricity Distribution (CICED)*, 2018, pp. 2362–2365.

Appendices

Appendix A: Details of the distribution network components.

Appendix A1: Data of the transformer.

Appendix A2: All data of the distribution line and cables.

Appendix B: The seventh power station feeder's half an hourly reading.

Appendix C: the PPU metering system readings table.

Appendix D: PPU PV power plant component data sheets.

Appendix E: Output result from the ETAP.

Appendix A: Details of the distribution network components.

25 - 200 kVA

250 - 400 kVA

Three Phase
Oil immersed
With Conservator Type,
25 - 2500 kVA
Transformers
Technical drawings

500 - 2500 kVA

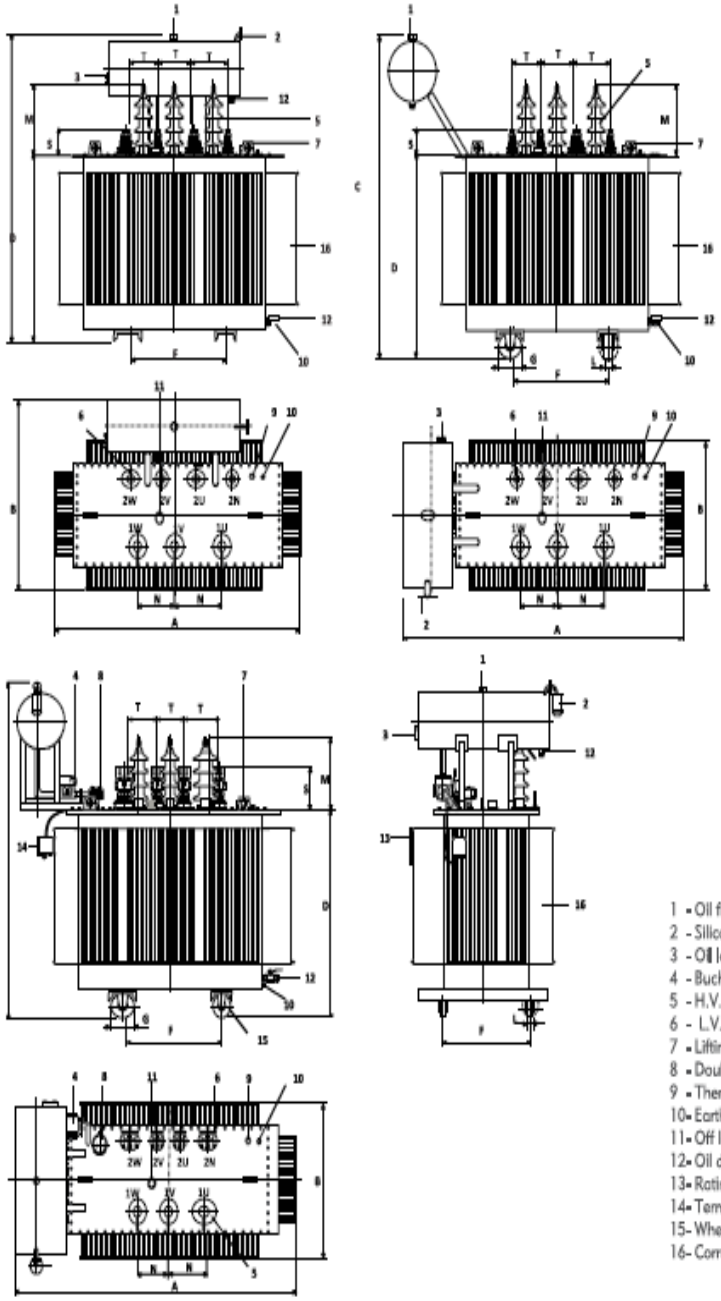

1 - Oil filling pipe
2 - Silicagel for dehydrating breather
3 - Oil level indicator
4 - Buchholz relay
5 - H.V.Bushings
6 - L.V.Bushings
7 - Lifting lugs
8 - Double contact thermometer
9 - Thermometer pocket
10- Earthing screws
11- Off load tap changer
12- Oil drain screws
13- Rating plate
14- Terminal box
15- Wheels
16- Corrugated walls

Power	Voltage	Oil Weight	Active Part Weight	Total Weight	Length A	Width B	Heigth C	D	F	ØG	L	M	N	S	T
kVA	kV	kg	kg	kg	mm	mm	mm	mm	mm	mm	mm	mm	mm	mm	mm
25	6,3–10,5	130	295	540	935	680	1170	700	520			310	210	138	150
	15,8	130	295	540	935	680	1245	700				385	220		
	33	120	225	410	920	730	1365	720				485	290		
40	6,3–10,5	150	400	650	975	730	1230	760	520			310	265	138	150
	15,8	150	400	650	975	730	1305	760				385	265		
	33	145	305	540	905	785	1450	805				485	330		
50	6,3–10,5	170	440	685	1000	750	1240	770	520			310	265	138	150
	15,8	170	440	685	1000	750	1315	770				385	265		
	33	155	345	570	920	800	1470	825				485	330		
63	6,3–10,5	190	495	760	1025	750	1280	810	520			310	265	138	150
	15,8	190	495	760	1025	750	1355	810				385	265		
	33	165	380	625	935	800	1490	845				485	330		
80	6,3–10,5	210	555	840	1055	750	1325	850	520			310	265	138	150
	15,8	210	555	840	1055	750	1400	850				385	265		
	33	180	420	685	955	810	1510	865				485	330		
100	6,3–10,5	240	665	980	1100	750	1385	910	520			310	265	138	150
	15,8	240	665	980	1100	750	1460	910				385	265		
	33	200	480	780	980	815	1540	895				485	350		
125	6,3–10,5	255	800	1155	1150	750	1425	950	520			310	265	138	150
	15,8	255	800	1155	1150	750	1500	950				385	265		
	33	220	555	890	1010	820	1575	930				485	350		
160	6,3–10,5	280	975	1345	1210	750	1480	1000	520			310	265	138	150
	15,8	280	975	1345	1210	750	1555	1000				385	265		
	33	245	650	1015	1060	830	1620	970				485	350		
200	6,3–10,5	300	1050	1450	1275	780	1525	1050	520			310	265	178	150
	15,8	300	1050	1450	1275	780	1600	1050				385	265		
	33	270	730	1130	1250	830	1645	990				485	350		
250	6,3–10,5	325	1140	1580	1355	700	1625	1105	520			310	265	178	150
	15,8	325	1140	1580	1355	700	1700	1105				385	265		
	33	295	815	1250	1550	700	1710	1015				485	350		
315	6,3–10,5	390	1405	1975	1500	720	1690	1170	670	150	50	310	330	178	150
	15,8	390	1405	1975	1500	720	1765	1170				385	330		
	33	360	995	1555	1590	765	1805	1105				485	350		
400	6,3–10,5	465	1700	2390	1660	740	1820	1250	670	150	50	310	330	178	150
	15,8	465	1700	2390	1660	740	1895	1250				385	330		
	33	440	1190	1875	1640	840	1950	1220				485	350		
500	6,3–10,5	510	1955	2750	1680	915	1835	1300	670	150	50	310	330	263	200
	15,8	510	1955	2750	1680	915	1910	1300				385	330		
	33	520	1440	2250	1700	895	2020	1270				485	350		
630	6,3–10,5	570	2235	3115	1700	1100	1875	1360	670	150	50	310	330	263	200
	15,8	570	2235	3115	1700	1100	1950	1360				385	330		
	33	605	1720	2650	1700	970	1950	1320				485	350		
800	6,3–10,5	630	2360	3245	1800	950	1980	1375	820	150	50	310	400	263	220
	15,8	630	2360	3245	1800	950	2055	1375				385			
	33	730	1980	3100	1840	1050	2155	1370				485			
1000	6,3–10,5	755	2890	4120	1950	980	2155	1545	820	200	70	310	400	340	230
	15,8	755	2890	4120	1950	980	2230	1545				385			
	33	770	2275	3525	2005	1035	2210	1425				485			
1250	6,3–10,5	810	3425	4700	1900	1100	2190	1580	820	200	70	310	400	340	240
	15,8	810	3425	4700	1900	1100	2265	1580				385			
	33	885	2440	3880	2000	1170	2255	1470				485			
1600	6,3–10,5	900	3395	4845	1900	1140	2215	1605	820	200	70	310	400	372	240
	15,8	900	3395	4845	1900	1140	2290	1605				385			
	33	1000	2825	4645	2070	1330	2410	1580				485			
2000	6,3–10,5	1100	4065	6030	2205	1300	2285	1625	1000	200	70	310	400	372	250
	15,8	1100	4065	6030	2205	1300	2360	1625				385			
	33	1085	3100	5240	2100	1385	2465	1630				485			
2500	6,3–10,5	1335	4765	7145	2150	1400	2315	1655	1000	200	70	310	400	450	260
	15,8	1335	4765	7145	2150	1400	2390	1655				385			
	33	1330	3915	6720	2270	1575	2485	1650				485			

ACSR

TEKNİK BİLGİLER

Orta ve yüksek gerilim iletim hatlarında kullanılırlar. TS EN 50182 Standardına uygun olarak alüminyum tellerden ve çinko kaplı çelik tellerden imal edilirler. İletkenler yedi veya daha fazla tellerden eş merkez tabakalı olarak örülürler. Eğer iletken birden fazla tabakadan oluşuyorsa bitişik tabakalar birbirine ters adım yönünde örülür. İstenildiğinde DIN, BS, ASTM, NF, CSA, EN standartlarına uygun üretim yapılabilir.

TECHNICAL DATA

They are used in medium and high voltage transmission lines. The aluminium wires and zinc coated steel wires are produced in accordance with TS EN 50182 standards. Conductors are stranded with seven or more wire as concentrically.If conductors are consist of more than one layer, than they are stranded in reverse direction to each other. Upon request they can be produced in accordance to DIN,BS, ASTM, NF, CSA, EN standards..

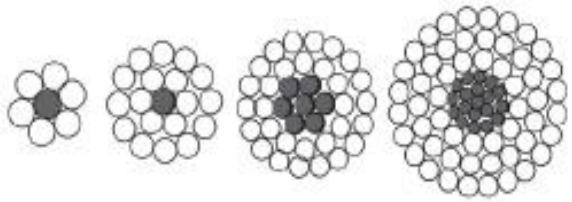

6 Al./1 St. 18 Al./1 St. 26 Al./7 St. 54 Al./19 St.

underground power cables

Medium &High Voltage

12/20 kV
Circular Stranded
Copper Conductors,
XLPE Insulated
PVC or PE Sheathed

USE:
For indoor installations, in cable ducts, outdoors and for laying in the ground for power stations, industrial plants and switching stations as well as a distribution cable in local supply systems and on slopes.
Permissible operating temperature: 90°C
Permissible short circuit temperature: 250°C
(for short-circuit duration up to 5 sec.)

SPECIFICATION:
H.C. circular compacted copper conductor, inner extruded thermosetting semiconductive layer, XLPE insulated, outer extruded thermosetting semiconductive layer, semiconductive tape, copper wire screen with a copper tape transverse helix, PVC or PE outer sheath.
According to Israeli Standard 1516 and IEC 502.

Current rating based on VDE 0298.
Similar to N2XSY or N2XS2Y (VDE 0273).

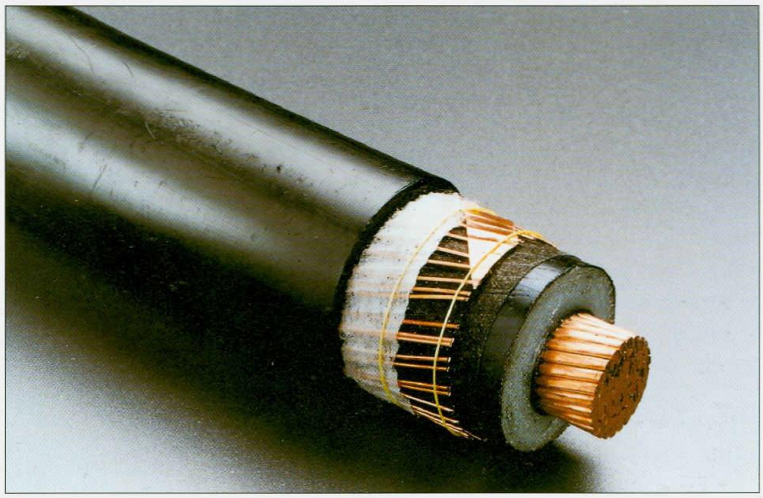

Catalog Number	Number of cores and nominal section of conductor	Minimum number of wires in conductor	Nominal thickness of insulation	Approx. outer diameter	Approx. weight	Current rating at 30°C in air Trefoil formation	Current rating at 20°C in ground Trefoil formation	Standard delivery lengths
	mm^2		mm	mm	kg/km	Amperes	Amperes	m
832753115	1x50/16	6	5.5	28	1150	238	223	1000
832753117	1x70/16	12	5.5	29	1400	296	273	1000
832753119	1x95/16	15	5.5	31	1700	358	325	1000
832754122	1x120/16	18	5.5	33	2000	412	368	1000
832754125	1x150/25	18	5.5	34	2400	466	410	1000
832754126	1x185/25	30	5.5	36	2800	532	463	1000
832755127	1x240/25	34	5.5	39	3400	627	534	1000
832755128	1x300/25	34	5.5	41	4100	715	601	500
832755129	1x400/25	53	5.5	47	5150	819	674	500

NOTES:
1) A special flame retardant construction can be supplied upon request.
2) A special moisture barrier construction can be supplied upon request.
(type of cable N2XS(F)2Y)

Appendix B: The seventh power station feeder's half an hourly readings.

Total Power profile for the power Transformer 1

	Avg Power (kW)	Avg Power (kW)	Avg Power (kW)
Time Step	January	July	yearly
00:00:00	1720.84	1545.95	1633.39
00:30:00	1607.77	1501.66	1554.71
01:00:00	1525.19	1409.45	1467.32
01:30:00	1435.80	1380.94	1408.37
02:00:00	1370.63	1336.02	1353.32
02:30:00	1339.29	1323.31	1331.30
03:00:00	1270.39	1291.87	1281.13
03:30:00	1249.85	1288.40	1269.12
04:00:00	1256.52	1270.46	1263.49
04:30:00	1274.49	1241.84	1258.17
05:00:00	1291.56	1232.79	1262.18
05:30:00	1355.93	1331.81	1343.87
06:00:00	1429.36	1380.22	1404.79
06:30:00	1585.17	1372.75	1478.96
07:00:00	1965.01	1441.43	1703.22
07:30:00	3027.82	1990.17	2508.99
08:00:00	3781.16	2514.86	3148.01
08:30:00	4334.14	3540.77	3937.45
09:00:00	4671.33	3996.27	4333.80
09:30:00	4664.16	4236.33	4450.24
10:00:00	4713.91	4399.63	4556.77
10:30:00	4816.22	4357.11	4586.66
11:00:00	4905.41	4374.32	4639.87
11:30:00	4748.31	4289.47	4518.89
12:00:00	4417.72	4233.94	4325.83
12:30:00	4387.57	3932.15	4159.86
13:00:00	4461.55	3926.59	4194.07
13:30:00	4707.31	3827.47	4267.39
14:00:00	4652.63	3823.94	4238.29
14:30:00	4896.52	4044.12	4470.32
15:00:00	4698.54	4059.36	4378.95
15:30:00	4446.33	4170.66	4308.50
16:00:00	3860.57	3996.47	3928.52
16:30:00	3648.47	3732.39	3690.43
17:00:00	3394.83	3317.76	3356.30
17:30:00	3124.87	3095.03	3109.95
18:00:00	2865.18	2783.26	2824.22
18:30:00	2681.60	2530.17	2605.89
19:00:00	2436.22	2302.49	2369.36
19:30:00	2402.40	2147.82	2275.11
20:00:00	2371.05	2014.31	2192.68
20:30:00	2327.24	1967.03	2147.13
21:00:00	2301.11	1910.07	2105.59
21:30:00	2230.89	1829.65	2030.27
22:00:00	2140.93	1716.69	1928.81
22:30:00	2083.08	1673.35	1878.21
23:00:00	1984.92	1625.27	1805.09
23:30:00	1866.86	1588.30	1727.58

PPU feeder Load Profile

	Avg Power (kW)	Avg Power (kW)	Avg Power (kW)
Time Step	January	Jun	yearly
00:00:00	683.70	580.19	631.94
00:30:00	656.75	569.55	613.15
01:00:00	631.21	559.73	595.47
01:30:00	604.59	553.65	579.12
02:00:00	580.31	538.02	559.17
02:30:00	569.87	522.95	546.41
03:00:00	554.69	529.76	542.22
03:30:00	545.85	529.13	537.49
04:00:00	541.90	518.35	530.12
04:30:00	528.56	522.56	525.56
05:00:00	536.58	508.98	522.78
05:30:00	541.56	492.38	516.97
06:00:00	548.91	491.93	520.42
06:30:00	561.96	476.95	519.45
07:00:00	594.95	488.57	541.76
07:30:00	641.51	542.89	592.20
08:00:00	697.37	586.49	641.93
08:30:00	810.45	661.86	736.15
09:00:00	866.57	675.10	770.84
09:30:00	912.37	733.68	823.03
10:00:00	955.72	779.64	867.68
10:30:00	1005.15	766.41	885.78
11:00:00	1056.91	754.43	905.67
11:30:00	1097.97	743.23	920.60
12:00:00	1097.40	751.90	924.65
12:30:00	1080.50	749.49	915.00
13:00:00	1060.51	717.60	889.06
13:30:00	1037.81	684.74	861.27
14:00:00	1038.83	700.73	869.78
14:30:00	1004.83	666.38	835.61
15:00:00	964.29	600.43	782.36
15:30:00	939.48	633.58	786.53
16:00:00	873.00	633.15	753.07
16:30:00	889.95	639.48	764.71
17:00:00	898.03	655.39	776.71
17:30:00	914.39	659.42	786.90
18:00:00	907.77	653.86	780.82
18:30:00	891.12	671.49	781.30
19:00:00	877.15	681.70	779.43
19:30:00	861.55	694.03	777.79
20:00:00	856.22	707.94	782.08
20:30:00	848.97	712.69	780.83
21:00:00	853.72	666.38	760.05
21:30:00	841.75	635.05	738.40
22:00:00	799.20	617.49	708.35
22:30:00	806.23	595.64	700.94
23:00:00	764.02	585.13	674.58
23:30:00	727.77	571.28	649.53

Zallum Feeder load profile			
	Avg Power (kW)	Avg Power (kW)	Avg Power (kW)
Time Step	January	July	yearly
00:00	1037.13	965.76	1001.45
00:30	951.02	932.11	941.56
01:00	893.98	849.71	871.85
01:30	831.21	827.29	829.25
02:00	790.32	797.99	794.15
02:30	769.42	800.36	784.89
03:00	715.70	762.11	738.91
03:30	704.00	759.27	731.63
04:00	714.62	752.11	733.37
04:30	745.92	719.28	732.60
05:00	754.98	723.81	739.39
05:30	814.36	839.43	826.90
06:00	880.46	888.29	884.37
06:30	1023.22	895.80	959.51
07:00	1370.06	952.87	1161.47
07:30	2386.31	1447.28	1916.80
08:00	3083.79	1928.36	2506.08
08:30	3523.69	2878.90	3201.30
09:00	3804.76	3321.17	3562.97
09:30	3751.79	3502.65	3627.22
10:00	3758.18	3619.99	3689.09
10:30	3811.07	3590.70	3700.88
11:00	3848.50	3619.90	3734.20
11:30	3650.33	3546.25	3598.29
12:00	3320.33	3482.04	3401.18
12:30	3307.06	3182.66	3244.86
13:00	3401.03	3208.99	3305.01
13:30	3669.50	3142.73	3406.11
14:00	3613.81	3123.21	3368.51
14:30	3891.69	3377.74	3634.71
15:00	3734.25	3458.93	3596.59
15:30	3506.85	3537.08	3521.96
16:00	2987.58	3363.33	3175.45
16:30	2758.52	3092.92	2925.72
17:00	2496.80	2662.37	2579.59
17:30	2210.48	2435.61	2323.05
18:00	1957.41	2129.40	2043.40
18:30	1790.49	1858.69	1824.59
19:00	1559.07	1620.79	1589.93
19:30	1540.85	1453.79	1497.32
20:00	1514.84	1306.37	1410.60
20:30	1478.27	1254.34	1366.30
21:00	1447.40	1243.69	1345.54
21:30	1389.14	1194.61	1291.88
22:00	1341.73	1099.20	1220.46
22:30	1276.85	1077.71	1177.28
23:00	1220.90	1040.14	1130.52
23:30	1139.08	1017.03	1078.05

Substation load profile	
Time Step	yearly
00:00	17.12
00:30	15.78
01:00	15.61
01:30	15.15
02:00	14.93
02:30	13.62
03:00	13.34
03:30	11.89
04:00	12.44
04:30	12.28
05:00	12.46
05:30	11.77
06:00	11.82
06:30	11.57
07:00	11.21
07:30	11.52
08:00	11.16
08:30	11.39
09:00	13.09
09:30	12.31
10:00	11.49
10:30	13.47
11:00	14.12
11:30	14.40
12:00	13.49
12:30	15.30
13:00	15.71
13:30	14.83
14:00	14.93
14:30	15.79
15:00	14.31
15:30	15.51
16:00	15.22
16:30	14.12
17:00	16.00
17:30	15.40
18:00	16.07
18:30	16.33
19:00	16.21
19:30	16.32
20:00	17.33
20:30	18.68
21:00	18.70
21:30	19.87
22:00	18.90
22:30	17.62
23:00	17.98
23:30	16.85

Appendix C: the PPU metering system readings table.

Active Power Profile									Yearly Active Power Profile	
	August		September		October		November			
Time Step	Import period (kW.h)	Export period (kW.h)	Import period (kW.h)	Export period (kW.h)	Import period (kW.h)	Export period (kW.h)	Import period (kW.h)	Export period (kW.h)	Import period (kW.h)	Export period (kW.h)
00:00	28.23	0.00	34.94	0.00	35.40	0.00	33.53	0.00	34.63	0.00
00:30	28.21	0.00	34.39	0.00	35.43	0.00	34.19	0.00	34.67	0.00
01:00	28.34	0.00	34.08	0.00	35.31	0.00	33.53	0.00	34.31	0.00
01:30	28.19	0.00	33.90	0.00	35.05	0.00	33.46	0.00	34.14	0.00
02:00	28.45	0.00	33.74	0.00	35.13	0.00	33.68	0.00	34.18	0.00
02:30	28.18	0.00	34.03	0.00	35.19	0.00	33.68	0.00	34.30	0.00
03:00	28.14	0.00	33.81	0.00	34.67	0.00	32.88	0.00	33.78	0.00
03:30	27.99	0.00	33.66	0.00	34.57	0.00	33.31	0.00	33.85	0.00
04:00	28.22	0.00	33.88	0.00	34.41	0.00	33.10	0.00	33.80	0.00
04:30	28.64	0.00	33.13	0.00	36.61	0.00	32.88	0.00	34.21	0.00
05:00	32.35	0.00	33.24	0.00	36.73	0.00	34.26	0.00	34.75	0.00
05:30	31.70	0.00	34.15	0.00	34.68	0.00	33.10	0.00	33.98	0.00
06:00	28.37	0.00	33.50	0.00	35.56	0.00	31.23	0.00	33.43	0.00
06:30	26.62	0.00	32.26	0.00	38.21	0.00	31.54	0.00	34.00	0.00
07:00	23.76	0.00	33.01	0.00	60.12	0.00	30.07	0.00	41.07	0.00
07:30	21.39	0.00	56.74	0.00	103.51	0.06	45.66	0.04	68.64	0.03
08:00	16.93	0.04	58.75	0.00	109.07	0.81	47.84	0.65	71.89	0.49
08:30	14.82	3.42	109.06	0.00	106.28	2.46	90.56	3.53	101.97	2.00
09:00	16.54	11.70	119.86	0.00	99.77	4.33	94.10	3.84	104.58	2.72
09:30	16.21	20.05	111.73	0.00	99.68	6.02	99.66	1.55	103.69	2.52
10:00	15.15	27.79	103.67	0.00	94.57	6.57	88.32	2.97	95.52	3.18
10:30	14.73	34.42	106.26	0.00	88.80	7.49	81.68	3.84	92.25	3.78
11:00	14.42	39.99	97.74	0.00	81.44	7.73	76.69	6.43	85.29	4.72
11:30	14.47	44.58	94.48	0.00	84.73	7.70	73.89	4.70	84.37	4.13
12:00	14.76	47.55	86.26	0.00	90.36	7.87	72.42	4.31	83.01	4.06
12:30	13.17	49.60	89.26	0.00	85.41	8.92	78.93	3.68	84.54	4.20
13:00	16.47	49.42	92.10	0.00	75.57	9.07	89.72	6.63	85.80	5.23
13:30	17.82	49.28	86.17	0.00	77.35	6.35	84.90	3.64	82.80	3.33
14:00	16.06	52.14	80.65	0.00	74.03	7.06	83.01	0.48	79.23	2.51
14:30	16.22	50.91	78.51	0.00	67.72	5.48	93.70	0.07	79.98	1.85
15:00	12.01	49.39	68.46	0.00	50.43	3.41	92.26	0.52	70.38	1.31
15:30	10.09	47.86	62.32	0.00	43.13	0.16	83.76	0.05	63.07	0.07
16:00	10.22	41.45	47.63	0.34	45.32	0.01	68.59	0.00	53.85	0.12
16:30	10.34	32.90	25.30	2.42	39.37	0.00	48.14	0.00	37.61	0.81
17:00	11.28	20.05	29.22	3.36	35.41	0.00	42.98	0.00	35.87	1.12
17:30	11.90	13.67	26.71	2.42	40.41	0.00	42.10	0.00	36.41	0.81
18:00	12.57	4.94	21.62	0.08	43.72	0.00	40.54	0.00	35.29	0.03
18:30	17.32	0.15	30.92	0.00	42.52	0.00	41.09	0.00	38.18	0.00
19:00	23.90	0.00	34.70	0.00	41.32	0.00	38.22	0.00	38.08	0.00
19:30	28.49	0.00	37.77	0.00	37.87	0.00	36.32	0.00	37.32	0.00
20:00	33.61	0.00	37.63	0.00	36.91	0.00	36.03	0.00	36.86	0.00
20:30	33.41	0.00	37.92	0.00	36.53	0.00	35.47	0.00	36.64	0.00
21:00	32.64	0.00	36.59	0.00	36.39	0.00	34.57	0.00	35.85	0.00
21:30	33.12	0.00	34.80	0.00	35.69	0.00	34.49	0.00	34.99	0.00
22:00	29.32	0.00	34.84	0.00	35.65	0.00	34.48	0.00	34.99	0.00
22:30	29.10	0.00	34.02	0.00	35.65	0.00	34.33	0.00	34.67	0.00
23:00	28.99	0.00	33.93	0.00	36.21	0.00	33.55	0.00	34.57	0.00
23:30	28.73	0.00	34.10	0.00	35.87	0.00	33.77	0.00	34.58	0.00

Reactive Power Profile									Yearly Active Power Profile	
	August		September		October		November			
Time Step	Import period (kVar.h)	Export period (kVar.h)	Import period (kVar.h)	Export period (kVar.h)	Import period (kVar.h)	Export period (kVar.h)	Import period (kVar.h)	Export period (kVar.h)	Import period (kVar.h)	Export period (kVar.h)
00:00	0.00	4.05	0.00	3.41	0.00	3.18	0.00	4.57	0.00	3.72
00:30	0.00	3.99	0.00	3.61	0.00	3.19	0.00	3.89	0.00	3.56
01:00	0.00	3.94	0.00	3.68	0.00	3.15	0.00	4.30	0.00	3.71
01:30	0.00	4.03	0.00	3.78	0.00	3.33	0.00	4.39	0.00	3.83
02:00	0.00	3.90	0.00	3.80	0.00	3.21	0.00	4.23	0.00	3.74
02:30	0.00	4.05	0.00	3.71	0.00	3.15	0.00	4.35	0.00	3.74
03:00	0.00	4.12	0.00	3.71	0.00	3.57	0.00	4.84	0.00	4.04
03:30	0.00	4.14	0.00	3.70	0.00	3.49	0.00	4.52	0.00	3.90
04:00	0.00	4.05	0.00	3.65	0.00	3.56	0.00	4.60	0.00	3.94
04:30	0.00	3.96	0.00	3.74	0.00	3.13	0.00	4.76	0.00	3.88
05:00	0.00	3.16	0.00	3.62	0.00	3.48	0.00	4.75	0.00	3.95
05:30	0.00	3.37	0.00	3.74	0.00	4.03	0.00	5.34	0.00	4.37
06:00	0.00	3.96	0.00	3.68	0.00	3.95	0.00	5.79	0.00	4.47
06:30	0.00	4.45	0.00	4.51	0.30	2.91	0.00	5.18	0.10	4.20
07:00	0.00	4.99	0.00	4.95	9.43	0.68	0.00	5.02	3.14	3.55
07:30	0.00	4.76	0.22	3.33	31.00	0.63	0.14	3.50	10.45	2.49
08:00	0.07	4.38	8.95	0.00	34.72	0.18	7.13	1.03	16.94	0.40
08:30	0.75	3.70	33.46	0.00	33.47	0.11	22.33	0.70	29.75	0.27
09:00	2.01	3.31	38.85	0.00	32.07	0.11	23.66	0.44	31.52	0.18
09:30	2.63	3.23	37.33	0.00	31.15	0.18	23.31	0.32	30.60	0.16
10:00	2.47	3.08	34.83	0.00	30.09	0.14	21.29	0.27	28.74	0.14
10:30	2.71	3.08	35.30	0.00	28.16	0.00	20.94	0.10	28.13	0.03
11:00	2.47	2.71	31.45	0.00	26.51	0.00	19.62	0.31	25.86	0.10
11:30	2.45	2.74	30.21	0.00	27.29	0.02	18.08	0.47	25.19	0.16
12:00	2.43	2.65	27.72	0.00	30.52	0.01	19.08	0.52	25.78	0.18
12:30	2.09	2.46	28.93	0.00	28.23	0.04	20.00	0.55	25.72	0.20
13:00	2.66	2.19	31.47	0.00	25.15	0.00	20.73	0.35	25.78	0.12
13:30	2.87	2.13	29.27	0.00	25.41	0.01	20.09	0.34	24.93	0.12
14:00	2.23	2.83	27.51	0.00	24.88	0.00	20.18	0.09	24.19	0.03
14:30	1.72	2.97	26.41	0.00	22.10	0.03	21.58	0.33	23.36	0.12
15:00	0.98	3.09	23.14	0.00	17.71	0.02	21.60	0.42	20.82	0.15
15:30	0.38	3.31	22.05	0.00	10.98	0.01	18.02	0.49	17.02	0.17
16:00	0.00	3.48	15.89	0.01	4.46	0.01	10.55	0.77	10.30	0.26
16:30	0.00	3.58	7.67	0.01	1.30	0.99	3.40	1.21	4.12	0.73
17:00	0.00	3.20	1.66	0.55	0.30	1.54	0.53	1.84	0.83	1.31
17:30	0.00	3.87	0.01	3.12	0.10	1.97	0.42	2.42	0.18	2.50
18:00	0.00	3.89	0.00	3.64	0.07	1.52	0.41	3.03	0.16	2.73
18:30	0.00	3.96	0.00	4.01	0.05	1.68	0.43	2.72	0.16	2.80
19:00	0.00	4.53	0.00	4.14	0.11	1.77	0.24	2.84	0.12	2.91
19:30	0.00	3.92	0.00	3.44	0.00	2.55	0.00	3.15	0.00	3.05
20:00	0.00	3.03	0.00	3.28	0.00	2.62	0.00	3.15	0.00	3.02
20:30	0.00	3.10	0.00	3.05	0.00	2.82	0.00	3.66	0.00	3.18
21:00	0.00	3.31	0.00	3.28	0.02	2.73	0.00	3.64	0.01	3.22
21:30	0.00	3.00	0.00	3.71	0.00	3.25	0.11	3.70	0.04	3.55
22:00	0.00	3.55	0.00	3.66	0.00	3.31	0.03	3.75	0.01	3.57
22:30	0.00	3.60	0.00	3.92	0.00	3.33	0.00	3.93	0.00	3.73
23:00	0.00	3.66	0.00	4.00	0.01	2.86	0.00	4.53	0.00	3.80
23:30	0.00	3.82	0.00	3.82	0.00	3.17	0.00	4.27	0.00	3.75

Appendix D: PPU PV power plant component data sheets.

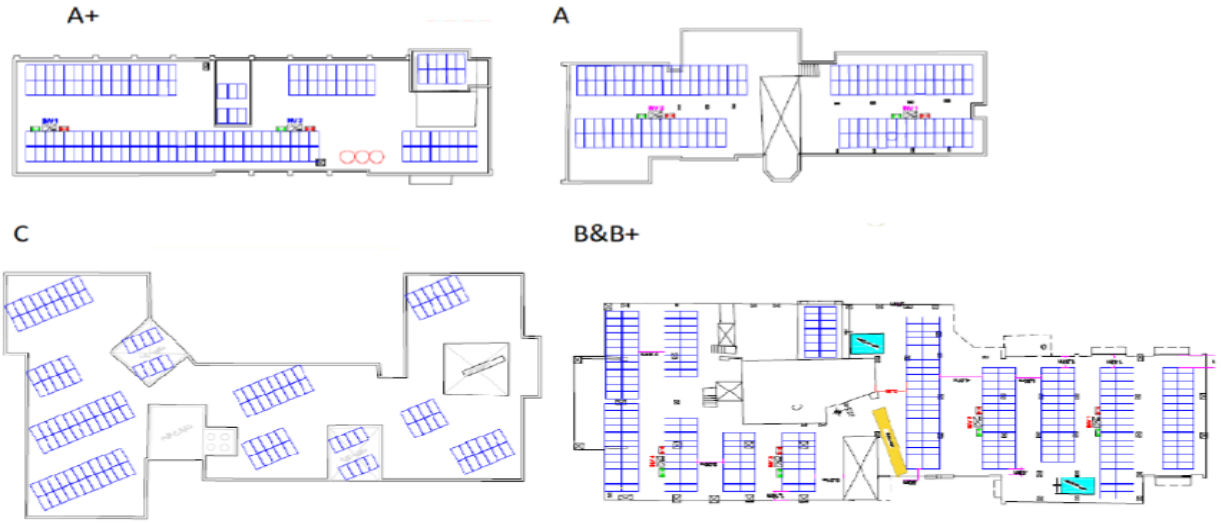

The new Q.POWER L-G5 is the result of the continued evolution of our polycrystalline solar modules. Thanks to improved power yield, excellent reliability and high-level operational safety, the new Q.POWER L-G5 generates electricity at a low cost (LCOE) and is suitable for a wide range of applications.

SUPERIOR YIELD
High power output thanks to advanced 6-busbar technology and outstanding performance under real-life conditions.

LOW LEVELISED COST OF ELECTRICITY
Higher yield per surface area, lower BOS costs, higher power classes and an efficiency rate of up to 17.5 %.

INNOVATIVE ALL-WEATHER TECHNOLOGY
Optimal yields, whatever the weather with excellent low-light and temperature behaviour.

EXTREME WEATHER RATING
High-tech aluminium alloy frame, certified for high snow (5400 Pa) and wind loads (2400 Pa).

MAXIMUM COST REDUCTIONS
Lower logistics costs due to higher module capacity per box.

A RELIABLE INVESTMENT
Inclusive 12-year product warranty and 25-year linear performance warranty[1].

EUPD RESEARCH TOP BRAND PV MODULES EUROPE 2017

Photon Q CELLS Best polycrystalline solar module 2014 Q.PRO-G2 235 174 modules tested

MECHANICAL SPECIFICATION

Format	1960 mm × 991 mm × 35 mm (including frame)
Weight	22.5 kg ± 5 %
Front Cover	3.2 mm thermally pre-stressed glass with anti-reflection technology
Back Cover	Multi-layer composite sheet
Frame	Anodised aluminium
Cell	6 × 12 polycrystalline solar cells
Junction box	Protection class IP67 or IP68, with bypass diodes
Cable	4 mm² Solar cable; (+) ≥ 1200 mm, (-) ≥ 1200 mm
Connector	Intermateable connector with H4, MC4

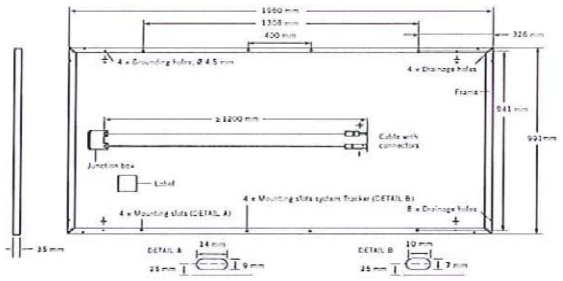

ELECTRICAL CHARACTERISTICS

POWER CLASS			315	320	325	330	335
MINIMUM PERFORMANCE AT STANDARD TEST CONDITIONS, STC[1] (POWER TOLERANCE +5 W / -0 W)							
Power at MPP[2]	P_{MPP}	[W]	315	320	325	330	335
Short Circuit Current*	I_{SC}	[A]	9.11	9.15	9.20	9.30	9.40
Open Circuit Voltage*	V_{OC}	[V]	45.7	45.8	46.0	46.1	46.3
Current at MPP*	I_{MPP}	[A]	8.50	8.61	8.67	8.76	8.87
Voltage at MPP*	V_{MPP}	[V]	37.1	37.2	37.5	37.7	37.8
Efficiency[2]	η	[%]	≥ 16.2	≥ 16.4	≥ 16.7	≥ 16.9	≥ 17.2
MINIMUM PERFORMANCE AT NORMAL OPERATING CONDITIONS, NOC[3]							
Power at MPP[2]	P_{MPP}	[W]	232	235	239	243	247
Short Circuit Current*	I_{SC}	[A]	7.37	7.40	7.44	7.52	7.60
Open Circuit Voltage*	V_{OC}	[V]	42.9	43.0	43.1	43.2	43.4
Current at MPP*	I_{MPP}	[A]	6.79	6.88	6.93	7.00	7.09
Voltage at MPP*	V_{MPP}	[V]	34.1	34.2	34.5	34.7	34.8

[1] 1000 W/m², 25 °C, spectrum AM 1.5 G [2] Measurement tolerances STC ± 3 %; NOC ± 5 % [3] 800 W/m², NOCT, spectrum AM 1.5 G * typical values, actual values may differ

Q CELLS PERFORMANCE WARRANTY

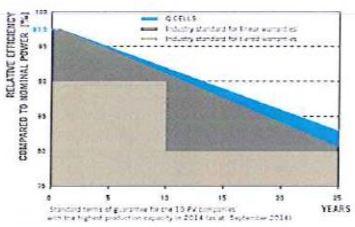

At least 97.5 % of nominal power during first year. Thereafter max. 0.7 % degradation per year.
At least 91.2 % of nominal power up to 10 years.
At least 82.0 % of nominal power up to 25 years.

All data within measurement tolerances. full warranties in accordance with the warranty terms of the Q CELLS sales organization of your respective country.

PERFORMANCE AT LOW IRRADIANCE

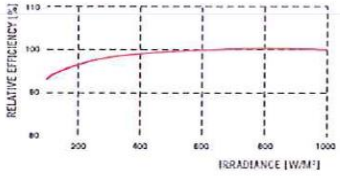

Typical module performance under low irradiance conditions in comparison to STC conditions (25 °C, 1000 W/m²).

TEMPERATURE COEFFICIENTS

Temperature Coefficient of I_{SC}	α	[%/K]	+0.05	Temperature Coefficient of V_{OC}	β	[%/K]	-0.31
Temperature Coefficient of P_{MPP}	γ	[%/K]	-0.40	Normal Operating Cell Temperature	NOCT	[°C]	45 ± 3

PROPERTIES FOR SYSTEM DESIGN

Maximum System Voltage	V_{SYS}	[V]	1000	Safety Class		II
Maximum Reverse Current	I_R	[A]	20	Fire Rating		C
Wind/Snow Load (Test-load in accordance with IEC 61215)		[Pa]	2400/5400	Permitted Module Temperature On Continuous Duty		-40 °C up to +85 °C

QUALIFICATIONS AND CERTIFICATES

IEC 61215, IEC 61730, Conformity to CE, Application Class A

PARTNER

NOTE: Installation instructions must be followed. See the installation and operating manual or contact our technical service department for further information on approved installation and use of this product.

Hanwha Q CELLS (Qidong) Co., Ltd.
No. 888 Linyang Road, Qidong City, Jiangsu Province, China | EMAIL sales@hanwha-qcells.com | WEB www.q-cells.com

Engineered in **Germany**

blueplanet
15.0 TL3
20.0 TL3

- Up to 98.4 % efficiency
- 2 MPP trackers, symmetrical and asymmetrical loading possible
- Wide input voltage range 200 V – 950 V
- Protection class IP65 for outdoor use
- Graphical display, multilingual menu, pre-configured country settings
- Data logger with web server
- Prepared for DC surge protection SPD 1+2

www.kaco-newenergy.com

EN 5001046-08-180123

Your retailer

The text and figures reflect the current technical state at the time of printing. Subject to technical changes. Errors and omissions excepted. This current version replaces all older versions. Download the most current version at: www.kaco-newenergy.com

Technical data

blueplanet 15.0 TL3 | 20.0 TL3

Electrical data	15.0 TL3	20.0 TL3
Input variables		
Maximum PV generator power	18000 W	24000 W
MPP range@Pnom	420V ... 800V	515V ... 800V
Operating range	200V - 950V	200V - 950V
Min. DC voltage / starting voltage	200V / 250V	200V / 250V
No-load voltage	1000 V	1000 V
Max. input current	2x20.0 A	2x20.0 A
Max. short circuit current [$I_{SC\,max}$]	2x22.4 A	2x22.4 A
Number of MPP trackers	2	2
Max. power/tracker	14.9 kW	15.0 kW
Number of strings	2x2	2x2
Output variables		
Rated output (@ 230 V)	15000 VA@230 V	20000 VA@230 V
Line voltage	400 V / 230 V (3 / N / PE)	400 V / 230 V (3 / N / PE)
Rated current	3x21.8 A	3x29.0 A
Rated frequency	50 Hz / 60 Hz	50 Hz / 60 Hz
cos phi	0.30 inductive ... 0.30 capacitive	0.30 inductive ... 0.30 capacitive
Number of grid phases	3	3
General electrical data		
Max. efficiency	98,0 %	98.4 %
Europ. efficiency	97.7 %	98.1 %
Night consumption	1.5 W	1.5 W
Switching plan	transformerless	transformerless
Grid monitoring	acc. to local requirements	acc. to local requirements
Mechanical data		
Display	graphical display + LEDs	graphical display + LEDs
Control units	4-way navigation + 2 buttons	4-way navigation + 2 buttons
Interfaces	standard: 2xEthernet, USB, RS485, fault signalling relay optional: 4-DI	standard: 2xEthernet, USB, RS485, fault signalling relay optional: 4-DI
Fault signalling relay	potential-free NOC max. 30 V / 1 A	potential-free NOC max. 30 V / 1 A
Connections	DC: solar connector, AC: cable connection M40 and terminal (max. cross-section: 16 mm² flexible, 10 mm² rigid)	DC: solar connector, AC: cable connection M40 and terminal (max. cross-section: 16 mm² flexible, 10 mm² rigid)
Ambient temperature	-25°C ... +60°C [1]	-25°C ... +60°C [1]
Cooling	forced convection	forced convection
Protection class	IP65	IP65
Noise emission	< 52 dB (A)	< 53 dB (A)
DC switch	integrated	integrated
Casing	aluminium casting	aluminium casting
HxWxD	690x420x200 mm	690x420x200 mm
Weight	46.6 kg	46.6 kg

[1] Power derating at high ambient temperatures

Appendix E: Output result from the ETAP.

2-Winding Transformer Input Data

Transformer		Rating					Z Variation			% Tap Setting		Adjusted	Phase Shift	
ID	Phase	MVA	Prim. kV	Sec. kV	% Z1	X1/R1	+ 5%	- 5%	% Tol.	Prim.	Sec.	% Z	Type	Angle
Power Tr.1	3-Phase	10.000	33.000	11.000	8.35	13.00	0	0	0	0	0	8.3500	Dyn	0.000
Power Tr.2	3-Phase	10.000	33.000	11.000	8.35	13.00	0	0	0	0	0	8.3500	Dyn	0.000
Subst. Tr.	3-Phase	0.400	11.000	0.400	4.00	1.50	0	0	0	0	0	4.0000	Dyn	0.000
T1	3-Phase	0.630	11.000	0.400	4.00	1.50	0	0	0	0	0	4.0000	Dyn	0.000
T2	3-Phase	0.160	11.000	0.400	4.00	1.50	0	0	0	0	0	4.0000	Dyn	0.000
T3	3-Phase	0.400	11.000	0.400	4.00	1.50	0	0	0	0	0	4.0000	Dyn	0.000
T4	3-Phase	1.000	11.000	0.400	5.00	3.50	0	0	0	0	0	5.0000	Dyn	0.000
T5	3-Phase	0.160	11.000	0.400	4.00	1.50	0	0	0	0	0	4.0000	Dyn	0.000
T6	3-Phase	0.250	11.000	0.400	4.00	1.50	0	0	0	0	0	4.0000	Dyn	0.000
T7	3-Phase	0.400	11.000	0.400	4.00	1.50	0	0	0	0	0	4.0000	Dyn	0.000
T8	3-Phase	0.250	11.000	0.400	4.00	1.50	0	0	0	0	0	4.0000	Dyn	0.000
T9	3-Phase	0.630	11.000	0.400	4.00	1.50	0	0	0	0	0	4.0000	Dyn	0.000
T10	3-Phase	0.250	11.000	0.400	4.00	1.50	0	0	0	0	0	4.0000	Dyn	0.000
T14	3-Phase	1.000	11.000	0.400	5.00	3.50	0	0	0	0	0	5.0000	Dyn	0.000
Tr. AK	3-Phase	5.000	11.000	0.400	8.35	13.00	0	0	0	0	0	8.3500	Dyn	0.000
Tr. SA	3-Phase	5.500	11.000	0.400	8.35	13.00	0	0	0	0	0	8.3500	Dyn	0.000
Tr.1	3-Phase	0.400	11.000	0.400	4.00	1.50	0	0	0	0	0	4.0000	Dyn	0.000
Tr.2	3-Phase	0.630	11.000	0.400	4.00	1.50	0	0	0	0	0	4.0000	Dyn	0.000
Tr.3	3-Phase	0.400	11.000	0.400	4.00	1.50	0	0	0	0	0	4.0000	Dyn	0.000
Tr.4	3-Phase	0.630	11.000	0.400	4.00	1.50	0	0	0	0	0	4.0000	Dyn	0.000
Tr.5	3-Phase	0.250	11.000	0.400	4.00	1.50	0	0	0	0	0	4.0000	Dyn	0.000
Tr.6	3-Phase	0.400	11.000	0.400	4.00	1.50	0	0	0	0	0	4.0000	Dyn	0.000
Tr.7	3-Phase	0.630	11.000	0.400	4.00	1.50	0	0	0	0	0	4.0000	Dyn	0.000
Tr.9	3-Phase	0.250	11.000	0.400	4.00	1.50	0	0	0	0	0	4.0000	Dyn	0.000
Tr.10	3-Phase	0.400	11.000	0.400	4.00	1.50	0	0	0	0	0	4.0000	Dyn	0.000
Tr.11	3-Phase	0.400	11.000	0.400	4.00	1.50	0	0	0	0	0	4.0000	Dyn	0.000
Tr.12	3-Phase	0.630	11.000	0.400	4.00	1.50	0	0	0	0	0	4.0000	Dyn	0.000
Tr.13	3-Phase	0.400	11.000	0.400	4.00	1.50	0	0	0	0	0	4.0000	Dyn	0.000
Tr.14	3-Phase	0.630	11.000	0.400	4.00	1.50	0	0	0	0	0	4.0000	Dyn	0.000
Tr.15	3-Phase	0.160	11.000	0.400	4.00	1.50	0	0	0	0	0	4.0000	Dyn	0.000
Tr.16	3-Phase	0.400	11.000	0.400	4.00	1.50	0	0	0	0	0	4.0000	Dyn	0.000
Tr.18	3-Phase	0.630	11.000	0.400	4.00	1.50	0	0	0	0	0	4.0000	Dyn	0.000
Tr.21	3-Phase	0.400	11.000	0.400	4.00	1.50	0	0	0	0	0	4.0000	Dyn	0.000
Tr.22	3-Phase	0.630	11.000	0.400	4.00	1.50	0	0	0	0	0	4.0000	Dyn	0.000
Tr.26	3-Phase	0.630	11.000	0.400	4.00	1.50	0	0	0	0	0	4.0000	Dyn	0.000
Tr.29	3-Phase	0.400	11.000	0.400	4.00	1.50	0	0	0	0	0	4.0000	Dyn	0.000
Tr.32	3-Phase	0.400	11.000	0.400	4.00	1.50	0	0	0	0	0	4.0000	Dyn	0.000
Tr.35	3-Phase	0.630	11.000	0.400	4.00	1.50	0	0	0	0	0	4.0000	Dyn	0.000

Branch Connections

CKT/Branch		Connected Bus ID		% Impedance, Pos. Seq., 100 MVA Base			
ID	Type	From Bus	To Bus	R	X	Z	Y
Power Tr.1	2W XFMR	Main Bus	Bus1	6.40	83.25	83.50	
Power Tr.2	2W XFMR	Main Bus	Bus21	6.40	83.25	83.50	
Subst. Tr.	2W XFMR	Bus1	subst. Tr.Bus	554.70	832.05	1000.00	
T1	2W XFMR	Bus3	Bus5	352.19	528.29	634.92	
T2	2W XFMR	Bus4	Bus6	1386.75	2080.13	2500.00	
T3	2W XFMR	Bus7	Bus8	554.70	832.05	1000.00	
T4	2W XFMR	Bus9	Bus10 (PPU)	137.36	480.76	500.00	
T5	2W XFMR	Bus11	Bus12	1386.75	2080.13	2500.00	
T6	2W XFMR	Bus13	Bus14	887.52	1331.28	1600.00	
T7	2W XFMR	Bus15	Bus16	554.70	832.05	1000.00	
T8	2W XFMR	Bus17	Bus18	887.52	1331.28	1600.00	
T9	2W XFMR	Bus 52	Bus 53	352.19	528.29	634.92	
T10	2W XFMR	Bus 54	Bus 55	887.52	1331.28	1600.00	
T14	2W XFMR	Bus9	Bus10 (PPU)2	137.36	480.76	500.00	
Tr. AK	2W XFMR	Bus AK	Bus AK low	12.81	166.51	167.00	
Tr. SA	2W XFMR	Bus SA	Bus SA low	11.64	151.37	151.82	
Tr.1	2W XFMR	Bus Z	Bus 20	554.70	832.05	1000.00	
Tr.2	2W XFMR	Bus 21	Bus 23	352.19	528.29	634.92	
Tr.3	2W XFMR	Bus 22	Bus 24	554.70	832.05	1000.00	
Tr.4	2W XFMR	Bus 22	Bus 25	352.19	528.29	634.92	
Tr.5	2W XFMR	Bus 22	Bus 26	887.52	1331.28	1600.00	
Tr.6	2W XFMR	Bus 27	Bus 29	554.70	832.05	1000.00	
Tr.7	2W XFMR	Bus 30	Bus 31	352.19	528.29	634.92	
Tr.9	2W XFMR	Bus 30	Bus 32	887.52	1331.28	1600.00	
Tr.10	2W XFMR	Bus 33	Bus 34	554.70	832.05	1000.00	
Tr.11	2W XFMR	Bus 35	Bus 36	554.70	832.05	1000.00	
Tr.12	2W XFMR	Bus 35	Bus 37	352.19	528.29	634.92	
Tr.13	2W XFMR	Bus 38	Bus 39	554.70	832.05	1000.00	
Tr.14	2W XFMR	Bus 41	Bus 42	352.19	528.29	634.92	
Tr.15	2W XFMR	Bus 43	Bus 44	1386.75	2080.13	2500.00	
Tr.16	2W XFMR	Bus 43	Bus 45	554.70	832.05	1000.00	
Tr.18	2W XFMR	Bus 61	Bus 62	352.19	528.29	634.92	
Tr.21	2W XFMR	Bus 43	Bus 46	554.70	832.05	1000.00	
Tr.22	2W XFMR	Bus 43	Bus 47	352.19	528.29	634.92	
Tr.26	2W XFMR	Bus 48	Bus 49	352.19	528.29	634.92	
Tr.29	2W XFMR	Bus 48	Bus 50	554.70	832.05	1000.00	

CKT/Branch		Connected Bus ID		% Impedance, Pos. Seq., 100 MVA Base			
ID	Type	From Bus	To Bus	R	X	Z	Y
Tr.32	2W XFMR	Bus 56	Bus 57	554.70	832.05	1000.00	
Tr.35	2W XFMR	Bus 56	Bus 58	352.19	528.29	634.92	
Tr.37	2W XFMR	Bus 59	Bus 60	352.19	528.29	634.92	
C1	Cable	Bus1	Bus2	17.30	13.80	22.13	
C2	Cable	Bus2	Bus7	6.96	5.55	8.90	
C3	Cable	Bus7	Bus9	7.52	6.00	9.62	
C4	Cable	Bus9	Bus15	2.31	1.84	2.95	
C5	Cable	Bus9	Bus11	0.75	0.60	0.96	
C6	Cable	Bus15	Bus17	1.25	1.00	1.60	
C8	Cable	Bus1	Bus Z	8.40	6.70	10.74	
C9	Cable	Bus21	Bus SA	38.31	30.57	49.01	
C10	Cable	Bus 22	Bus 27	0.88	0.70	1.12	
C12	Cable	Bus21	Bus AK	53.89	43.00	68.94	
C13	Cable	Bus 30	Bus 33	1.25	1.00	1.60	
C15	Cable	Bus 33	Bus 35	0.63	0.50	0.80	
C18	Cable	Bus 35	Bus 38	2.51	2.00	3.21	
C20	Cable	Bus 38	Bus 41	3.76	3.00	4.81	
Line1	Line	Bus2	Bus3	3.13	2.94	4.29	0.0000453
Line2	Line	Bus3	Bus4	2.39	2.24	3.27	0.0000345
Line3	Line	Bus13	Bus11	29.83	27.98	40.90	0.0004314
Line6	Line	Bus Z	Bus 21	14.17	13.29	19.43	0.0002049
Line7	Line	Bus 21	Bus 22	7.55	7.08	10.35	0.0001091
Line10	Line	Bus 27	Bus 28	8.06	7.55	11.04	0.0001165
Line12	Line	Bus 28	Bus 30	8.06	7.55	11.04	0.0001165
Line13	Line	Bus 43	Bus 28	9.85	9.23	13.50	0.0001424
Line15	Line	Bus 43	Bus 48	1.91	1.79	2.62	0.0000276
Line17	Line	Bus 48	Bus 51	1.91	1.79	2.62	0.0000276
Line20	Line	Bus 51	Bus 52	4.53	4.25	6.22	0.0000656
Line21	Line	Bus 52	Bus 54	1.91	1.79	2.62	0.0000276
Line23	Line	Bus 51	Bus 56	3.40	3.19	4.66	0.0000492
Line25	Line	Bus 56	Bus 59	4.53	4.25	6.22	0.0000656
Line26	Line	Bus 59	Bus 61	1.91	1.79	2.62	0.0000276

Bus Input Data

Bus			Initial Voltage		Load							
					Constant kVA		Constant Z		Constant I		Generic	
ID	kV	Sub-sys	% Mag.	Ang.	MW	Mvar	MW	Mvar	MW	Mvar	MW	Mvar
Bus1	11.000	1	100.0	0.0								
Bus2	11.000	1	100.0	0.0								
Bus3	11.000	1	100.0	0.0								
Bus4	11.000	1	100.0	0.0								
Bus5	0.400	1	100.0	0.0	0.223	0.095	0.056	0.024				
Bus6	0.400	1	100.0	0.0	0.057	0.024	0.014	0.006				
Bus7	11.000	1	100.0	0.0								
Bus8	0.400	1	100.0	0.0	0.140	0.060	0.035	0.015				
Bus9	11.000	1	100.0	0.0								
Bus10 (PPU)	0.400	1	100.0	0.0	0.494	0.150	0.088	0.038				
Bus10 (PPU)2	0.400	1	100.0	0.0								
Bus11	11.000	1	100.0	0.0								
Bus12	0.400	1	100.0	0.0	0.057	0.024	0.014	0.006				
Bus13	11.000	1	100.0	0.0								
Bus14	0.400	1	100.0	0.0	0.088	0.038	0.022	0.009				
Bus15	11.000	1	100.0	0.0								
Bus16	0.400	1	100.0	0.0	0.141	0.060	0.035	0.015				
Bus17	11.000	1	100.0	0.0								
Bus18	0.400	1	100.0	0.0	0.088	0.038	0.022	0.009				
Bus 20	0.400	1	100.0	0.0	0.109	0.046	0.027	0.012				
Bus21	11.000	1	100.0	0.0								
Bus 21	11.000	1	100.0	0.0								
Bus 22	11.000	1	100.0	0.0								
Bus 23	0.400	1	100.0	0.0	0.172	0.073	0.043	0.018				
Bus 24	0.400	1	100.0	0.0	0.109	0.046	0.027	0.012				
Bus 25	0.400	1	100.0	0.0	0.172	0.073	0.043	0.018				
Bus 26	0.400	1	100.0	0.0	0.066	0.029	0.017	0.007				
Bus 27	11.000	1	100.0	0.0								
Bus 28	11.000	1	100.0	0.0								
Bus 29	0.400	1	100.0	0.0	0.109	0.046	0.027	0.012				
Bus 30	11.000	1	100.0	0.0								
Bus 31	0.400	1	100.0	0.0	0.172	0.073	0.043	0.018				
Bus 32	0.400	1	100.0	0.0	0.066	0.029	0.017	0.007				

Bus			Initial Voltage		Load							
					Constant kVA		Constant Z		Constant I		Generic	
ID	kV	Sub-sys	% Mag.	Ang.	MW	Mvar	MW	Mvar	MW	Mvar	MW	Mvar
Bus 33	11.000	1	100.0	0.0								
Bus 34	0.400	1	100.0	0.0	0.109	0.046	0.027	0.012				
Bus 35	11.000	1	100.0	0.0								
Bus 36	0.400	1	100.0	0.0	0.109	0.046	0.027	0.012				
Bus 37	0.400	1	100.0	0.0	0.172	0.073	0.043	0.018				
Bus 38	11.000	1	100.0	0.0								
Bus 39	0.400	1	100.0	0.0	0.109	0.046	0.027	0.012				
Bus 41	11.000	1	100.0	0.0								
Bus 42	0.400	1	100.0	0.0	0.172	0.073	0.043	0.018				
Bus 43	11.000	1	100.0	0.0								
Bus 44	0.400	1	100.0	0.0	0.057	0.024	0.014	0.006				
Bus 45	0.400	1	100.0	0.0	0.109	0.046	0.027	0.012				
Bus 46	0.400	1	100.0	0.0	0.109	0.046	0.027	0.012				
Bus 47	0.400	1	100.0	0.0	0.172	0.073	0.043	0.018				
Bus 48	11.000	1	100.0	0.0								
Bus 49	0.400	1	100.0	0.0	0.172	0.073	0.043	0.018				
Bus 50	0.400	1	100.0	0.0	0.109	0.046	0.027	0.012				
Bus 51	11.000	1	100.0	0.0								
Bus 52	11.000	1	100.0	0.0								
Bus 53	0.400	1	100.0	0.0	0.223	0.095	0.056	0.024				
Bus 54	11.000	1	100.0	0.0								
Bus 55	0.400	1	100.0	0.0	0.066	0.029	0.017	0.007				
Bus 56	11.000	1	100.0	0.0								
Bus 57	0.400	1	100.0	0.0	0.109	0.046	0.027	0.012				
Bus 58	0.400	1	100.0	0.0	0.172	0.073	0.043	0.018				
Bus 59	11.000	1	100.0	0.0								
Bus 60	0.400	1	100.0	0.0	0.172	0.073	0.043	0.018				
Bus 61	11.000	1	100.0	0.0								
Bus 62	0.400	1	100.0	0.0	0.216	0.092	0.054	0.023				
Bus AK	11.000	1	100.0	0.0								
Bus AK low	0.400	1	100.0	0.0	1.396	0.676	0.349	0.169				
Bus SA	11.000	1	100.0	0.0								
Bus SA low	0.400	1	100.0	0.0	3.106	1.323	0.777	0.331				
Bus Z	11.000	1	100.0	0.0								
Main Bus	33.000	1	100.0	0.0								

Bus			Initial Voltage		Load							
					Constant kVA		Constant Z		Constant I		Generic	
ID	kV	Sub-sys	% Mag.	Ang.	MW	Mvar	MW	Mvar	MW	Mvar	MW	Mvar
subst. Tr.Bus	0.400	1	100.0	0.0	0.012	0.002	0.003	0.001				
Total Number of Buses: 69					9.128	3.910	2.247	0.978	0.000	0.000	0.000	0.000

Generation Bus				Voltage		Generation			Mvar Limits	
ID	kV	Type	Sub-sys	% Mag.	Angle	MW	Mvar	% PF	Max	Min
Bus10 (PPU)	0.400	Mvar/PF Control	1	100.0	0.0	0.210	0.000	100.0		
Main Bus	33.000	Swing	1	100.0	0.0					
						0.210	0.000			

Line/Cable Input Data

ohms or siemens/1000 m per Conductor (Cable) or per Phase (Line)

Line/Cable ID	Library	Size	Length Adj. (m)	% Tol.	#/Phase	T (°C)	R	X	Y
C1	15NCUS1	150	1380.0	0.0	1	75	0.151650	0.121000	
C2	15NCUS1	150	555.0	0.0	1	75	0.151650	0.121000	
C3	15NCUS1	150	600.0	0.0	1	75	0.151650	0.121000	
C4	15NCUS1	150	184.0	0.0	1	75	0.151650	0.121000	
C5	15NCUS1	150	60.0	0.0	1	75	0.151650	0.121000	
C6	15NCUS1	150	100.0	0.0	1	75	0.151650	0.121000	
C8	15NCUS1	150	670.0	0.0	1	75	0.151650	0.121000	
C9	15NCUS1	150	3057.0	0.0	1	75	0.151650	0.121000	
C10	15NCUS1	150	70.0	0.0	1	75	0.151650	0.121000	
C12	15NCUS1	150	4300.0	0.0	1	75	0.151650	0.121000	
C13	15NCUS1	150	100.0	0.0	1	75	0.151650	0.121000	
C15	15NCUS1	150	50.0	0.0	1	75	0.151650	0.121000	
C18	15NCUS1	150	200.0	0.0	1	75	0.151650	0.121000	
C20	15NCUS1	150	300.0	0.0	1	75	0.151650	0.121000	
Line1		120	105.0	0.0	1	75	0.361000	0.338556	0.0000036
Line2		120	80.0	0.0	1	75	0.361000	0.338556	0.0000036
Line3		120	1000.0	0.0	1	75	0.361000	0.338556	0.0000036
Line6		120	475.0	0.0	1	75	0.361000	0.338556	0.0000036
Line7		120	253.0	0.0	1	75	0.361000	0.338556	0.0000036
Line10		120	270.0	0.0	1	75	0.361000	0.338556	0.0000036
Line12		120	270.0	0.0	1	75	0.361000	0.338556	0.0000036
Line13		120	330.0	0.0	1	75	0.361000	0.338556	0.0000036
Line15		120	64.0	0.0	1	75	0.361000	0.338556	0.0000036
Line17		120	64.0	0.0	1	75	0.361000	0.338556	0.0000036
Line20		120	152.0	0.0	1	75	0.361000	0.338556	0.0000036
Line21		120	64.0	0.0	1	75	0.361000	0.338556	0.0000036
Line23		120	114.0	0.0	1	75	0.361000	0.338556	0.0000036
Line25		120	152.0	0.0	1	75	0.361000	0.338556	0.0000036
Line26		120	64.0	0.0	1	75	0.361000	0.338556	0.0000036

Line / Cable resistances are listed at the specified temperatures.

LOAD_FLOW_REPORT

Bus		Voltage		Generation		Load		Load Flow					XFMR
ID	kV	% Mag.	Ang.	MW	Mvar	MW	Mvar	ID	MW	Mvar	Amp	%PF	%Tap
Bus1	11.000	97.390	-2.6	0	0	0	0	Bus2	1.359	0.631	80.8	90.7	
								Bus Z	4.184	1.868	246.9	91.3	
								Main Bus	-5.557	-2.503	328.4	91.2	
								subst. Tr.Bus	0.014	0.003	0.8	98.0	
Bus2	11.000	97.059	-2.7	0	0	0	0	Bus1	-1.355	-0.628	80.8	90.7	
								Bus7	1.008	0.476	60.3	90.4	
								Bus3	0.347	0.152	20.5	91.6	
Bus3	11.000	97.043	-2.7	0	0	0	0	Bus2	-0.347	-0.152	20.5	91.6	
								Bus4	0.070	0.031	4.1	91.6	
								Bus5	0.277	0.121	16.3	91.6	
Bus4	11.000	97.041	-2.7	0	0	0	0	Bus3	-0.070	-0.031	4.2	91.6	
								Bus6	0.070	0.031	4.2	91.6	
Bus5	0.400	95.384	-3.3	0	0	0.273	0.116	Bus3	-0.273	-0.116	449.3	92.0	
Bus6	0.400	95.382	-3.3	0	0	0.069	0.030	Bus4	-0.069	-0.030	114.1	92.0	
Bus7	11.000	96.960	-2.7	0	0	0	0	Bus2	-1.007	-0.475	60.3	90.4	
								Bus9	0.833	0.398	50.0	90.2	
								Bus8	0.175	0.077	10.3	91.5	
Bus8	0.400	95.306	-3.3	0	0	0.172	0.074	Bus7	-0.172	-0.074	284.0	91.9	
Bus9	11.000	96.871	-2.7	0	0	0	0	Bus7	-0.832	-0.397	50.0	90.2	
								Bus15	0.285	0.125	16.9	91.6	
								Bus11	0.180	0.079	10.6	91.6	
								Bus10 (PPU)	0.367	0.194	22.5	88.4	
								Bus10 (PPU)2	0.000	0.000	0.0	0.0	
Bus10 (PPU)	0.400	95.403	-3.6	0.210	0.000	0.574	0.185	Bus9	-0.364	-0.185	617.9	89.2	
Bus10 (PPU)2	0.400	96.871	-2.7	0	0	0	0	Bus9	0.000	0.000	0.0	0.0	
Bus11	11.000	96.869	-2.7	0	0	0	0	Bus9	-0.180	-0.079	10.6	91.6	
								Bus13	0.110	0.048	6.5	91.7	
								Bus12	0.070	0.031	4.2	91.6	
Bus12	0.400	95.207	-3.3	0	0	0.069	0.030	Bus11	-0.069	-0.030	114.3	92.0	
Bus13	11.000	96.821	-2.7	0	0	0	0	Bus11	-0.110	-0.048	6.5	91.6	
								Bus14	0.110	0.048	6.5	91.6	
Bus14	0.400	95.159	-3.4	0	0	0.108	0.046	Bus13	-0.108	-0.046	178.6	92.0	
Bus15	11.000	96.861	-2.7	0	0	0	0	Bus9	-0.285	-0.125	16.9	91.6	
								Bus17	0.110	0.048	6.5	91.6	
								Bus16	0.175	0.077	10.4	91.6	
Bus16	0.400	95.200	-3.3	0	0	0.173	0.074	Bus15	-0.173	-0.074	285.6	92.0	

Bus		Voltage		Generation		Load		Load Flow					XFMR
ID	kV	% Mag.	Ang.	MW	Mvar	MW	Mvar	ID	MW	Mvar	Amp	%PF	%Tap
Bus17	11.000	96.860	-2.7	0	0	0	0	Bus15	-0.110	-0.048	6.5	91.6	
								Bus18	0.110	0.048	6.5	91.6	
Bus18	0.400	95.198	-3.3	0	0	0.108	0.046	Bus17	-0.108	-0.046	178.5	92.0	
Bus 20	0.400	95.625	-3.2	0	0	0.134	0.057	Bus Z	-0.134	-0.057	219.6	92.0	
Bus21	11.000	97.061	-2.6	0	0	0	0	Bus SA	3.857	1.963	234.0	89.1	
								Bus AK	1.731	0.910	105.8	88.5	
								Main Bus	-5.588	-2.873	339.8	88.9	
Bus 21	11.000	96.066	-2.9	0	0	0	0	Bus Z	-4.001	-1.767	238.9	91.5	
								Bus 22	3.788	1.675	226.3	91.5	
								Bus 23	0.212	0.093	12.6	91.7	
Bus 22	11.000	95.645	-3.0	0	0	0	0	Bus 27	3.346	1.474	200.7	91.5	
								Bus 21	-3.774	-1.662	226.3	91.5	
								Bus 24	0.135	0.059	8.1	91.7	
								Bus 25	0.212	0.092	12.7	91.7	
								Bus 26	0.082	0.037	4.9	91.2	
Bus 23	0.400	94.782	-3.4	0	0	0.210	0.090	Bus 21	-0.210	-0.090	347.8	92.0	
Bus 24	0.400	94.358	-3.5	0	0	0.133	0.057	Bus 22	-0.133	-0.057	221.5	92.0	
Bus 25	0.400	94.358	-3.5	0	0	0.210	0.089	Bus 22	-0.210	-0.089	348.8	92.0	
Bus 26	0.400	94.381	-3.4	0	0	0.081	0.035	Bus 22	-0.081	-0.035	135.0	91.6	
Bus 27	11.000	95.603	-3.0	0	0	0	0	Bus 22	-3.345	-1.473	200.7	91.5	
								Bus 28	3.211	1.414	192.6	91.5	
								Bus 29	0.134	0.059	8.1	91.7	
Bus 28	11.000	95.221	-3.1	0	0	0	0	Bus 27	-3.200	-1.404	192.6	91.6	
								Bus 30	1.120	0.490	67.4	91.6	
								Bus 43	2.080	0.914	125.2	91.6	
Bus 29	0.400	94.316	-3.5	0	0	0.133	0.057	Bus 27	-0.133	-0.057	221.5	92.0	
Bus 30	11.000	95.088	-3.1	0	0	0	0	Bus 33	0.826	0.360	49.7	91.6	
								Bus 28	-1.119	-0.489	67.4	91.6	
								Bus 31	0.211	0.092	12.7	91.7	
								Bus 32	0.081	0.037	4.9	91.2	
Bus 31	0.400	93.796	-3.6	0	0	0.209	0.089	Bus 30	-0.209	-0.089	350.1	92.0	
Bus 32	0.400	93.819	-3.6	0	0	0.081	0.035	Bus 30	-0.081	-0.035	135.5	91.6	
Bus 33	11.000	95.073	-3.1	0	0	0	0	Bus 30	-0.826	-0.360	49.7	91.7	
								Bus 35	0.691	0.302	41.6	91.7	
								Bus 34	0.134	0.059	8.1	91.7	
Bus 34	0.400	93.781	-3.6	0	0	0.133	0.057	Bus 33	-0.133	-0.057	222.3	92.0	
Bus 35	11.000	95.067	-3.1	0	0	0	0	Bus 33	-0.691	-0.302	41.6	91.7	
								Bus 38	0.346	0.151	20.8	91.6	
								Bus 36	0.134	0.059	8.1	91.7	

Bus		Voltage		Generation		Load		Load Flow					XFMR
ID	kV	% Mag.	Ang.	MW	Mvar	MW	Mvar	ID	MW	Mvar	Amp	%PF	%Tap
								Bus 37	0.211	0.092	12.7	91.7	
Bus 36	0.400	93.775	-3.6	0	0	0.133	0.057	Bus 35	-0.133	-0.057	222.4	92.0	
Bus 37	0.400	93.775	-3.6	0	0	0.209	0.089	Bus 35	-0.209	-0.089	350.2	92.0	
Bus 38	11.000	95.054	-3.1	0	0	0	0	Bus 35	-0.346	-0.151	20.8	91.7	
								Bus 41	0.211	0.092	12.7	91.6	
								Bus 39	0.134	0.059	8.1	91.7	
Bus 39	0.400	93.762	-3.6	0	0	0.133	0.057	Bus 38	-0.133	-0.057	222.4	92.0	
Bus 41	11.000	95.043	-3.1	0	0	0	0	Bus 38	-0.211	-0.092	12.7	91.7	
								Bus 42	0.211	0.092	12.7	91.7	
Bus 42	0.400	93.751	-3.6	0	0	0.209	0.089	Bus 41	-0.209	-0.089	350.3	92.0	
Bus 43	11.000	94.918	-3.1	0	0	0	0	Bus 28	-2.074	-0.909	125.2	91.6	
								Bus 48	1.525	0.669	92.1	91.6	
								Bus 44	0.070	0.031	4.2	91.5	
								Bus 45	0.134	0.059	8.1	91.7	
								Bus 46	0.134	0.059	8.1	91.7	
								Bus 47	0.211	0.092	12.7	91.6	
Bus 44	0.400	93.234	-3.8	0	0	0.069	0.029	Bus 43	-0.069	-0.029	115.8	92.0	
Bus 45	0.400	93.624	-3.6	0	0	0.133	0.057	Bus 43	-0.133	-0.057	222.6	92.0	
Bus 46	0.400	93.624	-3.6	0	0	0.133	0.057	Bus 43	-0.133	-0.057	222.6	92.0	
Bus 47	0.400	93.624	-3.6	0	0	0.209	0.089	Bus 43	-0.209	-0.089	350.6	92.0	
Bus 48	11.000	94.874	-3.1	0	0	0	0	Bus 43	-1.524	-0.668	92.1	91.6	
								Bus 51	1.179	0.517	71.2	91.6	
								Bus 49	0.211	0.092	12.8	91.6	
								Bus 50	0.134	0.059	8.1	91.7	
Bus 49	0.400	93.580	-3.6	0	0	0.209	0.089	Bus 48	-0.209	-0.089	350.7	92.0	
Bus 50	0.400	93.580	-3.6	0	0	0.133	0.057	Bus 48	-0.133	-0.057	222.7	92.0	
Bus 51	11.000	94.841	-3.1	0	0	0	0	Bus 48	-1.179	-0.517	71.2	91.6	
								Bus 52	0.356	0.157	21.5	91.5	
								Bus 56	0.823	0.360	49.7	91.6	
Bus 52	11.000	94.817	-3.1	0	0	0	0	Bus 51	-0.356	-0.157	21.5	91.5	
								Bus 54	0.081	0.036	4.9	91.2	
								Bus 53	0.274	0.121	16.6	91.5	
Bus 53	0.400	93.132	-3.8	0	0	0.271	0.115	Bus 52	-0.271	-0.115	456.2	92.0	
Bus 54	11.000	94.814	-3.1	0	0	0	0	Bus 52	-0.081	-0.037	4.9	91.2	
								Bus 55	0.081	0.037	4.9	91.2	
Bus 55	0.400	93.543	-3.6	0	0	0.081	0.035	Bus 54	-0.081	-0.035	135.8	91.6	
Bus 56	11.000	94.799	-3.1	0	0	0	0	Bus 51	-0.822	-0.360	49.7	91.6	
								Bus 59	0.477	0.209	28.8	91.6	
								Bus 57	0.134	0.059	8.1	91.7	

Bus		Voltage		Generation		Load		Load Flow					XFMR
ID	kV	% Mag.	Ang.	MW	Mvar	MW	Mvar	ID	MW	Mvar	Amp	%PF	%Tap
								Bus 58	0.211	0.092	12.8	91.6	
Bus 57	0.400	93.505	-3.7	0	0	0.133	0.057	Bus 56	-0.133	-0.057	222.8	92.0	
Bus 58	0.400	93.505	-3.7	0	0	0.209	0.089	Bus 56	-0.209	-0.089	350.8	92.0	
Bus 59	11.000	94.767	-3.1	0	0	0	0	Bus 56	-0.477	-0.209	28.8	91.6	
								Bus 61	0.266	0.117	16.1	91.6	
								Bus 60	0.211	0.092	12.8	91.6	
Bus 60	0.400	93.472	-3.7	0	0	0.209	0.089	Bus 59	-0.209	-0.089	350.9	92.0	
Bus 61	11.000	94.759	-3.2	0	0	0	0	Bus 59	-0.266	-0.117	16.1	91.6	
								Bus 62	0.266	0.117	16.1	91.6	
Bus 62	0.400	93.127	-3.8	0	0	0.263	0.112	Bus 61	-0.263	-0.112	442.2	92.0	
Bus AK	11.000	95.697	-2.8	0	0	0	0	Bus21	-1.709	-0.893	105.8	88.6	
								Bus AK low	1.709	0.893	105.8	88.6	
Bus AK low	0.400	93.958	-4.5	0	0	1.704	0.825	Bus AK	-1.704	-0.825	2908.4	90.0	
Bus SA	11.000	94.921	-2.9	0	0	0	0	Bus21	-3.781	-1.902	234.0	89.3	
								Bus SA low	3.781	1.902	234.0	89.3	
Bus SA low	0.400	91.608	-6.5	0	0	3.758	1.601	Bus SA	-3.758	-1.601	6435.8	92.0	
Bus Z	11.000	96.901	-2.7	0	0	0	0	Bus1	-4.165	-1.853	246.9	91.4	
								Bus 21	4.030	1.795	238.9	91.4	
								Bus 20	0.135	0.059	8.0	91.7	
* Main Bus	33.000	100.000	0.0	11.197	6.050	0	0	Bus1	5.582	2.829	109.5	89.2	
								Bus21	5.615	3.222	113.3	86.7	
subst. Tr.Bus	0.400	97.284	-2.7	0	0	0.014	0.003	Bus1	-0.014	-0.003	21.6	98.0	

* Indicates a voltage regulated bus (voltage controlled or swing type machine connected to it)

# Indicates a bus with a load mismatch of more than 0.1 MVA

Branch Losses Summary Report

Branch ID	From-To Bus Flow		To-From Bus Flow		Losses		% Bus Voltage		Vd % Drop in Vmag
	MW	Mvar	MW	Mvar	kW	kvar	From	To	
C1	1.359	0.631	-1.355	-0.628	4.1	3.3	97.4	97.1	0.33
C8	4.184	1.868	-4.165	-1.853	18.6	14.8	97.4	96.9	0.49
Power Tr.1	-5.557	-2.503	5.582	2.829	25.1	326.0	97.4	100.0	2.61
Subst. Tr.	0.014	0.003	-0.014	-0.003	0.0	0.0	97.4	97.3	0.11
C2	1.008	0.476	-1.007	-0.475	0.9	0.7	97.1	97.0	0.10
Line1	0.347	0.152	-0.347	-0.152	0.0	0.0	97.1	97.0	0.02
Line2	0.070	0.031	-0.070	-0.031	0.0	0.0	97.0	97.0	0.00
T1	0.277	0.121	-0.273	-0.116	3.4	5.1	97.0	95.4	1.66
T2	0.070	0.031	-0.069	-0.030	0.9	1.3	97.0	95.4	1.66
C3	0.833	0.398	-0.832	-0.397	0.7	0.5	97.0	96.9	0.09
T3	0.175	0.077	-0.172	-0.074	2.1	3.2	97.0	95.3	1.65
C4	0.285	0.125	-0.285	-0.125	0.0	0.0	96.9	96.9	0.01
C5	0.180	0.079	-0.180	-0.079	0.0	0.0	96.9	96.9	0.00
T4	0.367	0.194	-0.364	-0.185	2.5	8.8	96.9	95.4	1.47
T14	0.000	0.000	0.000	0.000			96.9	96.9	
Line3	0.110	0.048	-0.110	-0.048	0.0	-0.4	96.9	96.8	0.05
T5	0.070	0.031	-0.069	-0.030	0.9	1.3	96.9	95.2	1.66
T6	0.110	0.048	-0.108	-0.046	1.4	2.0	96.8	95.2	1.66
C6	0.110	0.048	-0.110	-0.048	0.0	0.0	96.9	96.9	0.00
T7	0.175	0.077	-0.173	-0.074	2.2	3.3	96.9	95.2	1.66
T8	0.110	0.048	-0.108	-0.046	1.4	2.0	96.9	95.2	1.66
Tr.1	-0.134	-0.057	0.135	0.059	1.3	1.9	95.6	96.9	1.28
C9	3.857	1.963	-3.781	-1.902	76.2	60.8	97.1	94.9	2.14
C12	1.731	0.910	-1.709	-0.893	21.9	17.5	97.1	95.7	1.36
Power Tr.2	-5.588	-2.873	5.615	3.222	26.8	348.9	97.1	100.0	2.94
Line6	-4.001	-1.767	4.030	1.795	29.4	27.4	96.1	96.9	0.84
Line7	3.788	1.675	-3.774	-1.662	14.0	13.1	96.1	95.6	0.42
Tr.2	0.212	0.093	-0.210	-0.090	2.0	3.1	96.1	94.8	1.28
C10	3.346	1.474	-3.345	-1.473	1.3	1.0	95.6	95.6	0.04
Tr.3	0.135	0.059	-0.133	-0.057	1.3	2.0	95.6	94.4	1.29
Tr.4	0.212	0.092	-0.210	-0.089	2.1	3.1	95.6	94.4	1.29
Tr.5	0.082	0.037	-0.081	-0.035	0.8	1.2	95.6	94.4	1.26
Line10	3.211	1.414	-3.200	-1.404	10.8	10.1	95.6	95.2	0.38
Tr.6	0.134	0.059	-0.133	-0.057	1.3	2.0	95.6	94.3	1.29
Line12	1.120	0.490	-1.119	-0.489	1.3	1.1	95.2	95.1	0.13

Branch ID	From-To Bus Flow		To-From Bus Flow		Losses		% Bus Voltage		Vd % Drop in Vmag
	MW	Mvar	MW	Mvar	kW	kvar	From	To	
Line13	2.080	0.914	-2.074	-0.909	5.6	5.1	95.2	94.9	0.30
C13	0.826	0.360	-0.826	-0.360	0.1	0.1	95.1	95.1	0.01
Tr.7	0.211	0.092	-0.209	-0.089	2.1	3.1	95.1	93.8	1.29
Tr.9	0.081	0.037	-0.081	-0.035	0.8	1.2	95.1	93.8	1.27
C15	0.691	0.302	-0.691	-0.302	0.0	0.0	95.1	95.1	0.01
Tr.10	0.134	0.059	-0.133	-0.057	1.3	2.0	95.1	93.8	1.29
C18	0.346	0.151	-0.346	-0.151	0.0	0.0	95.1	95.1	0.01
Tr.11	0.134	0.059	-0.133	-0.057	1.3	2.0	95.1	93.8	1.29
Tr.12	0.211	0.092	-0.209	-0.089	2.1	3.1	95.1	93.8	1.29
C20	0.211	0.092	-0.211	-0.092	0.0	0.0	95.1	95.0	0.01
Tr.13	0.134	0.059	-0.133	-0.057	1.3	2.0	95.1	93.8	1.29
Tr.14	0.211	0.092	-0.209	-0.089	2.1	3.1	95.0	93.8	1.29
Line15	1.525	0.669	-1.524	-0.668	0.6	0.5	94.9	94.9	0.04
Tr.15	0.070	0.031	-0.069	-0.029	0.9	1.3	94.9	93.2	1.68
Tr.16	0.134	0.059	-0.133	-0.057	1.3	2.0	94.9	93.6	1.29
Tr.21	0.134	0.059	-0.133	-0.057	1.3	2.0	94.9	93.6	1.29
Tr.22	0.211	0.092	-0.209	-0.089	2.1	3.1	94.9	93.6	1.29
Line17	1.179	0.517	-1.179	-0.517	0.4	0.3	94.9	94.8	0.03
Tr.26	0.211	0.092	-0.209	-0.089	2.1	3.1	94.9	93.6	1.29
Tr.29	0.134	0.059	-0.133	-0.057	1.3	2.0	94.9	93.6	1.29
Line20	0.356	0.157	-0.356	-0.157	0.1	0.0	94.8	94.8	0.02
Line23	0.823	0.360	-0.822	-0.360	0.3	0.2	94.8	94.8	0.04
Line21	0.081	0.036	-0.081	-0.037	0.0	0.0	94.8	94.8	0.00
T9	0.274	0.121	-0.271	-0.115	3.5	5.3	94.8	93.1	1.68
T10	0.081	0.037	-0.081	-0.035	0.8	1.2	94.8	93.5	1.27
Line25	0.477	0.209	-0.477	-0.209	0.1	0.1	94.8	94.8	0.03
Tr.32	0.134	0.059	-0.133	-0.057	1.3	2.0	94.8	93.5	1.29
Tr.35	0.211	0.092	-0.209	-0.089	2.1	3.1	94.8	93.5	1.29
Line26	0.266	0.117	-0.266	-0.117	0.0	0.0	94.8	94.8	0.01
Tr.37	0.211	0.092	-0.209	-0.089	2.1	3.1	94.8	93.5	1.29
Tr.18	0.266	0.117	-0.263	-0.112	3.3	5.0	94.8	93.1	1.63
Tr. AK	1.709	0.893	-1.704	-0.825	5.2	67.6	95.7	94.0	1.74
Tr. SA	3.781	1.902	-3.758	-1.601	23.2	301.0	94.9	91.6	3.31
					323.4	1289.6			